



**BEHAVIOUR OF CONCRETE STRUCTURES  
REPAIRED WITH A NOVEL AND  
SUSTAINABLE COMPOSITE JACKET**

A Thesis submitted by

**Ali Abdulkareem Mohammed**

BENH (Hons.) (Structural), MEng (Infrastructure)

For the award of

**Doctor of Philosophy**

**2021**

## ABSTRACT

Repairing deteriorating structures is a major challenge for many economies around the world. The use of fibre reinforced polymer (FRP) composite jackets has become a preferred solution in repairing bridge piles as they can be easily installed and form a robust single-piece repair system providing structural continuity along the hoop direction. Recently, a novel prefabricated glass-FRP (GFRP) jacket with innovative joining system that comprises two interlocking edges was developed. The actual performance of this jacket however is not fully explored and its structural contribution to the repaired structure is yet to be determined. This study focused on investigating the behaviour of damaged reinforced concrete (RC) structures repaired with the novel jacket and evaluating its effectiveness as prefabricated FRP repair system.

The grout plays a vital role in transferring the stresses between the damaged concrete structure and the FRP jacket, thus the most suitable grout system is determined as the first study. The effects of three types of grout infills, i.e. cementitious- concrete- and epoxy-based grout, on the structural behaviour of prefabricated GFRP tubes were investigated. The considered grouts have compressive strength and modulus of elasticity ranging from 10 MPa to 70 MPa and from 10 GPa to 35 GPa, respectively, which are the experimental parameters of this stage. The results showed that the brittle failure behaviour of the cementitious and epoxy grouts led to localised failure in the FRP repair system while the progressive cracking and crushing of the concrete infill resulted in effective utilisation of the high strength properties of the composite materials. The developed theoretical model accurately predicts the compressive behaviour of the grout-filled GFRP tubes. From this study, it was also determined that a cementitious grout is a suitable grout system due to its relatively high strength and stiffness as well as its ease of handling and installation.

The effectiveness of the novel FRP jacket as a repair system for RC columns with simulated corrosion damage was evaluated as the second study. Large scale circular and square columns were fabricated with 25% and 50% steel corrosion damage, and 50% and 100% concrete cover damage, then repaired with the FRP jacket and tested axially until failure. The results showed that the jacket restored the load-carrying capacity by 99% and 95% for columns with 25% and 50% corrosion damage, respectively, while the repaired columns with 50% and 100% concrete cover damage restored their axial load capacity by 95% and 82%, respectively. Moreover, the FRP

jacket was found to be 43% more effective in repairing circular columns than the square columns due to the better confinement provided by the GFRP jacket in the circular than in the square column. Theoretical model predicting the axial strength of repaired columns showed an excellent agreement with the experimental results.

Bridge piers are normally subjected to lateral loads from water, tides and waves which create flexural stresses. Thus, the flexural behaviour of seven RC square members with simulated damage repaired with the novel FRP jacket was investigated as the third study. The FRP jacket was found to be more effective in repairing concrete members under flexural load when the damage is located in the compression zone rather than in the tension zone. This effectiveness could be further increased by placing the joint away from the compression zone. The provision of epoxy and coarse aggregates inside the jacket surface improved the stress distribution and cracks propagation in the jacket with grout. A simplified fibre model analysis which considers the confined tensile and compressive properties of the grout reliably predicted the flexural capacity of the damaged beams repaired with the FRP jacket.

Finally, Finite Element (FE) analysis was conducted to gain a better understanding of the behaviour of the repaired columns and to evaluate the effect of joint strength on the effectiveness of the repair system. ABAQUS software package was utilised to develop the FE model using the information obtained from the experimental stages as inputs for the model. The behaviour of the repaired columns was simulated accurately by considering the damaged plasticity model for concrete, bilinear behaviour for steel and linear elastic behaviour of the FRP composites. The results of the FE analysis revealed that the joint of the jacket should be placed away from the damaged zone to minimise stress concentration and effectively utilise the jacket as a repair system. Moreover, joint with tensile strength of at least 20% of the novel GFRP jacket's hoop strength can significantly improve the capacity of the repaired column.

The results of this work provided a comprehensive evaluation on the effectiveness of the novel FRP repair system and detailed understanding on the behaviour of the damaged structures where the current system is sufficient for structural repair; however, further improvements are necessary to modify the joint to extend the jacket's application as a strengthening system. Moreover, this research successfully explored the benefits of this unique system and provided a safe design tools for engineers to effectively utilise the novel FRP jacket in repair applications.

## **CERTIFICATION OF THESIS**

This thesis is entirely the work of *Ali Abdulkareem Mohammed* except where otherwise acknowledged. The work is original and has not previously been submitted for any other award, except where acknowledged.

Principal Supervisor: *Professor Allan Manalo*

Associate Supervisor: *Professor Yan Zhuge*

Student and supervisors' signatures of endorsement are held at USQ.

## STATEMENT OF CONTRIBUTIONS

The scientific journal manuscripts produced from this study are a joint contribution of the collaborated authors. The details of the scientific contribution of each author are presented below:

**Manuscript 1:** Ali A. Mohammed, Allan C. Manalo, Wahid Ferdous, Yan Zhuge, PV Vijay, Ashraf Q. Alkinani and Amir Fam, (2020). “State-of-the-art of prefabricated composite jackets for structures repair” *Engineering Science and Technology, an International Journal*. (Top 10% journal; CiteScore: 4.85 and SNIP: 2.432).

DOI: <https://doi.org/10.1016/j.jestch.2020.02.006>

The overall contribution of Ali A. Mohammed was 60% to the concept development, manuscript structuring, drafting and revising the final submission. The co-authors contributed to the concept development, manuscript structuring, editing and providing important technical inputs.

**Manuscript 2:** Ali A. Mohammed, Allan C. Manalo, Gingham B. Maranan, Yan Zhuge and P.V. Vijay, (2018) “Comparative study on the behaviour of different infill materials for pre-fabricated fibre composite repair systems” *Construction & Building Materials*, vol. 172, pp. 770–780. (Top 10% journal; Impact Factor: 4.046 and SNIP: 2.369).

DOI: <https://doi.org/10.1016/j.conbuildmat.2018.04.025>

The overall contribution of Ali A. Mohammed was 60% to the concept development, design of experiments, experimental works, analysis and interpretation of data, drafting and revising the final submission. The co-authors contributed to the concept development, design of experiments, analysis and interpretation of data, editing and providing important technical inputs.

**Manuscript 3:** Ali A. Mohammed, Allan C. Manalo, Gingham B. Maranan, Yan Zhuge, P. V. Vijay, and John Pettigrew (2019) “Behavior of damaged concrete columns repaired with novel FRP jacket” *Journal of Composites for Construction*, vol. 23, issue (3): 04019013 (Top 10% journal; Impact Factor: 2.606 and SNIP: 1.811).

DOI: [https://doi.org/10.1061/\(ASCE\)CC.1943-5614.0000942](https://doi.org/10.1061/(ASCE)CC.1943-5614.0000942)

The overall contribution of Ali A. Mohammed was 60% to the concept development, design of experiments, experimental works, analysis and interpretation of data, drafting and revising the final submission. The co-authors contributed to the concept

development, design of experiments, analysis and interpretation of data, editing and providing important technical inputs.

**Manuscript 4:** Ali A. Mohammed, Allan C. Manalo, Gingham B. Maranan, Majid Muttashar, Yan Zhuge, PV Vijay, and John Pettigrew. “Effectiveness of a novel composite jacket in repairing damaged reinforced concrete structures subject to flexural loads” *Composite Structures*, vol. 233. (Top 10% journal; Impact Factor: 4.829 and SNIP: 2.035).

DOI: <https://doi.org/10.1016/j.compstruct.2019.111634>

The overall contribution of Ali A. Mohammed was 60% to the concept development, design of experiments, experimental works, analysis and interpretation of data, drafting and revising the final submission. The co-authors contributed to the concept development, design of experiments, analysis and interpretation of data, editing and providing important technical inputs.

**Manuscript 5:** Ali A. Mohammed, Allan C. Manalo, Wahid Ferdous, Yan Zhuge, PV Vijay and John Pettigrew. “Experimental and numerical evaluations on the behaviour of structures repaired using prefabricated FRP composites jacket” *Engineering Structures*, 210 (2020) 110358. (Top 10% journal; Impact Factor: 3.084 and SNIP: 2.089).

DOI: <https://doi.org/10.1016/j.engstruct.2020.110358>

The overall contribution of Ali A. Mohammed was 70% to the concept development, analysis, drafting and revising the final submission. The co-authors contributed to the concept development, design of experiments, analysis and interpretation of data, editing and providing important technical inputs.

## ACKNOWLEDGMENT

I would like to express my deepest gratitude to my principal supervisor *Professor Allan Manalo* for his scientific insight and unparalleled guidance during my PhD journey. He is advisor of life, not only research. I learned to be a good researcher and even better person from his rich academic and life experience. He is big brother and good friend and I am greatly indebted to him for his support and kindness.

I would also like to thank my associate supervisor Professor *Yan Zhuge*, and my co-authors: *Dr Ginghis Maranan, Mr John Pettigrew, Dr Majid Muttashar, Dr Wahid Ferdous, Assistant Professor P.V. Vijay, Mr Ashraf Alkinani* and *Professor Amir Fam* who directly contributed their knowledge to my research and publications.

I acknowledge the Ministry of Higher Education of Iraq, Australian government and Joinlox™ Pty. Ltd who made this research possible. This research has been supported by an Australian Government Research Training Program Scholarship.

Friends, colleagues, academic and professional staff at CFM, USQ, Toowoomba and beyond, thank you for the support and encouragement, laughs and good times, which kept my strength and determination at good levels to reach this stage.

Special thanks to *Dr Usama Hilo* and *Professor Jasim Hilo* for directing me to this path, taking the first step for me and helping me to complete this big task successfully.

My amazing parents, brothers and sisters, I cannot thank you enough for believing and trusting me to accomplish. Your endless support and encouragement are unapparelled.

The most special thank you goes to my beloved wife, *Haneen*, for your tremendous love and endless patience during the challenging periods which without I could not have been able to overcome this challenge. Presenting this research without statement of love to my adorable pigeon pair *Hasan* and *Emma* is not fair, because they are the joy and happiness of the present and the hope and promise of the future.

Thanks *God*, the greatest engineer behind this very systemic universe, for giving me the hope, health and strength to compete this work.

Finally, to those whom I failed to mention but have been a great part of this journey, thank you.

*Ali A. Mohammed*

## TABLE OF CONTENTS

<b>Abstract</b> .....	ii
<b>Certification of Thesis</b> .....	iv
<b>Statement of Contribution</b> .....	v
<b>Acknowledgment</b> .....	vii
<b>List of Figures</b> .....	ix
<b>List of Tables</b> .....	xi
<b>Abbreviations</b> .....	xii
Chapter 1 Introduction.....	1
Chapter 2 State-of-the-Art of Prefabricated Composite Jackets for Structures Repair	9
Chapter 3 Comparative study on the behaviour of different infill materials for pre- fabricated fibre composite repair systems.....	25
Chapter 4 Behaviour of damaged concrete columns repaired with novel FRP jacket	37
Chapter 5 Effectiveness of a novel composite jacket in repairing damaged reinforced concrete structures subject to flexural loads.....	52
Chapter 6 Experimental and numerical evaluations on the behaviour of structures repaired using prefabricated FRP composites jacket.....	68
Chapter 7 Conclusions.....	79
<b>References</b> .....	87
<b>Appendix A: Recognitions and Awards</b> .....	88
<b>Appendix B: Refereed Conference Papers and Project Poster</b> .....	89
<b>Appendix C: Full Experimental Results of Chapter 3</b> .....	91
<b>Appendix D: Revised Published Figures</b> .....	92

## LIST OF FIGURES

Figure 1.1	Novel GFRP Jacket.....	3
Figure 1.2	Flow diagram of the thesis.....	7
Figure 2.1	Demand increase on structural repairs from 2003 to 2018 based on Scopus.....	11
Figure 2.2	Splicing of timber piles.....	11
Figure 2.3	RC columns repair using RC and steel jackets.....	12
Figure 2.4	Wood pile repair.....	13
Figure 2.5	Waterfront structure repair, New York.....	13
Figure 2.6	Steel bridge pile repair.....	13
Figure 2.7	PileMedic™.....	13
Figure 2.8	Seismic repair method.....	14
Figure 2.9	GFRP composite pile repair system.....	14
Figure 2.10	GFRP jacket.....	15
Figure 2.11	Stress–strain curves.....	16
Figure 2.12	Stress–strain curves of confined concrete with FRP tubes of various thickness.....	17
Figure 2.13	Confinement effectiveness of FRP tubes with various stiffness.....	17
Figure 2.14	Joining systems.....	18
Figure 2.15	Confinement mechanism.....	19
Figure 2.16	The prefabricated composite pile repair system.....	21
Figure 2.17	Bridge piles repaired with FRP jacket.....	21
Figure 3.1	The pre-fabricated GFRP tube.....	28
Figure 3.2	Stacking sequence of the GFRP tube.....	28
Figure 3.3	Geometry and configuration of the test specimens.....	28
Figure 3.4	Roughened GFRP tube.....	29
Figure 3.5	Compression test set-up.....	29
Figure 3.6	Representative failure modes of the cylindrical infills.....	29
Figure 3.7	Representative stress-strain ( $\sigma_c - \epsilon_c$ ) curves of the cylindrical infill materials.....	30
Figure 3.8	Typical compression failure of hollow and filled GFRP tubes.....	31
Figure 3.9	Post-failure configuration of G-C2 and G-C2*.....	31
Figure 3.10	Axial stress-axial strain curves of the grout-filled GFRP tubes.....	31
Figure 3.11	Axial stress-hoop strain curves of the grout-filled GFRP tubes.....	32
Figure 3.12	Relation between the normalised axial stress and the normalised axial strain.....	33
Figure 3.13	Relationship between $\sigma_{iu}$ and $f_o$ .....	34
Figure 3.14	$\sigma_{gu}/\sigma_{iu}$ vs $\sigma_{l,a}/\sigma_{iu}$ .....	34
Figure 3.15	$\epsilon_{hu}/\epsilon_{iu}$ vs $(\epsilon_{hu}/\epsilon_{iu})^n (\sigma_{l,a}/\sigma_{iu})$ .....	34
Figure 3.16	Experimental and theoretical axial stress-axial strain curves of the grout-filled GFRP tubes.....	35
Figure 4.1	Existing prefabricated FRP repair system.....	39
Figure 4.2	Novel GFRP jacket.....	39
Figure 4.3	Test specimen details and configuration.....	41
Figure 4.4	Fabrication of column specimens.....	42
Figure 4.5	Installation of GFRP jacket and infill.....	42
Figure 4.6	Compression test set-up of columns.....	43

Figure 4.7	Failure modes of tested columns.....	44
Figure 4.8	Specific failures in components of repair system.....	45
Figure 4.9	Load-deformation curves.....	45
Figure 4.10	Strain development in repair system.....	46
Figure 4.11	Development of cracks in grout material and stress concentration in jacketed columns.....	46
Figure 4.12	FRP jacket effectiveness with different levels of steel damage.....	47
Figure 4.13	Configuration of partially confined compression member.....	48
Figure 4.14	Normalized $A_{ef}$ versus normalized $k$ .....	49
Figure 5.1	Novel GFRP jacket with novel joining system.....	54
Figure 5.2	Splitting tensile test set-up.....	55
Figure 5.3	Behaviour of grout-filled FRP tubes.....	55
Figure 5.4	Schematic diagram of the failure mode of grout-filled FRP tubes.....	56
Figure 5.5	Details and configuration of test specimens.....	56
Figure 5.6	Fabrication of beams reinforcement cage with simulated damage.....	57
Figure 5.7	Installation of GFRP jackets over the beams.....	57
Figure 5.8	Four-point static bending test set-up.....	58
Figure 5.9	Crack pattern of tested beams.....	59
Figure 5.10	Propagation of cracks in the grout infill.....	60
Figure 5.11	Failure mode of the tested specimens.....	61
Figure 5.12	Failure of the jacket.....	62
Figure 5.13	Load-deflection curves of the tested specimens.....	62
Figure 5.14	Load-strain curves of the tested beams.....	63
Figure 5.15	Load-strain curves of the tested beams.....	63
Figure 5.16	Load deflection curves of beams repaired with epoxy coated jacket.....	64
Figure 5.17	Basic assumptions in Fibre Model Analysis.....	64
Figure 5.18	Constitutive models for basic materials of RC beam.....	65
Figure 6.1	Novel GFRP Jacket.....	70
Figure 6.2	Fabrication of column specimens.....	71
Figure 6.3	Test set-up of columns.....	72
Figure 6.4	Failure mode of the tested columns.....	73
Figure 6.5	Experimental load-strain behaviour of the tested columns.....	73
Figure 6.6	Constitutive models of components materials.....	74
Figure 6.7	Modelled columns and repair system.....	75
Figure 6.8	Validation and numerical load-strain behaviour of the tested columns..	75
Figure 6.9	Failure mode of simulated columns.....	76
Figure 6.10	Level of joint strength improvement ( $f_{frph}/f_{frp}$ ) versus axial strength enhancement of the repaired member ( $P_c/P$ ).....	77
Figure 7.1	Novel FRP jacket utilisation in actual repair project.....	85

## LIST OF TABLES

Table 2.1	Summary of FRP composite application in the laboratory and on real structures.....	16
Table 3.1	Properties of GFRP coupons.....	28
Table 3.2	Peak axial load, compressive strength and its standard deviation, elastic modulus, and strain at peak of the cylindrical grout infills.....	30
Table 3.3	Peak axial load, peak axial stress and corresponding standard deviation and strains at rupture of grout-filled GFRP tubes.....	32
Table 3.4	Values of constants a, b, c, d, and n.....	34
Table 4.1	Properties of GFRP shell and joint.....	40
Table 4.2	Maximum axial load capacity, stiffness, and failure mode of tested columns.....	43
Table 4.3	Experimental and theoretical results.....	48
Table 5.1	Load, deformation and the failure mode of the tested beams.....	59
Table 5.2	Actual and predicted load (P, kN) and strain ( $\mu\epsilon$ ) values of RC beams.....	65
Table 6.1	Experimental test specimens.....	71
Table 6.2	Axial load capacity, stiffness and failure mode of the tested columns.....	72
Table 6.3	Material properties of concrete, grout, steel and GFRP.....	73

## ABBREVIATIONS

GFRP	Glass fibre reinforced polymer
RC	Reinforced concrete
$k_e$	Confinement effective coefficient
MOE	Modulus of elasticity
$A_c$	Cross-sectional area
$A_e$	Effectively confined concrete
$A_{ef}$	Normalised effective area
$D$	Diameter
$P$	Applied Load
$\sigma_{co}$	Original compressive strength of the column
$\sigma_{cc}$	Predicted compressive strength of the column
$\sigma_{l,a}$	Active confining pressure
$\epsilon_{hu}$	Rupture strain of FRP in the hoop direction
$\epsilon_{iu}$	Axial strain at peak load
$t_g$	Nominal thickness of FRP jacket
$E_f$	Elastic modulus of FRP
$h_f$	Height of the FRP jacket
$h_u$	Total height of the column

# Chapter 1

## Introduction

### *Background and motivation*

Maintaining the existing structures in service is a major challenge for many transport authorities around the world due to constant weathering and environmental attacks. Corrosion damage costs the Australian economy \$13 billion every year including the cost of lost production due to the delay in transporting goods and daily services and shutdowns to make repairs (Cassidy et al. 2015). In addition, it is estimated that more than \$15 billion annually is needed to maintain the reinforced concrete (RC) bridges in the US, Canada, and Europe (Azam et al. 2016). Compounding this problem is the recurring durability issues in the traditional repair techniques such as concrete and steel jacketing as they are made with the same materials as the existing structure, which will be affected again by the same factors that attacked the original structures at first place (Vandoros and Dritsos 2008). Moreover, concrete and steel jackets are bulky and heavy, and add weight to the repaired structures and may attract higher loads in seismic events (Beddiar et al. 2015). Implementation of these traditional repair systems is also difficult and costly in the repair of underwater structures. Hence, there has been an urgent need for an alternative technique to overcome the drawbacks of using traditional materials in a repair system.

The introduction of fibre reinforced polymer (FRP) composites as a repair system has become very popular because of their versatility due to their high strength, light weight and their ability to minimise the durability issues that accompanied the use of traditional material (Sakr et al. 2005). As a repair system, FRP composites can be applied either as wet lay-up or pre-fabricated systems (Manalo et al. 2014). In the wet lay-up, FRP repair systems are prepared and applied on site by impregnating liquid resins into fibres and then wrapping them around the existing structure. The pre-fabricated systems, on the other hand, are manufactured in a factory and delivered to a site in a ready for installation condition. Although many studies have shown that both systems are effective (Berthet et al. 2005), the pre-fabricated composite jacket is favoured over the wet lay-up method because it is easier, quicker, safer to install and can achieve a higher quality under well controlled manufacturing conditions.

Recently, a novel and sustainable pre-fabricated FRP jacket that can be quickly and safely installed due to its easy-fit and self-locking mechanical joining system has been developed (Figure 1.1). This innovative joining system comprises two interlocking edges that can easily fit into each other, similar to the teeth of a zipper. A FRP locking key is placed between the interlocking teeth, which can be slid or levered only one pitch length, thus causing wedging of the joint edges together with a uniform force distribution along the entire length of the joint. This repair system works by wrapping the prefabricated FRP jacket around the damaged structure and placing a grout infill between the jacket and the repaired structure, producing a cylindrical confinement. This system also serves as protective environmental shield and permanent formwork. Manalo et al. (2014) evaluated the effectiveness of this FRP jacket numerically, using Strand7 finite element (FE) program and experimentally subjecting the jacket to internal pressure. The results showed that the FRP jacket can sustain an internal pressure of up to 2 MPa, which substantially exceeds the industry standard for internal bursting pressure required of a concrete pile repair system and a permanent concrete formwork jacket. However, the actual behaviour of this prefabricated FRP repair system has not yet been fully investigated and its structural contribution to the damaged member is yet to be determined.

This thesis systemically investigated and evaluated the overall behaviour of the prefabricated FRP composite system in repairing damaged concrete structures. Firstly, the effect of different grout-infills' properties, such as compressive strength and modulus of elasticity, on the behaviour of the FRP repair system was studied. Secondly, the axial behaviour of the damaged RC columns repaired with the novel jacket was investigated. The effect of the level of corrosion damage, the concrete cover damage, the shape effect and the innovative joining system efficiency on the behaviour of the repaired column was studied under concentric axial loads. Thirdly, the effectiveness of the prefabricated FRP composite jacket in repairing RC members under flexural loads was investigated considering different parameters, i.e. joint location, damage location and jacket-grout bonding effect. Finally, FE analysis was conducted for a better understanding of the behaviour of the repaired columns with the prefabricated FRP jacket, particularly the behaviour inside the repaired part of the columns which was not visible during loading due to the jacket. The developed FE model was also used to investigate the effect of joint strength on the behaviour of the

repaired structures. This research, in general, provided useful and effective design tools for stakeholders and engineers to safely design a reliable repair system that can restore the strength of the damaged structure to its original condition.

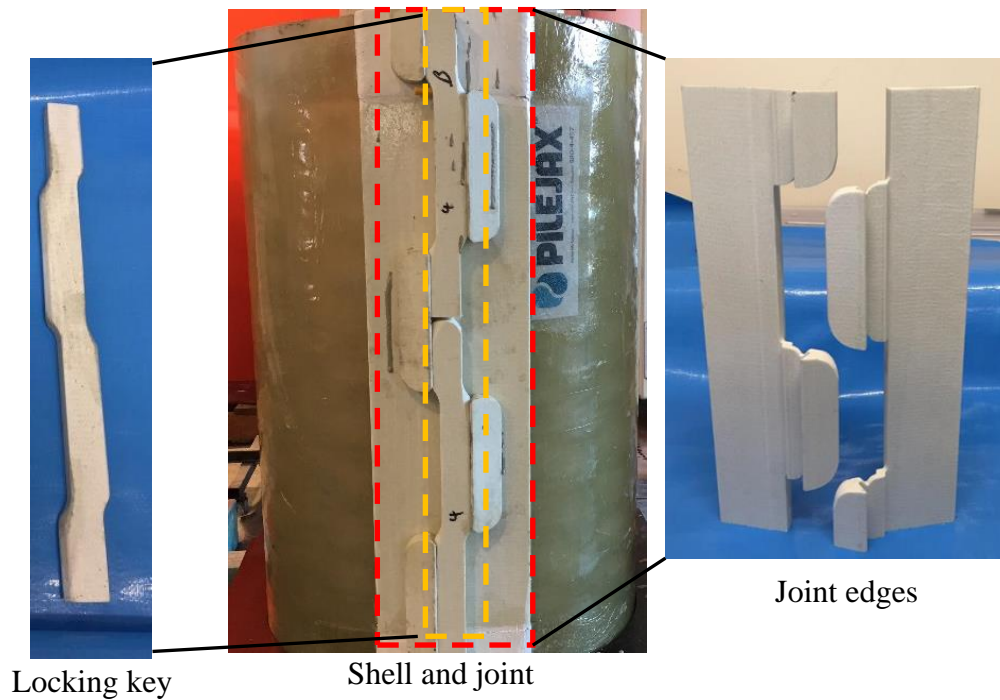


Figure 1.1. Novel GFRP jacket

### ***Objectives***

The main objective of this study is to investigate the behaviour of damaged structures repaired with the composite repair system, and to evaluate the efficiency of the prefabricated FRP jacket. The specific objectives of the study are:

1. Review the existing prefabricated FRP repair system and identify the factors affecting their performance.
2. Determine the effect of different grout infills' properties on the behaviour of the prefabricated FRP repair system.
3. Experimentally investigate the axial behaviour of damaged RC columns repaired with the prefabricated FRP jacket.
4. Experimentally investigate the flexural behaviour of damaged RC members repaired with the prefabricated FRP jacket.

5. Simulate the behaviour of the damaged members repaired with the prefabricated jacket numerically and investigate the effect of the critical design parameters affecting the behaviour of the repaired structure.

### ***Study limitations***

This thesis studied the behaviour of damaged concrete structures repaired with prefabricated FRP composite jacket. Only three types of grout currently used in industry practice (concrete, cementitious and epoxy based grout) were investigated. The diameter of the RC columns was limited to 250 mm based on the maximum load capacity of the testing equipment. For the jacketing system, a jacket with one diameter (450 mm) and one thickness (3 mm) was used for the repair of damaged compression and flexural members. The jacket diameter was based on the curvature of the joint, while the 3 mm thickness was sufficient as no failure was observed in the shell segment. A new approach was adopted to simulate the steel corrosion damage by cutting the longitudinal reinforcements in the test region and replacing them with non-structural PVC pipe (16-mm diameter) to prevent the concrete from occupying the steel volume and to maintain the alignment of the longitudinal reinforcement at both ends. This approach was adopted because the accelerated corrosion process takes significant time to simulate low levels of corrosion damage. In the FE modelling, for simplicity and to save computational efforts, the innovative joint was modelled as a lamina with different properties in the longitudinal and transverse directions instead of the actual geometry.

### ***Thesis organisation***

The outcome of this work is presented as a thesis by publication. It comprises an introduction that presents the research theme, an extensive review of the related literature, four major chapters that address the four main objectives of this research and with results that are presented in high quality international journals, a conclusion that summarises the general findings and contributions of this study, and some recommendations for future works. The five journal manuscripts that resulted from this research are the following:

**Manuscript 1: Ali A. Mohammed,** Allan C. Manalo, Wahid Ferdous, Yan Zhuge, PV Vijay, Ashraf Q. Alkinani and Amir Fam. “State-of-the-art of prefabricated composite jackets for structures repair” *Engineering Science and Technology, an International Journal*, (2020). (Top 10% journal; Impact Factor: 4.85 and SNIP: 2.432).

DOI: <https://doi.org/10.1016/j.jestch.2020.02.006>

**Manuscript 2: Ali A. Mohammed,** Allan C. Manalo, Gingham B. Maranan, Yan Zhuge and P.V. Vijay, (2018) “Comparative study on the behaviour of different infill materials for pre-fabricated fibre composite repair systems” *Construction & Building Materials*, vol. 172, pp. 770–780. (Top 10% journal; Impact Factor: 4.046 and SNIP: 2.369).

DOI: <https://doi.org/10.1016/j.conbuildmat.2018.04.025>

**Manuscript 3: Ali A. Mohammed,** Allan C. Manalo, Gingham B. Maranan, Yan Zhuge, P. V. Vijay, and John Pettigrew (2019) “Behavior of damaged concrete columns repaired with novel FRP jacket” *Journal of Composites for Construction*, vol. 23, issue (3): 04019013 (Top 10% journal; Impact Factor: 2.606 and SNIP: 1.811).

DOI: [https://doi.org/10.1061/\(ASCE\)CC.1943-5614.0000942](https://doi.org/10.1061/(ASCE)CC.1943-5614.0000942)

**Manuscript 4: Ali A. Mohammed,** Allan C. Manalo, Gingham B. Maranan, Majid Muttashar, Yan Zhuge, PV Vijay, and John Pettigrew. “Effectiveness of a novel composite jacket in repairing damaged reinforced concrete structures subject to flexural loads” *Composite Structures*, vol. 233. (Top 10% journal; Impact Factor: 4.829 and SNIP: 2.035).

DOI: <https://doi.org/10.1016/j.compstruct.2019.111634>

**Manuscript 5: Ali A. Mohammed, Allan C. Manalo, Wahid Ferdous, Yan Zhuge, PV Vijay and John Pettigrew.** “Experimental and numerical evaluations on the behaviour of structures repaired using prefabricated FRP composites jacket” *Engineering Structures*, 210 (2020) 110358. (Top 10% journal; Impact Factor: 3.084 and SNIP: 2.089).

DOI: <https://doi.org/10.1016/j.engstruct.2020.110358>

In addition, the significant findings from this research were presented in related national and international conferences, which are summarised in Appendix A.

The first objective of this study is to extensively review the existing prefabricated FRP repair system and identify the factors affecting their performance which is presented in Chapter 2. The current repair practice have been critically reviewed and suggestions were made for better rehabilitation techniques. This manuscript concluded that the proposed novel jacket with an innovative joining system can be a game changer in the construction industry and can breathe new life into key infrastructure.

The second objective of this study is to determine the effect of concrete, cementitious and epoxy grout infills’ properties on the behaviour of the prefabricated FRP repair system which is addressed in Chapter 3. The compressive strength and modulus of elasticity are the two most important mechanical characteristics of the grout that affect its functionality in terms of load transferability and effective utilisation of the FRP system. Three different types of grout with a wide range of compressive strength and elastic modulus used as infills with hollow GFRP tubes and subject to axial concentric loads. The study determined how the failure mode of the infill can affect the ultimate failure and the utilisation of prefabricated GFRP tubes

The third objective of this study is to investigate the axial behaviour of damaged RC columns repaired with the prefabricated FRP jacket and evaluate the jacket effectiveness in repairing damaged structures which is achieved in Chapter 4. The load-deformation response, mechanism of failure, strength and deformation capacity, reinforcement, concrete and jacket component strain were thoroughly investigated. The results of the extensive experimental investigation showed that the joint is capable of providing structural continuity along the hoop and the jacket is able

to restore the axial strength and stiffness of RC column with steel corrosion and concrete cover damage.

Chapter 5 addressed the fourth objective of this study and focused on the effectiveness of the novel composite jacket in repairing damaged RC structures subject to flexural loads. Full-scale beams were prepared and tested under four-point static loads to evaluate the effects of damage location in the concrete member, joint location and internal surface coating of the jacket. The results showed that the behaviour of the repaired system is governed by the tensile cracking of the grout and the failure of teeth at the joint. The FRP jacket is found to be more effective in repairing concrete members under flexural load when the damage is located at the top rather than at the bottom of the member.

The final objective of this study is to numerically simulate the behaviour of the damaged members repaired with the prefabricated jacket which has been addressed in Chapter 6. The FE analysis was implemented using ABAQUS/Explicit and accurately simulated the behaviour of the repaired columns. The results from this simulation were extended to investigate the effect of joint strength on the behaviour of the repaired structures.

For better understanding the link among the studies and manuscripts, the flow of the thesis is graphically presented in Figure 1.2.

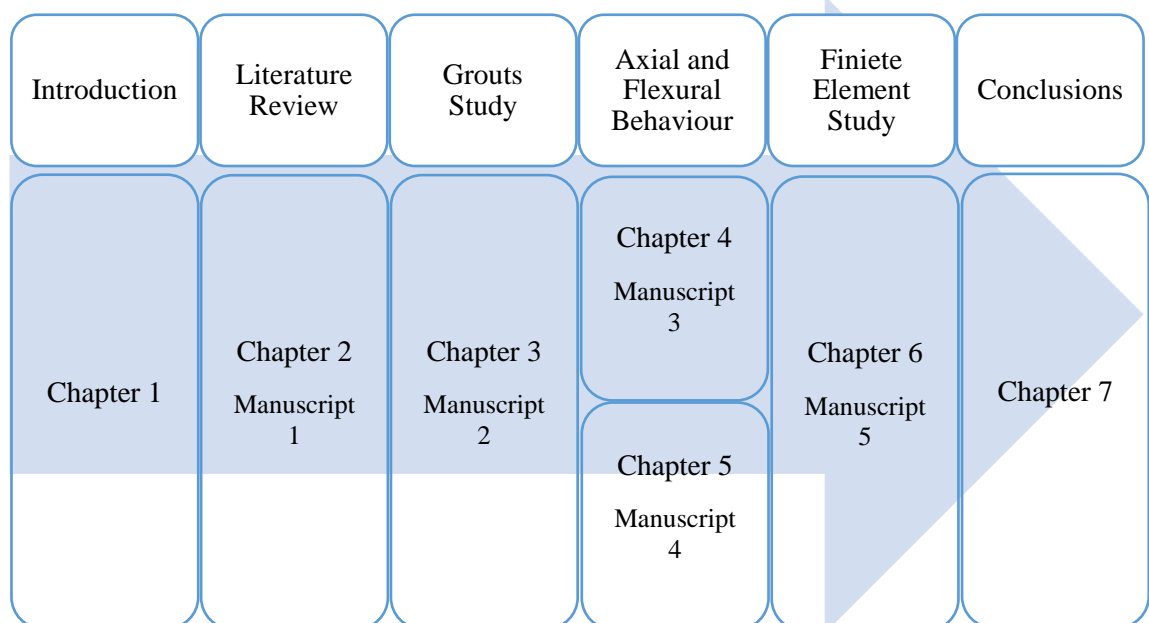


Figure 1.2. Flow diagram of the thesis

## *Summary*

Most of the available prefabricated FRP repair systems lack an effective joining system that is capable of providing structural continuity along the hoop direction. In order to overcome this limitation, a novel FRP composite jacket with innovative FRP joining system has recently been developed. Evaluating the effectiveness of this novel FRP jacket and understanding the behaviour of damaged members repaired with the proposed jacket is the main motivation of this research. The effect of various types of grout with different mechanical properties on the behaviour of the repair system were investigated. Moreover, the behaviour of RC members with simulated steel corrosion and concrete cover damaged casted and repaired with the novel jacket subjected to axial and flexural loads were studied. Finally, FE model was also developed to simulate the behaviour of the repaired structure and gain an in-depth understanding of the system components. The results of these works are presented in the succeeding chapters.

## **Chapter 2**

### **State-of-the-Art of Prefabricated Composite Jackets for Structures Repair**

Chapter 2 presents a critical review about the current practice and new opportunities of using prefabricated composite jackets for structural repair of deteriorating concrete structures. The state-of-the-art review highlighted the many drawbacks of using traditional repair systems including concrete and steel jacketing, in repairing damaged structures. It also summarised research, development and practice in prefabricated FRP repair systems. Moreover, the most important factors affecting the effectiveness of prefabricated FRP repair system were identified and their effect was analysed. From state-of-the-art review, concrete, shrinkage compensating or expansive cementitious grout and epoxy-based grout are identified as the most common grouts for the prefabricated FRP repair system wherein their compressive strength and modulus of elasticity significantly affect the effective transfer of loads from the repaired structure to the FRP repair system. However, this can only be achieved if the prefabricated FRP repair system can provide structural continuity along the hoop direction through its joining system. Thus, the FRP jacket with novel joining system provides the construction industry with a repair system that can breathe in a new life into aging and deteriorating structures. The performance benefits of this novel FRP jacket should however be investigated, its contribution to the structural integrity of the repaired structure to be determined and to fully explore the potential and effectiveness of this novel composite repair system. This has been the main motivation of this study as addressed in Chapters 3 to 6.

HOSTED BY



ELSEVIER

Contents lists available at ScienceDirect

# Engineering Science and Technology, an International Journal

journal homepage: [www.elsevier.com/locate/jestch](http://www.elsevier.com/locate/jestch)

## Review

# State-of-the-art of prefabricated FRP composite jackets for structural repair

Ali A. Mohammed<sup>a,b,\*</sup>, Allan C. Manalo<sup>a</sup>, Wahid Ferdous<sup>a</sup>, Yan Zhuge<sup>c</sup>, P.V. Vijay<sup>d</sup>, Ashraf Q. Alkinani<sup>e</sup>, Amir Fam<sup>f</sup>

<sup>a</sup> Centre for Future Materials (CFM), School of Civil Engineering and Surveying, University of Southern Queensland, Toowoomba 4350, Australia

<sup>b</sup> Environmental Engineering Department, College of Engineering, The University of Mustansiriyah, Baghdad, Iraq

<sup>c</sup> School of Natural & Built Environments, University of South Australia, Adelaide 5001, Australia

<sup>d</sup> Department of Civil and Environmental Engineering West Virginia University, WV 26506, USA

<sup>e</sup> School of Civil Engineering, Universiti Sains Malaysia, Penang, 14300, Malaysia

<sup>f</sup> Department of Civil Engineering, Queen's University, Kingston, ON, K7L 3N6, Canada

## ARTICLE INFO

### Article history:

Received 1 October 2019

Revised 16 February 2020

Accepted 17 February 2020

Available online xxxx

### Keywords:

Damage

Structural rehabilitation

Structural repair

Prefabricated FRP composite jacket

Deterioration

FRP

Composites

Jacketing

Joints

## ABSTRACT

Fibre reinforced polymer (FRP) composites have attracted significant attention in repairing existing and deteriorating structures since the traditional rehabilitation techniques have several limitations in terms of durability, self-weight and complex installation process. Prefabricated FRP composite jackets are the preferred solution in repairing bridge piles located both underwater and above the waterline as they can be easily placed around the damaged pile to form a robust single-piece repair system. The structural continuity of the jacket in such a repair system is critical for effectively utilising its maximum strength. This study presents an extensive review of the current practices and new opportunities for using prefabricated composite jackets for structural repair. Important design considerations to effectively utilise prefabricated FRP composite jackets in repairing structures are presented and analysed. The review also identifies the challenges and highlights the future directions of research to increase the acceptance and use of emerging composite repair systems.

© 2020 Karabuk University. Publishing services by Elsevier B.V. This is an open access article under the CC BY-NC-ND license (<http://creativecommons.org/licenses/by-nc-nd/4.0/>).

## Contents

1. Introduction . . . . .	00
2. Current jacket repair systems . . . . .	00
3. Prefabricated FRP composites repair systems. . . . .	00
4. Factors affecting structural repair using prefabricated FRP repair system . . . . .	00
4.1. Condition of the existing structures. . . . .	00
4.1.1. Environmental conditions . . . . .	00
4.1.2. Level of damage . . . . .	00
4.2. FRP composite jacket . . . . .	00
4.2.1. Thickness. . . . .	00
4.2.2. Fibre type and orientation . . . . .	00
4.3. Joining system . . . . .	00
4.4. Grouting system . . . . .	00
5. Existing models to evaluate effectiveness of prefabricated FRP repair systems. . . . .	00
6. Discussion and future research . . . . .	00

\* Corresponding author at: Centre for Future Materials (CFM), School of Civil Engineering and Surveying, University of Southern Queensland, Toowoomba 4350, Australia.

E-mail addresses: [ali.mohammed@usq.edu.au](mailto:ali.mohammed@usq.edu.au) (A.A. Mohammed), [allan.manalo@usq.edu.au](mailto:allan.manalo@usq.edu.au) (A.C. Manalo), [wahid.ferdous@usq.edu.au](mailto:wahid.ferdous@usq.edu.au) (W. Ferdous), [yan.zhuge@unisa.edu.au](mailto:yan.zhuge@unisa.edu.au) (Y. Zhuge), [p.vijay@mail.wvu.edu](mailto:p.vijay@mail.wvu.edu) (P.V. Vijay), [ashrafqays@student.usm.my](mailto:ashrafqays@student.usm.my) (A.Q. Alkinani), [amir.fam@queensu.ca](mailto:amir.fam@queensu.ca) (A. Fam).

Peer review under responsibility of Karabuk University.

<https://doi.org/10.1016/j.jestch.2020.02.006>

2215-0986/© 2020 Karabuk University. Publishing services by Elsevier B.V.

This is an open access article under the CC BY-NC-ND license (<http://creativecommons.org/licenses/by-nc-nd/4.0/>).

Please cite this article as: A. A. Mohammed, A. C. Manalo, W. Ferdous et al., State-of-the-art of prefabricated FRP composite jackets for structural repair, Engineering Science and Technology, an International Journal, <https://doi.org/10.1016/j.jestch.2020.02.006>

7. Conclusions .....	00
Declaration of Competing Interest .....	00
Acknowledgements .....	00
References .....	00

## 1. Introduction

Across the globe, civil infrastructure, including highway bridges, roads, railways, ports, and airports is critical for economic development and progress. However, keeping this infrastructure in an efficient working condition is costly and challenging. Steel, timber and concrete structures are vulnerable to harsh weathering attacks including chloride and sulphate penetration, especially in marine or mining environments, that affect their integrity and cause their performance to deteriorate significantly [1,2]. For example, many coastal bridges experience corrosion after only 30 years of service, which is early, considering that they are designed for a service life of about 100 years [3]. A report on the durability of concrete structures cited in Nkurunziza et al. [4] stated that the cost of repairs and restoration constitutes a high percentage of infrastructure expenditure in many countries including Australia, the USA, Canada, and European Union countries. The Commonwealth Scientific and Industrial Research Organisation (CSIRO) reported that corrosion damage costs the Australian economy more than \$13 billion per year [5]. In the USA, around 40% of the 575,000 country's bridges are structurally and/or functionally defective due to steel corrosion [4]. The same problem exists in Canada wherein it is estimated that more than 40% of bridges constructed 40-years ago are suffering from significant steel corrosion [4]. Jumaat et al. [6] indicated that investments in maintenance and repair works on existing buildings represent about 50% of the total expenditure in construction. In most applications, repairing the damaged structures is preferable and more economical than replacing them due to the high cost of the new design, material, machinery and labour, plus the long extended service life of the effectively repaired structure. Hence, many industries and research agency are trying to optimise the current repair techniques and develop more effective ones. The Scopus database search conducted using the keyword "structural repair" was limited to engineering as a subject area and to article as a source type. It showed that the number of studies conducted on structural repair has been significantly increased from 2003 to 2018 (Fig. 1), highlighting the demand and necessity for an effective repair technique.

Rehabilitation of damaged and deteriorating structures with jackets made of concrete, steel, fibre-reinforced polymer (FRP)

composites is now common and has been widely adopted as these jackets have high economic benefits by minimising the time the structure is off-service. Use of these jackets also results in significant savings in the amount of time and resources by decreasing the delay in daily operational services to a considerable level. Concrete jackets are used to retrofit damaged reinforced concrete (RC) structures with steel corrosion damage and concrete spalling. Many studies have shown that RC jackets can effectively restore the structural functionality of these deteriorated members [7–10]. In addition, steel jackets are also used to strengthen and retrofit RC members with structural defects [11–14]. The versatility of FRP composite materials has rendered them essential in civil applications [15–17], especially for strengthening and rehabilitation of civil infrastructure [18]. Many glass-FRP (GFRP) repair systems have already been used globally for rehabilitating damaged concrete, steel and timber structures and extending their service lives [19–24]. Similarly, Carbon-FRP (CFRP) is also good alternative to be used in seismic repairs and/or when more confinement pressure is required to achieve enhanced structural capacities due to their higher mechanical properties compared to GFRP jackets [25–33]. The availability of this wide range of composite jacket repair systems necessitates a targeted approach to evaluate the advantages and disadvantages of each technique in order to fully explore their potential in repairing damaged and deteriorating structures.

This study presents a systematic review of current practices for the repair of structures using prefabricated composite jackets and discusses the factors affecting structural repair using these jackets. The information on recent developments in prefabricated composite jackets for repairing structures helps to understand their performance and identify the critical factors in their application. Also, the paper identifies the gap in the state-of-art repair systems, and makes recommendations for new areas of research and development that need further exploration to increase the acceptance and use of emerging and new composite repair systems.

## 2. Current jacket repair systems

Splicing deteriorating steel and timber structures involves replacing the damaged part with a new section of the same material. For instance, a common practice for repairing corroded steel structures is bolting or welding a new steel section onto them

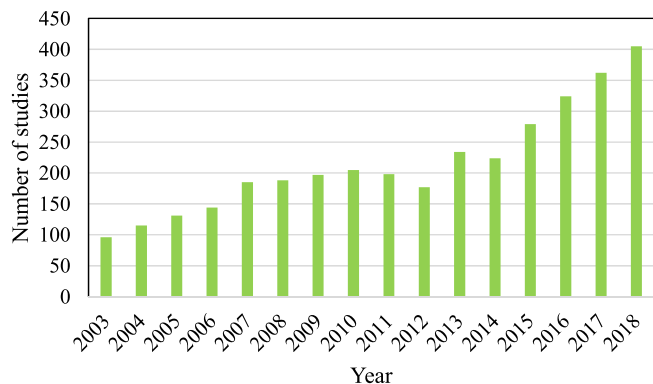


Fig. 1. Demand increase on structural repairs from 2003 to 2018 based on Scopus.



Fig. 2. Splicing of timber piles [21].



Fig. 3. RC columns repair using RC and steel jackets. a) RC jacket [8] b) steel jacket [14].

[34]. This technique was used for the first time in France in 1943, when rectangular steel bars were welded between a row of rivets to strengthen an old steel bridge [35]. Similarly, splicing timber structures involves removing the damaged portion of an old pile and splicing a new piece using metallic bolts, as depicted in Fig. 2 [21]. An example of this technique is the Kaase timber bridges repair in Ghana where 25 year-old decayed wood piles were replaced with new members made of the same type of original timber that the bridge was built with [36].

Fig. 3 shows RC and steel jackets in actual practice. Concrete jacketing is one of the earliest and most popular rehabilitation techniques for poorly detailed or deficient concrete and steel structures. RC jacketing/encasement has been utilised as a repair method for corroded steel and damaged wooden piles suffering from significant section loss [37]. Hawkswood [37] listed several cases of corroded steel piles successfully repaired using RC jackets including the 14 tubular steel piles (610 mm diameter) used in Cork, Ireland and the 84H steel piles used on a fishing jetty in Lunenburg, Canada. For repairing the damaged structure, steel angle reinforcement was welded at the required location prior to concrete encasement. On the other hand, steel jackets normally consist of steel angles or plates and batten with different thickness, width and spacing [38] have been mostly used for strengthening square or rectangular sections. They are relatively easier to install, and have smaller thickness in comparison with the RC jackets. Cement or epoxy mortar fills the gap between the jacket and column. Several studies have been conducted investigating the effectiveness of steel jackets for repairing and strengthening RC structures [39–43]. Abdel-Hay and Fawzy [14] repaired the damaged RC columns with steel jackets wherein the corrosion was simulated by eliminating the stirrups in the middle third of RC columns. The jacket was anchored to the column using 10 pieces of 6 mm diameter anchor bolts on each side and an injection plaster was used to fill the gap between the steel jacket and the retrofitted column. The results showed that the repaired columns failed by concrete crushing outside the strengthened part at load of at least 90% of the ultimate load of the original columns.

Repairing the damaged and old structures using traditional materials like timber, concrete and steel is effective to some extent, especially in the short term. However, the repair approaches are interrelated with various aspects such as material compatibility, load transfer, connections, effectiveness, future maintenance, repair-downtime and environmental conditions, among other factors. As an example, the effectiveness of splicing damaged wooden piles is compromised due to the improper bearing vertical load

transfer because of the gap in the splice between the surfaces of the two wooden pile portions [21]. Moreover, marine borers and shipworms enter through these gaps and attack the untreated wood. RC and steel jackets, on the other hand, are heavy and bulky, which enlarge the retrofitted members' size and reduce the free space of the structure. They also significantly increase the overall structural self-weight that affects the foundation and/or attracts more loads in seismic events [44]. Moreover, the anchorage of steel reinforcement for RC and steel jackets is a complex task. In the case of offshore structures, the production of the facility needs to be shut down during the so called "hot works" for safety reasons which significantly increases the total cost of welding repairs. In addition, steel jackets are not suitable for concrete structures in corrosive environments such as marine environments or a bridge subjected to de-icing salts [13]. Furthermore, repairing deteriorating structures using the same type of material that they were originally built with is impractical and ineffective in the long term because the repaired part will be subjected to the same condition that caused the deterioration to the original structure and the repair cycles may never end. More durable and reliable repair systems and materials with long-term effectiveness such as FRP composites are therefore warranted.

### 3. Prefabricated FRP composites repair systems

FRP composites offer unique benefits over conventional materials for strengthening and rehabilitation of civil infrastructure. In addition to their corrosion resistance characteristics, which is their primary feature, the ease of installation of the FRP composites makes them highly effective in addressing the drawbacks of conventional materials and repair practices like aggressive marine environments, limited access, self-weight and complexity of RC and steel jackets [45]. The availability in various forms including flexible thin sheets that can be wrapped around beams and columns is a remarkable advantage over rigid steel plates. Moreover, the superior properties of the FRP composites like lightweight, high strength, high fatigue capacity particularly for carbon-FRP, high impact strength, and durability [46], favoured it over the traditional repair techniques and qualified it for effective rehabilitating and strengthening applications to damaged RC and steel structures [47–49]. In addition to the strength requirements, FRP composites can also serve as a protective shield for the structural members against harsh environmental and weathering conditions such as chloride ions penetration, marine borers and waves which can

rapidly cause concrete to weaken and deteriorate [21]. These favourable properties of FRP composites led to their gaining worldwide acceptance and significant attention from both researchers and construction industries. FRP composites have been effectively utilised in restoring the structural strength of damaged wooden piers in marine wharves [21], rehabilitating steel bridges [23], retrofit of corroded and severely cracked RC bridge bents [31], seismic repair of bridge columns with severe concrete crushing, and longitudinal steel bars fracture and buckling [25,26], rehabilitation of severely damaged precast RC columns connected with grouted splice sleeves and epoxy-anchored headed steel bars [50] and enhancing the strength and ductility of RC structures [51–56]. Based on their manufacturing method, FRP repair/strengthening systems are classified into two groups: wet lay-up and prefabricated systems [57].

Many researchers have successfully demonstrated the effectiveness of external wet lay-up FRP wrapping in repairing and strengthening RC structures [58–62]. In a study conducted by Sen and Mullins [19] pre-impregnated wet lay-up FRP repair systems were used for emergency repair of underwater circular RC piles in Tampa Bay, Florida, USA. The access to the piles in the deep waters was provided by divers for single isolated piles, and a custom-designed, lightweight modular scaffolding system was assembled around the piles in the same bent. The evaluation conducted by the authors two years after the wrapping indicated that the repair was successful and can be adopted in future projects. Manalo et al. [49] showed that a prepeg CFRP system can effectively restore the original stiffness and load carrying capacity of I-shaped steel beams with simulated crack and 80% corrosion damage. Saafi and Asa [63] also followed the wet lay-up method to impregnate an E-glass jacket with epoxy to repair 30-year-old circular wooden poles in Alabama, USA. The wet lay-up FRP composite jacket was 5 mm thick and wrapped around the pole for a length of 850 mm at 2 m distance from the bottom. Cantilever bending tests showed that the repaired poles can restore the load capacity by more than 85%. These studies showed that wet lay-up FRP wrapping is an effective technique in repairing deteriorated structures. This technique is also preferable when urgent rehabilitation is required but demands good work quality in terms of preparing and installing the FRP jacket. Moreover, if the repair work is underwater, it will be much more difficult to execute, monitor and cure the wet lay-up systems, especially when more than one layer is required. There are also safety concerns in the styrene emission while preparing the jacket which restricts the full employment of this technique [64]. Therefore, the prefabricated systems have been a preferred technique in rehabilitating structures under water or in areas that are hard to access.

Prefabricated composite repair systems are manufactured at specialized plants and delivered to a site in ready for installation packages. These repair systems are preferable to the wet lay-up

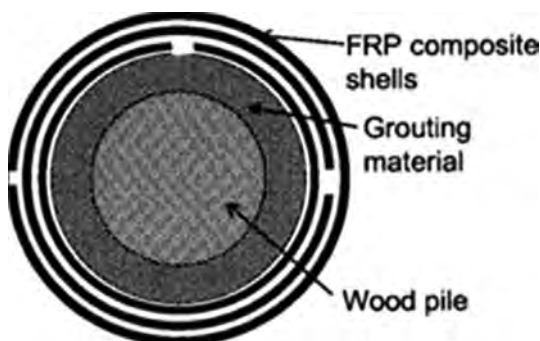


Fig. 4. Wood pile repair [21].

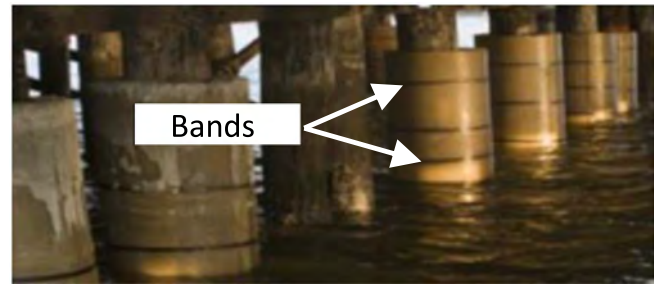


Fig. 5. Waterfront structure repair, New York [66].

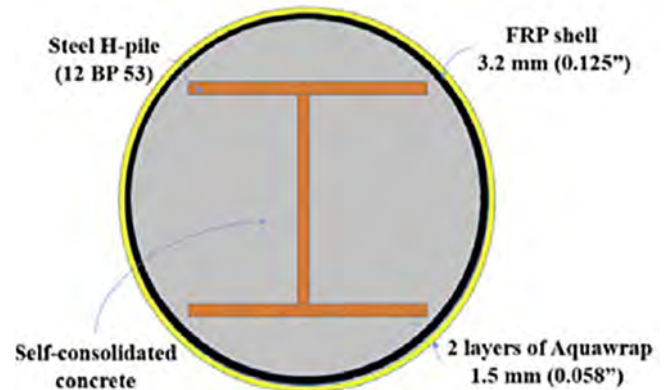


Fig. 6. Steel bridge pile repair [23].

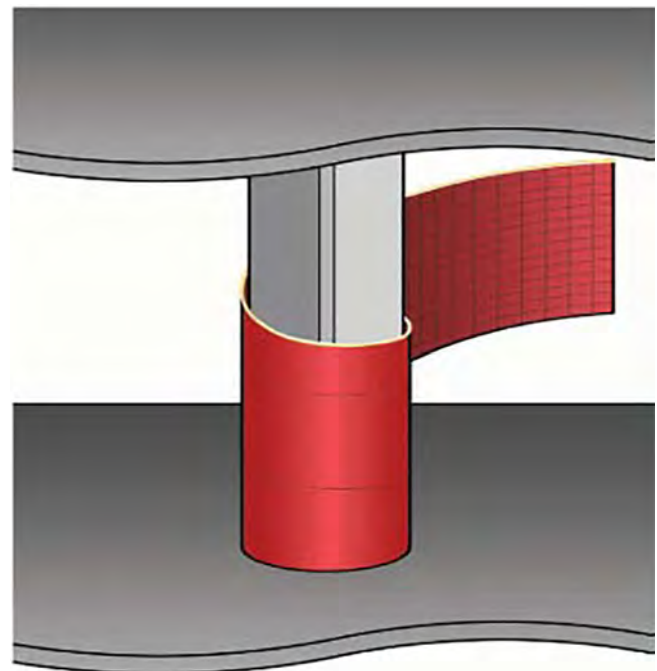


Fig. 7. PileMedic™ [67].

technique as they are produced under well controlled manufacturing conditions, and are easier, quicker and safer to install and require less onsite labour [64,65]. Prefabricated FRP jackets are becoming widely used for regular and under water structural repairs as they serve as a permanent formwork and protective shield. The gap between the FRP shell and the treated structural

member is filled with non-shrink grout or concrete. Several examples are available in the literature [21,23,66–68] regarding this technique and these will be discussed in detail in the following sections.

Lopez-Anido et al. [21] suggested the use of 3.3 mm thick pre-fabricated FRP composite shells as a repair system to protect and restore the structural integrity of circular damaged wooden piles in Portland Harbor, Maine, USA (Fig. 4). The proposed repair system comprised a minimum of two FRP prefabricated shells which were kept together by straps or temporary strips along the circumferential direction. Another prefabricated FRP repair system consisting of woven mat and chopped strand fabrics with single seam FRP shell was used to repair waterfront structures in New York City as shown in Fig. 5 [66]. In addition to the strength contribution, both systems served as an environmental protective shield to the core pile and a permanent formwork to the grout.

Vijay et al. [23] used both pre-cured FRP shells and prepreg fabrics to repair the corroded H-steel piles of East Lynn Lake Campground Bridge in Wayne County, West Virginia USA (Fig. 6). Self-consolidating concrete was used to fill the gap between the FRP shells and the H-steel piles where the FRP shell worked as a permanent formwork to the grout. The installation process for this repair system required the prefabricated FRP shells to be installed first before applying the prepreg fabrics which needed a few days to cure prior to grouting. Hence, extended installation time and high manpower costs were incurred in this practice. Ehsani [67] developed the FRP seamless jacket PileMedic™, which consists of thin and flexible fabric laminates up to 1500 mm wide for pile repairs. However, it did not serve as a formwork in the construction of columns or piers because of their spiral wrapping method as shown in Fig. 7. Beddiar et al. [68] used a GFRP prefabricated jacket consisting of three identical shells connected together by stepped lap joints with shrinkage-compensating cement mortar as infill between the shells and the square column. The experimental results demonstrated that the axial load capacity and ductility increased by 31% and 74%, respectively, compared to the unjacketed concrete specimens. However, this came at the expense of 100% increase in the cross sectional area. Karagah et al. [69] implemented a large-scale experimental study to demonstrate the structural performance of submerged corroded I-shaped steel bridge piles repaired using two different types of grout-filled FRP jackets. The first one consisted of two plies of prefabricated flexible CFRP wrapped around the piles and bonded using an underwater curing adhesive. The second type consisted of a two-layered FRP system wherein the first layer was fabricated using two plies of GFRP



Fig. 9. GFRP composite pile repair system [70].

installed around the pile using marine adhesive and screws, while the second layer consisted of one CFRP layer installed over the GFRP layer using a wet lay-up technique. The results showed that both repair systems were capable of restoring and enhancing the axial strength of the piles with the second type providing 11% higher enhancement than the first one.

Wu and Pantelides [25,26] proposed a rapid seismic repair method for RC bridge columns, which designed were designed under current codes, with minimal intervention. The repair method involves a CFRP cylindrical shell, epoxy-anchored headed steel bars, and steel collar with studs around the original column as shown in Fig. 8. The CFRP shell, consisting of unidirectional laminates in the hoop and vertical direction, encloses the headed bars and is filled with non-shrink concrete to shift the location of column plastic hinge. Vertical fibres were provided in the CFRP shell to increase tensile capacity of the shell in the axial direction to avoid the circumferential cracks [25,26,50]. Steel collar with shear studs improved the bond between original column and repair concrete to increase structural integrity of the whole CFRP “donut”. Fig. 9 shows a prototype of a GFRP composite pile repair system



Fig. 8. Seismic repair method [26].



Fig. 10. GFRP jacket [71].

that was successfully utilised for underwater repair trials of piles at the Missingham Bridge in Northern NSW, Australia in 2005 [70]. Fig. 10 depicts another FRP repair system with a tongue and groove joining system installed around bridge piles with metal screws being bolted through the joints. As shown in the summary of the existing prefabricated FRP repair systems presented in Table 1, the tongue and groove joining system with metal screws is the most common technique in the actual applications of the FRP repair system due to its ease and rapid fitment. However, the durability of the use of metal screws in the technique is always a concern as they do not have the same characteristics as the FRP shell in resisting the severe environmental conditions. The failure of the joining system results in opening of the jacket leading to its functional loss. Hence, the effectiveness of the prefabricated FRP composite jacket for repair of structures depends mostly on the joining technique as it is responsible to provide complete continuity for the repair system. Therefore, there is an urgent need to innovate an effective joining system for the prefabricated FRP repair system that can assure the structural continuity along the hoop direction.

#### 4. Factors affecting structural repair using prefabricated FRP repair system

Prefabricated FRP repair systems work by placing the flexible FRP shell around the degraded structure and then filling the gap between the shell and the repaired structure with a non-shrink grout infill. The long-term effectiveness of the repair system mainly depends on the durability of the FRP jackets which depends on their inherent properties. Hollaway [74] presented durability considerations to effectively utilize FRP composites in various environments. For example, aramid fibres are not recommended be used in alkaline and acidic environments and UV exposure while careful consideration is suggested when using glass fibres in alkaline environment due to the presence of silica in the glass. On the other hand, carbon fibres are resistant to the ingress of alkali or solvents, but experience galvanic corrosion. Thus, the ACI-Committee [57] introduced an environmental reduction factor

for FRP repair systems to account for the durability effects under different exposure conditions.

The structural effectiveness of the repair system is associated with several factors which have to be considered in the design of the repair system, including the conditions of the existing structures and the properties and dimensions of its components, i.e. FRP jacket, joining system and grouting system. The effect of these factors on the repair system is discussed as follows:

##### 4.1. Condition of the existing structures

The condition of a deteriorated structure and the extent of its damage are critical parameters for assessment before proceeding with any repair strategy. It is also important to consider the existing site and environmental conditions prior to selecting an appropriate repair technique.

###### 4.1.1. Environmental conditions

Structures in aggressive environments are susceptible to durability problems due to the external environmental attacks which affect their serviceability and structural reliability. Davis [75] classified the marine environment infrastructure (e.g. piles) into different zones: submerged (the part of pile extending from 0.3 m to 1.0 m below mean low tide to mud line), tidal (the part of pile extending between mean high tide and mean low tide which is subjected to wet-dry cycles), splash (the part of pile above the mean high tide where it is subjected to wetting by water drops) and atmospheric zones (the top part of the pile where it is subjected to minimal wetting by waves splash). The parts of structures located in the tidal region are considered to be the most critical members [76] since they are subjected to both physical and chemical attacks. Safedian and Ramezani-pour [77] also identified that the tidal and the splash zones are subjected to the most aggressive weathering attacks, which commonly cause reinforcement corrosion due to chloride ion ingress in the concrete [78]. Furthermore, the motion of waves and tides in the tidal zone cause physical collision, erosion and abrasion [79]. Steel structures in such environments are susceptible to section loss due to corrosion damage which degrades their structural performance [80,81]. For example, the East Lynn Lake Campground Bridge was narrowed to one traffic lane and then closed completely after finding steel section losses of up to 60% in its piles [23]. As another example, marine borers and organisms can cause extensive damage to wooden marine piles. In Portland Harbor, Maine, USA, several wooden piles were severely decayed due to the surrounding harsh environment and were classified as structurally deficient [21].

Aggressive soil and acid attacks are other types of harsh environments that cause significant structural degradation and loss of performance [82–86]. There are concerns about iron, steel and other metals being embedded in aggressive soils as they exhibit significant rates of corrosion. Montgomery [87] reported on another issue: severe sulphuric acid attack damaged the pile foundation of chemical plants located on the Atlantic coast of the USA, which resulted in up to 130 mm settlement of concrete columns. Concrete, however, would not have been seriously damaged by sulphate attacks if moderate sulphate resisting or highly sulphate resisting cement were to be used, depending on the extent of the exposure [88].

###### 4.1.2. Level of damage

Corrosion of steel reinforcement is the most substantial degrading problem faced by RC structures. It is responsible for concrete cracking, bond strength weakening, loss in steel cross-section, and loss of serviceability and structural functionality [89–96]. Manalo et al. [97] indicated that simulating 50% steel corrosion in circular RC columns of 1 m height and 250 mm diameter

**Table 1**  
Summary of FRP composite application in the laboratory and on real structures.

Reference	Description	Joining system	Level of Development	Advantages	Disadvantages
Lopez-Anido et al. [21]	Circular GFRP shells made of unidirectional E-glass layers (0° and 90°) and chop strand layer.	Two overlapping open shells strapped together.	R&D	Rapid installation Permanent formwork	Outer metal straps are susceptible deterioration which lead to jacket opening.
Van Erp et al. [70]	Circular GFRP composite pile repair system	Composite pins	Prototype	Rapid installation Permanent formwork	No continuity along the hoop
Williams [66]	Single seam circular GFRP jacket made up of chop strand and woven mat impregnated with epoxy resin.	Tongue and groove with metal screws	Application	Rapid installation Permanent formwork	Screws and outer bands are susceptible deterioration which lead to jacket opening.
Ehsani [67]	Thin, flexible and continuous GFRP jacket wrapped spirally along the pile.	Seamless jacket	Application	Rapid installation	This system cannot serve as a form work due to its wrapping technique.
Strong-Tie [71]	Round, H-pile, square/rectangular or octagonal GFRP jacket	Tongue and groove with metal screws	Application	Rapid installation Permanent formwork Various shapes	Screws are susceptible deterioration which lead to jacket opening.
Beddiar et al. [68]	Three identical GFRP segment bonded together to form a cylindrical shell.	Bonded stepped lap joint	R&D	Permanent formwork	Complex and poor continuity along the hoop
Vijay et al. [23]	Circular GFRP shells and prepreg GFRP fabrics for wrapping	GFRP prepreg fabrics wrapping	Application	Permanent formwork	Long installation time and high labour cost
Five Star [72]	Five Star PileForm round, H-pile or square/rectangular GFRP jackets	Tongue and groove with metal screws	Application	Rapid installation Permanent formwork Various shapes	Screws are susceptible deterioration which lead to jacket opening.
FiberSystems [73]	Combined carbon and glass FRP circular jacket	Bonded overlapping joint	Application	Rapid installation Permanent formwork	Poor continuity along the hoop
Karagah et al. [69]	CFRP or combined CFRP and GFRP jacket where the CFRP layer installed over the GFRP shell using wet lay-up technique.	Bonded overlapping joint	R&D	Rapid installation Permanent formwork	Poor continuity along the hoop
Wu and Pantelides [25,26]	CFRP cylindrical shell "donut" and epoxy-anchored headed steel bars	Bonded overlapping joint	R&D	Seismic repair Permanent formwork	Limited to columns' ends repair due to the headed steel bars anchorage.

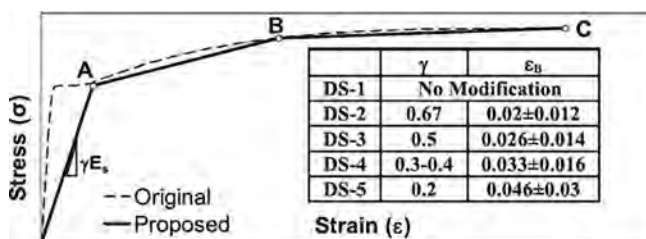


**Fig. 11.** Stress–strain curves.

resulted in 56% reduction in the axial load capacity due to the loss in the area of steel which resulted in a minor eccentricity effect. Experiments by Torres-Acosta et al. [94] showed that the increase in the depth of rebar corrosion damage was the most significant parameter in reducing the flexural strength of corroded RC beams as it initiates localised failure. The exposed reinforcement due to concrete cover spalling affects the structural performance of the damaged member because the reinforcement loses its structural integrity and composite action with concrete. A study carried out by Cairns and Zhao [98] showed that in a rectangular beam with no concrete cover at the bottom, 50% loss in flexural capacity was found due to bond strength loss between the steel and the concrete. In another study, Vosooghi and Saiidi [30] developed a

trilinear stress–strain relationship (Fig. 11) to estimate the existing strain in the longitudinal bars of damaged columns based on five visual damage states (DS) that were defined as follow: DS-1 (flexural cracks), DS-2 (minimal spalling and possible shear cracks), DS-3 (extensive cracks and spalling), DS-4 (visible lateral and/or longitudinal reinforcing bars), and DS-5 [compressive failure of the concrete core edge with only a few longitudinal bars may exhibit slight buckling (imminent failure)]. A reduction factor was used, based on the damage state, to modify the original slope of the first branch of Fig. 11. In the same figure, Point A represents the yield stress and the strain associated with the modified stiffness, Point B is associated with the maximum strain in the longitudinal steel at a given damage state, and Point C is the modified ultimate point accounting for strain rate effect. Another important factor to consider in the repair is the bond slip effects of the existing steel bars if they were still embedded in the damaged concrete [99], or directly interact with new and confined concrete [100]. Harajli [99] developed a bond-slip relationship predicting the bond degradation response of bond-critical regions in reinforced concrete members when retrofitted using external FRP jackets including the effects of steel bar diameter, ratio of concrete cover and concrete compressive strength. Moreover, Wu and Pantelides [100] incorporated the effect of bond-slip in the model they developed to accurately simulate the seismic performance of repaired column-to-cap beam/footing connections using CFRP jacket.

Steel structures, and even galvanised steel after the consumption of galvanic protection, will corrode, when exposed to harsh environments, and their strength capacity is reduced accordingly. Beaulieu et al. [101] reported that 25% and 40% simulated corrosion in steel angle members resulted in a decrease by 24% and 42%, respectively, of their compressive strength due to the loss in the cross sectional area. For timber structures, wooden piles with more than 50% loss in their cross-sectional area need to be replaced as it is hard to estimate the residual strength capacity of degraded structures and decide when they are no longer safe [102]. Pizzo et al. [103] observed an average reduction of 70% in residual compressive strength of decayed wooden piles due to the mass loss and the alteration in chemical composition of the wood. These results are in agreement with those established by Klaassen [104] and Schniewind [105]. The reparability threshold is driven by the results of the initial repair design where the residual strength of the original section is assessed and the additional strength from the FRP repair system is calculated. The summation of both is then compared with the design load. The economic aspect is also considered as another criteria for the repair. An appropriate, cost-effective, reliable, and safe repair system is therefore needed to restore the capacity of such deteriorating structures to an acceptable level of service.

#### 4.2. FRP composite jacket

Thickness, fibre type and fibre orientation are the three main material parameters that influence the effectiveness of an FRP jacket system. This section discusses how each parameter affects the behaviour of an FRP jacket.

##### 4.2.1. Thickness

The FRP jacket thickness has substantial effects on the strength and ductility of repaired columns. In addition, it is directly related with the exerted confinement pressure of the FRP jacket as the confinement effectiveness increases with higher thickness [106]. Berthet et al. [107] and Li et al. [108] indicated that FRP wraps with higher thickness significantly enhance the strength and ductility of wrapped concrete columns. A study conducted by Hajsadeghi et al. [51] showed that concrete columns wrapped with five FRP sheets had higher axial stress and axial strain capacity in comparison with the columns wrapped with one or three layers because of the increase in the confining pressure with the increase in thickness. Other research by Parvin and Jamwal [109] revealed that the axial strength increased with the increase of the wrap thickness for all FRP-wrapped columns. On the other hand, the average hoop strain decreases as the number of sheets or the thickness of FRP jackets is

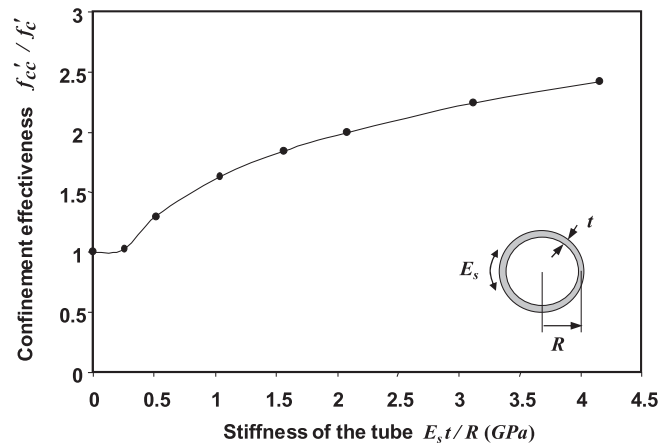


Fig. 13. Confinement effectiveness of FRP tubes with various stiffness [115].

increased because they are inversely related [110,111]. This effect was also demonstrated by Fam and Rizkalla [112] as shown in the Figs. 12 and 13. Increasing the FRP jacket thickness has the same effect on steel and timber structures because the exerted confining pressure is what matters the most [63,113]. However, for hollow steel tubes, Teng et al. [113] indicated that once the thickness of jacket reaches a specific threshold for which the dominant behaviour is the inward buckling deformations of the hollow steel tube, an additional increase in the thickness of jacket will not result in noteworthy further benefits as the jacket does not provide good resistance to inward buckling deformations [113].

Regarding the thickness of prefabricated and ready-to-install FRP jackets, there is no specified upper limit value since they are manufactured in specialised plants as one integral part. However, there is a limitation on the thickness of multilayer FRP laminate strengthening system as additional layers increase the number of potential failure modes because failure can occur in the adhesive between each layer which increases the risk of failure within the FRP. For example, VicRoads [114] limits the layers of FRP strengthening system to maximum of 2 layers for pultruded plates, and 3 layers for FRP fabrics.

##### 4.2.2. Fibre type and orientation

The magnitude of the confining stresses exerted by the prefabricated FRP jacket is the main factor that affects the repair system effectiveness, and it is highly influenced by the fibres' type and orientation regardless of the core material type whether it is concrete, steel or timber [116–119]. For example, glass fibres are more cost competitive than carbon fibres, but the latter have superior characteristics, while aramid fibres have lower compressive load capacities compared to other fibre types [52]. Fibres are oriented along the load direction to resist axial loads. However, in prefabricated FRP jackets, fibres are oriented in the circumference direction to produce higher lateral stresses which, in return, results in higher axial load capacity. Moreover, additional fibres with an inclination of various angles with respect to the hoop and longitudinal directions are used to provide resistance against multi-axial strains, increase the structural integrity of the whole FRP shell and behave in a more ductile manner at failure [26,51]. Finally, increasing the confining pressure significantly increases the ductility enhancement ratio [106,107,120].

#### 4.3. Joining system

Many techniques were adopted to join the jacket's ends and encapsulate the damaged member. The type of joining system

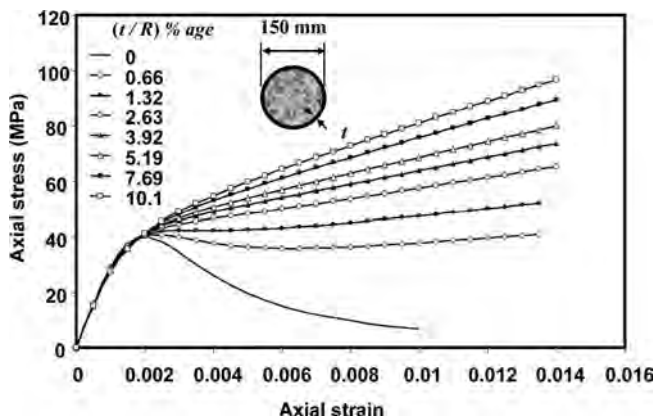
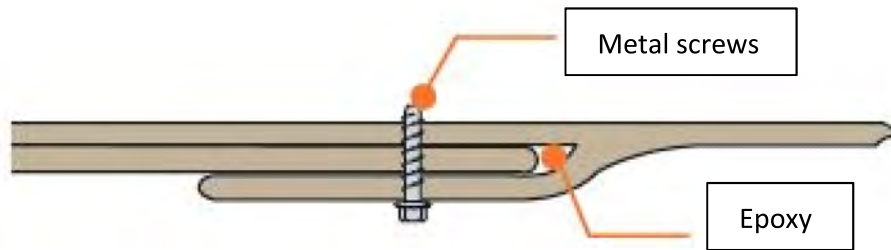
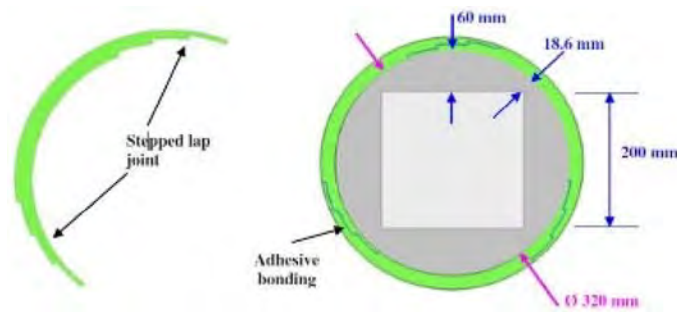


Fig. 12. Stress–strain curves of confined concrete with FRP tubes of various thickness [115].



a) Tongue-and-groove joining technique [121]



b) Stepped lap [68]

Fig. 14. Joining systems.

can affect the durability and the utilisation limit of the repair system. For example, the joint will have different capacities to resist the weathering and environmental attack if it was made from materials different to that of the jacket body. The premature jacket failure limits the full utilisation of the FRP repair system. Many joining systems were proposed and designed in a way to address the aforementioned concerns; however, their performances varied significantly from each other.

In the repair system proposed by Lopez-Anido et al. [21], the splits in FRP shells were aligned away from each other to avoid a weakness line along the entire height of the shell. The interior surface of each shell was glued to the outer surface of the next shell using epoxy. Circumferential metal straps or temporary bands were then used to hold the shells together and achieve the structural restoration. As shown in Fig. 14a, slip-joint/tongue-and-groove is another popular joining technique to connect the ends of the FRP jacket [121]. Epoxy and self-taping metal screws were also used to hold the tongue in the groove and increase the reliability of the joint. This technique was adopted to repair waterfront structures in New York City [66]. In addition, steel bands were used in the adopted repair system to hold the jacket and contain the infill. The metal screws damage the FRP shell and affect the stress flow by developing stress concentration regions which eventually affect the fatigue resistance and the lifespan of the FRP shell. Another method is that used by Vijay et al. [23] where additional water-curable GFRP prepregs were applied on the outer surface of the FRP shell to keep jacket ends together and prevent them from opening. An alternative seamless FRP repair system was proposed by Ehsani [67] consisted of flexible FRP laminates that can be spirally wrapped around the damaged member. Finally, a stepped lap joint technique was proposed and used by Beddiar et al. [68] to join the FRP jacket ends together (Fig. 14b). Each step was measured to be 40 mm in length to provide sufficient overlapping for the jacket ends in addition to being glued together using epoxy.

There are concerns about the capability of commercially available prefabricated FRP repair systems to provide effective structural continuity and actual confinement in the hoop direction. For instance, the joint and the bands consisting of metallic material are prone to corrosion. Moreover, using extra FRP layers and/or epoxy increases the installation time as they require additional time to cure, which increases the installation/labour cost. These limitations can be overcome by integrating an innovative and sustainable joining system with the FRP jacket.

#### 4.4. Grouting system

Studies on the effect of grouting systems on the effectiveness of prefabricated FRP repair systems are limited. However, the grout is a key player in transferring the stresses between the damaged core and the outer FRP shell and developing the composite action within the repair system. The functionality of the grout, with regard to load transferability and effective employment of the FRP jacket, is dependent on its compressive strength and modulus of elasticity [23,122,123]. Grout thickness, on the other hand, is insignificant in the case of a grout with stiffness higher than 20 GPa, while in the case of a low stiffness grout, the thinner grout is better than thicker grout for bringing together an effective composite action among different components of the jacket system, thus producing lower strains in the core [124]. Mohammed et al. [122] revealed that the behaviour of the prefabricated FRP jacket is strongly affected by the compressive strength and the modulus of elasticity of the infill. Localised failure was observed in the FRP repair system due to the brittle cracking and crushing behaviour of the cementitious and epoxy grouts while the progressive failure of the concrete infill resulted in effective utilisation of the high strength characteristics of the FRP repair system. The authors also concluded that the high compressive strength of the grout infill restrained its ability to transfer the stresses uniformly around the

FRP jacket due to increased brittleness. The numerical analyses conducted by Sum and Leong [125] showed that increasing the epoxy grout stiffness resulted in better stress transfer and more effective utilisation of the composite sleeve as a repair system for high pressure steel pipelines due to the enhanced composite action of the repair system. In another study, Deb and Bhattacharyya [126] highlighted the importance of the bond strength between the infill and the FRP shell as it can influence the effectiveness of the prefabricated FRP jacket because any discontinuity or voids presence would induce non-uniform stresses in the FRP shell leading to premature failure.

The grout is a vital part in the FRP repair system as it provides a smooth surface for the FRP shell and refill of the lost profile of the damaged structure which will assure a full contact among the components of repair system [123]. In addition, the grout infill is necessary when the original structure requires shape modification, i.e. from square or rectangular to a circular section for more effective confinement [127–129]. In order to eliminate separation from the FRP shell due to shrinkage, Fam and Rizkalla [115] used expansive cement in the concrete fill to fully engage the tube from the onset of applying the system through some active confinement. It is important therefore that the effect of these parameters are considered in the design of a prefabricated FRP repair system.

**5. Existing models to evaluate effectiveness of prefabricated FRP repair systems**

It is well established that using an FRP jacket to laterally confine the concrete significantly increases its strength and ductility. Over the last two decades, substantial amounts of research have been carried out to understand and model the axial behaviour of FRP-confined concrete. As a result, about 80 stress–strain models have been developed [120,130] considering the various shapes of columns, i.e. square, rectangular, circular and elliptical [131,132]. The majority of the available models can be categorised into two groups as suggested by Lam and Teng [120]: (a) design-oriented models [133–142], and (b) analysis-oriented models [115,143–151]. In design-oriented models, the compressive strength, ultimate strain and stress–strain behaviour are predicted using closed-form equations based directly on the interpretation of experimental results. In analysis-oriented models, stress–strain curves are generated using an incremental numerical procedure to capture the interaction between the FRP jacket and concrete core. They are, therefore, more appropriate for incorporation in non-linear finite element analysis in computer-based numerical analysis software [120]. In contrast, design-oriented models are specifically suitable for direct implementation in design calculations as they offer an approach that is familiar to engineers for calculating the strength of FRP-confined RC structures. Hence, the design-oriented models are widely adopted in repair system applications.

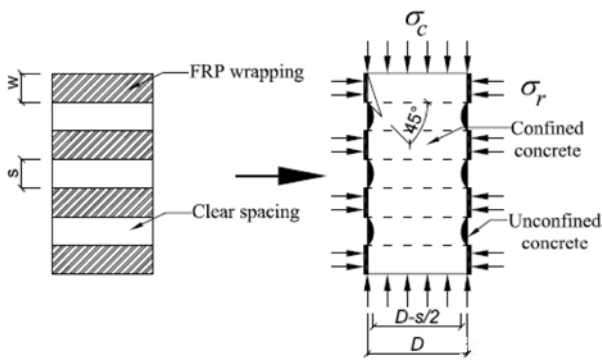
Most of the previous research work on RC columns retrofitting using FRP composites, focused on columns wrapped fully with FRP jackets to assure the confinement continuity along their longitudinal axes [111,152]. Only a small number of studies investigated columns wrapped partially with FRP composites yet also showed an increase in strength and ductility, in comparison with equivalent unconfined columns [153–157]. However, concrete columns partially confined with FRP composite are less efficient in nature than fully-confined columns due to the presence of the unconfined areas along their heights (Fig. 15a). Mander et al. [158] proposed a model to determine the effective confining pressure on the concrete core, and it has been utilised in several subsequent studies [153,159,160]. Fig. 15a shows the effectively confined areas of the concrete core where the confining pressure is assumed to be fully developed due to arching action. The arching effect is described with assumed second-degree parabola with initial slope of 45°. Hence, a confinement effective coefficient ( $k_e$ ) is introduced to consider the partial wrapping effects as shown in Eq. (1):

$$k_e = \frac{A_e}{A_c} = \left(1 - \frac{s}{2D}\right)^2 \tag{1}$$

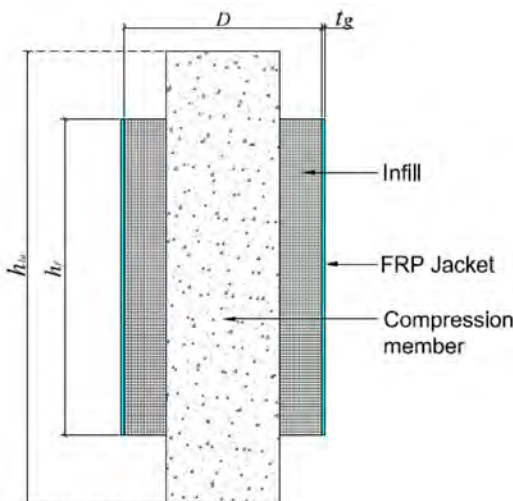
where  $A_c$  and  $A_e$  are the cross-sectional area and the effectively confined concrete area respectively;  $s$  is the clear spacing between two FRP strips and  $D$  is the diameter. Consequently, the active confining pressure ( $\sigma_{l,a}$ ) on the columns wrapped partially with FRP composites can be calculated as stated in Eq. (2):

$$\sigma_{l,a} = \frac{2t_g E_f \epsilon_{hu}}{D} \times k_e \tag{2}$$

where the first term accounts for the jacket properties as  $t_g$  is the nominal thickness of FRP jacket;  $E_f$  is the elastic modulus of FRP; and  $\epsilon_{hu}$  is the rupture strain of FRP in the hoop direction. However, since the partial confinement in most pile repair systems is carried out using one large FRP segment as mentioned in the existing literature, Mohammed et al. [161] proposed a confinement effective coefficient ( $h_j/h_{tu}$ ) considering the height of the FRP jacket ( $h_j$ ) and the total height of the column ( $h_{tu}$ ) instead of the confined area (Fig. 15b) to predict the maximum axial load of the damaged RC concrete columns repaired using prefabricated FRP jackets and



a) Concrete column partially confined with FRP strips [153]



b) Concrete column partially confined with one FRP segment [161]

**Fig. 15.** Confinement mechanism.

cementitious infill. The active confining pressure on the concrete columns wrapped partially with one FRP segment was calculated as stated in Eq. (3):

$$\sigma_{l,a} = \frac{2t_g E_f \varepsilon_{hu}}{D} \times \frac{h_f}{h_{lu}} \quad (3)$$

Moreover, the model developed by Mohammed et al. [161] considered the level of damage in the original structure while predicting the axial strength of the repaired column as detailed in Eq. (4)

$$\sigma_{cc} = \sigma_{co} + \left( \frac{5t_g E_f \varepsilon_{hu}}{d_{gi}} \times \frac{h_f}{h_{lu}} - 1.3\sigma_{co} \right) \times \left[ 1.22 \left( \frac{A_{ef}}{A_{undamaged}} \right) - 1.28 \right] \quad (4)$$

where  $\sigma_{cc}$  and  $\sigma_{co}$  are the predicted and the original compressive strength of the column, respectively, and  $A_{ef}$  and  $A_{undamaged}$  are the normalised effective area and the original area, respectively. Moreover, the jacket strain at the moment of joint failure was considered, while the grout was considered to be of the same material type as that of the core. This model showed a close agreement between the experimental and the predicted values of the repaired RC columns. However, the developed theoretical model might be only applicable to the prefabricated FRP repair system investigated in that research and further verification and/or calibrations are recommended for other different types of repair systems with different core materials, i.e. steel or timber.

Finally, for the steel structures, there are several models available to predict their strength and behaviour when strengthened with FRP wrapping [113,162–165], but there are no theoretical models to predict the behaviour and/or strength capacity of damaged steel structures repaired with prefabricated FRP jackets, and similarly for timber structures. Hence, further theoretical investigation in the area of repairing steel and timber structures using prefabricated FRP repair system is recommended.

## 6. Discussion and future research

The damage level of existing structures is closely associated with the severity of the surrounding environmental conditions. The highest level of damage is found at the tidal zones as those areas are subjected to both physical (waves) and chemical attacks (chloride ion ingress). RC and steel jackets are commonly used to repair these damaged structures despite the fact that they are heavy and bulky repair systems. They also significantly increase the size and weight of the retrofitted member which is not desirable, especially during seismic events, as they tend to attract higher loads due to their increased rigidity [44]. Furthermore, using the same original material for repair with the presence of the same environment will cause similar damage again and the repair cycle may never end. Hence, more research is being conducted to use the prefabricated FRP composite jackets in structural repair to overcome the drawbacks of using traditional materials in a repair system.

The effectiveness of the prefabricated repair system depends on the properties of the jacket (thickness, fibre type and orientation) and its joining system to maintain the jacket continuity around the damaged member. The confinement effectiveness increases with the increase of the jacket's thickness as the exerted confinement pressure is higher for thicker jackets [106]. Carbon fibres are also used when higher effectiveness is required because they have superior properties compared to those of glass and aramid fibres, and they are oriented along the circumference axis [52]. The grout, on the other hand, is essential to connect the repair system components by transferring the loads between the damaged core and the composite FRP shell. The grout's compressive strength and modulus of elasticity [23,122,123] are the two critical mechan-

ical properties that affect its functionality in terms of load transferability and effective utilisation of the FRP system. High compressive strength grout reduces the repair system effectiveness as it has limited capacity in transferring the load uniformly due to the increased brittleness. Further research considering various types of cost-effective grouts with a different range of properties should be conducted to optimise the design and utilisation of the repair system.

Interestingly, the original compressive strength of the core material can affect the strength gain of the confined structure. The very low strength confined concrete experience severe crushing under axial load [122]. In the developing countries, the very low strength concrete is commonly used in RC structures where it should be noted that the concrete core can be significantly damaged without any remarkable deformation in FRP jacket which will not result in any additional axial load carrying capacity for the repaired column despite the use of confining jackets. For normal strength confined cores (20–50 MPa), the strength gains depend only on the confinement pressure generated by FRP jackets and it increases with higher confinement pressure. In case of high strength cores, the strength gain is a function of both the confinement ratio and the maximum compressive strength of the core. The strength gain, however, decreases marginally with the increase in the compressive strength of the core. In the same way, the hoop strain capacity of the FRP shell declines as the core's compressive strength increases. The main reason for the decline is the high material brittleness which increases with the core compressive strength regardless of its type i.e., concrete, steel or timber. In concrete, the increased brittleness drives the micro-cracks to be developed in heterogeneous manner which is considered the main reason for this deficiency [110], while in steel and timber, the increased brittleness decreases the Poisson's ratio effects and more internal stresses will be generated resulting in local failure of the core and consequently of the FRP jacket. Moreover, the original shape of the core structure can affect the overall behaviour of the repaired structure as several studies showed that the confinement mechanism of prefabricated FRP shells is less competent for square/rectangular columns in comparison with circular columns [68,100,130]. Prefabricated FRP composite jackets have an excellent in-plane tensile strength but, as they are quite thin, possess relatively small out-of-plane bending strength. Hence, the tensile hoop stresses in the composite jacket generate confining pressure that uniformly confines the whole area of a circular column. At the same time, non-uniform confining pressures are exerted by the prefabricated FRP jackets onto square/rectangular cross sections. Concentrated confining pressures are generated at the corners of square/rectangular columns rather than on the sides because confining pressures on the sides result from the flexural behaviour of the composite shell rather than its behaviour in tension [58]. Nevertheless, there are concerns about the ability of the commercially available prefabricated FRP repair systems to provide effective structural continuity and actual confinement in the hoop direction. These concerns have motivated the development of a prefabricated FRP repair system with an easy-fit and self-locking mechanical joining system (Fig. 16). The novel joining system consists of two interlocking edges and a locking key to provide a uniform force distribution along the entire height of the joint. This joint design was inspired by the way in which clams attach themselves to rock ledges using anchors through hundreds of small filaments. These filaments can produce a strong hold when their strength is combined (Fig. 16b).

Manalo et al. [64] identified the most effective joint materials that can provide a scenario of structural continuity in the hoop direction and effective confinement to the repaired structure. Mohammed et al. [161] conducted a large-scale experimental investigation to evaluate the effectiveness of the novel FRP repair

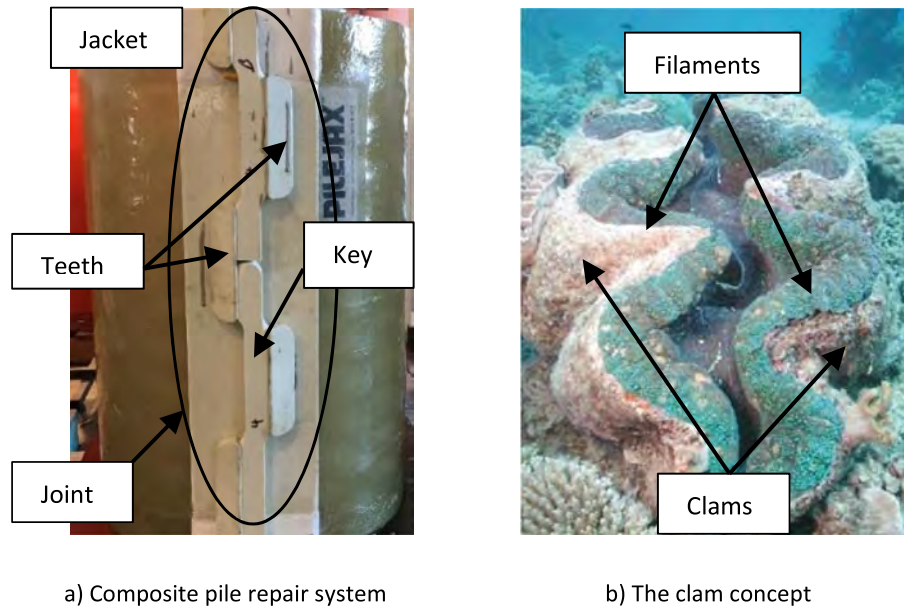


Fig. 16. The prefabricated composite pile repair system.



Fig. 17. Bridge piles repaired with FRP jacket [166].

system in repairing RC concrete piles. Concrete columns with simulated steel corrosion and concrete cover damage were repaired with an FRP jacket that partially covered the columns' height. The gap between the pile and the jacket was filled with grout prior to axial compressive loading of the test specimens. The compression testing results showed that FRP jacket could restore the stiffness and the axial strength capacity of the damaged columns to the original levels of the undamaged columns [161]. This repair system has been successfully used to rehabilitate a road bridge located at the Gold Coast in Queensland, Australia (Fig. 17). It was chosen over other rehabilitation jackets for its benefits: cost-effectiveness, rapid fitment, safety, and ease of installation [166]. Mohammed et al. [161] however recommended further modifications on the current joining system design to fully utilise the jacket capacity and expand the application of the prefabricated repair system to strengthening situations.

Important parameters such corrosion level, concrete cover loss, shape, grout infill properties, jacket thickness and the integrity of the joint should be taken into consideration while designing and constructing using the prefabricated FRP repair system. The cost effective prefabricated composite jacket is being further explored

and investigated with a focus on developing the next generation of efficient and reliable structural composite repair methods. The current model for damaged RC columns repaired with prefabricated jacket can be developed further to include additional factors like the type of grouting system and the degree of damage within the core structure.

## 7. Conclusions

This paper critically reviews the existing jacketing techniques to repair and strengthen existing damaged or deteriorating infrastructure. It focuses on prefabricated FRP composite jackets and identifies the parameters that affect the effectiveness of this type of repair system. From this critical review, the following conclusions and recommendations can be drawn:

- Repairing the damaged structures using either concrete or steel jackets or timber splicing is impractical in infrastructure exposed to aggressive environments. Using these conventional materials will lead to never-ending repair cycles as they are subjected to the same environment which caused damage to the existing structure.
- FRP composite jacketing systems offer superior properties in terms of corrosion resistance, lightweight and durability compared to conventional repair systems and are compatible with steel, concrete and timber structures.
- Prefabricated FRP composite repair systems are preferable to the wet lay-up as the former systems are easier, quicker, safer to install, require fewer workers on site, lead to less resource wastage and have higher quality as they are manufactured under well controlled conditions.
- The design of an effective joint is key to providing structural continuity for prefabricated FRP composite jackets. The joining schemes should offer a composite repair system that is easy, quick and safe to install, and can be easily implemented for prefabricated FRP repair systems.
- The effectiveness of the prefabricated FRP composite jackets is governed by the thickness and orientation of the fibres within the jacket, the type and properties of infill grout, and the level

of damage and shape of the existing structures. Understanding the effects of these design parameters will lead to an optimal and safe design of prefabricated FRP jacket repair systems.

- Available models to predict the strength and behaviour of strengthened structures with FRP composite jackets do not account for the level of damage in the existing structures. The development of numerical and/or analytical models that systematically consider the effect of key parameters upon the overall response of repaired structures is needed to achieve a reliable and safe repair system.

From the above findings, the prefabricated composite jacket with an innovative joining system can be a game changer in the construction industry and can breathe new life into key infrastructure. The low cost-to-performance benefits of this type of repair system should be fully explored and its contribution to the structural capacity of the repaired structure should be determined. Next generation joining schemes with FRP prefabricated systems can offer a rapid and effective repair solution for deteriorating and structurally deficient structures.

### Declaration of Competing Interest

The authors declare that they have no known competing financial interests or personal relationships that could have appeared to influence the work reported in this paper.

### Acknowledgements

The authors gratefully acknowledge Joinlox Pty Ltd., Australia for the financial, materials, and technical support in conducting this study. The authors are also grateful to the Innovation Connections Fund given by the Australian Government for the successful implementation of this research project. The second author acknowledges the scholarship granted by the Australian Government Endeavour Executive Leadership Award to undertake his professional development at the Centre for Integration of Composites into Infrastructure (CICI), West Virginia University, Morgantown, USA.

### References

- [1] X. Shi, N. Xie, K. Fortune, J. Gong, Durability of steel reinforced concrete in chloride environments: An overview, *Constr. Build. Mater.* 30 (2012) 125–138.
- [2] S.A. Mangi, M.H. Wan Ibrahim, N. Jamaluddin, M.F. Arshad, S. Shahidan, Performances of concrete containing coal bottom ash with different fineness as a supplementary cementitious material exposed to seawater, *Eng. Sci. Technol. Int. J.* 22 (3) (2019) 929–938.
- [3] A. Shayan, A. Xu, Realising 100-year bridge design life in an aggressive environment: review of the literature, 2016.
- [4] G. Nkurunziza, A. Debaiky, P. Cousin, B. Benmokrane, Durability of GFRP bars: A critical review of the literature, *Prog. Struct. Mat. Eng.* 7 (4) (2005) 194–209.
- [5] M. Cassidy, J. Waldie, S. Palanisamy, A Method to Estimate the Cost of Corrosion for Australian Defence Force Aircraft, (2015).
- [6] M. Jumaat, M. Kabir, M. Obaydullah, A review of the repair of reinforced concrete beams, *J. Appl. Sci. Res.* 2 (6) (2006) 317–326.
- [7] B.J. Bett, R.E. Klingner, J.O. Jirsa, Lateral load response of strengthened and repaired reinforced concrete columns, *Struct. J.* 85 (5) (1988) 499–508.
- [8] S. Dritsos, C. Taylor, K. Vadoros, Seismic strengthening of reinforced concrete structures by concrete jacketing, *Proceedings of the 7th International Conference on Structural Faults and Repair*, 1997, pp. 391–402.
- [9] U. Ersoy, A.T. Tankut, R. Suleiman, Behavior of jacketed columns, *Struct. J.* 90 (3) (1993) 288–293.
- [10] M.M. Kassem, F. Mohamed Nazri, E. Noroozinejad Farsangi, On the quantification of collapse margin of a retrofitted university building in Beirut using a probabilistic approach, *Eng. Sci. Technol. Int. J.* (2019).
- [11] R. Su, L. Wang, Axial strengthening of preloaded rectangular concrete columns by precambered steel plates, *Eng. Struct.* 38 (2012) 42–52.
- [12] J. Garzón-Roca, J. Ruiz-Pinilla, J.M. Adam, P.A. Calderón, An experimental study on steel-caged RC columns subjected to axial force and bending moment, *Eng. Struct.* 33 (2) (2011) 580–590.
- [13] J. Li, J. Gong, L. Wang, Seismic behavior of corrosion-damaged reinforced concrete columns strengthened using combined carbon fiber-reinforced polymer and steel jacket, *Constr. Build. Mater.* 23 (7) (2009) 2653–2663.
- [14] A.S. Abdel-Hay, Y.A.G. Fawzy, Behavior of partially defected R.C columns strengthened using steel jackets, *HBRC J.* 11 (2) (2015) 194–200.
- [15] İ. Demir, S. Güzelkücü, Ö. Sevim, Effects of sulfate on cement mortar with hybrid pozzolan substitution, *Eng. Sci. Technol. Int. J.* 21 (3) (2018) 275–283.
- [16] Y.J. Kim, State of the practice of FRP composites in highway bridges, *Eng. Struct.* 179 (2019) 1–8.
- [17] E. Guades, T. Aravinthan, M. Islam, A. Manalo, A review on the driving performance of FRP composite piles, *Compos. Struct.* 94 (6) (2012) 1932–1942.
- [18] L.C. Hollaway, J.-G. Teng, *Strengthening and Rehabilitation of Civil Infrastructures using Fibre-Reinforced Polymer (FRP) Composites*, Elsevier, 2008.
- [19] R. Sen, G. Mullins, Application of FRP composites for underwater piles repair, *Compos. B Eng.* 38 (5) (2007) 751–758.
- [20] F. Faleschini, J. Gonzalez-Libreros, M.A. Zanini, L. Hofer, L. Sneed, C. Pellegrino, Repair of severely-damaged RC exterior beam-column joints with FRP and FRM composites, *Compos. Struct.* 207 (2019) 352–363.
- [21] R. Lopez-Anido, A.P. Michael, T.C. Sandford, B. Goodell, Repair of wood piles using prefabricated fiber-reinforced polymer composite shells, *J. Perform. Constr. Facil.* 19 (1) (2005) 78–87.
- [22] A.C. Manalo, A.A. Mohammed, G. Maranan, in: *Novel Composites Jacket for Repair of Concrete Columns*, Special Publication 327, 2018, p. 12.
- [23] P. Vijay, P.R. Soti, H.V. GangaRao, R.G. Lampo, J.D. Clarkson, Repair and Strengthening of Submerged Steel Piles Using GFRP Composites, *J. Bridge Eng.* (2016), 04016038.
- [24] A.A. Mohammed, A.C. Manalo, G.B. Maranan, M. Muttashar, Y. Zhuge, P. Vijay, J. Pettigrew, Effectiveness of a novel composite jacket in repairing damaged reinforced concrete structures subject to flexural loads, *Compos. Struct.* (2019), 111634.
- [25] R.-Y. Wu, C.P. Pantelides, Rapid seismic repair of reinforced concrete bridge columns, *ACI Struct. J.* 114 (5) (2017) 1339.
- [26] R.-Y. Wu, C.P. Pantelides, Rapid repair and replacement of earthquake-damaged concrete columns using plastic hinge relocation, *Compos. Struct.* 180 (2017) 467–483.
- [27] R.-Y. Wu, C.P. Pantelides, Seismic evaluation of repaired multi-column bridge bent using static and dynamic analysis, *Constr. Build. Mater.* 208 (2019) 792–807.
- [28] R.D. Iacobucci, S.A. Sheikh, O. Bayrak, Retrofit of square concrete columns with carbon fiber-reinforced polymer for seismic resistance, *Struct. J.* 100 (6) (2003) 785–794.
- [29] A. Balsamo, A. Colombo, G. Manfredi, P. Negro, A. Prota, Seismic behavior of a full-scale RC frame repaired using CFRP laminates, *Eng. Struct.* 27 (5) (2005) 769–780.
- [30] A. Vosoghi, M.S. Saiidi, Design guidelines for rapid repair of earthquake-damaged circular RC bridge columns using CFRP, *J. Bridge Eng.* 18 (9) (2012) 827–836.
- [31] C.P. Pantelides, J. Gergely, Carbon-fiber-reinforced polymer seismic retrofit of RC bridge bent: Design and in situ validation, *J. Compos. Constr.* 6 (1) (2002) 52–60.
- [32] Ö. zğür Yurdakul, Ö. Avşar, Structural repairing of damaged reinforced concrete beam-column assemblies with CFRPs, *Struct. Eng. Mech.* 54 (3) (2015) 521–543.
- [33] Ö. Yurdakul, O. Tunaboyu, L. Routil, Ö. Avşar, Stochastic-Based Nonlinear Numerical Modeling of Shear Critical RC Beam Repaired with Bonded CFRP Sheets, *J. Compos. Constr.* 23 (5) (2019) 04019042.
- [34] M. Gholami, A.R.M. Sam, J.M. Yatim, M.M. Tahir, A review on steel/CFRP strengthening systems focusing environmental performance, *Constr. Build. Mater.* 47 (2013) 301–310.
- [35] F. Klaiber, K. Dunker, T. Wipf, W. Sanders Jr, *Methods of strengthening existing highway bridges*, Transportation Research Board, Washington, D.C., 1987.
- [36] R.K. Lumor, J.S. Ankrah, S. Bawa, E.A. Dadzie, O. Osei, Rehabilitation of timber bridges in Ghana with case studies of the Kaase Modular Timber Bridge, *Eng. Fail. Anal.* 82 (2017) 514–524.
- [37] M. Hawkswood, *Marine Pile Repairs by Concrete Encasement*, Innovative Coastal Zone Management, ICE, Belfast UK, 2011.
- [38] N. Islam, M. Hoque, Strengthening of reinforced concrete columns by steel jacketing: a state of review, *Asian Trans. Eng. (ATE ISSN: 2221-4267)* 5 (2015).
- [39] A. Tarabia, H. Albakry, Strengthening of RC columns by steel angles and strips, *Alexandria Engineering Journal* 53 (3) (2014) 615–626.
- [40] V. Badalamenti, G. Campione, M.L. Mangiavillano, Simplified model for compressive behavior of concrete columns strengthened by steel angles and strips, *J. Eng. Mech.* 136 (2) (2009) 230–238.
- [41] E. Choi, Y.-S. Chung, K. Park, J.-S. Jeon, Effect of steel wrapping jackets on the bond strength of concrete and the lateral performance of circular RC columns, *Eng. Struct.* 48 (2013) 43–54.
- [42] N. Areemit N. Faeksin P. Niyom P. Phonsak Strengthening of deficient RC columns by steel angles and battens under axial load Proceedings of the Thirteenth East Asia-Pacific Conference on Structural Engineering and Construction (EASEC-13), The Thirteenth East Asia-Pacific Conference on Structural Engineering and Construction (EASEC-13) 2013 pp. 1-5-6.

- [43] J.M. Adam, S. Ivorra, F.J. Pallarés, E. Giménez, P.A. Calderón, Axially loaded RC columns strengthened by steel caging finite element modelling, *Constr. Build. Mater.* 23 (6) (2009) 2265–2276.
- [44] S.P.B. Waghmare, Materials and jacketing technique for retrofitting of structures, *Int. J. Adv. Eng. Res. Studies* 1 (1) (2011) 15–19.
- [45] N. Delatte, *Failure, Distress and Repair of Concrete Structures*, Elsevier, 2009.
- [46] M. Sakr, M. El Naggar, M. Nehdi, Interface characteristics and laboratory constructability tests of novel fiber-reinforced polymer/concrete piles, *J. Compos. Constr.* 9 (3) (2005) 274–283.
- [47] S. Pessiki, K.A. Harries, J.T. Kestner, R. Sause, J.M. Ricles, Axial behavior of reinforced concrete columns confined with FRP jackets, *J. Compos. Constr.* 5 (4) (2001) 237–245.
- [48] J. Teng, J. Chen, S.T. Smith, L. Lam, Behaviour and strength of FRP-strengthened RC structures: a state-of-the-art review, *Proceedings of the institution of civil engineers-structures and buildings* 156(1) (2003) 51–62.
- [49] A. Manalo, C. Sirimanna, W. Karunasena, L. McGarva, P. Falzon, Pre-impregnated carbon fibre reinforced composite system for patch repair of steel I-beams, *Constr. Build. Mater.* 105 (2016) 365–376.
- [50] J.E. Parks, D.N. Brown, M. Ameli, C.P. Pantelides, Seismic repair of severely damaged precast reinforced concrete bridge columns connected with grouted splice sleeves, *ACI Struct. J.* 113 (3) (2016) 615.
- [51] M. Hajsadeghi, F.J. Alaei, A. Shahmohammadi, Investigation on behaviour of square/rectangular reinforced concrete columns retrofitted with FRP jacket, *J. Civ. Eng. Manage.* 17 (3) (2011) 400–408.
- [52] J.G. Teng, *FRP-strengthened RC structures*, Wiley, 2002.
- [53] Y.-F. Wu, T. Liu, D. Oehlers, Fundamental principles that govern retrofitting of reinforced concrete columns by steel and FRP jacketing, *Adv. Struct. Eng.* 9 (4) (2006) 507–533.
- [54] L. Lam, J. Teng, Ultimate condition of fiber reinforced polymer-confined concrete, *J. Compos. Constr.* 8 (6) (2004) 539–548.
- [55] A. Nanni, M.S. Norris, FRP jacketed concrete under flexure and combined flexure-compression, *Constr. Build. Mater.* 9 (5) (1995) 273–281.
- [56] P. Rochette, P. Labossiere, Axial testing of rectangular column models confined with composites, *J. Compos. Constr.* 4 (3) (2000) 129–136.
- [57] ACI-Committee, *Guide for the Design and Construction of Externally Bonded FRP Systems for Strengthening Concrete Structures* (ACI 440.2R-08), American Concrete Institute, Farmington Hills, MI, 2008.
- [58] T. Norris, H. Saadatmanesh, M.R. Ehsani, Shear and flexural strengthening of R/C beams with carbon fiber sheets, *J. Struct. Eng.* 123 (7) (1997) 903–911.
- [59] P. Alagusundaramoorthy, I. Harik, C. Choo, Flexural behavior of R/C beams strengthened with carbon fiber reinforced polymer sheets or fabric, *J. Compos. Constr.* 7 (4) (2003) 292–301.
- [60] S.A. Taleb, A.S. Salem, Bending and Shear Behavior of a Composite Beam Strengthened and Double-Confined with FRP-Jacket, *Procedia Eng.* 114 (2015) 165–172.
- [61] Z.C. Tetta, L.N. Koutas, D.A. Bournas, Textile-reinforced mortar (TRM) versus fiber-reinforced polymers (FRP) in shear strengthening of concrete beams, *Compos. B Eng.* 77 (2015) 338–348.
- [62] F. Ribeiro, J. Sena-Cruz, F.G. Branco, E. Júlio, Hybrid FRP jacketing for enhanced confinement of circular concrete columns in compression, *Constr. Build. Mater.* 184 (2018) 681–704.
- [63] M. Saafi, E. Asa, Extending the service life of electric distribution and transmission wooden poles using a wet layup FRP composite strengthening system, *J. Perform. Constr. Facil.* 24 (4) (2010) 409–416.
- [64] A.C. Manalo, W. Karunasena, C. Sirimanna, G.B. Maranan, Investigation into fibre composites jacket with an innovative joining system, *Constr. Build. Mater.* 65 (2014) 270–281.
- [65] W. Ferdous, Y. Bai, T.D. Ngo, A. Manalo, P. Mendis, New advancements, challenges and opportunities of multi-storey modular buildings—A state-of-the-art review, *Eng. Struct.* 183 (2019) 883–893.
- [66] J. Williams, F.R.P. Pile, Jacket Solution has no "Pier" in Timber, *Pile Restoration* (2009).
- [67] M. Ehsani, FRP super laminates present unparalleled solutions to old problems, *Reinf. Plast.* 53 (6) (2009) 40–45.
- [68] A. Beddiar, R. Zitoun, F. Collombet, Y. Grunevald, M. Abadlia, N. Bourahla, Compressive behaviour of concrete elements confined with GFRP-prefabricated bonded shells, *Eur. J. Environ. Civ. Eng.* 19 (1) (2015) 65–80.
- [69] H. Karagah, M. Dawood, A. Belarbi, Experimental study of full-scale corroded steel bridge piles repaired underwater with grout-filled fiber-reinforced polymer jackets, *J. Compos. Constr.* 22 (3) (2018) 04018008.
- [70] G. Van Erp, C. Cattell, T. Heldt, Fibre composite structures in Australia's civil engineering market: an anatomy of innovation, *Prog. Struct. Mat. Eng.* 7 (3) (2005) 150–160.
- [71] Strong-Tie, FX-70 Structural Piling Repair and Protection System <https://www.strongtie.com/products/rps/fx70> 2013 2018)
- [72] Five Star, Five Star PileForm fiberglass reinforced plastic pile rehabilitation jackets, 2016. <https://www.fivestarproducts.com/pileform-f-jacket.html>.
- [73] FiberSystems, FiberSystems supplies composite pile jackets, *Reinforced Plastics* 61(2) (2017) 65.
- [74] L.C. Holloway, A review of the present and future utilisation of FRP composites in the civil infrastructure with reference to their important in-service properties, *Constr. Build. Mater.* 24 (12) (2010) 2419–2445.
- [75] J.R. Davis, *Corrosion: Understanding the basics*, Asm Int. (2000).
- [76] P.K. Mehta, Durability of concrete in marine environment—A review, *Spec. Publ.* 65 (1980) 1–20.
- [77] M. Safehian, A.A. Ramezani-pour, Assessment of service life models for determination of chloride penetration into silica fume concrete in the severe marine environmental condition, *Constr. Build. Mater.* 48 (2013) 287–294.
- [78] S. Tang, Z. Li, E. Chen, H. Shao, Non-steady state migration of chloride ions in cement pastes at early age, *RSC Adv.* 4 (89) (2014) 48582–48589.
- [79] Z. Li, *Advanced Concrete Technology*, John Wiley & Sons, 2011.
- [80] J.G. Castañó, C.A. Botero, A.H. Restrepo, E.A. Agudelo, E. Correa, F. Echeverría, Atmospheric corrosion of carbon steel in Colombia, *Corros. Sci.* 52 (1) (2010) 216–223.
- [81] X. Liu, A. Nanni, P.F. Silva, R.A. Laboube, Rehabilitation of steel bridge columns with FRP composite materials, *Proc. CCC* (2001) 10–12.
- [82] H. Grube, W. Rechenberg, Durability of concrete structures in acidic water, *Cem. Concr. Res.* 19 (5) (1989) 783–792.
- [83] U. Schneider, W. Piasta, The behaviour of concrete under Na<sub>2</sub> S<sub>04</sub> solution attack and sustained compression or bending, *Mag. Concr. Res.* 43 (157) (1991) 281–289.
- [84] M.T. Bassuoni, M.L. Nehdi, Durability of self-consolidating concrete to sulfate attack under combined cyclic environments and flexural loading, *Cem. Concr. Res.* 39 (3) (2009) 206–226.
- [85] J. Ju, L. Weng, S. Mindess, A. Boyd, Damage assessment and service life prediction of concrete subject to sulfate attack, *Materials Science of Concrete: Sulfate Attack Mechanisms* (1999).
- [86] S.A. Mangi, M.H. Wan Ibrahim, N. Jamaluddin, M.F. Arshad, R. Putra Jaya, Short-term effects of sulphate and chloride on the concrete containing coal bottom ash as supplementary cementitious material, *Eng. Sci. Technol. Int. J.* 22 (2) (2019) 515–522.
- [87] M.W. Montgomery Repair and replacement of acid-damaged piles, *International Conference on Case Histories in Geotechnical Engineering*, St 1984 Louis, Missouri
- [88] B. Mather, Concrete durability, *Cem. Concr. Compos.* 26 (1) (2004) 3–4.
- [89] J.G. Cabrera, Deterioration of concrete due to reinforcement steel corrosion, *Cem. Concr. Compos.* 18 (1) (1996) 47–59.
- [90] C. Lee, J. Bonacci, M.D. Thomas, M. Maalej, S. Khajehpour, N. Hearn, S. Pantazopoulou, S. Sheikh, Accelerated corrosion and repair of reinforced concrete columns using carbon fibre reinforced polymer sheets, *Can. J. Civ. Eng.* 27 (5) (2000) 941–948.
- [91] C. Fang, K. Lundgren, L. Chen, C. Zhu, Corrosion influence on bond in reinforced concrete, *Cem. Concr. Res.* 34 (11) (2004) 2159–2167.
- [92] T. El Maaddawy, A. Chahrour, K. Soudki, Effect of fiber-reinforced polymer wraps on corrosion activity and concrete cracking in chloride-contaminated concrete cylinders, *J. Compos. Constr.* 10 (2) (2006) 139–147.
- [93] Y. Du, L.A. Clark, A.H. Chan, Impact of reinforcement corrosion on ductile behavior of reinforced concrete beams, *ACI Struct. J.* 104 (3) (2007) 285.
- [94] A.A. Torres-Acosta, S. Navarro-Gutierrez, J. Terán-Guillén, Residual flexure capacity of corroded reinforced concrete beams, *Eng. Struct.* 29 (6) (2007) 1145–1152.
- [95] J. Rodriguez, L. Ortega, J. Casal, Load carrying capacity of concrete structures with corroded reinforcement, *Constr. Build. Mater.* 11 (4) (1997) 239–248.
- [96] D.V. Val, Deterioration of strength of RC beams due to corrosion and its influence on beam reliability, *J. Struct. Eng.* 133 (9) (2007) 1297–1306.
- [97] A.C. Manalo, A.A. Mohammed, G.B. Maranan, Novel Composites Jacket for Repair of Concrete Structures, *Proceedings of the 13th Fiber Reinforced Polymer for Reinforced Concrete Structures (FRPRCS13)*, Anaheim, California, United States of America, 2017.
- [98] J. Cairns, Z. Zhao, Behaviour of concrete beams with exposed reinforcement, *Proceedings of the Institution of Civil Engineers: Structures and Bridges*, 1993.
- [99] M. Harajli, Bond stress-slip model for steel bars in unconfined or steel FRC, or FRP confined concrete under cyclic loading, *J. Struct. Eng.* 135 (5) (2009) 509–518.
- [100] R.-Y. Wu, C.P. Pantelides, Concentrated and distributed plasticity models for seismic repair of damaged RC bridge columns, *J. Compos. Constr.* 22 (5) (2018) 04018044.
- [101] L.-V. Beaulieu, F. Legeron, S. Langlois, Compression strength of corroded steel angle members, *J. Constr. Steel Res.* 66 (11) (2010) 1366–1373.
- [102] U.S. Army, U.S. Navy, U.S. Air Force, Chapter 2: Timber structures, *Maintenance of Waterfront Facilities* 1978.
- [103] B. Pizzo, N. Macchioni, C. Capretti, E. Pecoraro, L. Sozzi, L. Fiorentino, Assessing the wood compressive strength in pile foundations in relation to diagnostic analysis: The example of the Church of Santa Maria Maggiore, Venice, *Constr. Build. Mater.* 114 (2016) 470–480.
- [104] R.K. Klaassen, Bacterial decay in wooden foundation piles—Patterns and causes: A study of historical pile foundations in the Netherlands, *Int. Biodeterior. Biodegrad.* 61 (1) (2008) 45–60.
- [105] A.P. Schniewind, Physical and mechanical properties of archaeological wood, *Physical and mechanical properties of archaeological wood.* (225) (1990) 87–109.
- [106] T. Ozbakkaloglu, Compressive behavior of concrete-filled FRP tube columns: Assessment of critical column parameters, *Eng. Struct.* 51 (2013) 188–199.
- [107] J. Berthet, E. Ferrier, P. Hamelin, Compressive behavior of concrete externally confined by composite jackets. Part A: experimental study, *Constr. Build. Mater.* 19 (3) (2005) 223–232.
- [108] G. Li, S. Kidane, S.-S. Pang, J. Helms, M.A. Stubblefield, Investigation into FRP repaired RC columns, *Compos. Struct.* 62 (1) (2003) 83–89.

- [109] A. Parvin, A.S. Jamwal, Performance of externally FRP reinforced columns for changes in angle and thickness of the wrap and concrete strength, *Compos. Struct.* 73 (4) (2006) 451–457.
- [110] J.C. Lim, T. Ozbakkaloglu, Hoop strains in FRP-confined concrete columns: experimental observations, *Mater. Struct.* 48 (9) (2015) 2839–2854.
- [111] S.T. Smith, S.J. Kim, H. Zhang, Behavior and effectiveness of FRP wrap in the confinement of large concrete cylinders, *J. Compos. Constr.* 14 (5) (2010) 573–582.
- [112] A.Z. Fam, S.H. Rizkalla, Confinement model for axially loaded concrete confined by circular fiber-reinforced polymer tubes, *Struct. J.* 98 (4) (2001) 451–461.
- [113] J.G. Teng, T. Yu, D. Fernando, Strengthening of steel structures with fiber-reinforced polymer composites, *J. Constr. Steel Res.* 78 (2012) 131–143.
- [114] VicRoads, Code of Practice: FRP for strengthening of bridge structures, in: *V. Roads* (Ed.), 2018.
- [115] A. Fam, S. Rizkalla, Behavior of axially loaded concrete-filled circular FRP tubes, *ACI Struct. J.* 98 (3) (2001) 280–289.
- [116] W.-K. Hong, H.-C. Kim, Behavior of concrete columns confined by carbon composite tubes, *Can. J. Civ. Eng.* 31 (2) (2004) 178–188.
- [117] H. Kim, K.H. Lee, Y.H. Lee, J. Lee, Axial behavior of concrete-filled carbon fiber-reinforced polymer composite columns, *Struct. Des. Tall Spec. Build.* 21 (3) (2012) 178–193.
- [118] T. Vincent, T. Ozbakkaloglu, Influence of fiber orientation and specimen end condition on axial compressive behavior of FRP-confined concrete, *Constr. Build. Mater.* 47 (2013) 814–826.
- [119] M.R. Bambach, H.H. Jama, M. Elchalakani, Axial capacity and design of thin-walled steel SHS strengthened with CFRP, *Thin-Walled Struct.* 47 (10) (2009) 1112–1121.
- [120] L. Lam, J. Teng, Design-oriented stress-strain model for FRP-confined concrete, *Constr. Build. Mater.* 17 (6) (2003) 471–489.
- [121] Simpson Strong-Tie, FX-70<sup>®</sup> Structural Piling Repair and Protection System, 2018. <https://www.strongtie.com/products/rps/fx70>.
- [122] A.A. Mohammed, A.C. Manalo, G.B. Maranan, Y. Zhuge, P.V. Vijay, Comparative study on the behaviour of different infill materials for pre-fabricated fibre composite repair systems, *Constr. Build. Mater.* 172 (2018) 770–780.
- [123] M. Shamsuddoha, M.M. Islam, T. Aravinthan, A. Manalo, K.-T. Lau, Characterisation of mechanical and thermal properties of epoxy grouts for composite repair of steel pipelines, *Mater. Des.* 52 (2013) 315–327.
- [124] M. Shamsuddoha, Behaviour of Infilled Rehabilitation System with Composites for Steel Pipe, University of Southern Queensland, 2014.
- [125] W. Sum, K. Leong, Numerical study of annular flaws/defects affecting the integrity of grouted composite sleeve repairs on pipelines 0731684413503721, *J. Reinf. Plast. Compos.* (2013).
- [126] A. Deb, S. Bhattacharyya, Investigation into the effect of bonding on FRP-wrapped cylindrical concrete columns, *J. Compos. Constr.* 14 (6) (2010) 706–719.
- [127] H. Saadatmanesh, M. Ehsani, L. Jin, Seismic retrofitting of rectangular bridge columns with composite straps, *Earthquake Spectra* 13 (2) (1997) 281–304.
- [128] Z. Yan, C.P. Pantelides, Concrete column shape modification with FRP shells and expansive cement concrete, *Constr. Build. Mater.* 25 (1) (2011) 396–405.
- [129] Z. Yan, C.P. Pantelides, L.D. Reaveley, Posttensioned FRP composite shells for concrete confinement, *J. Compos. Constr.* 11 (1) (2007) 81–90.
- [130] T. Ozbakkaloglu, J.C. Lim, T. Vincent, FRP-confined concrete in circular sections: Review and assessment of stress-strain models, *Eng. Struct.* 49 (2013) 1068–1088.
- [131] D.A. Moran, C.P. Pantelides, Elliptical and circular FRP-confined concrete sections: A Mohr-Coulomb analytical model, *Int. J. Solids Struct.* 49 (6) (2012) 881–898.
- [132] D.A. Moran, C.P. Pantelides, L.D. Reaveley, Mohr-coulomb model for rectangular and square FRP-confined concrete, *Compos. Struct.* 209 (2019) 889–904.
- [133] Y. Xiao, H. Wu, Compressive behavior of concrete confined by carbon fiber composite jackets, *J. Mater. Civ. Eng.* 12 (2) (2000) 139–146.
- [134] L. Lam, J. Teng, Strength models for fiber-reinforced plastic-confined concrete, *J. Struct. Eng.* 128 (5) (2002) 612–623.
- [135] J. Berthet, E. Ferrier, P. Hamelin, Compressive behavior of concrete externally confined by composite jackets: Part B: Modeling, *Constr. Build. Mater.* 20 (5) (2006) 338–347.
- [136] Z. Yan, C. Pantelides, Design-oriented model for concrete columns confined with bonded FRP jackets or post-tensioned FRP shells, *Proceedings of the 8th International Symposium on Fiber Reinforced Polymer Reinforcement for Concrete Structures*, University of Patras, 2007.
- [137] J. Teng, T. Jiang, L. Lam, Y. Luo, Refinement of a design-oriented stress-strain model for FRP-confined concrete, *J. Compos. Constr.* 13 (4) (2009) 269–278.
- [138] H.-L. Wu, Y.-F. Wang, L. Yu, X.-R. Li, Experimental and computational studies on high-strength concrete circular columns confined by aramid fiber-reinforced polymer sheets, *J. Compos. Constr.* 13 (2) (2009) 125–134.
- [139] M.F. Fahmy, Z. Wu, Evaluating and proposing models of circular concrete columns confined with different FRP composites, *Compos. B Eng.* 41 (3) (2010) 199–213.
- [140] T. Yu, J. Teng, Design of concrete-filled FRP tubular columns: provisions in the Chinese technical code for infrastructure application of FRP composites, *J. Compos. Constr.* 15 (3) (2010) 451–461.
- [141] J.C. Lim, T. Ozbakkaloglu, Confinement model for FRP-confined high-strength concrete, *J. Compos. Constr.* 18 (4) (2013) 04013058.
- [142] G. Lin, T. Yu, J. Teng, Design-Oriented Stress-Strain Model for Concrete under Combined FRP-Steel Confinement 04015084, *J. Compos. Constr.* (2015).
- [143] M.R. Spoelstra, G. Monti, FRP-confined concrete model, *J. Compos. Constr.* 3 (3) (1999) 143–150.
- [144] A. Mirmiran, M. Shahawy, Behavior of concrete columns confined by fiber composites, *J. Struct. Eng.* 123 (5) (1997) 583–590.
- [145] S.P.C. Marques, D.C.D.S.C. Marques, J. Lins da Silva, M.A.A. Cavalcante, Model for analysis of short columns of concrete confined by fiber-reinforced polymer, *J. Compos. Constr.* 8 (4) (2004) 332–340.
- [146] D.A. Moran, C.P. Pantelides, Stress-strain model for fiber-reinforced polymer-confined concrete, *J. Compos. Constr.* 6 (4) (2002) 233–240.
- [147] B. Binici, An analytical model for stress-strain behavior of confined concrete, *Eng. Struct.* 27 (7) (2005) 1040–1051.
- [148] T. Jiang, J. Teng, Analysis-oriented stress-strain models for FRP-confined concrete, *Eng. Struct.* 29 (11) (2007) 2968–2986.
- [149] C. Aire, R. Gettu, J. Casas, S. Marques, D. Marques, Concrete laterally confined with fibre-reinforced polymers (FRP): experimental study and theoretical model, *Materiales de Construcción* 60 (297) (2010) 19–31.
- [150] Q. Xiao, J. Teng, T. Yu, Behavior and modeling of confined high-strength concrete, *J. Compos. Constr.* 14 (3) (2010) 249–259.
- [151] J. Teng, G. Lin, T. Yu, Analysis-oriented stress-strain model for concrete under combined FRP-steel confinement, *J. Compos. Constr.* 19 (5) (2014) 04014084.
- [152] O. Chaallal, M. Shahawy, M. Hassan, Performance of axially loaded short rectangular columns strengthened with carbon fiber-reinforced polymer wrapping, *J. Compos. Constr.* 7 (3) (2003) 200–208.
- [153] T.M. Pham, M.N. Hadi, J. Yousef, Optimized FRP wrapping schemes for circular concrete columns under axial compression, *J. Compos. Constr.* 19 (6) (2015) 04015015.
- [154] T. Turgay, Z. Polat, H. Koksall, B. Doran, C. Karakoç, Compressive behavior of large-scale square reinforced concrete columns confined with carbon fiber reinforced polymer jackets, *Mater. Des.* 31 (1) (2010) 357–364.
- [155] T.E. Maaddawy, Strengthening of eccentrically loaded reinforced concrete columns with fiber-reinforced polymer wrapping system: experimental investigation and analytical modeling, *J. Compos. Constr.* 13 (1) (2009) 13–24.
- [156] F. Colomb, H. Tobbi, E. Ferrier, P. Hamelin, Seismic retrofit of reinforced concrete short columns by CFRP materials, *Compos. Struct.* 82 (4) (2008) 475–487.
- [157] J.-J. Zeng, Y.-C. Guo, W.-Y. Gao, W.-P. Chen, L.-J. Li, Stress-strain behavior of concrete in circular concrete columns partially wrapped with FRP strips, *Compos. Struct.* 200 (2018) 810–828.
- [158] J.B. Mander, M.J.N. Priestley, R. Park, Theoretical Stress-Strain Model for Confined Concrete, *J. Struct. Eng.* 114 (8) (1988) 1804–1826.
- [159] H. Saadatmanesh, M.R. Ehsani, M.-W. Li, Strength and ductility of concrete columns externally reinforced with fiber composite straps, *Struct. J.* 91 (4) (1994) 434–447.
- [160] T.M. Pham, J. Yousef, M.N. Hadi, T.M. Tran, Effect of different FRP wrapping arrangements on the confinement mechanism, *Procedia Eng.* 142 (2016) 306–312.
- [161] A.A. Mohammed, A.C. Manalo, G.B. Maranan, Y. Zhuge, P. Vijay, J. Pettigrew, Behavior of damaged concrete columns repaired with novel FRP jacket, *J. Compos. Constr.* 23 (3) (2019) 04019013.
- [162] T.V. Parry, S. Wronski, Selective reinforcement of an aluminium alloy by adhesive bonding with uniaxially aligned carbon fibre/epoxy composites, *Composites* 12 (4) (1981) 249–255.
- [163] M. Tavakkolizadeh, H. Saadatmanesh, Fatigue Strength of Steel Girders Strengthened with Carbon Fiber Reinforced Polymer Patch, *J. Struct. Eng.* 129 (2) (2003) 186–196.
- [164] A. Shaat, A. Fam, Fiber-Element Model for Slender HSS Columns Retrofitted with Bonded High-Modulus Composites, *J. Struct. Eng.* 133 (1) (2007) 85–95.
- [165] M.R. Bambach, M. Elchalakani, Plastic mechanism analysis of steel SHS strengthened with CFRP under large axial deformation, *Thin-Walled Struct.* 45 (2) (2007) 159–170.
- [166] J. Solan, USQ, Joinlox collaborate on prefabricated composite repair system, *Composites World*, 2017.

## **Chapter 3**

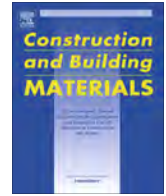
### **Comparative study on the behaviour of different infill materials for pre-fabricated fibre composite repair systems**

Chapter 2 highlighted that the high strength of the FRP composite material can be effectively utilised if the grout can efficiently transfer the stresses between the damaged structure and the external FRP jacket. This chapter investigated the behaviour of prefabricated FRP system filled with different types of grouts commonly used by the industry. Concrete-, cementitious- and epoxy-based grout infills with compressive strength and modulus of elasticity ranging from 10 MPa to 70 MPa and from 10 GPa to 35 GPa, respectively, have been considered and used as infills for GFRP tubes of 100 mm diameter and 200 mm height. The bond effect was also investigated as an additional parameter by coating the inner surface of the tube by epoxy and 5 mm coarse aggregate. All specimen type, 3 replicates each, were tested under concentric axial loading until failure. The results showed a strength and strain enhancement by only 1.3 and 1.0, respectively, for the GFRP repair system filled with epoxy grouts but up to 6.2 and 38 times, respectively, for the tubes filled with the lowest strength and modulus concrete. The 3 replicates for each specimen types behaved almost the same. Moreover, the provision of epoxy and coarse aggregates inside the GFRP tube surface enhanced the stress transfer between the tube and infill which consequently improved the load capacity and ductility by at least 10%. Furthermore, localised failure was observed in the FRP repair system due to the brittle cracking and crushing behaviour of the cementitious and epoxy grouts while the progressive failure of the concrete infill resulted in effective utilisation of the high strength characteristics of the FRP repair system. Moreover, the high compressive strength of the infill material limited its capacity to transfer the stresses uniformly around the tubes due to the increased brittleness. A theoretical model was developed to accurately predict the compressive behaviour of infills and grout-filled GFRP tubes which accounts for the experimental axial and hoop FRP rupture strains. From this work, cementitious grout was found effective as a practical infill between prefabricated FRP jacket and damaged RC structures due to its sufficiently high workability, compressive strength and stiffness. The behaviour of damaged structures repaired with FRP jacket and filled with this grouting system under compression and bending were then investigated in Chapters 4 and 5, respectively.



Contents lists available at ScienceDirect

# Construction and Building Materials

journal homepage: [www.elsevier.com/locate/conbuildmat](http://www.elsevier.com/locate/conbuildmat)

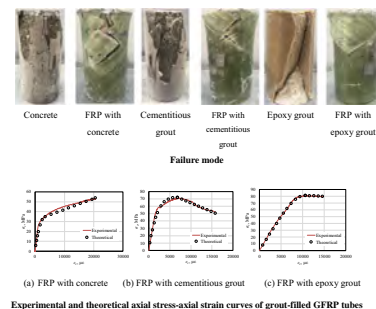
## Comparative study on the behaviour of different infill materials for pre-fabricated fibre composite repair systems

Ali A. Mohammed<sup>a,b</sup>, Allan C. Manalo<sup>a,\*</sup>, Gingham B. Maranan<sup>c</sup>, Yan Zhuge<sup>d</sup>, P.V. Vijay<sup>e</sup><sup>a</sup> Centre for Future Materials (CFM), School of Civil Engineering and Surveying, University of Southern Queensland, Toowoomba 4350, Australia<sup>b</sup> Environmental Engineering Department, College of Engineering, The University of Mustansiriyah, Baghdad, Iraq<sup>c</sup> Civil Engineering, School of Engineering, Faculty of Science and Engineering, University of Waikato, Hamilton 3216, New Zealand<sup>d</sup> School of Natural & Built Environments, University of South Australia, Adelaide 5001, Australia<sup>e</sup> Department of Civil and Environmental Engineering West Virginia University, Morgantown, WV 26506, United States

### HIGHLIGHTS

- Constituent behaviour and mechanical properties of concrete-, shrinkage compensating cementitious- and epoxy-grout infills.
- Behaviour of GFRP tubes filled with different types of grout-infills.
- Pre-fabricated FRP composite repair system for deficient structures.
- Theoretical model development to predict the overall behaviour of composite repair systems with different infill materials.

### GRAPHICAL ABSTRACT



Experimental and theoretical axial stress-axial strain curves of grout-filled GFRP tubes

### ARTICLE INFO

#### Article history:

Received 3 December 2017

Received in revised form 29 March 2018

Accepted 3 April 2018

#### Keywords:

Grout-infills

New composite materials

Systems and strengthening techniques

FRP tube

Composite jacket

Characterization of FRP and FRC materials/systems

### ABSTRACT

Prefabricated fibre-reinforced polymer (FRP) composite jacket is now becoming an effective repair system for deteriorating piles and columns exposed to marine environment. This system works by providing grout infills between the annulus of the existing structure and the composite jacket. Few studies are however available on the optimal grouting materials that can effectively transfer the stresses between the existing structure and the FRP jacket. This study is investigating the effect of cementitious, concrete and epoxy-based grout infills on the structural behaviour of pre-fabricated glass-FRP (GFRP) tubes. The considered grouts have compressive strength and modulus of elasticity ranging from 10 MPa to 70 MPa and from 10 GPa to 35 GPa, respectively. The experimental results showed that the behaviour of the composite repair system is highly dependent on the modulus of elasticity and the compressive strength of the grout infill. The brittle failure behaviour of the cementitious and epoxy grouts led to localised failure in the FRP repair system while the progressive cracking and crushing of the concrete infill resulted in effective utilisation of the high strength properties of the composite materials. Theoretical analysis of the overall compressive behaviour has also been conducted and showed very good agreement with the experimental results.

© 2018 Elsevier Ltd. All rights reserved.

### 1. Introduction

The increasing problems of deteriorating reinforced concrete (RC) civil infrastructure have resulted in many of them becoming out of service due to safety concerns. These damaged structures need to be either replaced or retrofitted so that they can continue to remain in service. It is estimated that more than \$5 billion

\* Corresponding author.

E-mail addresses: [ali.mohammed@usq.edu.au](mailto:ali.mohammed@usq.edu.au) (A.A. Mohammed), [allan.manalo@usq.edu.au](mailto:allan.manalo@usq.edu.au) (A.C. Manalo), [gmaranan@waikato.ac.nz](mailto:gmaranan@waikato.ac.nz) (G.B. Maranan), [yan.zhuge@unisa.edu.au](mailto:yan.zhuge@unisa.edu.au) (Y. Zhuge), [p.vijay@mail.wvu.edu](mailto:p.vijay@mail.wvu.edu) (P.V. Vijay).

annually is needed to maintain the RC bridges in each of the countries like US, Canada, and Europe [1]. In Australia, the corrosion-induced damages cost the economy more than \$13 billion per year due to lost production and shutdowns to make repairs as reported by the Commonwealth Scientific and Industrial Research Organisation (cited in Cassidy et al. [2]). In most cases, it is more economical to repair the existing damaged structures than to replace them. Adopting effective rehabilitation and strengthening techniques can be economically beneficial by minimizing the off-service time of the structure, and eventually saving a significant amount of resources. Due to the limitations of the traditional rehabilitation techniques, such as concrete and steel jacketing, in terms of the material weight and the complexity of steel anchorage [3], the introduction of versatile fibre-reinforced polymer (FRP) composites for strengthening and rehabilitation of civil infrastructure has been essential and very valuable. The superior characteristics of this advanced material, such as high strength, corrosion resistance, lightweight, high fatigue resistance, high impact resistance, and durability [4], enabled it to be successfully utilised for strengthening and rehabilitating damaged and/or deteriorating concrete and steel structures, [5–8], especially those that are located in harsh environments such as marine and mining areas.

Pre-fabricated composite jackets are becoming increasingly used in repairing structures especially for under water applications. These composite repair systems are manufactured at specialised plants, thereby achieving high quality and uniformity. Moreover, they can be easily installed at site by placing the jacket around the damaged structure and serving as a permanent formwork. An appropriate grout is then placed to fill the gap between the jacket and the existing structure. The pre-fabricated FRP jacket provides protective shield and induces lateral confining passive pressure, which eventually strengthens the damaged structure. Lopez-Anido et al. [9] proposed a repair system utilizing FRP shells with two different types of grouting systems, cement-based structural grout and expanding polyurethane chemical grout, to provide protection and structural restoration for deteriorated wood piles. Williams (cited in Manalo et al. [10]) utilised pre-fabricated FRP pile jackets consisting of chop strands and woven mats impregnated with epoxy resin in the rehabilitation of New York City waterfront structures to restore its structural strength. A 3/8" lightweight stone concrete was utilised as the grout infill to prevent the weight increase that could cause structural damage to the pier. Vijay et al. [11] used pre-cured FRP shells for encasing and rehabilitating the water-submerged steel H-piles of a bridge in the USA. The space between the FRP shells and the steel piles was filled with self-consolidating concrete to strengthen and protect the piles from further deterioration. Considering the behaviour of the repair system components, Shamsuddoha et al. [12] highlighted the effectiveness of using FRP composites and grout infills for steel pipeline repairs. In these applications, the repair systems have been successfully implemented by providing grout infills between the annulus of the existing structure and the prefabricated composite jackets.

The effectiveness of the pre-fabricated FRP jacket in repairing damaged or deteriorating structures is highly dependent on the performance of the grout infill. The grout plays a vital role in transferring the stresses between the core structure and the external FRP jacket to develop the composite action [13]. The compressive strength and modulus of elasticity are the two most important mechanical characteristics of the grout that affect its functionality in terms of load transferability and effective utilisation of the FRP system [11,12]. Sum and Leung [13] conducted a numerical analysis on a composite sleeve and epoxy grouts over a pipe subjected to internal pressure. The results indicated that a stiffer epoxy grout is preferable because it is more effective in stress transfer and makes the repair system act compositely. The bond between the grout and the FRP

jacket is another factor that affects the efficiency of the FRP repair system because any discontinuity and/or voids would lead to generating non-uniform stresses onto the FRP jackets that could lead to premature failure [14]. The grout is necessary to assure a full contact between the system components as it provides a smooth bed for the FRP jacket and refill of the damaged profile of the existing structure [12]. Moreover, it is essential when shape modification is required, i.e. modifying the original structure from square/rectangular to a circular section for better confinement [15,16].

A number of studies have used several types of grouts as infill for the pre-fabricated FRP repair system [9,11,17–20]; however, these studies did not consider the structural contribution of the grout infills. There is a need therefore to have a better understanding on the mechanical properties of the grout infills and how they affect the stress development on the composite repair system. In this study, the properties of three different grout materials and the structural behaviour of a FRP repair system filled with different grouts are evaluated. The results of this study provide information on the important characteristics of the grouting materials that will be useful to effectively utilise the inherent properties of the pre-fabricated composite repair systems.

## 2. Experimental program

The material properties and procedures employed in the study are presented and discussed in this section.

### 2.1. Material properties

#### 2.1.1. Infills

Three different types of infills were considered in this study: (1) concrete-grout infill, (2) shrinkage compensating cementitious-grout infill, and (3) epoxy-grout infill. These grout infills were selected based on their market availability and current industry practice, with taking into consideration the compressive strength and elastic modulus of the infills. For the concrete-grout infill, three different compressive strength grades, i.e. Grade 1, Grade 2 and Grade 3, of commercially available normal concrete made up of Portland cement, water, sand, and gravels with maximum aggregate size of 10 mm were used. The shrinkage-compensating cementitious grout was made up of cement powder with 0.3 mm maximum particle size. Its shrinkage-compensating feature allowed the final product to be volumetrically stable during the initial stage of curing and prevented cracking due to plastic shrinkage. Following the recommended procedure in the technical data sheet [21], a water-to-cement weight ratio of 0.175 was adopted to obtain a flowable grout that suits filling applications while avoiding the formation of voids. A high strength chemical epoxy grout [22] was used in this study and consisted of two main components; the polyurethane (Part A) and binder (Part B). After the proper mixing of these components, special graded aggregate and fillers for epoxy compounds were added to the mix to produce the desired grout mortar.

#### 2.1.2. GFRP tubes

Fig. 1 shows the prefabricated glass-fibre-reinforced polymer (GFRP) tubes that were manufactured using the filament winding method with E-glass fibres and vinyl ester resin. Experimental approaches in accordance with the ISO 527-1:1995 [23] and ISO 14126:1999 [24] were adopted to ascertain the tensile and compressive properties of the GFRP tubes. The test coupons were cut from the large GFRP laminates, with the same lay-up and composition as the GFRP tubes, using the water jet cutting machine. The results of the material characterisation are listed in Table 1. As can be seen from the table, the GFRP tubes had average tensile strength ( $f_f$ ) and tensile modulus ( $E_f$ ) equivalent to 297 MPa and 24 GPa, respectively. The compressive strength ( $f'_f$ ) and compressive modulus ( $E'_f$ ) on the other hand, were equal to 180 MPa and 30 GPa, respectively.

Burnout test was also conducted, in accordance with ISO 1172-96 [25], to determine the fibre content ratio and fibre stacking sequence of the GFRP tubes. The test revealed that the GFRP tube material has 67.6% fibre content by weight. As depicted in Fig. 2, the GFRP tube had a stacking sequence of  $-45^\circ/+45^\circ/-45^\circ/+45^\circ$  with respect to the hoop direction. Such configuration is effective in managing multi-axial stresses and in achieving more ductile behaviour at failure [26,27].

### 2.2. Test specimens

Three replicates were prepared for each type of specimen, yielding a total of 36 specimens including three (3) hollow GFRP tubes, fifteen (15) infill cylinders, fifteen (15) grout-filled GFRP tubes, and three (3) filled GFRP tubes with the internal surface roughened with epoxy and 5 mm size course aggregates. The specimens were cured and tested after seven days.



Fig. 1. The pre-fabricated GFRP tube.

Fig. 3 shows the geometry and configuration of the tested specimens. The average height ( $h_i$ ) and diameter ( $d_i$ ) of the infill cylinders were 200 mm and 100 mm, respectively, while the average thickness ( $t_g$ ), height ( $h_g$ ), and internal diameter ( $d_{gi}$ ) of GFRP tubes were 3, 200 and 100 mm, respectively. The GFRP tubes were roughened by coating the inner surface with a thin layer of epoxy and 5 mm coarse aggregates (Fig. 4) to investigate the influence of the bonding between the GFRP tubes and the infills. These tubes were filled with Grade 2 concrete.

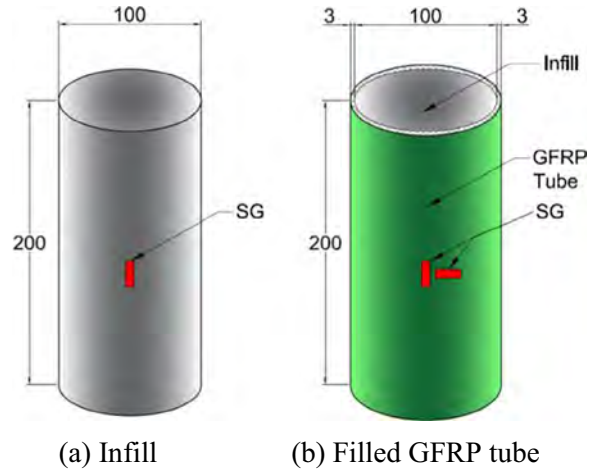


Fig. 3. Geometry and configuration of the test specimens.

Grades 1, 2, and 3 cylindrical concrete infills were labelled as C1, C2, and C3, respectively, and were collectively labelled as C#. The cylindrical cementitious-grout and epoxy-grout infills were labelled as CG and EG, respectively. The grout-filled GFRP tubes were then identified by adding the prefix G- to the infill label while the hollow GFRP tubes were named as H-Tube. The filled GFRP tubes with roughened internal surface were identified by adding the symbol \*. For example, the specimen named as G-EG stands for GFRP tubes filled with epoxy-grout while G-C2\* represents the specimen with roughened GFRP tubes and filled with Grade 2 concrete-grout infill. The concrete-filled GFRP tubes were collectively called as G-C#.

2.3. Test set-up and procedure

The mechanical properties of the test specimens were determined using the uniaxial compression test in accordance with the ASTM C39/C39M [28] as shown in Fig. 5. The specimens were vertically positioned at the centre of the loading

Table 1  
Properties of GFRP coupons.

Test	Test standard	Dimensions (mm)		Property	Value	Standard deviation
		Length	Width			
Tensile	ISO 527-1:1995 [1]	250	25	Peak stress, MPa ( $f_f$ )	297	45
				Modulus, GPa ( $E_f$ )	24	-
				Peak strain, $\mu\epsilon$ ( $\epsilon_{fu}$ )	11,268	-
Compression	ISO 14126:1999 [2]	140	12.75	Peak stress, MPa ( $f'_f$ )	180	38
				Modulus, GPa ( $E'_f$ )	30	-
				Peak strain, $\mu\epsilon$ ( $\epsilon'_{fu}$ )	11,001	-
Burnout	ISO 1172:1998 [3]	50	15	Fibre content	67.65%	0.31

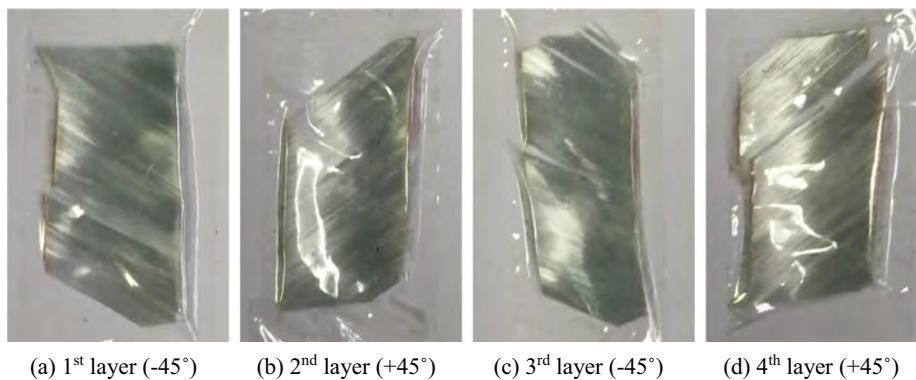


Fig. 2. Stacking sequence of the GFRP tube.



Fig. 4. Roughened GFRP tube.

plates. The monotonically increasing loads were applied using the 2000 kN SANS servo-hydraulic compression testing machine at a displacement rate of 3.0 mm/min. The machine was equipped with a digital acquisition system that measured and recorded the applied loads and corresponding deformations. The axial and lateral strains were measured using strain gauges (SG) glued longitudinally and transversely at the mid-height of the specimens and were captured using the System 5000 data logger. A calibrated 2000 kN load cell attached to the logger was also used to synchronise the deformation readings obtained from the SANS machine and the strain readings captured from the data logger.

### 3. Results and observations

#### 3.1. Behaviour of infill materials

This section summarises the results obtained from the compression tests of infills.

##### 3.1.1. Failure mode

Fig. 6 shows the representative failure modes of the tested cylindrical infill specimens after the compression test. Visible crushing and cracking were observed at the top section of the concrete and cementitious grout cylinders during the test. As the applied load increased, the cracks spread and propagated downward with increased crushing. At failure, C1 (Fig. 6a), C2 (Fig. 6b), and C3 (Fig. 6c) underwent concrete crushing coupled with the formation of longitudinal cracks throughout the height of each specimen. In general, as the compression strength of concrete increases, the degree of aggregate separation and crushing severity decreases while the width of cracks increases. CG (Fig. 6d) exhibited nearly similar failure mode as the concrete specimens, but with a sharp and sudden break in the form of a large vertical crack throughout the height of the cylinder.

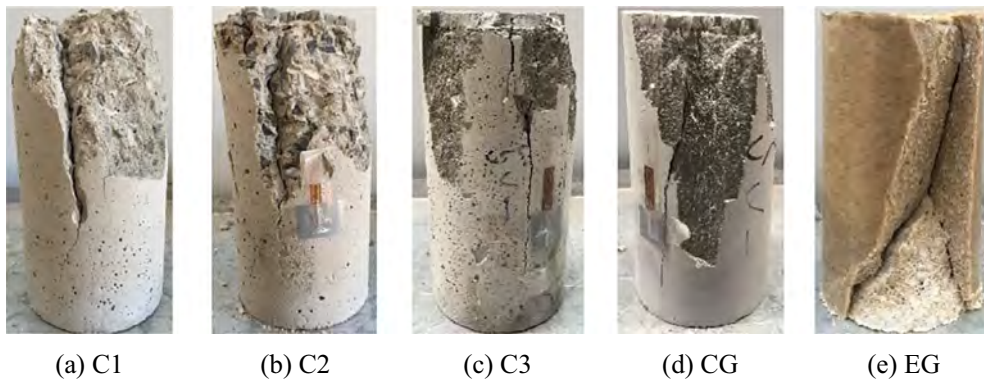


a. Infill



b. Filled GFRP tube

Fig. 5. Compression test set-up.



(a) C1

(b) C2

(c) C3

(d) CG

(e) EG

Fig. 6. Representative failure modes of the cylindrical infills.

The failure of EG (Fig. 6e), on the other hand, was governed by the combination of cone formation at the bottom and large fracture without crushing at both ends. The cone formation can be attributed to the frictional force between the top and bottom plates, and the specimen surfaces which creates horizontal stresses and eventually forms cones at the ends [28]. However, no cone was formed at the top due to the presence of the cap which minimised/eliminated the friction force. Interestingly, similar failure pattern was observed by Shamsuddoha et al. [12] but without the cone formation as the frictional force was marginal due to the relatively low axial applied load. This specimen underwent the most violent compression failure among all the other infills, wherein a loud snapping sound was heard at failure.

### 3.1.2. Stress-strain behaviour

Fig. 7 presents the typical relationship between the axial stress ( $\sigma_c$ ) and the axial strain ( $\epsilon_c$ ) of the tested cylindrical infills. As shown in the figure, C<sup>#</sup> exhibited a linear elastic behaviour, wherein the load increased rapidly with the deformation. As can be expected, the elastic modulus increases with the compressive strength. A short nonlinear behaviour prior to peak load was observed, owing to the simultaneous crushing and cracking of the specimen. After reaching the maximum load, the load dropped progressively. C3 showed the fastest degradation followed by C2 and C1, respectively. In the case of CG, the axial stress increased rapidly with the axial strain; however, CG did not show any post-peak response as the curve dropped immediately after failure. The typical stress-strain curve of EG was composed of a short linear segment followed by a long nonlinear segment prior to peak, owing to the high deformability characteristic of the epoxy grout, which was then followed by a short decreasing stress-strain segment.

### 3.1.3. Compressive strength, modulus of elasticity, and axial strain at peak

Table 2 summarises the experimental results obtained from the compression tests of cylindrical infills including the average axial load capacity ( $P_{iu}$ ), the average peak compressive strength ( $\sigma_{iu}$ )

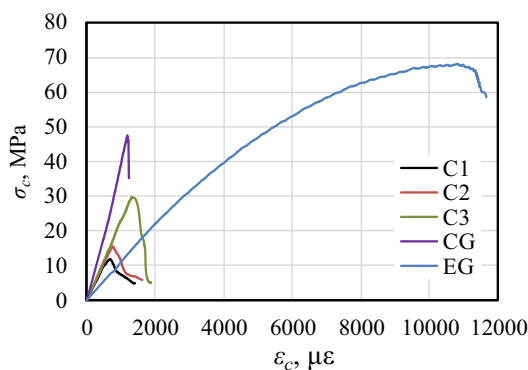


Fig. 7. Representative stress-strain ( $\sigma_c - \epsilon_c$ ) curves of the cylindrical infill materials.

Table 2  
Peak axial load, compressive strength and its standard deviation, elastic modulus, and strain at peak of the cylindrical grout infills.

Specimen	$P_{iu}$ , kN	$\sigma_{iu}$ , MPa	$s_i$ , MPa	$MOE_i$ , GPa	$\epsilon_{iu}$ , $\mu\epsilon$
C1	99.1	12.6	1.4	18.4	662
C2	136.5	17.4	4.4	19.5	755
C3	215.8	27.5	3.1	26.8	1312
CG	378.4	48.2	1.1	34.3	1178
EG	619.5	78.9	4.6	10.0	10,800

and corresponding standard deviation ( $s_{iu}$ ), the modulus of elasticity ( $MOE_i$ ), and the axial strain at peak ( $\epsilon_{iu}$ ). The  $P_{iu}$  of C1, C2, and C3 were 99.1 kN, 136.5 kN, and 215.8 kN, respectively, which translate to  $\sigma_{iu}$  of 12.6 MPa, 17.4 MPa, and 27.5 MPa respectively. CG and EG, on the other hand yielded  $P_{iu}$  of 378.4 kN and 619.5 kN that were equivalent to  $\sigma_{iu}$  of 48.2 MPa and 78.9 MPa, respectively. The values of  $s_{iu}$  ranged from 1.4 MPa to 4.6 MPa, suggesting a good precision among the obtained results.

The  $MOE_i$  values were taken from the regression analysis of the linear segment of the stress-strain curves. As expected, C3 (26.8 GPa) yielded the highest  $MOE_i$  among the concrete infills followed by C2 (19.5 GPa) and C1 (18.4 GPa), respectively. CG exhibited the highest  $MOE_i$  (34.3 GPa) among the tested cylindrical infills. Interestingly, the experimental MOE of the concrete-grout and cementitious-grout infills were more or less comparable to the theoretical values obtained from the established empirical formula (Eq. (1)) for normal concrete:

$$MOE_i = 4700\sqrt{\sigma_{iu}} \quad (1)$$

Although EG yielded the highest  $\sigma_{iu}$  among infills, it produced the least  $MOE_i$  (10 GPa). This value was equivalent to the  $MOE_i$  (11 GPa) reported by Shamsuddoha et al. [12] for epoxy-based grout with relatively similar material composition as the epoxy grout adopted in this study.

The magnitude of  $\epsilon_{iu}$  increases with the compressive strength of the concrete infills, wherein C3 (1312  $\mu\epsilon$ ) yielded the largest value followed by C2 (755  $\mu\epsilon$ ) and C1 (662  $\mu\epsilon$ ), respectively. The  $\epsilon_{iu}$  of CG and EG, on the other hand, were equivalent to 1178  $\mu\epsilon$  and 10,800  $\mu\epsilon$ , respectively.

### 3.2. Behaviour of hollow and filled GFRP tubes

This section summarises the results obtained from the compression tests of hollow GFRP tubes and grout-filled GFRP tubes.

#### 3.2.1. Failure mode

Fig. 8 shows the typical mode of failure of the hollow and grout-filled GFRP tubes. As shown in Fig. 8a, the hollow GFRP tubes experienced localised crushing just below the loading point (end crushing). Then, the damage was transferred axially to the body by forming a large crack with continuous fibre rupture. Sounds of resin cracking and fibres rupturing were heard before the final failure. Filling the GFRP tubes with grout infills, however, modified the failure from axial to hoop failure. For all the grout-filled GFRP tubes, the failure was initiated by the development of cracks and crushing of the core infills. White spots appeared onto the body of the tubes, especially at the potential failure zones due to the tensioning of fibres. The mechanism and extent of fibre rupture, however, were different for each type of grout infill.

G-C<sup>#</sup> exhibited a failure mode that was characterised by the longitudinal cracks perpendicular to the fibre orientation. G-C1 (Fig. 8b) exhibited the most violent and most severe degree of failure among the G-C<sup>#</sup> specimens, owing to the rupture of fibres through its entire height, followed by G-C2 (Fig. 8c) and G-C3 (Fig. 8e), respectively, which exhibited local fibre rupture at the top portion. Interestingly, this localised failure was also reported

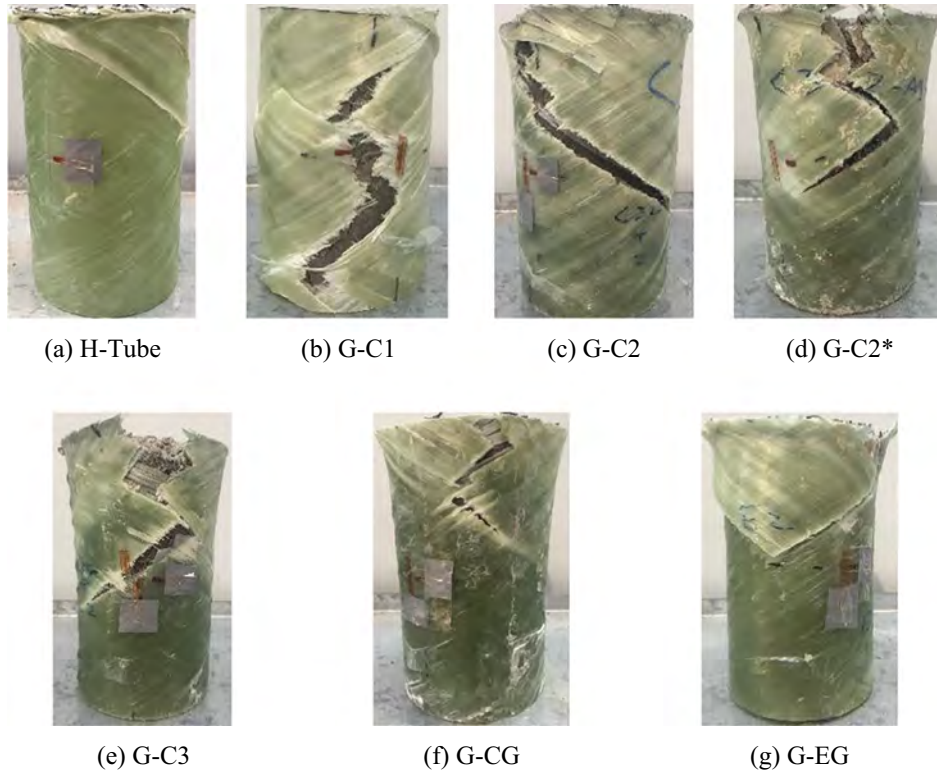


Fig. 8. Typical compression failure of hollow and filled GFRP tubes.

by Vincent and Ozbakkaloglu [29] for FRP-tube encased specimens. The curing of concrete inside the tube resulted in a localised concrete shrinkage at the top because the evaporation takes place only in this region. Hence, the concrete shrinkage should be avoided in the practical engineering applications. G-CG (Fig. 8f) also exhibited similar failure mode as G-C3 specimens but with shorter cracks and less violent failure. On the other hand, more localised failure was observed in G-EG (Fig. 8g). An upside down triangle-shaped FRP rupture was observed in the upper part of G-EG, which seems to be a replicate of the top fracture that was observed in EG (Fig. 6e).

Fig. 8d presents the post-failure configuration of G-C2\*. As can be seen in the figure, G-C2\* exhibited nearly similar failure as G-C2, but with a lesser degree of fibre's rupture. G-C2\* appeared to confine the fibre rupture along the height of the tube and prevented the propagation of fibre rupture around the tube, suggesting the influence of internal surface roughening. In fact, it was evident in G-C2 (Fig. 9a) that the whole concrete cylinder was completely detached from the surface of the tubes while G-C2\* showed otherwise (Fig. 9b), wherein some concrete was attached to the tubes owing to the epoxy grout and concrete gravel that enhanced the bonding between the concrete infill and the tube.

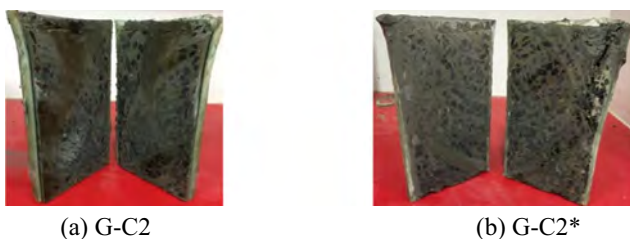


Fig. 9. Post-failure configuration of G-C2 and G-C2\*.

### 3.2.2. Stress-strain behaviour

Fig. 10 shows the representative axial stress-axial strain ( $\sigma_c - \epsilon_c$ ) curves of the grout-filled GFRP tubes. The typical  $\sigma_c - \epsilon_c$  behaviour of G-C# specimens was embodied by a monotonically increasing bi-linear curve. It is an increasing type of  $\sigma_c - \epsilon_c$  curve, wherein both of the significantly enhanced compressive strength and ultimate strain were reached at the same time [30]. The initial rapidly ascending linear segment represents the elastic region wherein the axial behaviour of the G-C# was comparable to that of their corresponding infills, which can be expected since the behaviour of the specimen at this stage was governed by the core infills. As long as the axial stress is lower than the compressive strength of the concrete core, the core dilation will be insignificant to activate the passive confinement of the low modulus GFRP tube and hence, will not influence the overall behaviour of the specimen [31,32]. In fact, negligible hoop strain readings up until an applied stress equivalent to the compressive strength of the infills were recorded during the test as shown in Fig. 11. Furthermore, this can be mathematically proven by calculating the axial rigidity

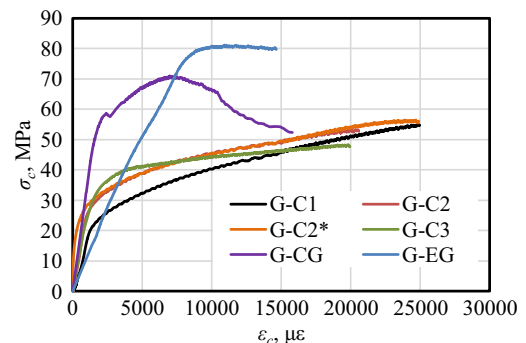


Fig. 10. Axial stress-axial strain curves of the grout-filled GFRP tubes.

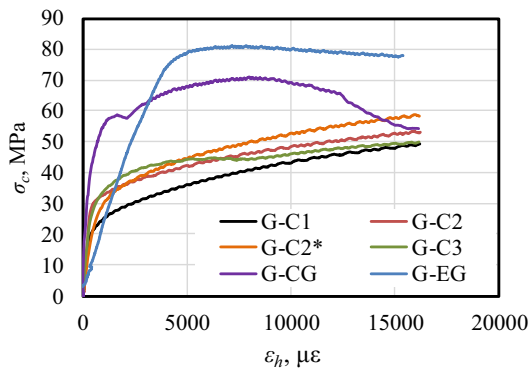


Fig. 11. Axial stress-hoop strain curves of the grout-filled GFRP tubes.

( $EA$ ) of the filled GFRP tube system, wherein the  $EA$  of C1, C2, and C3 were equivalent to 97.2%, 97.4% and 97.6% of the overall  $EA$  of G-C1, G-C2, and G-C3, respectively, suggesting that more loads were attracted by the infills during the elastic stage. The next segment was represented by another linear segment with a reduced slope ( $E_2$ ) that embodied the plastic hardening behaviour of the specimens. The infills undergo more severe crushing and cracking that fully activated the passive confinement of the tubes as evidenced by the large amount of strain values obtained along the hoop direction. At this stage, the GFRP tube mainly governed the behaviour of the specimens. The GFRP tubes filled with C1 infill yielded the highest  $E_2$  than those filled with C2 and C3, respectively. The specimens did not show any response after reaching their peaks. A nonlinear behaviour was observed between the two linear segments that indicated the initiation and propagation of concrete crushing and cracking, and the partial activation of the tubes.

The typical  $\sigma_c - \varepsilon_c$  curve of G-CG (Fig. 10) specimens, on the other hand, can be categorised as a decreasing type featured by a post-peak descending branch [30]. A slight load drop occurred after the initial peak. This drop marked the transition from linear to non-linear behaviour and was not observed in concrete infills having compressive strength lower than that of the cementitious-grout infills (48.9 MPa). Vincent and Ozbakkaloglu [29] reported that this phenomenon happened in specimens filled with high strength and ultra-high strength concrete (59 MPa to 112 MPa) and not in the specimens filled with normal strength concrete (34.8 MPa to 38.0 MPa). However, this phenomenon will start to transpire at a stress ranges from 38.0 MPa to 48.9 MPa. After reaching the peak or the confined compressive strength, a softening segment occurred. At this stage, more severe infill crushing and cracking transpired concomitant with fibre rupture and crushing of matrix of the GFRP tubes. The compressive stress at FRP rupture was higher than that of the compressive strength of the infill, suggesting that CG were still sufficiently confined.

The  $\sigma_c - \varepsilon_c$  behaviour of G-EG specimens can be represented by a bilinear curve. The initial linear branch was similar to that of the cylindrical epoxy grouts. The second linear segment tend to show

the plateau behaviour of the specimens. A short nonlinear transition zone transpired in between the two segments that marked the beginning of the GFRP tube's confinement.

G-C2\* exhibited nearly identical shape of stress-axial strain behaviour as G-C2. Nevertheless, these specimens showed different hoop strain readings at comparable loads. At lower loads, G-C2\* yielded higher hoop strains than G-C2, suggesting the early activation of the passive confinement of the GFRP tubes in G-C2\*. At higher loads, however, lower hoop strains were recorded for G-C2\* compared to G-C2, which tend to suggest that the circumferential stresses are more uniformly distributed in G-C2\* compared to G-C2. Further studies are suggested to verify these findings.

In general, upon exceeding the strength of the infills, all the filled GFRP specimens produced higher axial strains than hoop strains for the same magnitude of applied stress. This observation is in contrast with the earlier findings [31], wherein the lateral strains increase more quickly than the axial strains. The discrepancy may be due to the difference between the fibre stacking sequence. The GFRP tubes used in the study had a stacking sequence of  $-45^\circ/+45^\circ/-45^\circ/+45^\circ$  with respect to hoop direction while the previous study utilised tubes with the principal fibres oriented perpendicular to the column axis ( $0^\circ$  orientation). Additional research works are recommended to verify this finding.

### 3.2.3. Ultimate strength

Table 3 summarises the average peak load ( $P_{gu}$ ) and the peak stress ( $\sigma_{gu}$ ) and corresponding standard deviation ( $s_g$ ) of the filled GFRP tubes. The  $P_{gu}$  and  $\sigma_{gu}$  of G-C1, G-C2, and G-C3 were 692.7 kN and 78.5 MPa, 599.5 kN and 67.9 MPa, and 498.2 kN and 56.5 MPa, respectively. It was obvious from the results that the strength of filled GFRP tubes decreases as the compression strength of the concrete core infill increases. The  $P_{gu}$  were 616 kN and 798 kN for G-CG and G-EG, respectively, which are equivalent to  $\sigma_{gu}$  of 78.4 MPa and 101.6 MPa, respectively. The recorded  $P_{gu}$  and  $\sigma_{gu}$  were 639.0 kN and 72.4, respectively, for G-C2\* that translate to an increase of approximately 7%.

### 3.2.4. Axial and hoop strains

The average axial and hoop strains at peak stress ( $\varepsilon_{gu}$  and  $\varepsilon_{hu}$ , respectively) and at FRP rupture ( $\varepsilon_{g,rupt}$  and  $\varepsilon_{h,rupt}$ , respectively) in the grout-filled GFRP tubes are also presented in Table 3. G-C1 (24850  $\mu\varepsilon$ ) produced the highest  $\varepsilon_{gu}$  followed by G-C2 (20900  $\mu\varepsilon$ ) and G-C3 (19780  $\mu\varepsilon$ ), respectively. G-CG yielded the lowest  $\varepsilon_{gu}$  equivalent to 6980  $\mu\varepsilon$  and  $\varepsilon_{g,rupt}$  of 16,140  $\mu\varepsilon$  while the  $\varepsilon_{gu}$  and  $\varepsilon_{g,rupt}$  for G-EG were equivalent to 10,800  $\mu\varepsilon$  and 15,390  $\mu\varepsilon$ , respectively. In the case of concrete-filled GFRP tubes,  $\varepsilon_{g,rupt}$  and  $\varepsilon_{h,rupt}$  were equivalent to their  $\varepsilon_{gu}$  and  $\varepsilon_{hu}$ , respectively. The  $\varepsilon_{gu}$  of G-C2\* was 18% larger than that of G-C2. As can be expected, the GFRP tubes failed in an approximately the same magnitude of  $\varepsilon_{h,rupt}$ , with an average value of 16,050  $\mu\varepsilon$ .

### 3.2.5. Strength and strain enhancement ratios

Fig. 12 shows the typical relationship between the normalised axial stress, which is the results of dividing  $\sigma_{gu}$  by  $\sigma_{iu}$ , and the normalised axial strain, which is the results of dividing  $\varepsilon_{gu}$  by  $\varepsilon_{iu}$ . Based

Table 3  
Peak axial load, peak axial stress and corresponding standard deviation and strains at rupture of grout-filled GFRP tubes.

Specimen	$P_{gu}$ , kN	$\sigma_{gu}$ , MPa	$s_g$ , MPa	$\frac{\sigma_{gu}}{\sigma_{iu}}$	$\varepsilon_{gu}$ , $\mu\varepsilon$	$\varepsilon_{hu}$ , $\mu\varepsilon$	$\varepsilon_{g,rupt}$ , $\mu\varepsilon$	$\varepsilon_{h,rupt}$ , $\mu\varepsilon$	$\frac{\varepsilon_{gu}}{\varepsilon_{iu}}$	$\mu$	$\varepsilon_{g5}$ , $\mu\varepsilon$	$\mu$	$U_T$ , MPa
G-C1	692.7	78.5	11.4	6.2	24,850	16,200	24,850	16,200	37.6	4266	24,850	5.8	1.01
G-C2	599.5	67.9	5.0	4.1	20,900	16,230	20,900	16,230	27.7	3235	20,900	6.5	0.88
G-C2*	639.0	72.4	2.5	4.4	20,240	16,180	24,665	16,180	32.7	3448	24,665	7.2	1.13
G-C3	498.2	56.5	3.6	2.2	19,780	16,170	19,780	16,170	15.1	2108	19,780	9.4	0.83
G-CG	645.1	73.1	0.3	1.6	6980	7990	16,116	16,140	5.9	2131	10,976	5.2	0.93
G-EG	798.5	90.5	7.2	1.3	10,800	7170	15,200	15,390	1.0	9048	10,914	1.2	0.84

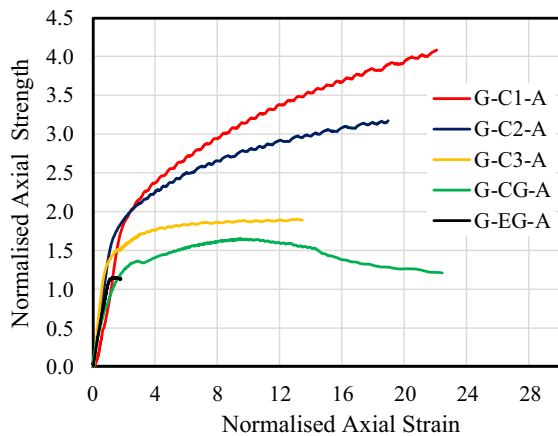


Fig. 12. Relation between the normalised axial stress and the normalised axial strain.

on the figure, the enhancement of the strength and strain of the concrete-filled GFRP tubes were comparable to each other when the applied stress was lower than the compressive strength of the cylindrical infills. At higher applied stress, however, G-C1 yielded the highest strength and strain gain followed by the tubes filled with Grade 2 and 3, respectively. Table 3 presents the strength enhancement ratio ( $\sigma_{gu}/\sigma_{iu}$ ) and strain enhancement ratio ( $\varepsilon_{gu}/\varepsilon_{iu}$ ) of the concrete-filled GFRP tubes. Based on the table, the highest strength and strain gain ratios were observed in GFRP tubes filled with Grade 1 concrete (6.2 and 37.6, respectively) followed by the tubes filled with Grades 2 (4.1 and 27.7, respectively) and 3 (2.2 and 15.1, respectively), respectively.

Next to G-C<sup>#</sup> specimens, G-CG exhibited  $\sigma_{gu}/\sigma_{iu}$  and  $\varepsilon_{gu}/\varepsilon_{iu}$  equivalent to 1.6 and 5.9, respectively. G-EG exhibited the least  $\sigma_{gu}/\sigma_{iu}$  (1.3) and  $\varepsilon_{gu}/\varepsilon_{iu}$  (1.0). The  $\sigma_{gu}/\sigma_{iu}$  and  $\varepsilon_{gu}/\varepsilon_{iu}$  of G-C2\* were 1.1 and 1.2 times that of their corresponding values in G-C2, respectively.

### 3.2.6. Ductility and energy absorption

Table 3 also shows the ductility ( $\mu$ ) and energy absorption ( $U_T$ ) of the tested filled GFRP tubes. The parameter  $\mu$  was calculated by taking the ratio of the post-peak strain at a stress  $0.85\sigma_{gu}$  ( $\varepsilon_{85}$ ) to the elastic strain limit ( $\varepsilon_1$ ), wherein  $\varepsilon_1$  was determined from the ratio between  $\sigma_{gu}$  and  $MOE_i$ . The parameter  $U_T$ , on the other hand, was determined by taking the area under the stress-strain of the specimen.

It can be seen from the table that  $\mu$  increased in the order of G-C1 (5.8), G-C2 (6.5), and G-C3 (9.4) following the ductility of the corresponding infills. Opposite trend, however, was observed in terms of  $U_T$ , wherein G-C1 (1.01 MPa) exhibited the highest followed by G-C2 (0.88 MPa) and G-C3 (0.83 MPa), respectively. The opposite trend of  $U_T$  is attributed to the low  $\varepsilon_{g,rupt}$  values of G-C3 and G-C2 in comparison with G-C1. G-EG produced the least  $\mu$  (1.2) and  $U_T$  (0.84 MPa), respectively, while G-CG yielded 5.2 and 0.93 MPa, respectively. G-C2\* yielded  $\mu$  and  $U_T$  that were 11% and 28%, respectively, higher than that of G-C2.

## 4. Discussion

### 4.1. Effect of concrete grade on the behaviour of GFRP tubes

This section presents the effects of the concrete grade on the behaviour of the GFRP tubes. In general, the amount of stress needed to activate the passive confinement of the GFRP tubes decreases with the compression strength of the concrete. This is

attributed to the low compression resistance of C1 infills, which underwent early crushing and cracking at lower applied stress. The advance activation of the passive confinement resulted in the enhancement of the performance of the GFRP tubes. In general, the strength and strain enhancement ratio decrease when the compressive strength of the concrete core infill increase. This result may be explained by the fact that the concrete brittleness increases with its strength, thereby changing the crack pattern development from heterogenic micro-cracks to localised macro-cracks [33]. The localised crack pattern limits the stress distribution along and around the GFRP tubes as was apparent in the failure configuration of the specimens. The fibre rupture transpired along the height of G-C1 while those with higher strength concrete (G-C2 and G-C3) experienced local fibre rupture mainly at the upper section of the GFRP tube.

Interestingly, the same trend of straight gain was reported by Vincent and Ozabakkaloglu [29]. According to their study, the FRP tube-encased specimens with normal strength concrete yielded the highest strength enhancement ratio followed by the high strength concrete and the ultra-high strength concrete, respectively. Berthet et al. [31] also reported the same trend, but for specimens with concrete core having compressive strength of 100–200 MPa only. Further studies are recommended to verify these differences.

### 4.2. Effect of infill types on the behaviour of GFRP tubes

Different stress-strain behaviour were observed upon filling the GFRP tubes with different types of infills. The concrete-, cementitious-, and epoxy-filled GFRP tubes yielded increasing, decreasing, and plateauing stress-strain curves, respectively. This observation could be attributed to the post-peak response of the infills, wherein the cylindrical concrete infills yielded a degrading stress-strain curves. The cylindrical cementitious grout did not show any post peak response while the cylindrical epoxy grout showed a decreasing post-peak response, but at a faster rate compared to cylindrical concrete infills. The concrete-filled GFRP tubes showed the highest strength and strain enhancement ratios while the epoxy-filled GFRP tubes showed the least. This finding suggested that the epoxy grout was not effectively confined. This can be attributed to the high deformability and insufficient stress absorption of the epoxy grout, which immediately stressed the GFRP tube as soon as the load was applied. Shamsuddoha et al. [34] reported that, for pipeline repairs using FRP systems, the low stiffness epoxy grout did not absorb the stress from the steel and hence, did not transfer the stress efficiently to the FRP. It is important to note however that the epoxy grouts considered by Shamsuddoha et al. [34] has a MOE of only up to 10 GPa which is slightly lower than that of the epoxy grouts used in this study. On the other hand, the ductility tend to increase with the concrete compressive strength; however, an opposite trend was found in terms of the energy absorption. Upon using different types of grout infills, no trend was found with respect to the ductility and the energy absorption. This could be expected since each type of infill have different material composition and mechanical properties.

### 4.3. Effect of surface preparation on the behaviour of filled GFRP tubes

The modification of the internal surface of GFRP tubes, by coating the surface with 5 mm coarse aggregates using epoxy grout as the adhesive, eliminated the presence of gaps in the GFRP tube-infill interface and enhanced the stress transfer between the infill and the GFRP tube, which consequently improved the load capacity, ductility, and energy absorption of the filled GFRP tubes. The good adhesion between the infill and the GFRP tube caused the early activation of the GFRP tubes and hence, the improvement

of the overall performance. This observation corroborates Deb and Bhattacharyya [14] findings for FRP bonding effects.

**5. Theoretical modelling**

This section details the development of theoretical models that can predict the ultimate strength, ultimate strain and stress-strain curve of the tested grout-filled GFRP tubes. The developed equations will assist in evaluating on how the important characteristics of the infill materials would affect the overall behaviour of the composite repair system. This will be useful in selecting the most suitable infill that will meet the requirement of different FRP repair system’s application, and to effectively utilise the inherent properties of composite materials.

**5.1. Development of prediction equations for the FRP system**

Different stress-strain ( $\sigma_c - \epsilon_c$ ) models were adopted in this study to develop prediction equations for the tested grout-filled GFRP tubes as they reasonably described the behaviour of the tested specimens. For concrete-filled GFRP tubes, with an increasing type of stress-strain curve, the expression proposed by Lam and Teng [30] for FRP-confined concrete (Eq. (2)) was used. The symbols  $E_c$ ,  $f'_{cc}$ , and  $\epsilon_{cu}$  were replaced with  $MOE_i$ ,  $\sigma_{gu}$ , and  $\epsilon_{gu}$ , respectively.

$$\sigma_c = \begin{cases} MOE_i \epsilon_c - \frac{(MOE_i - E_2)^2}{4f_o} \epsilon_c^2 & \text{for } 0 \leq \epsilon_c \leq \epsilon_t \\ f_o + E_2 \epsilon_c & \text{for } \epsilon_t \leq \epsilon_c \leq \epsilon_{gu} \end{cases} \quad (2)$$

$$\epsilon_t = \frac{2f_o}{MOE_i - E_2} \quad (a)$$

$$E_2 = \frac{\sigma_{gu} - f_o}{\epsilon_{gu}} \quad (b)$$

where  $f_o$  = stress-axis intercept of the second linear segment,  $\epsilon_t$  = strain at which the parabolic segment meets the second linear segment, and  $E_2$  = slope of the second linear segment. The relation between  $\sigma_{iu}$  and  $f_o$  of concrete infills is shown in Fig. 13. Based on the regression analysis,  $f_o$  can be predicted using the equation below:

$$f_o = 10.4\sigma_{iu}^{0.4} \quad (3)$$

The peak stress ( $\sigma_{gu}$ ) and strain at peak ( $\epsilon_{gu}$ ) were estimated using Eqs. (4) and (5), respectively, wherein the characters  $\sigma_{l,a}$  (Eq. (6)),  $t_g$ ,  $d_{gi}$ ,  $\epsilon_{iu}$ , and  $\epsilon_{hu}$  were used in place of  $f_{l,a}$  (maximum confining pressure),  $t$ ,  $d$ ,  $\epsilon_{co}$ , and  $\epsilon_{h,rup}$  respectively:

$$\frac{\sigma_{gu}}{\sigma_{iu}} = a \frac{\sigma_{l,a}}{\sigma_{iu}} + b \quad (4)$$

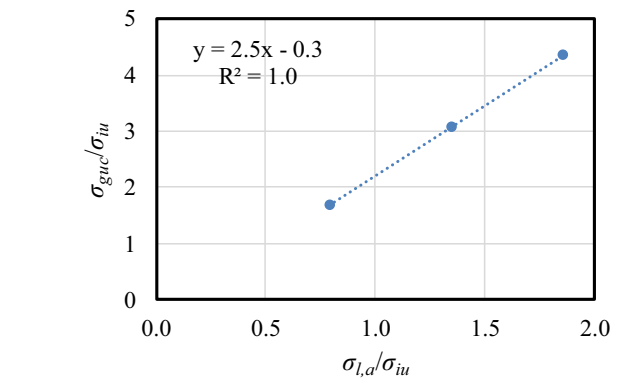


Fig. 14.  $\sigma_{gu}/\sigma_{iu}$  vs  $\sigma_{l,a}/\sigma_{iu}$ .

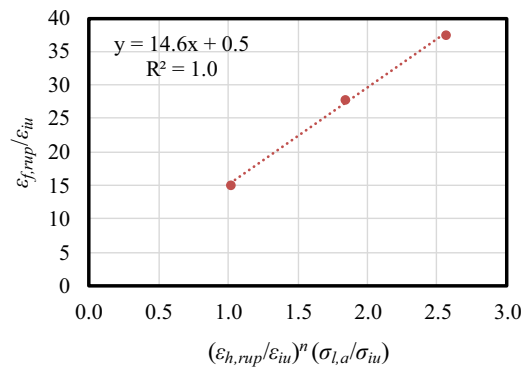


Fig. 15.  $\epsilon_{hu}/\epsilon_{iu}$  vs  $(\epsilon_{hu}/\epsilon_{iu})^n (\sigma_{l,a}/\sigma_{iu})$ .

**Table 4**  
Values of constants  $a$ ,  $b$ ,  $c$ ,  $d$ , and  $n$ .

Specimen	$a$	$b$	$c$	$d$	$n$
G-C#	2.5	-0.3	14.6	0.5	0.1
G-CG	2.5	-0.3 k	14.6	0.5 k	0.1
G-EG	2.5	-0.3 k	14.6/k	0.5 k	0.1 k <sup>2</sup>

\* Note:  $k = 3$ .

$$\frac{\epsilon_{gu}}{\epsilon_{iu}} = c \left( \frac{\sigma_{l,a}}{\sigma_{iu}} \right) \left( \frac{\epsilon_{hu}}{\epsilon_{iu}} \right)^n + d \quad (5)$$

$$\sigma_{l,a} = \frac{2E_f t_g \epsilon_{hu}}{d_{gi}} \quad (6)$$

The constants  $a$ ,  $b$ ,  $c$ ,  $d$  and  $n$  were determined from the regression analysis (Figs. 14 and 15) of the experimental results and are summarised in Table 4.

The initial ascending linear and nonlinear stress-strain segments of cementitious- and epoxy-filled GFRP tubes ( $0 \leq \epsilon_c \leq \epsilon_{gu}$ ) were modelled using Popovics’ [35] equation while the post-peak descending segment ( $\epsilon_{gu} < \epsilon_c \leq \epsilon_{g,rup}$ ) was linearly modelled using Wei and Wu’s equations [36]. Eqs. (4)–(6) were also used to estimate  $\sigma_{gu}$  and  $\epsilon_{gu}$ ; however, a modification factor  $k$ , equivalent to 3, was included to constants  $b$ ,  $c$ ,  $d$ , and  $n$  as shown in Table 4.

Fig. 16 presents the comparison between the theoretical and experimental stress-strain curves of the tested filled GFRP tubes. It can be seen from the figure that there is a good agreement between the two curves. Further experimental works, however, are recommended to enhance the accuracy the proposed models in predicting the behaviour of GFRP tubes filled with infills of different physical and mechanical properties.

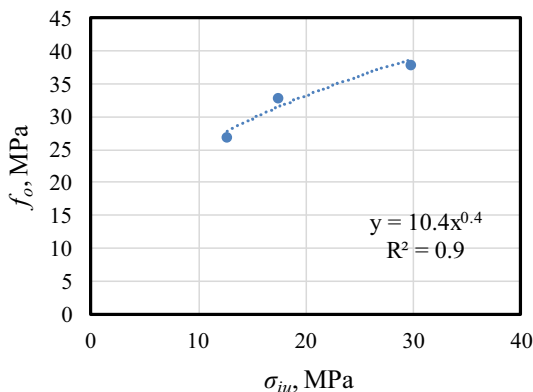


Fig. 13. Relationship between  $\sigma_{iu}$  and  $f_o$ .

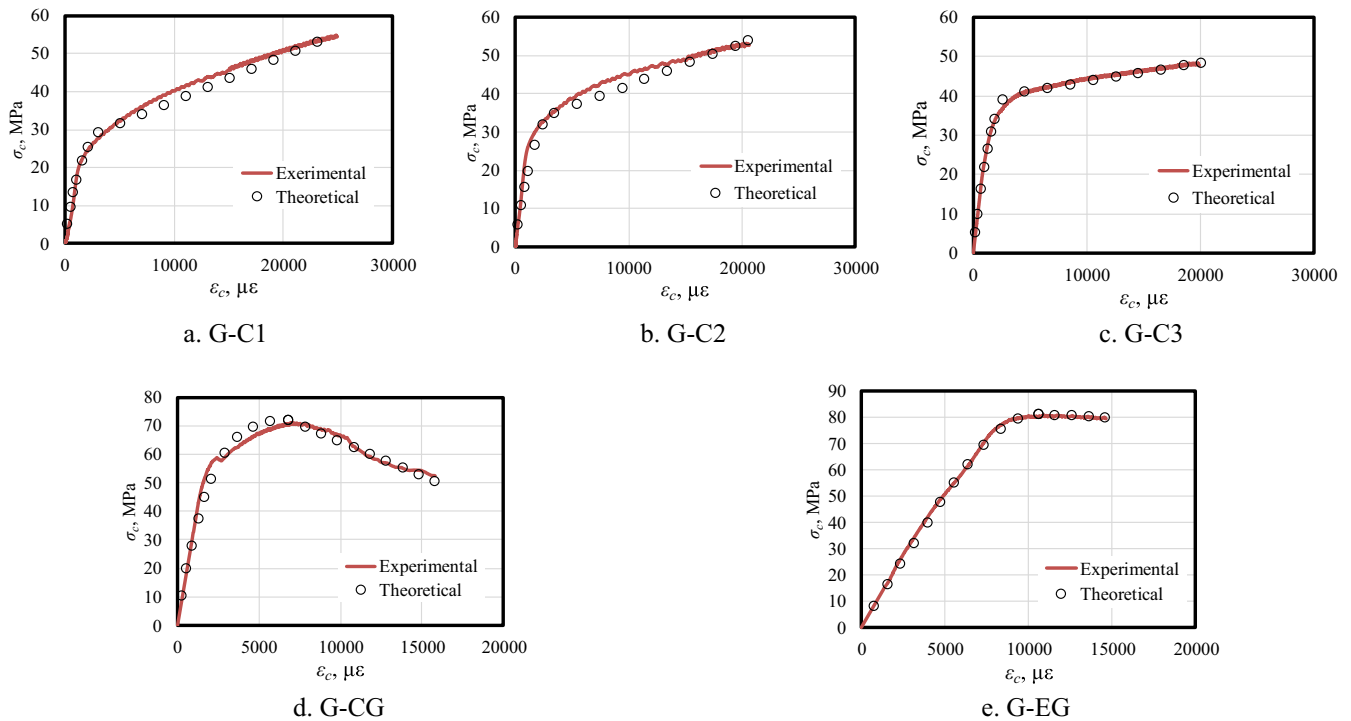


Fig. 16. Experimental and theoretical axial stress-axial strain curves of the grout-filled GFRP tubes.

## 6. Conclusions

The effects of filling the GFRP tubes with concrete, cementitious and epoxy grouts on the behaviour of a simulated prefabricated composite repair system was investigated in this study. Based on the experimental results, the following conclusions were derived:

- The behaviour of the infill materials was largely dependent on the modulus of elasticity and the compressive strength of the grout infill. High compressive strength and high modulus cementitious and epoxy grouts failed in a more brittle manner than the concrete infill. After the peak load, the concrete-, cementitious-, and epoxy-filled GFRP tubes yielded increasing, decreasing, and plateauing stress-strain curves.
- The type of the grout infill determined the overall behaviour of the composite repair system. The brittle failure behaviour of the cementitious and epoxy grouts lead to localised failure in the FRP repair system while the progressive cracking and crushing of the concrete infill resulted in effective utilisation of the high strength properties of the composite materials.
- The high compressive strength of the infill material limited its capacity to transfer the stresses uniformly around the tubes due to the increased brittleness. This resulted in the strength and strain enhancement ratios of only 1.3 and 1.0, respectively for the GFRP repair system filled with epoxy grouts but up to 6.2 and 38 times, respectively for the tubes filled with the lowest strength and modulus concrete.
- The provision of epoxy and coarse aggregates inside the GFRP tube surface enhanced the stress transfer between the tube and infill. This consequently improved the load capacity, ductility and energy absorption by at least 10%. Furthermore, this prevented the propagation of fibre rupture around the composite repair system leading to a more ductile behaviour than the one without roughened surface.
- The developed model accurately predicted the overall compressive behaviour of GFRP tubes filled with grouts of different com-

pressive strength and Modulus of Elasticity. This model is very useful in determining the appropriate elastic and strength properties of the grout infill for repairing existing structures with prefabricated composite jackets.

## Conflict of interest

There is no conflict of interest.

## Acknowledgement

The authors gratefully acknowledge Joinlox™ Pty. Ltd., Australia for the financial, materials and technical support in conducting this study.

## References

- [1] R. Azam, A.K. El-Sayed, K. Soudki, Behaviour of reinforced concrete beams without stirrups subjected to steel reinforcement corrosion, *J. Civil Eng. Manage.* 22 (2) (2016) 146–153.
- [2] M. Cassidy, J. Waldie, S. Palanisamy, A Method to Estimate the Cost of Corrosion for Australian Defence Force Aircraft, (2015).
- [3] N. Delatte, *Failure, Distress and Repair of Concrete Structures*, Elsevier, 2009.
- [4] M. Sakr, M. El Naggar, M. Nehdi, Interface characteristics and laboratory constructability tests of novel fiber-reinforced polymer/concrete piles, *J. Compos. Constr.* 9 (3) (2005) 274–283.
- [5] S. Pessiki, K.A. Harries, J.T. Kestner, R. Sause, J.M. Ricles, Axial behavior of reinforced concrete columns confined with FRP jackets, *J. Compos. Constr.* 5 (4) (2001) 237–245.
- [6] J. Teng, J. Chen, S.T. Smith, L. Lam, Behaviour and strength of FRP-strengthened RC structures: a state-of-the-art review, *Proc. Inst. Civil Eng. Struct. Build.* 156 (1) (2003) 51–62.
- [7] T. Ozbakkaloglu, J.C. Lim, T. Vincent, FRP-confined concrete in circular sections: review and assessment of stress-strain models, *Eng. Struct.* 49 (2013) 1068–1088.
- [8] A. Manalo, C. Sirimanna, W. Karunasena, L. McGarva, P. Falzon, Pre-impregnated carbon fibre reinforced composite system for patch repair of steel I-beams, *Constr. Build. Mater.* 105 (2016) 365–376.
- [9] R. Lopez-Anido, A.P. Michael, T.C. Sandford, B. Goodell, Repair of wood piles using prefabricated fiber-reinforced polymer composite shells, *J. Perform. Construct. Facil.* 19 (1) (2005) 78–87.

- [10] A.C. Manalo, W. Karunasena, C. Sirimanna, G.B. Maranan, Investigation into fibre composites jacket with an innovative joining system, *Constr. Build. Mater.* 65 (2014) 270–281.
- [11] P. Vijay, P.R. Soti, H.V. GangaRao, R.G. Lampo, J.D. Clarkson, Repair and strengthening of submerged steel piles using GFRP composites, *J. Bridge Eng.* (2016). 04016038.
- [12] M. Shamsuddoha, M.M. Islam, T. Aravinthan, A. Manalo, K.-T. Lau, Characterisation of mechanical and thermal properties of epoxy grouts for composite repair of steel pipelines, *Mater. Des.* 52 (2013) 315–327.
- [13] W. Sum, K. Leong, Numerical study of annular flaws/defects affecting the integrity of grouted composite sleeve repairs on pipelines, *J. Reinf. Plast. Compos.* (2013). 0731684413503721.
- [14] A. Deb, S. Bhattacharyya, Investigation into the effect of bonding on FRP-wrapped cylindrical concrete columns, *J. Compos. Constr.* 14 (6) (2010) 706–719.
- [15] Z. Yan, C.P. Pantelides, Concrete column shape modification with FRP shells and expansive cement concrete, *Constr. Build. Mater.* 25 (1) (2011) 396–405.
- [16] H. Saadatmanesh, M. Ehsani, L. Jin, Seismic retrofitting of rectangular bridge columns with composite straps, *Earthquake Spectra* 13 (2) (1997) 281–304.
- [17] A. Beddiar, R. Zitoun, F. Collombet, Y. Grunevald, M. Abadlia, N. Bourahla, Compressive behaviour of concrete elements confined with GFRP-prefabricated bonded shells, *Eur. J. Environ. Civ. Eng.* 19 (1) (2015) 65–80.
- [18] Z. Yan, C.P. Pantelides, L.D. Reaveley, Posttensioned FRP composite shells for concrete confinement, *J. Compos. Constr.* 11 (1) (2007) 81–90.
- [19] J. Teng, L. Lam, Compressive behavior of carbon fiber reinforced polymer-confined concrete in elliptical columns, *J. Struct. Eng.* 128 (12) (2002) 1535–1543.
- [20] J. Williams, FRP Pile Jacket Solution has no 'Pier' in Timber Pile Restoration, 2009.
- [21] Bluey, Technical Data Sheet: BluCem GP60 Construction Grout, 2017.
- [22] Chemrite, Technical Data Sheet: Chemrite Pad Grout, Chemrite Technologies, 2014.
- [23] ISO 527-1, ISO 527-1:1995 Plastics – determination of tensile properties: General principles, International Organization for Standardization., 1995.
- [24] ISO 14126, ISO 14126: 1999-Fibre-Reinforced Plastic Composites. Determination of Compressive Properties in the In-Plane Direction, International Organization for Standardization., 1999.
- [25] ISO 1172, ISO 1172, Textile glass reinforced plastics, Prepregs, moulding compounds and laminates 1996 Determination of the textile-glass and mineral-filler content, Calcination methods International Organization for Standardization. 1996S.
- [26] M. Hajsadeghi, F.J. Alaei, A. Shahmohammadi, Investigation on behaviour of square/rectangular reinforced concrete columns retrofitted with FRP jacket, *J. Civil Eng. Manage.* 17 (3) (2011) 400–408.
- [27] A. Parvin, A.S. Jamwal, Performance of externally FRP reinforced columns for changes in angle and thickness of the wrap and concrete strength, *Compos. Struct.* 73 (4) (2006) 451–457.
- [28] ASTM C39/C39M, ASTM C39/C39M-15a Standard Test Method for Compressive Strength of Cylindrical Concrete Specimens, ASTM International, 2015.
- [29] T. Vincent, T. Ozbakkaloglu, Influence of concrete strength and confinement method on axial compressive behavior of FRP confined high-and ultra high-strength concrete, *Compos. B Eng.* 50 (2013) 413–428.
- [30] L. Lam, J. Teng, Design-oriented stress-strain model for FRP-confined concrete, *Construct. Build. Mater.* 17 (6) (2003) 471–489.
- [31] J. Berthet, E. Ferrier, P. Hamelin, Compressive behavior of concrete externally confined by composite jackets. Part A: Exp. Study, *Constr. Build. Mater.* 19 (3) (2005) 223–232.
- [32] A. Boumarafi, A. Abouzied, R. Masmoudi, Harsh environments effects on the axial behaviour of circular concrete-filled fibre reinforced-polymer (FRP) tubes, *Compos. B Eng.* 83 (2015) 81–87.
- [33] T. Ozbakkaloglu, E. Akin, Behavior of FRP-confined normal-and high-strength concrete under cyclic axial compression, *J. Compos. Constr.* 16 (4) (2011) 451–463.
- [34] M. Shamsuddoha, Behaviour of Infilled Rehabilitation System with Composites for Steel Pipe, University of Southern Queensland, 2014.
- [35] S. Popovics, A numerical approach to the complete stress-strain curve of concrete, *Cem. Concr. Res.* 3 (5) (1973) 583–599.
- [36] Y.-Y. Wei, Y.-F. Wu, Unified stress-strain model of concrete for FRP-confined columns, *Constr. Build. Mater.* 26 (1) (2012) 381–392.

## **Chapter 4**

### **Behaviour of damaged concrete columns repaired with novel FRP jacket**

Chapter 3 provided a better understanding on the overall behaviour of GFRP tubes filled with different grout material and provided information on the most practical infill for the prefabricated FRP jacket. This chapter investigates the axial behaviour of large scale RC columns with simulated damage and repaired with the novel FRP jacket. Nine large scale circular columns (1000 mm in height and 250 mm in diameter) and one large scale square column (1000 mm in height and 220 mm x 220 mm in cross-section) were fabricated with 25% and 50% simulated steel corrosion and 50% and 100% concrete cover damage. The steel corrosion damage was achieved by cutting the longitudinal reinforcement in the test region and replacing them with non-structural PVC pipe (16-mm diameter), while bubble wraps were wrapped around the steel reinforcement cages to simulate the concrete cover damage. The damaged specimens were then repaired with 450 mm diameter, 700 mm height and 3 mm thick novel FRP jacket, and tested under concentric axial load until failure. The study found out that the jacket is capable of restoring the axial strength by 99% and 95% for RC columns with 25% and 50% steel corrosion damage, respectively. While the repaired columns with 50% and 100% concrete cover damage restored their axial load capacity by 95% and 82%, respectively. Also, it showed the novel FRP repair system was more effective in repairing circular than square columns due to the stress concentration at the corners of the latter. The study concluded that the current system is sufficient for structural repair; however, further improvements are necessary to modify the joint to extend the jacket's application as a strengthening system. In addition, the developed theoretical equation that accounts for the partial confinement effect (jacket height/column height) accurately calculated the ultimate axial strength of the damaged column repaired with the prefabricated FRP jacket. The effect of eccentricity induced from asymmetric simulated damage was neglected in the developed theoretical model as the provision of the FRP jacket stabilised the damaged section. As the bridge piles are subjected to both, axial and lateral loads, understanding the flexural behaviour of damaged RC members repaired with the FRP jacket was implemented in Chapter 5.



# Behavior of Damaged Concrete Columns Repaired with Novel FRP Jacket

Ali A. Mohammed<sup>1</sup>; Allan C. Manalo<sup>2</sup>; Ginghis B. Maranan<sup>3</sup>;  
Yan Zhuge<sup>4</sup>; P. V. Vijay<sup>5</sup>; and John Pettigrew<sup>6</sup>

**Abstract:** Jacketing using prefabricated fiber reinforced polymer (FRP) composite shells is an attractive repair system for deteriorating structures exposed to the marine environment. However, most available techniques lack an effective joining system capable of providing structural continuity along the hoop direction. This paper addresses the evaluation of the efficiency of a FRP jacket with an innovative joining system and the behavior of damaged concrete columns repaired with jackets considering several parameters, that is, level of steel corrosion, level of concrete cover damage, and the shape effect. The results showed that the jacket restored the load-carrying capacity by 99% and 95% for columns with 25% and 50% corrosion damage, respectively. Moreover, the jacket effectively restored the axial load capacity of columns with 50% and 100% concrete cover damage by 95% and 82%, respectively. The proposed system was more effective in circular columns because the axial load capacity of the repaired columns was 43% higher than the square columns. A theoretical analysis of the axial load capacity of the repaired columns indicated an excellent agreement with the experimental results. DOI: [10.1061/\(ASCE\)CC.1943-5614.0000942](https://doi.org/10.1061/(ASCE)CC.1943-5614.0000942). © 2019 American Society of Civil Engineers.

**Author keywords:** Prefabricated FRP composite jacket; novel pile repair system; damaged concrete columns; FRP joint.

## Introduction

Reinforced concrete (RC) structures subjected to harsh environments such as marine or mine-water discharge exposure will undergo severe weathering attacks, resulting in corrosion of the steel reinforcement (Shi et al. 2012). Moreover, marine structures built of RC and timber members usually corrode and/or deteriorate in the splash zone due to the wet-dry cycles, chlorine ingress, and the secondary attacks of marine borers (Baileys 1995; Bazinet et al. 1999; Chellis 1961). Such damaged infrastructure needs repair, replacement, or retrofit to remain in service. More than an estimated \$15 billion annually is spent to maintain the RC bridges in countries such as the United States, Canada, and Europe (Azam et al. 2016). In Australia, corrosion-induced damages cost the economy more than \$13 billion per year from production- and shutdown-related losses during repairs (Cassidy et al. 2015).

<sup>1</sup>Ph.D. Candidate, School of Civil Engineering and Surveying, Centre for Future Materials, Univ. of Southern Queensland, Toowoomba, QLD 4350, Australia. Email: ali.mohammed@usq.edu.au

<sup>2</sup>Associate Professor, School of Civil Engineering and Surveying, Centre for Future Materials, Univ. of Southern Queensland, Toowoomba, QLD 4350, Australia (corresponding author). Email: allan.manalo@usq.edu.au

<sup>3</sup>Lecturer, School of Engineering, Faculty of Science and Engineering, Univ. of Waikato, Hamilton 3216, New Zealand. Email: gmaranan@waikato.ac.nz

<sup>4</sup>Professor, School of Natural and Built Environments, Univ. of South Australia, Adelaide 5001, Australia. Email: yan.zhuge@unisa.edu.au

<sup>5</sup>Assistant Professor, Dept. of Civil and Environmental Engineering, West Virginia Univ., Morgantown, WV 26506. Email: p.vijay@mail.wvu.edu

<sup>6</sup>CEO, Joinlox Pty Ltd., Brisbane, QLD 4105, Australia. Email: johnp@joinlox.com

Note. This manuscript was submitted on June 4, 2018; approved on November 7, 2018; published online on March 12, 2019. Discussion period open until August 12, 2019; separate discussions must be submitted for individual papers. This paper is part of the *Journal of Composites for Construction*, © ASCE, ISSN 1090-0268.

In most cases, repairing rather than replacing the existing damaged structures is more economical. Hence, adopting effective rehabilitation and strengthening techniques can be economically beneficial by minimizing the off-service time of the structure, eventually saving a significant amount of resources. The RC jacket (Vandoros and Dritsos 2008) and the steel jacket (Belal et al. 2015) are very popular as repairing/strengthening techniques for concrete structures. However, the use of versatile fiber-reinforced polymer (FRP) composites has been highly beneficial in addressing some of the limitations of the traditional materials and rehabilitation techniques, such as limited access, sensitive marine environments, weight and complexity of steel anchorage, and others (Delatte 2009; Manalo et al. 2012). The superior characteristics of FRP, such as high strength, corrosion resistance, lightweight, high fatigue resistance, high impact resistance, and durability (Maranan et al. 2016; Muttashar et al. 2017; Sakr et al. 2005), have enabled end users to successfully implement them to rehabilitate damaged and/or deteriorated civil infrastructure (Manalo et al. 2016; Ozbakkaloglu et al. 2013; Pessiki et al. 2001; Teng et al. 2003).

Significant work has been done regarding the utilization of FRP composite materials in the construction industry. For example, FRP composites have been investigated for use as structural elements in construction, such as concrete-filled FRP tubes (CFFT) (Abdallah et al. 2018; Mohamed et al. 2010; Mohamed and Masmoudi 2010). In contrast, as an external confining/repair material, FRP composites can be applied as either a wet lay-up or prefabricated systems (ACI 2008; Manalo et al. 2014; Mohammed et al. 2017). In the wet lay-up, FRP jackets are fabricated onsite by impregnating liquid resins into fibers and then wrapping them around the existing structure. In contrast, the prefabricated systems are manufactured in a factory and delivered to a site ready to be installed. Although many studies have indicated that both systems are effective (Berthet et al. 2005; Nanni and Norris 1995; Teng 2002), the prefabricated composite jacket is favored over the wet lay-up method because the former is easier, quicker, safer to install, and can achieve higher quality under well-controlled manufacturing conditions.

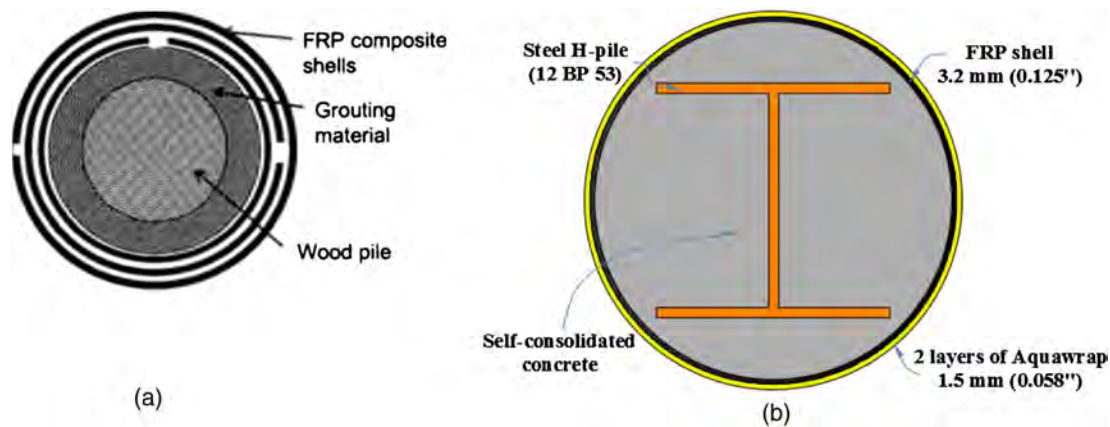


**Fig. 1.** Existing prefabricated FRP repair system: (a) wood pile repair (reprinted from Lopez-Anido et al. 2005, © ASCE); and (b) waterfront structure repair, New York (reprinted from Vijay et al. 2016, © ASCE).

Prefabricated FRP composite jackets are becoming increasingly used to repair regular and underwater structural applications. Once installed, the prefabricated FRP jacket acts as a protective shield and induces lateral confining passive pressure, which eventually strengthens the damaged structure.

Lopez-Anido et al. (2005) proposed a repair system with SCRIMP FRP shells for the protection and structural restoration of deteriorated wood piles [Fig. 1(a)]. This repair system consists of two FRP composite shells that are held together with circumferential metal straps or temporary bands to achieve structural restoration. However, the authors have pointed out that the metal straps could severely deteriorate, which could lead to the opening of FRP shells and the loss of repair system functionality. A prefabricated pile jacket repair system is manufactured with molded fiberglass construction products (MFG-CP) and utilized in the rehabilitation of New York City waterfront structures (Williams 2009). This system used mechanically fastened joint and steel bands to hold the jacket and contain the grout infill. The joint and bands were made of metallic materials that are prone to corrosion. Vijay et al. (2016) combined the use of precured glass FRP (GFRP) shells and water-curable GFRP prepreg fabrics for encasing, wrapping, and rehabilitating twenty water-submerged steel H-piles of a bridge in the United States [Fig. 1(b)]. The annulus between the GFRP shells and the steel piles was filled with self-consolidating concrete. However, the installation of this system requires a two-stage process wherein the precured GFRP shells are installed first and then wrapped with a wet fabric, which increases the installation time and labor cost. A few days of cure time is required for the prepreg fabrics before grouting. However, the ability of commercially available prefabricated composite repair systems to provide simplified structural continuity and effective confinement in the circumferential direction is always a concern. Therefore, a need exists to develop an innovative and effective joining system for a FRP repair system.

Recently, a new type of FRP composite jacket (Fig. 2) that can be quickly and safely installed due to its easy-fit and self-locking mechanical joining system has been developed (Joinlox 2014). This innovative joining system is comprised of two interlocking edges that can easily fit into each other, similar to the teeth of a zipper. A FRP locking key is placed between the interlocking teeth, which can be slid or levered only one pitch length, thus causing wedging of the joint edges together with a uniform force distribution along the entire length of the joint. Manalo et al. (2014) determined the most suitable joint materials and assessed the capacity and behavior of this system when subjected to internal pressure.

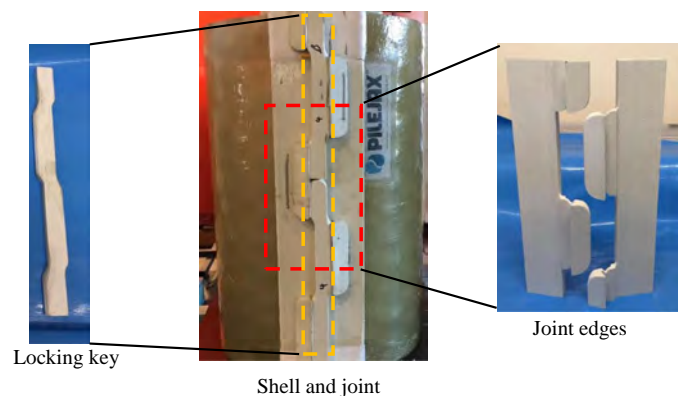


**Fig. 2.** Novel GFRP jacket.

They concluded that this jacket, with its new innovative joining system, can provide a case of structural continuity and confinement to the repaired structure. However, the performance benefits of this FRP jacket have yet to be fully explored, and its contribution to the structural capacity of the repaired structure is not yet understood. This study provides a better understanding of the actual performance of RC structures repaired and partially confined with the novel FRP jacket system. This information is critical for evaluating the efficiency of this new repair system and its application to actual rehabilitation projects.

## Experimental Program

### Materials

#### Novel GFRP Jacket

The GFRP jacket consists of the GFRP shell and the innovative GFRP joining system (Fig. 2). The GFRP shell was fabricated by the filament winding method, whereas the GFRP joint was made through a pultrusion process. The joint was then attached to the jacket using epoxy and FRP pins at the ends. A burnout test was conducted in accordance with ISO 1172 (ISO 1996) to determine the materials' fiber content ratio and fiber stacking sequence. The test revealed that the GFRP shell had 67.6% fiber content by weight and a stacking sequence of  $-45^\circ / +45^\circ / -45^\circ / +45^\circ$ .

**Table 1.** Properties of GFRP shell and joint

Test and standard	Part	Dimensions (mm)		Property	Value	Standard deviation	Coefficient of variation
		Length	Width				
Tensile (ISO 527-1:1995)	GFRP jacket	250	25	Peak stress, MPa ( $f_{fg}$ )	297	45	15.2
				Modulus, GPa ( $E_{fg}$ )	24	2	8.3
				Peak strain, $\mu\epsilon$ ( $\epsilon_{fug}$ )	11,268	483	4.3
	Joint longitudinal	250	25	Peak stress, MPa ( $f_{fjl}$ )	256	14	5.5
				Modulus, GPa ( $E_{fjl}$ )	25	1	4.0
				Peak strain, $\mu\epsilon$ ( $\epsilon_{fujl}$ )	10,000	312	3.1
	Joint transverse	72	25	Peak stress, MPa ( $f_{fjt}$ )	37	2	5.4
				Modulus, GPa ( $E_{fjt}$ )	11	2	18.2
				Peak strain, $\mu\epsilon$ ( $\epsilon_{fuit}$ )	3,500	129	3.7
Compression (ISO 14126:1999)	Jacket	140	12.75	Peak stress, MPa ( $f'_{fg}$ )	180	38	21.1
				Modulus, GPa ( $E'_{fg}$ )	30	2	6.7
				Peak strain, $\mu\epsilon$ ( $\epsilon'_{fug}$ )	11,001	381	3.5
	Joint longitudinal	140	12.75	Peak stress, MPa ( $f'_{fjl}$ )	394	21	5.3
				Modulus, GPa ( $E'_{fjl}$ )	26	2	7.7
				Peak strain, $\mu\epsilon$ ( $\epsilon'_{fujl}$ )	15,000	395	2.6
Burnout (ISO 1172:1996)	Jacket	50	15	Fiber content	67.65%	0.31	0.5
	Joint	—	—	Fiber content	66.05%	0.26	0.4

with respect to the hoop direction. Such a configuration is effective in managing multiaxial stresses and in achieving more ductile behavior at failure (Hajsadeghi et al. 2011; Parvin and Jamwal 2006). The joint also had a fiber content ratio of 66.0% and consisted of several longitudinal fiber, chopped strand, and woven mat layers.

Experimental approaches in accordance with ISO 527-1 (ISO 1995) and ISO 14126 (ISO 1999) were followed to ascertain the tensile and compressive properties of the GFRP shell and joint. The test coupons were cut directly from one of the jackets along the axial/longitudinal direction using the water jet cutting machine. At least six replicates were tested for each specimen type. The results of the FRP material characterization are listed in Table 1. Although three properties indicated a coefficient of variation higher than 15%, these are acceptable because they represent the true properties of the materials given that they were cut directly from the actual jacket. This variation in the test results can be attributed to the discontinuity of  $+45^\circ$  fibers in the tested coupons and some defects during jacket fabrication, that is, nonuniform resin distribution, but are expected not to affect the overall behavior of the columns.

### Grout-Infill

A shrinkage-compensating-cementitious-grout infill, commercially known as BluCem GP60, was used to fill the annulus between the jacket and the RC columns. This grout was made up of cement powder with a 0.3-mm maximum particle size. The shrinkage-compensating feature allowed the grout to be volumetrically stable during the initial curing stage and prevented cracking from plastic shrinkage. Following the specified procedure in the technical data sheet (Bluey 2017), a water-to-cement weight ratio of 0.175 was adopted to obtain a flowable and fillable grout without void formation. This grout infill was selected because of its relatively high stiffness, which made it effective in transferring loads and stresses from the repaired structure to the FRP jacket (Shamsuddoha et al. 2013). The constituent behavior and the mechanical properties of the cementitious-grout infill were reported by Mohammed et al. (2018), and the compressive strength ( $f'_{cgi}$ ) and modulus of elasticity ( $E'_{cgi}$ ) of the cementitious-grout infill were 48.2 MPa and 34.3 GPa, respectively.

### Reinforcing Steel

Deformed steel bars (Australian/New Zealand Standard 2001) with a nominal diameter ( $\phi_s$ ) of 16 mm and a yield strength ( $f_y$ ) of 500 MPa were used to reinforce the circular column specimens in the longitudinal direction, whereas plain steel bars (Australian/New Zealand Standard 2001) with a  $\phi_s$  of 10 mm and a  $f_y$  of 250 MPa were used as transverse reinforcement.

### Concrete

A commercially produced ready-mix concrete with a proprietary mixture consisting of fine and medium sands, 10-mm coarse aggregates, water, and normal portland cement, were used to cast the column specimens. The average slump of the fresh concrete, following ASTM C143/C143M (ASTM 2005), was 135 mm. Concrete cylinders were prepared and cured in accordance with ASTM C31/C31M (ASTM 2012). The average 28-day compressive strength ( $f'_{cc}$ ) and modulus of elasticity ( $E_c$ ) of the concrete equaled 30.5 MPa and 26 GPa, respectively, determined in accordance with the ASTM C39/C39M (ASTM 2015).

### Test Specimens

Fig. 3 summarizes the details and configurations of the columns tested in this study. Nine large-scale circular concrete columns (250-mm diameter by 1,000-mm height) and one large-scale square concrete column (220 mm by 220 mm by 1,000 mm height) were cast and tested up to failure. All of the columns were longitudinally reinforced with eight 16-mm steel bars (equivalent to 3.28% of the column's gross cross-sectional area) and were transversely reinforced with steel ties spaced uniformly at 50 mm center-to-center with a 30-mm concrete cover. The column size was designed based on the maximum capacity of the test equipment. Because the accelerated corrosion process takes significant time to simulate low levels of corrosion damage and is suitable mostly for small-scale specimens, that is, RC cylinders (da Fonseca et al. 2014; Maaddawy 2008), a new approach was adopted to simulate the steel corrosion damage by cutting the longitudinal reinforcement in the test region and replacing them with nonstructural PVC pipe (16-mm diameter) to prevent the concrete from occupying the steel volume and to maintain the alignment of the longitudinal reinforcement at both

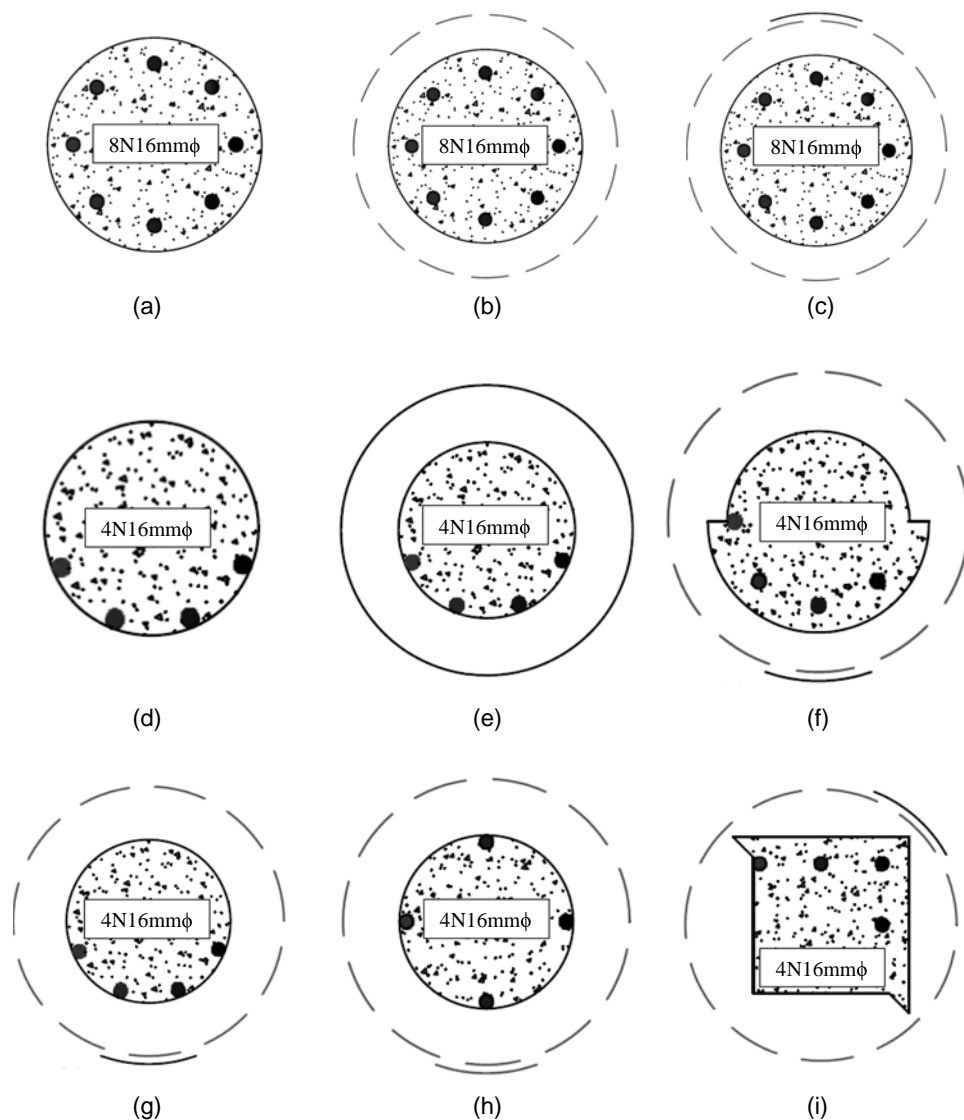


**Fig. 3.** Test specimen details and configuration: (a) C-0-0; (b) C-0-0-S; (c) C-0-0-J; (d) C-50-100; (e) C-50-100-G; (f) C-50-50-J; (g) C-50-100-J; (h) C-50-100-J\*; and (i) S-50-50-J.

ends [Fig. 4(a)]. A similar approach was adopted by Manalo et al. (2016), Liu et al. (2005), and Karagah et al. (2018) for which the flanges of S steel sections were machined to represent the section loss due to corrosion, and local buckling was observed within the corroded region in the latter study. In actual situations with severe corrosion, the lateral ties in a steel corroded column are not functional and should not be considered in the design. Not using lateral ties within specific locations of the columns ensures that the failure will occur in those locations. This approach also makes the column the weakest in this area, and the jacket is applied in this location for strength restoration. Similarly, lateral ties were not provided in the middle third height of the undamaged control column to ensure that it will fail in this location and within the capacity of the test machine. A similar approach was implemented by Abdel-Hay and Fawzy (2015) to study the effect of the partial strengthening of defected columns using steel jackets. This approach will also ensure that the confinement effects measured from the experimental works for repaired and damaged columns are provided solely by the jacket. Finally, this approach enabled the development of an empirical equation to calculate the confined compressive strength of the concrete columns repaired by the novel FRP jacket. However, bubble

wraps were wrapped around the steel reinforcement cages (prior to concrete casting) to simulate the concrete cover damage [Fig. 4(b)]. The bubble wraps were removed after the hardening of the concrete. GFRP jackets measuring 450 mm in diameter and 700 mm in length were then placed around the damaged section to partially cover the columns' height [Fig. 5(a)] followed by filling the annulus with the grout [Fig. 5(b)]. These steps simulate the repair of columns with damage in the splash zone, which is necessary because the GFRP jacket implemented in this study was designed as a repair system and not for strengthening. This approach will result in the jacket and the grout not being subjected to direct axial loads but to lateral stresses generated from the expansion of the column in the radial direction. The jacket diameter was based on the curvature of the joint and serves as a formwork to contain the grout. The location of the FRP joint was based on the current practice of the industry collaborator as well as to address the concerns of the asset owners that the joint may be the pathway for moisture to reach the damaged locations of the existing structure.

The test specimens were labeled in the following manner: shape of the column-percentage of the steel corrosion-percentage of concrete cover damage type of repair system. The first letters C and S

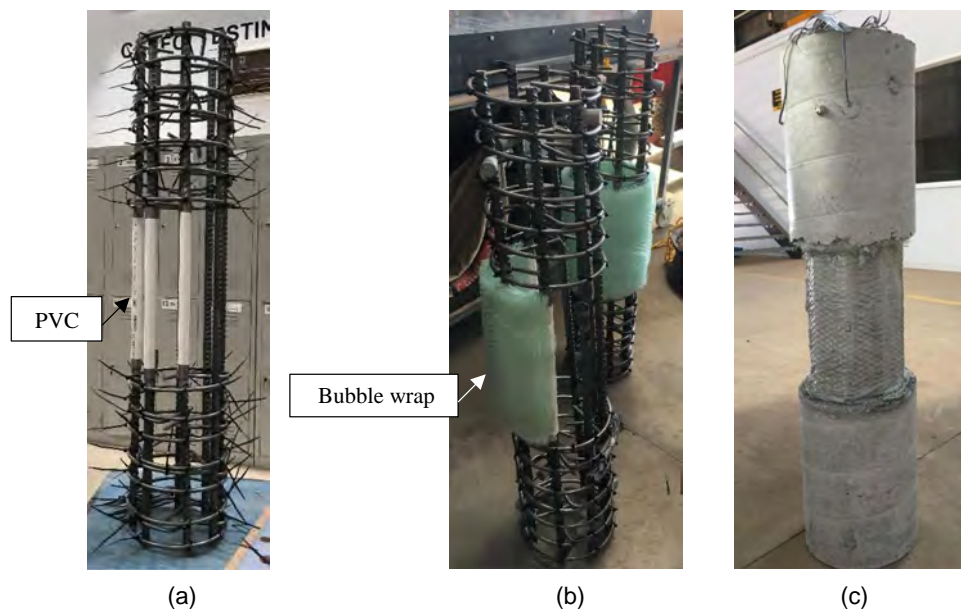


**Fig. 4.** Fabrication of column specimens: (a) corrosion damage; (b) concrete cover damage; and (c) damaged column.

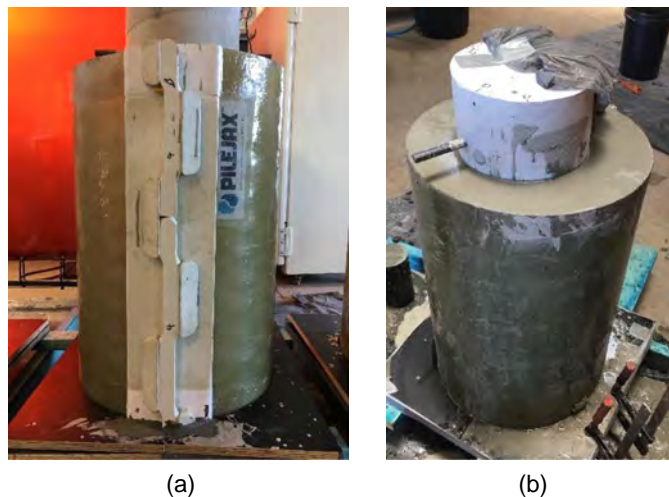


**Fig. 5.** Installation of GFRP jacket and infill: (a) placing the jacket; and (b) grout-filled annulus.

stand for circular and square column, respectively, and the last letters G, J, and S identify the columns repaired with grout only, GFRP jacket, and GFRP sleeve (continuous GFRP shell), respectively.

The first circular column C-0-0 [Fig. 3(a)] served as the control undamaged specimen. The second and third circular columns represented by C-0-0-S [Fig. 3(b)] and C-0-0-J [Fig. 3(c)], respectively, were prepared without any damages and were wrapped with GFRP sleeve and jacket, respectively, to evaluate the strengthening efficiency of the joint on the repair system, respectively. The fourth column C-50-100 [Fig. 3(d)], with 50% steel corrosion and 100% concrete cover damage, served as the damaged control specimen. The fifth specimen C-50-100-G [Fig. 3(e)] is similar to the previous one (C-50-100) but is repaired with grout only to determine the grout contribution. To investigate the influence of steel corrosion, the sixth and seventh columns designated by C-25-50-J

and C-50-50-J [Fig. 3(f)], respectively, were fabricated by removing 25% and 50% of the steel area in the test region, respectively. Column C-25-50-J is not depicted in Fig. 3 to maintain the symmetrical shape of the figure and because it is similar to C-50-50-J [Fig. 3(f)] with two additional longitudinal bars. In contrast, the effect of concrete cover damage was studied by casting the eighth column C-50-100-J [Fig. 4(g)] with 100% concrete cover removed but with a similar level of steel corrosion (50%) as column C-50-50-J. The ninth column C-50-100-J\* [Fig. 3(h)] had the same amount of steel corrosion and spalled concrete cover as column C-50-100-J\* but with a symmetrical steel reinforcement arrangement. Hence, the symbol \* at the end was used to distinguish it from the previous column.

To investigate the shape effect, a square column with almost a similar cross-sectional area as the circular columns was also cast and tested. The square column (S-50-50-J) was prepared with 50% corrosion and 50% concrete cover loss [Fig. 3(i)], comparable to that of C-50-50-J. All of the damaged columns were repaired using the GFRP jacket, which is represented by the dashed circle in Fig. 3, whereas the double line represents the joint location with respect to the repaired column.

### Test Program and Instrumentation

Fig. 6 shows the test setup and instrumentation employed in this study. The columns were supported at both ends with two pairs of 10-mm thick steel collars/clamps, with an inner radius of 127 mm, to prevent end crushing, thereby ensuring failure at the test region. Neoprene rubber (3-mm thickness) also helped to fill the gaps between the clamps and specimens. The top and bottom ends, which were smoothed and leveled evenly during the casting process, were provided with 3-mm thick neoprene rubber during testing to ensure uniform distribution of the applied load across the cross section. Strain gauges were mounted onto critical portions of the concrete, longitudinal reinforcement, and GFRP jacket generally positioned at the midheight of the test region.

The columns were subjected to monotonically increasing axial concentric loads and were tested to failure in displacement control mode using a hydraulic jack, and both the pre and postpeak

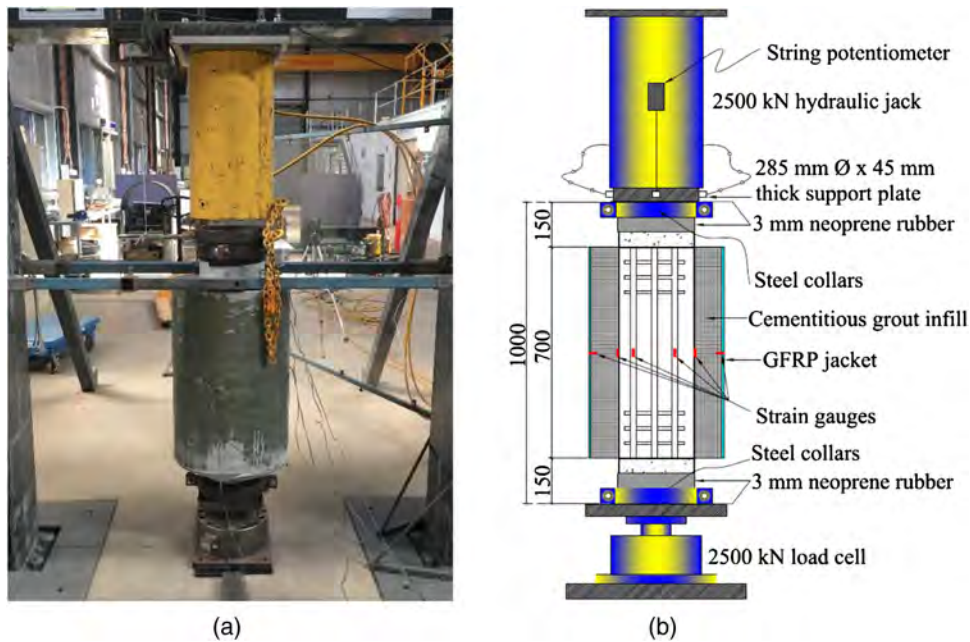


Fig. 6. Compression test set-up of columns: (a) actual test setup; and (b) schematic diagram (dimensions in millimeters).

behavior were observed. The magnitude of the applied load was measured with a 2,500-kN capacity load cell, whereas the corresponding deformations were measured with a string pot. The strain, load, and deflection readings were recorded with the system 5,000 data logger, whereas the failure modes were manually observed and recorded.

## Results and Observations

This section details the results and observations of the specimens that have been collected during the experimental stage. The results of this stage are summarized in Table 2, which presents the maximum axial load capacity, stiffness, and failure mode of the tested columns.

### Failure Mode

Fig. 7 shows the post-failure overview of the tested columns, and Fig. 8 depicts the specific failure pattern in different components of

**Table 2.** Maximum axial load capacity, stiffness, and failure mode of tested columns

Specimen	$P_u$ (kN)	$k$ (kN/mm)	Failure mode
C-0-0	2,319	279	Concrete crushing and steel buckling
C-50-100	1,028	170	Concrete crushing and steel buckling
C-50-100-G	1,218	281	Concrete crushing and steel buckling followed by grout cracking and broken into large pieces
C-0-0-S <sup>a</sup>	2,467	285	Concrete cracking/crushing at top and bottom ends
C-0-0-J	2,403	285	Concrete crushing and steel buckling followed by grout stressed radially
C-25-50-J	2,298	284	and jacket tensioned circumferentially
C-50-50-J	2,208	291	followed by joint failure at the teeth
C-50-100-J	1,905	290	
C-50-100-J*	1,902	288	
S-50-50-J	1,271	291	

<sup>a</sup>This specimen did not fail at this load level.

the repair system. Column C-0-0 exhibited slight cracking and spalling near the top and bottom ends prior to the peak load. However, right after reaching the peak load, column C-0-0 failed suddenly from the simultaneous crushing of the concrete and local buckling of the steel bars [Fig. 7(a)]. The columns failed in a very brittle manner accompanied by a loud explosive sound. A well-formed cone on both ends characterized the post-failure configuration of column (C-0-0). Severe crushing was also observed in the core concrete at the test region of the column. A similar failure mode was observed in column C-50-100 [Fig. 7(d)], but with global buckling of steel reinforcement and much lower load magnitude given the simulated damages. Several minor cracks were observed on the grout surface of C-50-100-G. Because the grout is not directly subjected to axial load but to lateral/radial stress, the expansion of the column in the radial direction resulted in rebar buckling and tensile gracing of the grout and then splitting into large pieces [Fig. 7(e)].

Different failure modes were observed in columns repaired with FRP jackets. As shown in Fig. 7(c), the failure of column C-0-0-J was initiated by the crushing of the concrete and buckling of the longitudinal steel bars, which pushed the concrete and grout radially outwards and tensioned the jacket circumferentially. Although buckling of PVC pipes was observed in specimens with simulated steel corrosion, it did not contribute to the overall strength and did not affect the overall failure behavior of the tested columns because of the significantly lower modulus of polyvinyl chloride (only approximately 4 GPa) relative to steel bars. Thus, the observed buckling of PVC pipe was only secondary to the crushing of the adjacent concrete. Several hairline cracks were observed in the grout. With an increase in the applied load, minor concrete cracking and crushing were observed outside the jacketed section near the loading and support points, whereas hairline cracks that developed in the grout increased in number and width. Prior to the peak load, the crack underneath the joint widened significantly, wherein sounds of resin cracking and fiber rupturing were heard, followed by jacket failure at the joint from rupturing of the teeth [Fig. 8(a)] and complete opening of the jacket [Fig. 8(c)]. However, no damage was observed in the GFRP shell. At failure, the cementitious grout infill



**Fig. 7.** Failure modes of tested columns: (a) C-0-0; (b) C-0-0-S; (c) C-0-0-J; (d) C-50-100; (e) C-50-100-G; (f) C-50-50-J; (g) C-50-100-J; (h) C-50-100-J\*; and (i) S-50-50-J.

broke down into large pieces with signs of inadequate bonding to the GFRP jackets and the repaired columns [Fig. 8(b)]. Finally, crushing of the core concrete was observed.

As indicated in Figs. 7(f–h), columns C-25-50-J, C-50-50-J, C-50-100-J, and C-50-100\* exhibited similar a failure mode to C-0-0-J, except that the grout started cracking at lower loads and higher severity. Moreover, the cracking load of the grout decreases

with increasing damage given a reduction in the strength of the core column. Interestingly, column C-0-0-S did not fail, and the sleeve had no signs of damage along its height. The test was stopped after reaching the maximum loading capacity of the test equipment. However, minor hairline cracks were observed in the grout, whereas wide cracks and marginal concrete spalling were observed in concrete at the top and bottom of the jacket, which created stress concentration.



**Fig. 8.** Specific failures in components of repair system: (a) rupture of the GFRP jacket's teeth; (b) large pieces of broken grout infill; and (c) debonded GFRP jacket and grout infill.

The square column S-50-50-J exhibited compression failure typified by concrete crushing and local buckling of the steel bars in the test region [Fig. 7(i)]. Although the ultimate failure was controlled by the jacket, its failure was similar to that of the circular columns. However, sounds of resin cracking and fiber rupturing were louder and lasted longer relative to that of the circular specimens.

### Load-Deformation Response

Fig. 9 presents the relationships between the axial load ( $P$ ) and deformation of the tested columns. The load-deformation of column C-0-0 consisted of a relatively linear ascending segment up to an applied load of 2,260 kN, with a stiffness of 279 kN/mm (the slope of the initial segment of the load-deformation curve, particularly between 30% and 60% of the maximum load). Ultimately, the column failed at 2,319 kN and could not sustain more load. Similar behavior was observed in column C-50-100, which behaved linearly until the failure load (1,027 kN) but with a stiffness of 170 kN/mm. Column C-50-100-G failed at a load almost similar to that of the damaged column with no repair but with a stiffness similar to that of the undamaged column. The jacketed specimen with zero damage (C-0-0-J) indicated ascending linear behavior with a stiffness of 285 kN/mm. When the load reached 2,000 kN, a slight drop in the stiffness and nonlinear behavior were observed until the final failure (2,403 kN), which is attributed to the cracking of grout as indicated in Fig. 11(a). Similar behavior was observed in other circular jacketed specimens. However, the degree of non-linearity increases due to the widening of the radial cracking in the grout. Nevertheless, columns C-25-50-J and C-50-50-J yielded axial strength and stiffness of 2,298 kN and 284 kN/mm, and

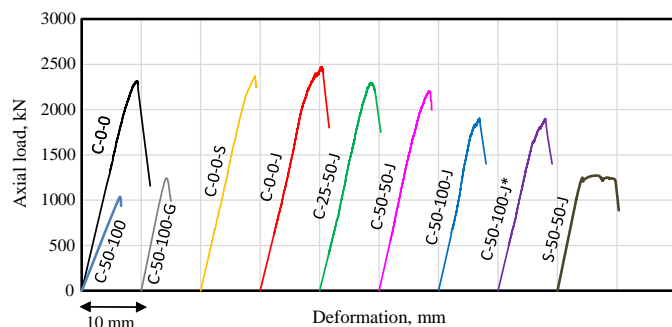


**Fig. 9.** Load-deformation curves.

2,208 kN and 291 kN/mm, respectively. Columns C-50-100-J and C-50-100-J\* exhibited axial strength and stiffness of 1,905 kN and 290 kN/mm, and 1,902 kN and 288 kN/mm, respectively. Finally, although column C-0-0-S did not fail, the descending branch of the load-deformation curve is the result of unloading of the specimen when the load cell reached its capacity.

The load-deformation behavior of the square column (S-50-50-J) was linear up to the first peak with a stiffness of 291 kN/mm, whereas the post-peak behavior was characterized by a flat plateau representing the progressive failure of the specimen until the joint failure.

### Load-Strain Behavior of the Repair System

Fig. 10(a) depicts the strain development in the components of the repair system in column C-50-50-J. In the elastic region, the concrete and the steel behaved linearly with almost zero hoop strain in the GFRP jacket and joint as the load was mainly carried by the concrete core column until a strain level of 500  $\mu\epsilon$ . Once the applied load in column C-50-50-J reached 1,100 kN—almost equivalent to the failure load of the damaged-unrepaired specimen (C-50-100)—the load was transferred mostly to the steel reinforcing bar and the steel strain increased nonlinearly and rapidly, whereas the concrete exhibited crushing and cracking that resulted in damage of the strain gauges bonded to the concrete. At this stage, the grout started to effectively carry and transfer the radial stresses, which were being generated due to the lateral expansion of the core column to the FRP repair system, and stressed it circumferentially. The lateral expansion caused an increase in the strain readings of the jacket and the joint, as indicated in Fig. 10(a), which explains the linear behavior of the load-deformation curves at that load level of the repaired specimens.

However, several hairline cracks originating from the column, propagating toward the jacket, and distributed along the circumference were observed in the grout prior to the final failure, whereas the width of the crack underneath the joint dramatically increased, as depicted in Fig. 11(a). Interestingly, higher strain readings were recorded in the joint rather than the jacket. This finding can be attributed to the discontinuity of the joint and its low transverse stiffness, which is less than that of the GFRP jacket, leading to premature failure of the joint without the GFRP jacket reaching its failure stress. A similar failure mechanism was observed in the square column [Fig. 10(b)] but with no minor crack development along the circumference. The jacket failed immediately after reaching the load level of 1,250 kN without fully deriving the benefits of confinement effects due to the stress concentration at the corners

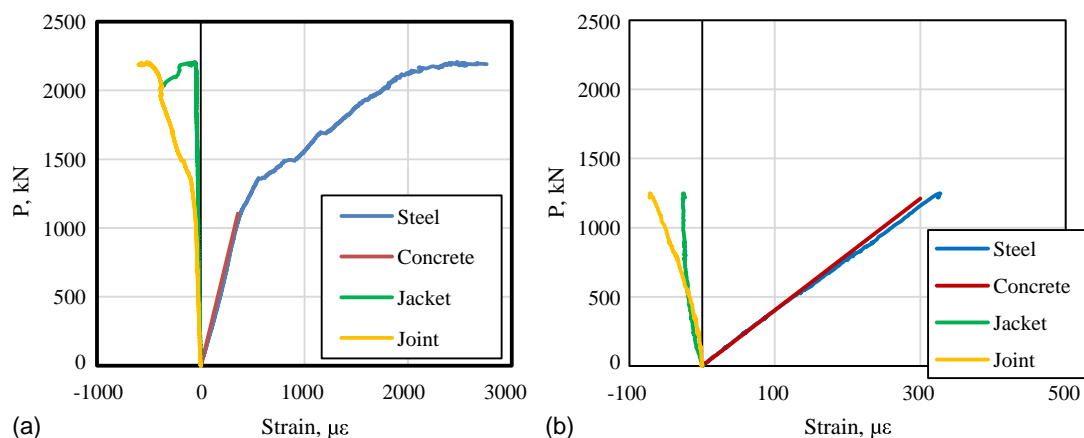


Fig. 10. Strain development in repair system.

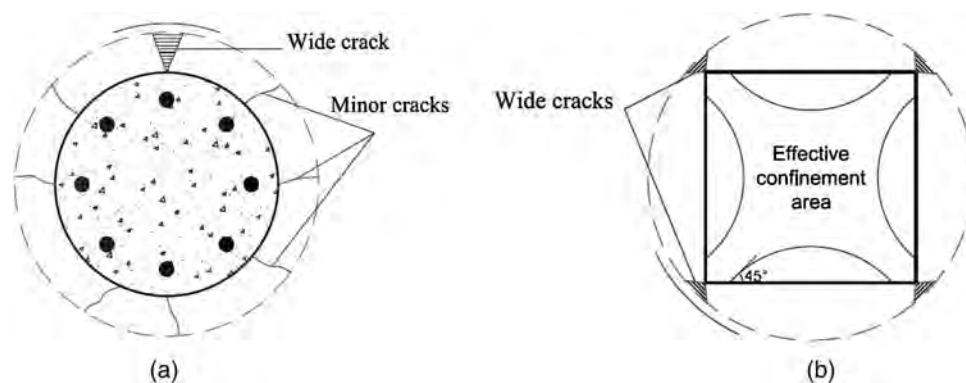


Fig. 11. Development of cracks in grout material and stress concentration in jacketed columns: (a) circular section; and (b) square section.

and the joint, as indicated in Fig. 11(b). The stress concentration is due to the geometry of the square columns for which more effective confinement occurs at the corners rather than the sides. This finding can be explained by the fact that, in square columns, the confining pressure near the corners is generated from tensioning of the FRP jacket along the hoop direction, whereas it is more due to the flexural behavior of the FRP jacket on the sides (ACI 2008; Lam and Teng 2003; Yan and Pantelides 2011; Yan et al. 2007). However and as indicated by Yan and Pantelides (2011), although the utilization of grout restores the membrane action and enhances the confinement, the stress concentration will not have been eliminated near the corners. Finally, in column S-50-50-J, the joint failed at a lower strain relative to its failure in column C-50-50-J. This result can be attributed to the action of additional flexural forces on the FRP jacket at the flat side of the square columns, resulting in the development of bending moments at the joint.

## Discussion

### Effectiveness in Repairing RC Columns with Steel Corrosion

The effectiveness of the FRP jacket in repairing concrete columns with steel corrosion was evaluated by studying the behavior of columns C-25-50-J and C-50-50-J and compared with the behavior of control specimens. The results indicate that simulating 50% corrosion and 100% concrete cover removal in column C-50-100 resulted in a 56% reduction in the axial load capacity in comparison

with column C-0-0. This experimental failure load is 10% lower than the theoretical value (1,127 kN) due to the moment generated from the applied load on the eccentric/undamaged steel bars. In contrast, the use of the grout alone in C-50-100-G has no significant structural contribution given its low tensile strength because the grout is not directly subjected to axial load but to lateral/radial stress.

Repair using the FRP jacket helped stabilize the damaged column by reducing the eccentricity effect of the corroded steel that resulted in extending the linear behavior of the steel bars to an applied load of 1,200 kN, as indicated in Fig. 10(a). The subsequent nonlinear behavior of the steel bars, however, was not obvious in the load-deformation curve (Fig. 9) as the activation of the repair system helped the columns sustain higher axial loads when maintaining their original stiffness, further demonstrating the effectiveness of FRP jackets. Moreover, the axial load capacity of columns C-25-50-J and C-50-50-J was 99% and 95%, respectively, of the strength of the undamaged column (C-0-0). These results show that, at these damage levels, the GFRP jacket is effective in restoring the damaged columns to their original strength. In addition, the GFRP jacket restored 100% of the axial stiffness. In contrast, using a simple and flexible GFRP jacket, Kaya et al. (2015) were only able to restore 67% of the elastic axial stiffness of steel columns with 60% simulated corrosion damage.

The effects of the location of the corroded steel bars on the repair system effectiveness were investigated by studying the behavior of columns C-50-100-J and C-50-100-J\*. Column C-50-100-J\* yielded almost a similar strength as column C-50-100-J, suggesting that the GFRP jacket is efficient irrespective of the location of

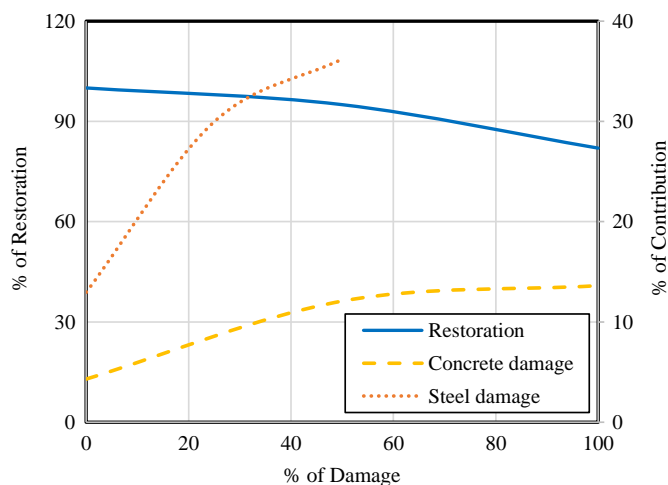


**Fig. 12.** FRP jacket effectiveness with different levels of steel damage.

the corroded steel bars in terms of strength restoration because the jacket helps with better stress distribution and stabilization of columns with steel corrosion. This phenomenon was likely also caused by the small reinforcement ratio in the investigated columns. However, a different scenario of slender columns was reported by Tapan and Aboutaha (2011), in which the authors stated that the corrosion of steel bars on the compression side of the column section causes more significant reduction than the tension side deterioration.

Fig. 12 indicates that with an increase in the steel corrosion level, the strength restoration of the damaged specimens decreases slightly. However, that decrease comes with a significant increase in the contribution of the repair system, from 13% to 30% and from 30% to 36% for 0% to 25% and 25% to 50% steel corrosion, respectively. This increase can be explained by the substantial loss in the strength capacity of the damaged columns, resulting in more loads being carried by the FRP jacket system through confinement effects. This observation corroborates the findings of Karagah et al. (2018) for GFRP and CFRP jackets for which the measured axial strength capacity of the repaired pile decreases as the corrosion level increases.

### Effectiveness in Repairing Columns with Damaged Concrete Cover

Comparative evaluations of the behavior of columns C-50-50-J and C-50-100-J were done to investigate the effectiveness of the FRP jacket in repairing columns with concrete cover damage. The column with a 50% spalled concrete cover (C-50-50-J) restored 95% of the capacity relative to the undamaged specimen. The effective restoration is attributed to the grout infill that replaced the volume of the spalled concrete cover and with the help of the FRP jacket, which provided confinement to the grout and the core column. However, increasing the level of concrete cover damage from 50% in C-50-50-J to 100% in C-50-100-J—equal to 42% of the overall cross-sectional area—resulted in reducing the strength restoration by 13%, as shown in Fig. 12. This reduction is attributed to the lower friction, bonding, and interaction development between the undamaged steel reinforcement and the cementitious grout. In other words, column C-50-50-J had damaged concrete cover on only one side, whereas the concrete cover damage was all over the circumference in column C-50-100-J, with full exposure of the steel bars. According to Bae et al. (2005) and Lee et al. (2003), the steel reinforcement bars exhibit better performances and higher axial load capacities with the original concrete cover more than the

addition of replacement/repair material at a later stage for the concrete cover because the original material can provide better support, interaction, and integration with the steel.

### Effectiveness in Repairing Circular and Square Columns

The effectiveness of the FRP jacket in repairing circular and square columns with damage was evaluated by comparing the behavior of columns C-50-50-J and S-50-50-J. These columns almost share the same cross-sectional area (approximately 49,000 mm<sup>2</sup>) and level of damage (50% steel corrosion and 50% concrete cover damage). Interestingly, the axial load capacity of the damaged FRP jacketed square column was 43% lower than that of the comparable circular column. This difference can be attributed to the lower level of confinement provided by the GFRP jacket in the square column than the circular column. Placing the joint in alignment with the corner resulted in earlier/premature failure due to high stress concentration in this location relative to the flat sides of the square columns (Pessiki et al. 2001; Pham et al. 2013; Yan and Pantelides 2011). However, column S-50-50-J exhibited more ductile behavior than column C-50-50-J before the final failure because the progression of the fiber rupture at the jacket joint was slower given the low failure load and the lower confinement effect of the GFRP in the square section relative to the circular column.

### Efficiency of Novel GFRP Joint

The efficiency of the novel joint of the jacket against a nonjointed sleeve was evaluated by comparing the behavior of columns C-0-0-J and C-0-0-S along with column C-0-0. The use of the GFRP jacket enhanced the strength of the undamaged column (C-0-0-J) by just 4%, suggesting that this jacket as tested is suitable for restoring the capacity of damaged columns but not for additional strengthening, which requires the use of additional reinforcement during the repair. The GFRP sleeve appears to be able to carry higher strains to failure and provides better strength enhancement than the GFRP jacket with a joint given the continuity of fibers in the sleeve. Nevertheless, the average hoop/transverse strain reading at the joint was 598  $\mu\epsilon$ , which is only 17% of the joint transverse strain capacity as mentioned in Table 1. This finding could be attributed to the multiaxial stresses generated at the joint region due to the joint geometry. Moreover, Teng and Lam (2004) indicated that the reduction in the hoop strain capacity was attributed to the FRP curvature effects and the cracked concrete/grout causing nonuniform deformation. American Concrete Institute (ACI 2008) introduced a strain efficiency factor that ranges from 0.57 to 0.61 for FRP confined concrete, although other researchers reported results outside this range (Bisby and Take 2009; Chen et al. 2010; Smith et al. 2010). However, the decrease in the joint strain capacity resulted in limited utilization of the FRP shell because the average hoop strain reading on the jacket at failure is 1,200  $\mu\epsilon$ . However, this level of hoop confinement is enough to restore the original capacity of a damaged concrete pile due to the relatively high thickness of the jacket (+3 mm).

However, the design of the current system is sufficient to restore the strength of damaged columns to their undamaged load capacity levels, but modifications can be made to extend the application of the system for additional strengthening purposes.

### Theoretical Modeling

This section details the development of the theoretical model that can predict the maximum axial load capacity of the jacketed columns. The developed equations will assist structural engineers

**Table 3.** Experimental and theoretical results

Column	$A_{c-ef}$ (mm <sup>2</sup> )	$A_{s-ef}$ (mm <sup>2</sup> )	$A_{ef}$ <sup>a</sup> (mm <sup>2</sup> )	Experimental				Theoretical to experimental ratio	
				$\sigma_{co}$ [MPa ( $P_{co}$ , kN)]	$\sigma_{cc}$ [MPa ( $P_{cc}$ , kN)]	$\sigma_{cc} - \sigma_{co}$ (MPa)	$K^a$		
C-0-0	47,479	1,608	59,598	31.9 (2,319)	—	0	—	—	
C-0-0-J	47,479	1,608	59,598 [1.00]	—	33.7 (2,403)	1.8	0.03 [1.00]	34.1 (2,422)	1.01
C-25-50-J	37,112	1,206	46,201 [0.78]	—	45.7 (2,298)	13.8	0.19 [7.77]	45.4 (2,288)	0.99
C-50-50-J	37,112	804	43,171 [0.72]	—	48.7 (2,208)	16.8	0.24 [9.45]	48.0 (2,181)	0.99
C-50-100-J	26,744	804	32,804 [0.55]	—	56.2 (1,905)	24.3	0.34 [13.70]	56.7 (1,919)	1.01

<sup>a</sup>Values in brackets represent the normalized  $A_{ef}$  and  $k$ .

involved in rehabilitation projects when selecting the appropriate repair method. Additionally, the equations will be useful in determining the extent of the damage for which the selected repair method can restore the structural integrity of the damaged member.

### Development of Prediction Equations

Table 3 summarizes the confined axial load capacity  $P_{cc}$  (C-0-0-J, C-25-50-J, C-50-50-J, and C-50-100-J) and unconfined axial load capacity  $P_{co}$  (C-0-0) of the columns.  $P_{co}$  and  $P_{cc}$  are the experimental axial load capacities of the control and jacketed tested columns, respectively. The confined and unconfined compressive strength of the columns ( $\sigma_{cc}$  and  $\sigma_{co}$ , respectively) were determined using Eqs. (1) and (2), respectively

$$\sigma_{co} = \frac{P_{co} - f_y A_{s-ef}}{A_{c-ef} - A_{s-ef}} \quad (1)$$

$$\sigma_{cc} = \frac{P_{cc} - f_y A_{s-ef}}{A_{c-ef} - A_{s-ef}} \quad (2)$$

where  $A_{c-ef}$  = undamaged effective concrete area;  $A_{s-ef}$  = undamaged effective steel area; and  $f_y$  = yield strength of the longitudinal steel reinforcement, which is 500 MPa. Note that the measured longitudinal strain in the steel bars in column C-0-0 at maximum load is at 2,500 microstrains, indicating that the steel bars yielded even without ties in the middle third of the column. This result can occur because of the buckling load of the unsupported 300-mm long longitudinal steel bars is significantly higher than the load for it to yield. However, the effect of the eccentricity induced from the partial cover removal and partial rebar removal was not considered in the theoretical model because the provision of the jacket and grout was observed to stabilize the column and eliminate the eccentricity effect. This phenomenon can also be due to the reduced contribution from the steel bars (reinforcement ratio reduced from 3.28% to 1.00% or less of the column's gross cross-sectional area) in the repaired section due to the increased cross-sectional area of the column provided by the grout and the jacket.

The prediction model for confined infills developed by Mohammed et al. (2018) was used and modified to develop a model that can predict the compressive strength of partially-confined undamaged and damaged columns  $\sigma_{cc}$  (Fig. 13). From Mohammed et al. (2018), the enhancement of the strength of concrete infills ( $\sigma_{gu} - \sigma_{iu}$ ) due to confinement can be written as

$$\sigma_{gu} - \sigma_{iu} = 2.5\sigma_{l,a} - 1.3\sigma_{iu} \quad (3)$$

where  $\sigma_{iu}$  and  $\sigma_{gu}$  are the compressive strength of infills and filled GFRP tubes, respectively, in (Mohammed et al. 2017); and  $\sigma_{l,a}$  = lateral confinement pressure. From this equation, the enhancement of the strength of partially confined columns ( $\sigma_{cc} - \sigma_{co}$ ) can be expressed as

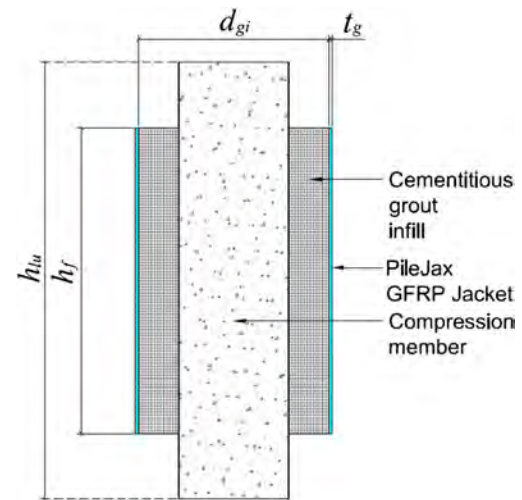


**Fig. 13.** Configuration of partially confined compression member.

$$\sigma_{cc} - \sigma_{co} = (2.5\sigma_{l,a} - 1.3\sigma_{iu}) \times k \quad (4)$$

The confining pressure ( $\sigma_{l,a}$ ) is calculated from Eq. (5) using the experimental results of the current study as inputs, that is,  $t_g = 3$  mm;  $d_{gi} = 450$  mm;  $E_f = 24,150$  MPa; and  $\varepsilon_{hu} = 1,200 \mu\varepsilon$

$$\sigma_{l,a} = \frac{2t_g E_f \varepsilon_{hu}}{d_{gi}} \times \frac{h_f}{h_{iu}} \quad (5)$$

The factor  $h_f/h_{iu}$  accounts for the influence of partial confinement, where  $h_f$  and  $h_{iu}$  are the length of the FRP jacket (700 mm) and the unsupported length of the column (1,000 mm), respectively. The concept of the partial confinement influence factor of this research is similar to the approach proposed by Mander et al. (1988) and has been utilized in several subsequent studies (Pham et al. 2015, 2016; Saadatmanesh et al. 1994). However, because the partial confinement here is provided by one large segment of the FRP jacket and not with several small strips, as mentioned in the existing literature, the confined length/height is considered instead of the confined area in this study. In contrast, the variable  $k$  considers the effect of the simulated damages. For each  $\sigma_{cc} - \sigma_{co}$ , the corresponding value of  $k$  was determined. Then, the normalized  $k$  (in terms of the undamaged area  $A_{undamaged}$  of C-0-0-J) was plotted against the normalized area of column  $A_{ef}$  (in terms of the area of C-0-0-J), as indicated in Fig. 14.  $A_{ef}$  is calculated using Eq. (6), wherein the modular ratio  $n$  is determined from Eq. (7) (equivalent to 7.53 when the steel elastic modulus  $E_s = 200,000$  MPa and the concrete elastic modulus  $E_c = 4700\sqrt{31.9} = 26546$  MPa)

$$A_{ef} = A_{c-ef} + nA_{s-ef} \quad (6)$$

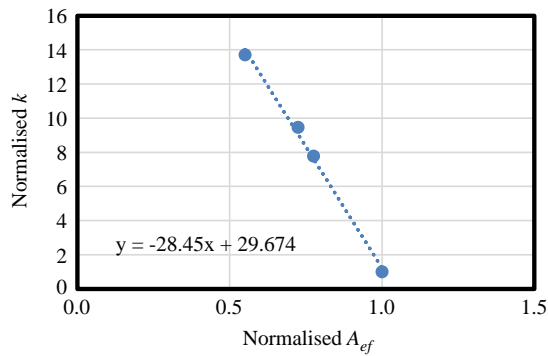


Fig. 14. Normalized  $A_{ef}$  versus normalized  $k$ .

$$n = \frac{E_s}{E_c} \quad (7)$$

By regression analysis, an expression for  $k$  is determined as

$$k = 0.043 \left[ 29.674 - 28.45 \left( \frac{A_{ef}}{A_{undamaged}} \right) \right] \quad (8)$$

Finally, by substituting Eqs. (8)–(4),  $\sigma_{cc}$  can be computed as

$$\sigma_{cc} = (2.5\sigma_{l,a} - 1.3\sigma_{co}) \times -0.043 \left[ 29.67 - 28.45 \left( \frac{A_{ef}}{A_{undamaged}} \right) \right] + \sigma_{co}$$

$$\sigma_{cc} = \sigma_{co} + \left( \frac{5t_g E_f \varepsilon_{hu}}{d_{gi}} \times \frac{h_f}{h_{lu}} - 1.3\sigma_{co} \right) \times \left[ 1.22 \left( \frac{A_{ef}}{A_{undamaged}} \right) - 1.28 \right] \quad (9)$$

where the term  $\frac{5t_g E_f \varepsilon_{hu}}{d_{gi}}$  represents the jacket properties. Using Eq. (9), the jacket properties can be determined with respect to the designated compressive strength.

Finally, given the failure of the joint at a hoop strain of only 1,200  $\mu\varepsilon$ , this system was suggested for use only for repair and strength restoration. The recommendation was made to improve the joint to extend the system application to strengthening.

### Comparison between Theoretical and Experimental Results

The maximum axial load capacity of the columns obtained from the theoretical models are compared with the experimental values of the tested specimens, as indicated in Table 3. The comparison indicates that an excellent agreement exists between the predicted and experimental values of the columns. Therefore, the theoretical model is validated by the test results and can be used for further applications. However, to be noted is that the developed theoretical equation may only apply to the repair system investigated in this study and may need calibration for other types of prefabricated composite repair systems.

### Conclusions

The behavior of damaged RC columns repaired using a novel FRP jacket system was investigated. Based on the experimental results, the following conclusions were made:

- The behavior of the prefabricated FRP jacket with infill evaluated in this study is governed by the capacity of the grout infill followed by the failure of the teeth at the joint location.

- The GFRP jacket was effective in restoring the axial load capacity of the RC columns with 25% and 50% corrosion damage, by 99% and 95%, respectively, as the repair system stabilized and restored the strength of the damaged columns.
- The GFRP jacket restored the axial load capacity by 95% for the specimen with a 50% spalled concrete cover. However, this percentage decreased by 13% in the specimen with 100% spalled concrete cover due to the change in the interaction/bond between the undamaged steel bars and the grout infill.
- The GFRP jacket was more effective in repairing circular than square columns as the damaged square column exhibited 43% lower axial load capacity than that of the circular section due to the stress concentration at the corners with the joint location. This information is useful for designers and engineers to better understand the capability and existing limitations of the investigated composite repair system.
- The current system is sufficient for structural repair; however, further improvements are necessary to modify the joint to extend the jacket's application as a strengthening system.
- The developed model accurately predicted the ultimate axial load capacity of the RC damaged columns repaired with the FRP jacket. This model is very useful in determining the extent of damage for which the FRP jacket is capable of restoring the structural integrity of a damaged column member.

### Acknowledgments

The authors gratefully acknowledge Joinlox Pty Ltd., Australia for the financial, materials, and technical support in conducting this study. The authors are also grateful to the Innovation Connections Fund given by the Australian Government for the successful implementation of this research project.

### References

- Abdallah, M. H., H. M. Mohamed, R. Masmoudi, and A. Moussa. 2018. "Analytical modeling of moment-curvature behavior of steel and CFRP RC circular confined columns." *Compos. Struct.* 189: 473–487. <https://doi.org/10.1016/j.compstruct.2018.01.110>.
- Abdel-Hay, A. S., and Y. A. G. Fawzy. 2015. "Behavior of partially defected R.C columns strengthened using steel jackets." *HBRC J.* 11 (2): 194–200. <https://doi.org/10.1016/j.hbrj.2014.06.003>.
- ACI (American Concrete Institute). 2008. *Guide for the design and construction of externally bonded FRP systems for strengthening concrete structures*. ACI 440.2R. Farmington Hill, MI: ACI.
- ASTM. 2005. *Standard test method for slump of hydraulic-cement concrete*. ASTM C143/C143M. West Conshohocken, PA: ASTM.
- ASTM. 2012. *Standard practice for making and curing concrete test specimens in the field*. ASTM C31/C31M. West Conshohocken, PA: ASTM.
- ASTM. 2015. *Standard test method for compressive strength of cylindrical concrete specimens*. ASTM C39/C39M. West Conshohocken, PA: ASTM.
- Australian/New Zealand Standard. 2001. *Steel reinforcing materials*. AS/NZS4671. Sydney, Australia: Australian/New Zealand Standard.
- Azam, R., A. K. El-Sayed, and K. Soudki. 2016. "Behaviour of reinforced concrete beams without stirrups subjected to steel reinforcement corrosion." *J. Civ. Eng. Manage.* 22 (2): 146–153. <https://doi.org/10.3846/13923730.2014.897979>.
- Bae, S., A. M. Mieses, and O. Bayrak. 2005. "Inelastic buckling of reinforcing bars." *J. Struct. Eng.* 131 (2): 314–321. [https://doi.org/10.1061/\(ASCE\)0733-9445\(2005\)131:2\(314\)](https://doi.org/10.1061/(ASCE)0733-9445(2005)131:2(314)).
- Baileys, R. T. 1995. "Timber structures and the marine environment." In *Proc., Ports '95*, 703–710. Reston, VA: ASCE.
- Bazinet, S., L. Cercone, and F. Worth. 1999. "Innovative FRP piling repair without the use of coffer dams." In *Proc., Int. Sampe Symp. and*

- Exhibition*, 2201–2206. Diamond Bar, CA: Society for the Advancement of Material and Process Engineering.
- Belal, M. F., H. M. Mohamed, and S. A. Morad. 2015. “Behavior of reinforced concrete columns strengthened by steel jacket.” *HBRC J.* 11 (2): 201–212. <https://doi.org/10.1016/j.hbrj.2014.05.002>.
- Berthet, J., E. Ferrier, and P. Hamelin. 2005. “Compressive behavior of concrete externally confined by composite jackets. Part A: Experimental study.” *Constr. Build. Mater.* 19 (3): 223–232. <https://doi.org/10.1016/j.conbuildmat.2004.05.012>.
- Bisby, L. A., and W. A. Take. 2009. “Strain localisations in FRP-confined concrete: New insights.” *Proc. Inst. Civ. Eng. Struct. Build.* 162 (5): 301–309. <https://doi.org/10.1680/stbu.2009.162.5.301>.
- Bluey. 2017. *Technical data sheet: BluCem GP60 construction grout*. Murarrie, QLD, Australia: Bluey.
- Cassidy, M., J. Waldie, and S. Palanisamy. 2015. “A method to estimate the cost of corrosion for Australian defence force aircraft.” In *Proc., 16th Australian Int. Aerospace Congress*. Melbourne, Australia: Barton, ACT, Australia: Engineers Australia.
- Chellis, R. 1961. “Deterioration and preservation of piles.” In *Pile foundations*, 339–372. New York: McGraw-Hill.
- Chen, J., J. Ai, and T. Stratford. 2010. “Effect of geometric discontinuities on strains in FRP-wrapped columns.” *J. Compos. Constr.* 14 (2): 136–145. [https://doi.org/10.1061/\(ASCE\)CC.1943-5614.0000053](https://doi.org/10.1061/(ASCE)CC.1943-5614.0000053).
- da Fonseca, B. S., A. Castela, M. A. Silva, R. Duarte, M. Ferreira, and M. Montemor. 2014. “Influence of GFRP confinement of reinforced concrete columns on the corrosion of reinforcing steel in a salt water environment.” *J. Mater. Civ. Eng.* 27 (1): 04014107. [https://doi.org/10.1061/\(ASCE\)MT.1943-5533.0001039](https://doi.org/10.1061/(ASCE)MT.1943-5533.0001039).
- Delatte, N. 2009. *Failure, distress and repair of concrete structures*. Amsterdam: Elsevier.
- Hajsadeghi, M., F. J. Alaei, and A. Shahmohammadi. 2011. “Investigation on behaviour of square/rectangular reinforced concrete columns retrofitted with FRP jacket.” *J. Civ. Eng. Manage.* 17 (3): 400–408. <https://doi.org/10.3846/13923730.2011.594155>.
- ISO. 1995. *Plastics-determination of tensile properties: General principles*. ISO 527-1. Geneva: ISO.
- ISO. 1996. *Textile glass reinforced plastics, prepregs, moulding compounds and laminates, determination of the textile-glass and mineral-filler content, calcination methods*. ISO 1172. Geneva: ISO.
- ISO. 1999. *Fibre-reinforced plastic composites. Determination of compressive properties in the in-plane direction*. ISO 14126. Geneva: ISO.
- Joinlox™. 2014. “PileJax™-Pile Repair Jackets.” Accessed May 19, 2016. <http://www.joinlox.com/pilejax/>.
- Karagah, H., M. Dawood, and A. Belarbi. 2018. “Experimental study of full-scale corroded steel bridge piles repaired underwater with grout-filled fiber-reinforced polymer jackets.” *J. Compos. Constr.* 22 (3): 04018008. [https://doi.org/10.1061/\(ASCE\)CC.1943-5614.0000847](https://doi.org/10.1061/(ASCE)CC.1943-5614.0000847).
- Kaya, A., M. Dawood, and B. Gencturk. 2015. “Repair of corroded and buckled short steel columns using concrete-filled GFRP jackets.” *Constr. Build. Mater.* 94: 20–27. <https://doi.org/10.1016/j.conbuildmat.2015.06.040>.
- Lam, L., and J. Teng. 2003. “Design-oriented stress-strain model for FRP-confined concrete in rectangular columns.” *J. Reinf. Plast. Compos.* 22 (13): 1149–1186. <https://doi.org/10.1177/0731684403035429>.
- Lee, H.-S., T. Kage, T. Noguchi, and F. Tomosawa. 2003. “An experimental study on the retrofitting effects of reinforced concrete columns damaged by rebar corrosion strengthened with carbon fiber sheets.” *Cem. Concr. Res.* 33 (4): 563–570. [https://doi.org/10.1016/S0008-8846\(02\)01004-9](https://doi.org/10.1016/S0008-8846(02)01004-9).
- Liu, X., A. Nanni, and P. F. Silva. 2005. “Rehabilitation of compression steel members using FRP pipes filled with non-expansive and expansive light-weight concrete.” *Adv. Struct. Eng.* 8 (2): 129–142. <https://doi.org/10.1260/1369433054038029>.
- Lopez-Anido, R., A. P. Michael, T. C. Sandford, and B. Goodell. 2005. “Repair of wood piles using prefabricated fiber-reinforced polymer composite shells.” *J. Perform. Constr. Facil.* 19 (1): 78–87. [https://doi.org/10.1061/\(ASCE\)0887-3828\(2005\)19:1\(78\)](https://doi.org/10.1061/(ASCE)0887-3828(2005)19:1(78)).
- Maaddawy, T. E. 2008. “Behavior of corrosion-damaged RC columns wrapped with FRP under combined flexural and axial loading.” *Cem. Concr. Compos.* 30 (6): 524–534. <https://doi.org/10.1016/j.cemconcomp.2008.01.006>.
- Manalo, A. C., T. Aravinthan, H. Mutsuyoshi, and T. Matsui. 2012. “Composite behaviour of a hybrid FRP bridge girder and concrete deck.” *Adv. Struct. Eng.* 15 (4): 589–600. <https://doi.org/10.1260/1369-4332.15.4.589>.
- Manalo, A. C., W. Karunasena, C. Sirimanna, and G. B. Maranan. 2014. “Investigation into fibre composites jacket with an innovative joining system.” *Constr. Build. Mater.* 65: 270–281. <https://doi.org/10.1016/j.conbuildmat.2014.04.125>.
- Manalo, A. C., C. Sirimanna, W. Karunasena, L. McGarva, and P. Falzon. 2016. “Pre-impregnated carbon fibre reinforced composite system for patch repair of steel I-beams.” *Constr. Build. Mater.* 105: 365–376. <https://doi.org/10.1016/j.conbuildmat.2015.12.172>.
- Mander, J. B., M. J. N. Priestley, and R. Park. 1988. “Theoretical Stress-Strain Model for Confined Concrete.” *J. Struct. Eng.* 114 (8): 1804–1826. [https://doi.org/10.1061/\(ASCE\)0733-9445\(1988\)114:8\(1804\)](https://doi.org/10.1061/(ASCE)0733-9445(1988)114:8(1804)).
- Maranan, G., A. Manalo, B. Benmokrane, W. Karunasena, and P. Mendis. 2016. “Behavior of concentrically loaded geopolymer-concrete circular columns reinforced longitudinally and transversely with GFRP bars.” *Eng. Struct.* 117: 422–436. <https://doi.org/10.1016/j.engstruct.2016.03.036>.
- Mohamed, H. M., H. M. Abdel-Baky, and R. Masmoudi. 2010. “Nonlinear stability analysis of concrete-filled fiber-reinforced polymer-tube columns: Experimental and theoretical investigation.” *ACI Struct. J.* 107 (6): 699–708.
- Mohamed, H. M., and R. Masmoudi. 2010. “Axial load capacity of concrete-filled FRP tube columns: Experimental versus theoretical predictions.” *J. Compos. Constr.* 14 (2): 231–243. [https://doi.org/10.1061/\(ASCE\)CC.1943-5614.0000066](https://doi.org/10.1061/(ASCE)CC.1943-5614.0000066).
- Mohammed, A. A., A. C. Manalo, G. B. Maranan, Y. Zhuge, and J. Pettigrew. 2017. “FRP jacket assembly for retrofitting concrete structures.” In *Proc., 6th Asia-Pacific Conf. FRP in Structures*. Kingston, ON, Canada: International Institute for FRP in Construction.
- Mohammed, A. A., A. C. Manalo, G. B. Maranan, Y. Zhuge, and P. V. Vijay. 2018. “Comparative study on the behaviour of different in-fill materials for pre-fabricated fibre composite repair systems.” *Constr. Build. Mater.* 172: 770–780. <https://doi.org/10.1016/j.conbuildmat.2018.04.025>.
- Muttashar, M., A. Manalo, W. Karunasena, and W. Lokuge. 2017. “Flexural behaviour of multi-celled GFRP composite beams with concrete infill: Experiment and theoretical analysis.” *Compos. Struct.* 159: 21–33. <https://doi.org/10.1016/j.compstruct.2016.09.049>.
- Nanni, A., and M. S. Norris. 1995. “FRP jacketed concrete under flexure and combined flexure-compression.” *Constr. Build. Mater.* 9 (5): 273–281. [https://doi.org/10.1016/0950-0618\(95\)00021-7](https://doi.org/10.1016/0950-0618(95)00021-7).
- Ozbakkaloglu, T., J. C. Lim, and T. Vincent. 2013. “FRP-confined concrete in circular sections: Review and assessment of stress-strain models.” *Eng. Struct.* 49: 1068–1088. <https://doi.org/10.1016/j.engstruct.2012.06.010>.
- Parvin, A., and A. S. Jamwal. 2006. “Performance of externally FRP reinforced columns for changes in angle and thickness of the wrap and concrete strength.” *Compos. Struct.* 73 (4): 451–457. <https://doi.org/10.1016/j.compstruct.2005.02.019>.
- Pessiki, S., K. A. Harries, J. T. Kestner, R. Sause, and J. M. Ricles. 2001. “Axial behavior of reinforced concrete columns confined with FRP jackets.” *J. Compos. Constr.* 5 (4): 237–245. [https://doi.org/10.1061/\(ASCE\)1090-0268\(2001\)5:4\(237\)](https://doi.org/10.1061/(ASCE)1090-0268(2001)5:4(237)).
- Pham, T. M., L. V. Doan, and M. N. S. Hadi. 2013. “Strengthening square reinforced concrete columns by circularisation and FRP confinement.” *Constr. Build. Mater.* 49: 490–499. <https://doi.org/10.1016/j.conbuildmat.2013.08.082>.
- Pham, T. M., M. N. Hadi, and J. Youssef. 2015. “Optimized FRP wrapping schemes for circular concrete columns under axial compression.” *J. Compos. Constr.* 19 (6): 04015015. [https://doi.org/10.1061/\(ASCE\)CC.1943-5614.0000571](https://doi.org/10.1061/(ASCE)CC.1943-5614.0000571).
- Pham, T. M., J. Youssed, M. N. Hadi, and T. M. Tran. 2016. “Effect of different FRP wrapping arrangements on the confinement mechanism.” *Procedia Eng.* 142: 307–313. <https://doi.org/10.1016/j.proeng.2016.02.051>.

- Saadatmanesh, H., M. R. Ehsani, and M.-W. Li. 1994. "Strength and ductility of concrete columns externally reinforced with fiber composite straps." *Struct. J.* 91 (4): 434–447.
- Sakr, M., M. El Naggar, and M. Nehdi. 2005. "Interface characteristics and laboratory constructability tests of novel fiber-reinforced polymer/concrete piles." *J. Compos. Constr.* 9 (3): 274–283. [https://doi.org/10.1061/\(ASCE\)1090-0268\(2005\)9:3\(274\)](https://doi.org/10.1061/(ASCE)1090-0268(2005)9:3(274)).
- Shamsuddoha, M., M. M. Islam, T. Aravinthan, A. Manalo, and K.-T. Lau. 2013. "Effectiveness of using fibre-reinforced polymer composites for underwater steel pipeline repairs." *Compos. Struct.* 100: 40–54. <https://doi.org/10.1016/j.compstruct.2012.12.019>.
- Shi, X., N. Xie, K. Fortune, and J. Gong. 2012. "Durability of steel reinforced concrete in chloride environments: An overview." *Constr. Build. Mater.* 30: 125–138. <https://doi.org/10.1016/j.conbuildmat.2011.12.038>.
- Smith, S. T., S. J. Kim, and H. Zhang. 2010. "Behavior and effectiveness of FRP wrap in the confinement of large concrete cylinders." *J. Compos. Constr.* 14 (5): 573–582. [https://doi.org/10.1061/\(ASCE\)CC.1943-5614.0000119](https://doi.org/10.1061/(ASCE)CC.1943-5614.0000119).
- Tapan, M., and R. S. Aboutaha. 2011. "Effect of steel corrosion and loss of concrete cover on strength of deteriorated RC columns." *Constr. Build. Mater.* 25 (5): 2596–2603. <https://doi.org/10.1016/j.conbuildmat.2010.12.003>.
- Teng, J. G. 2002. *FRP-strengthened RC structures*. Hoboken, NJ: Wiley.
- Teng, J. G., J. Chen, S. T. Smith, and L. Lam. 2003. "Behaviour and strength of FRP-strengthened RC structures: A state-of-the-art review." *Proc. Inst. Civ. Eng. Struct. Build.* 156 (1): 51–62. <https://doi.org/10.1680/stbu.2003.156.1.51>.
- Teng, J. G., and L. Lam. 2004. "Behavior and modeling of fiber reinforced polymer-confined concrete." *J. Struct. Eng.* 130 (11): 1713–1723. [https://doi.org/10.1061/\(ASCE\)0733-9445\(2004\)130:11\(1713\)](https://doi.org/10.1061/(ASCE)0733-9445(2004)130:11(1713)).
- Vandoros, K. G., and S. E. Dritsos. 2008. "Concrete jacket construction detail effectiveness when strengthening RC columns." *Constr. Build. Mater.* 22 (3): 264–276. <https://doi.org/10.1016/j.conbuildmat.2006.08.019>.
- Vijay, P., P. R. Soti, H. V. GangaRao, R. G. Lampo, and J. D. Clarkson. 2016. "Repair and strengthening of submerged steel piles using GFRP composites." *J. Bridge Eng.* 21 (7): 04016038. [https://doi.org/10.1061/\(ASCE\)BE.1943-5592.0000903](https://doi.org/10.1061/(ASCE)BE.1943-5592.0000903).
- Williams, J. 2009. *FRP pile jacket solution has no 'pier' in timber pile restoration*. Independence, KS: MFG Construction Products.
- Yan, Z., and C. P. Pantelides. 2011. "Concrete column shape modification with FRP shells and expansive cement concrete." *Constr. Build. Mater.* 25 (1): 396–405. <https://doi.org/10.1016/j.conbuildmat.2010.06.013>.
- Yan, Z., C. P. Pantelides, and L. D. Reaveley. 2007. "Posttensioned FRP composite shells for concrete confinement." *J. Compos. Constr.* 11 (1): 81–90. [https://doi.org/10.1061/\(ASCE\)1090-0268\(2007\)11:1\(81\)](https://doi.org/10.1061/(ASCE)1090-0268(2007)11:1(81)).

## **Chapter 5**

### **Effectiveness of a novel composite jacket in repairing damaged reinforced concrete structures subject to flexural loads**

Chapter 4 presented a detailed understanding on the compressive behaviour of damaged RC piles repaired with the novel prefabricated jacket and presented a valid evaluation on the jacket effectiveness as a repair system. Since bridge piers, wharves and jetties, where the prefabricated FRP jackets are commonly used, are subjected to lateral loads from water, tides and waves which create flexural stresses in the member in addition to the axial service loads. Thus, investigating the flexural behaviour of the damaged members repaired with FRP jacket is very important and the focus of this chapter. Four-point bending test was conducted on eight large-scale square concrete beams (220 mm by 220 mm in cross-section and 3000 mm in length) with 37.5% simulated steel corrosion and repaired with the prefabricated FRP jacket. The damage location in the beam, joint location and internal surface coating of the FRP jacket were the main parameters investigated in this study. The study found out that the effectiveness of the novel repair system was highly influenced by the tensile strength of the grout infill and the joint capacity. Moreover, the results showed that the FRP jacket is more effective in repairing flexural members with the damage located at the top than at the bottom. Only 55% restoration of the original flexural strength of the beam was achieved when the damage was at the bottom whereas 114% strength restoration was achieved when the damage was at the top. Placing the joint away from the compression zone resulted in 53% higher flexural strength capacity compared to the case when the joint was at the compression zone. In addition, the provision of epoxy and coarse aggregate coating inside the GFRP jacket surface resulted in better stress distribution and cracks propagation in the grout than the one without coating which increased the flexural strength capacity by 12%. The simplified fibre model analysis accurately predicted the flexural strength of the repaired beams considering confined mechanical properties of the grout. Finally, for both axial and flexural investigation, a further investigation on the behaviour of internal parts of the retrofitted members that were covered by the jacket is necessary to identify the effect of critical design parameters. This was the key motivation to conduct finite element analysis as a final stage of this research.



## Effectiveness of a novel composite jacket in repairing damaged reinforced concrete structures subject to flexural loads



Ali A. Mohammed<sup>a,b</sup>, Allan C. Manalo<sup>a,\*</sup>, Gingham B. Maranan<sup>c</sup>, Majid Muttashar<sup>d</sup>, Yan Zhuge<sup>e</sup>, P.V. Vijay<sup>f</sup>, John Pettigrew<sup>g</sup>

<sup>a</sup> Centre for Future Materials (CFM), School of Civil Engineering and Surveying, University of Southern Queensland, Toowoomba 4350, Australia

<sup>b</sup> Environmental Engineering Department, College of Engineering, The University of Mustansiriyah, Baghdad, Iraq

<sup>c</sup> Civil Engineering, School of Engineering, Faculty of Science and Engineering, University of Waikato, Hamilton 3216, New Zealand

<sup>d</sup> Department of Civil Engineering, College of Engineering, University of Thi-Qar, Thi-Qar, Iraq

<sup>e</sup> School of Natural & Built Environments, University of South Australia, Adelaide 5001, Australia

<sup>f</sup> Department of Civil and Environmental Engineering, West Virginia University, Morgantown, WV 26506, USA

<sup>g</sup> Joinlox Pty Ltd, Unit 2, 30 Walker Street, Brisbane, Queensland 4105, Australia

### ARTICLE INFO

#### Keywords:

Prefabricated FRP composite jacket  
Composite repair system  
Damaged concrete beams  
FRP joint

### ABSTRACT

This study evaluates the effectiveness of a novel composite repair system consisting of prefabricated fibre reinforced polymer (FRP) jacket with joint and grout infill for damaged concrete structures subject to flexural loads. Full-scale beams were prepared and tested under four-point static loads to evaluate the effects of damage location in the concrete member, joint location and internal surface coating of the jacket. The results showed that the behaviour of the repaired system is governed by the tensile cracking of the grout and failing of teeth at the joint. The FRP jacket is found to be more effective in repairing concrete members under flexural load when the damage is located at the top than at the bottom of the member. This effectiveness can be further increased by placing the joint of the composite jacket away from the compression zone. Moreover, the provision of epoxy and coarse aggregates inside the jacket surface resulted in better stress distribution and cracks propagation in the grout than the one without. Finally, a simplified fibre model analysis which considers the confined tensile and compressive properties of the grout reliably predicted the flexural capacity of the damaged beams repaired with the FRP jacket.

### 1. Introduction

The corrosion of steel reinforcement induced by the ingress of chloride ions is the most common cause of the deterioration of reinforced concrete (RC) structures [1,2]. The steel corrosion is usually accompanied with a reduction in the cross-sectional area of the corroded bars, loss of bond between bars and concrete, volume expansion and stresses in the adjacent concrete causing cracking and spalling of the concrete cover [3–5]. In the past few decades, a large number of research were conducted to evaluate the impact of steel corrosion on the structural behaviour of RC structures [6–10]. Manalo et al. [11] indicated that simulating a 50% corrosion in a circular RC columns of 1 m height and 250 mm diameter resulted in a 56% reduction in the axial load capacity. Torres-Acosta et al. [12] experimentally showed that the increase in the level of corrosion damage was the most

important factor reducing the flexural load capacity of corroded RC beams. The damaged or deteriorated infrastructure needs repair, replacement or retrofit to remain in service. It is estimated that more than \$5 billion is spent annually in maintaining RC bridges in countries like US, Canada and Europe [13]. In Australia, the corrosion-induced damages cost the economy more than \$13 billion per year due to production and shutdown related losses during repairs as reported by the Commonwealth Scientific and Industrial Research Organisation as per Cassidy et al. [14]. Hence, adopting an effective rehabilitation and retrofitting technique can be economically beneficial by minimizing the off-service time in repairing aging and damaged structures.

RC jackets [15,16] and steel jackets [17,18] are traditionally used as repair techniques for concrete structures. However, the use of versatile fibre-reinforced polymer (FRP) composites has increased in the last two decades as it addresses the limitations of the currently available

\* Corresponding author.

E-mail addresses: [ali.mohammed@usq.edu.au](mailto:ali.mohammed@usq.edu.au) (A.A. Mohammed), [allan.manalo@usq.edu.au](mailto:allan.manalo@usq.edu.au) (A.C. Manalo), [gmaranan@waikato.ac.nz](mailto:gmaranan@waikato.ac.nz) (G.B. Maranan), [yan.zhuge@unisa.edu.au](mailto:yan.zhuge@unisa.edu.au) (Y. Zhuge), [p.vijay@mail.wvu.edu](mailto:p.vijay@mail.wvu.edu) (P.V. Vijay), [johnp@joinlox.com](mailto:johnp@joinlox.com) (J. Pettigrew).

<https://doi.org/10.1016/j.compstruct.2019.111634>

Received 22 November 2018; Received in revised form 10 October 2019; Accepted 30 October 2019

Available online 02 November 2019

0263-8223/ © 2019 Elsevier Ltd. All rights reserved.

rehabilitation techniques such as limited access, sensitive marine environments, heavy weight and complexity of steel anchorage and others [19]. The superior characteristics of FRP such as high strength, corrosion resistance, lightweight, high fatigue resistance, high impact resistance and durability [20–23] have made them the materials of choice for rehabilitating damaged and deteriorated civil infrastructure [24–30].

As a repair system, FRP composites can be applied either as wet lay-up or pre-fabricated systems [31–33]. In the wet lay-up, FRP repair systems are prepared and applied on site by impregnating liquid resins into fibres and then wrapping them around the existing structure. The pre-fabricated systems, on the other hand, are manufactured in a factory and delivered to a site in ready for installation condition. Although many studies have shown that both systems are effective [34–38], the pre-fabricated composite jacket is favoured over the wet lay-up method because it is easier, quicker, safer to install and can achieve a higher quality under well controlled manufacturing conditions. Vijay et al. [39] combined the use of pre-cured glass FRP (GFRP) shells and water-curable GFRP prepreg fabrics for encasing, wrapping and rehabilitating 20 water-submerged steel H-piles of a bridge in the USA. Their experimental results showed an increase of 38% in the axial compressive strength of concrete cylinders repaired by this system. The installation of this system, however, requires a two-stage process wherein the pre-cured GFRP shells are installed first and then wrapped with a wet fabric. Karagah et al. [40] conducted a full-scale experimental investigation to study the behaviour of I-shaped steel bridge piles with corrosion damage repaired underwater using two different types of grout-filled FRP jackets. The first one consisted of two plies of pre-fabricated flexible CFRP wrapped around the piles and bonded using an underwater curing adhesive. The second type consisted of a two-layered FRP system wherein the first layer was fabricated using two plies of GFRP installed around the pile using marine adhesive and screws, while the second layer consisted of one CFRP layer installed over the GFRP layer using a wet-layup technique. The results showed that both repair systems were able to restore and enhance the axial capacity of the piles with the second type providing 11% higher enhancement than the first one. Beddiar et al. [41] used GFRP prefabricated jacket consisting of three identical shells connected by stepped lap joints as a strengthening and repair system. The gap between the shells and the column was filled with shrinkage-compensating cement mortar. The experimental results have demonstrated increases in the axial load capacity and durability by 31% and 74%, respectively, when compared to the un-jacketed concrete specimens. Lopez-Anido et al. [42] proposed a repair system consisting of two FRP composite shells which are held together with circumferential metal straps or temporary bands for the protection and structural restoration of deteriorated wood piles. Many other studies have demonstrated the effectiveness of using FRP composite jackets in restoring/upgrading the compressive strength of columns and bridge piers [43–49]. Bridge piers however are also subjected to lateral loads from water, tides and waves which create flexural stresses in the member, but there is still very limited studies on the flexural behaviour of those structural members when repaired with a composite jacket.

Recently, a new type of FRP composite jacket (Fig. 1), that can be quickly and safely installed due to its easy-fit and self-locking mechanical joining system has been developed [50]. This innovative joining system comprises of two interlocking edges that can easily fit into each other like the teeth of a zipper. A FRP locking key is placed between the interlocking teeth, which can be slid or levered only one pitch length, thus causing wedging of the joint edges and resulting in a uniform force distribution along the entire length of the joint. The jacket can be applied over the entire length of the structure or just over the damaged portion to restore the capacity of the corrosion-damaged concrete member. Manalo et al. [32] determined the most suitable joint materials and assessed the capacity and behaviour of this system when subjected to an internal pressure. Mohammed et al. [51] investigated the important characteristics of the grouting materials that will



Fig. 1. Novel GFRP jacket with novel joining system.

effectively utilise the inherent properties of this composite repair system. Furthermore, Mohammed et al. [52] evaluated the efficiency of this novel repair system in restoring the axial strength of reinforced concrete columns with different levels of simulated corrosion. However, the performance benefits of this FRP jacket are not yet fully evaluated and its contribution to the bending capacity of the repaired structure is yet to be explored. This study provides a better understanding on the structural performance of reinforced concrete structures repaired with the novel FRP jacket system under flexural loads. This information is critical for evaluating the efficiency of this new repair system and its application to actual rehabilitation projects.

## 2. Experimental program

### 2.1. Materials

#### 2.1.1. Reinforcing steel

Deformed steel bars [53] with a nominal diameter ( $\phi_s$ ) of 16 mm and a manufacture specified yield strength ( $f_y$ ) of 500 MPa were used to reinforce the square beam specimens in the longitudinal direction, while plain steel bars [53] with a  $\phi_s$  of 10 mm and a  $f_y$  of 250 MPa were used as transverse reinforcement.

#### 2.1.2. Concrete

A commercially produced ready mix concrete with a proprietary mixture consisting of fine and medium sand, 10 mm coarse aggregates, water and normal Portland cement, were used to cast the beam specimens from one batch. The average slump of the fresh concrete, following the ASTM C143/C143M-15 [54], was 135 mm. Eight concrete cylinders were prepared, cured and tested in accordance with the ASTM C31/C31M-12 and ASTM C39/C39M-15a [55,56]. The average 28-day compressive strength ( $f'_{co}$ ) and modulus of elasticity ( $E_c$ ) of the concrete were determined to be 35 MPa and 28 GPa, respectively.

#### 2.1.3. GFRP jacket

The GFRP jacket evaluated in this study consists of two main integrated parts, GFRP shell and innovative GFRP joining system. Both the GFRP jacket and the joint are made of E-glass fibres impregnated with vinyl ester resin. The GFRP shell was fabricated by the filament winding method, while the GFRP joint was made through the pultrusion process. Burnout tests were conducted in accordance with ISO 1172-96 [57], which revealed that the GFRP shell has a 67.6% fibre content by weight and a stacking sequence of  $-45^\circ/+45^\circ/-45^\circ/+45^\circ$  with respect to the hoop direction. This configuration is effective in resisting multi-axial stresses and in providing a more ductile behaviour at failure [58,59]. The joint had a fibre content ratio of 66.0% and consisted of several layers of longitudinal fibres, chopped strand and woven mat layers.

The tensile and compressive properties of the GFRP shell and joint were determined by coupon testing in accordance with the ISO 527-

1:1995 [60] and ISO 14126:1999 [61], respectively. The test coupons were cut directly from one of the jackets along the longitudinal direction using a water jet cutting machine. The test results revealed that the jacket has ultimate strength and strain equal to 297 MPa and 11,268  $\mu\epsilon$ , respectively, in tension, and 180 MPa and 11,001  $\mu\epsilon$ , respectively, in compression. The result also showed that the joint has ultimate tensile strength and peak strain equal to 256 MPa and 10,000  $\mu\epsilon$ , respectively, along the longitudinal direction, and 37 MPa and 3500  $\mu\epsilon$ , respectively, along the transverse direction. Lastly, the ultimate compressive strength and peak strain of the joint were equal to 394 MPa and 15,000  $\mu\epsilon$ , respectively.

#### 2.1.4. Grout-infill

A shrinkage-compensating-cementitious-grout infill, commercially known as BluCem GP60, was used to fill the annulus between the jacket and the RC beams. This grout was made up of cement powder with a maximum particle size of 0.3 mm. This grout infill was selected because of its relative high stiffness, which made it effective in transferring loads and stresses from the repaired structure to the FRP jacket [62]. Following the specified procedure in the technical data sheet [63], a water-to-cement weight ratio of 0.175 was adopted to obtain a flowable and fillable grout without void formation. The constituent behaviour and the mechanical properties of the cementitious-grout infill were reported by Mohammed et al. [51], wherein the compressive strength ( $f'_{cg}$ ) and modulus of elasticity ( $E'_{cg}$ ) of the cementitious-grout infill were 48.2 MPa and 34.3 GPa, respectively. In addition, the behaviour of grout-filled GFRP tubes under split-tensile load was determined in accordance with the ASTM C496/C496M [64] (Fig. 2). Strain gauges were mounted at the mid-length along the hoop direction of the tube. Fig. 3 shows that the stress increased linearly with the strain up to an applied stress of 7 MPa at a strain of 2700  $\mu\epsilon$  (Point A). Point A represents the initiation of crushing of the cementitious grout at the top and bottom of the cylinder near the loading points as shown in Fig. 4a. When the stress reached a value of 8 MPa at a strain of 5000  $\mu\epsilon$  (Point B), the grout experienced severe and wide splitting tensile cracking (Fig. 4b). Since the grout was confined by the GFRP tube, it was capable of carrying an ultimate stress of 10 MPa at a strain equal to 9000  $\mu\epsilon$  (Point C). Next, the grout was crushed and displaced towards the ends and fell off as depicted in Fig. 4c, which resulted in the decrease in load capacity as noted at point D.

#### 2.2. Test specimens

Fig. 5 summarises the details and configurations of the beams tested in this study. Eight large-scale square concrete beams (220 mm by 220 mm in cross-section and 3000 mm in length) were cast and tested to failure. All of the beams were reinforced with eight 16 mm longitudinal steel bars, 3 bars at top layer, 2 bars at middle layer and 3 bars at



Fig. 2. Splitting tensile test set-up.

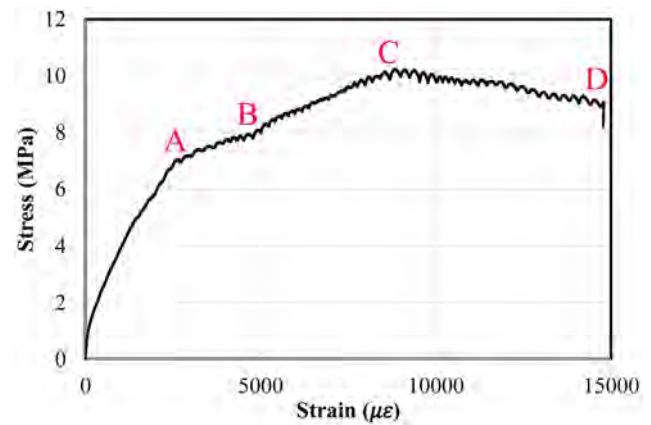


Fig. 3. Behaviour of grout-filled FRP tubes.

bottom layer, (equivalent to 3.23% of the beam's gross cross-sectional area) and plain steel stirrups spaced at 50 mm centre-to-centre (to avoid shear failure). The beams were provided with a clear concrete cover of 25 mm. The area of the beam, concrete core and reinforcement ratio are similar to those of 250 mm diameter circular columns investigated under compression by Mohammed et al. [52]. However, due to the difficulty and practical consideration in manufacturing 3.0 m long circular beams, beams with square section having a similar cross-sectional area were manufactured. In field conditions with severe corrosion, the stirrups in a steel corroded beam are not functional, and should not be considered in the design. Thus, lateral ties were not provided within the damage locations of the beams to ensure that the concrete confinement (if any) in the repaired region is provided solely by the FRP jacket system as was also implemented by Abdel-Hay and Fawzy [65].

Since the accelerated corrosion process takes significant amount of time in simulating low levels of corrosion damage [66,67], the steel corrosion damage was simulated by cutting and removing the bottom most longitudinal reinforcement for a length of 300 mm in the test region of the beam and replaced with a non-structural PVC pipe (1 mm thick and 16 mm internal diameter). The PVC pipe also prevented the concrete from occupying the steel location and volume, maintained the alignment of longitudinal reinforcement (Fig. 6) and ensured that all specimens had the same level of simulated corrosion damage. Similar approach was adopted by Manalo et al. [68], Karagah et al. [40] and Liu et al. [69] where the flanges of S steel sections were machined to represent the section loss due to corrosion. In actual systems, the corrosion damage would most probably occur in non-homogeneous manner. However, simulating this corrosion in the laboratory is difficult. In the current study, the approach of discontinuing the steel bars to simulate corrosion-damage is believed to cause more detrimental effect on the flexural behaviour of the reinforced concrete members as the tensile reinforcement cannot resist any force. GFRP jackets measuring 450 mm in diameter and 700 mm in length were then placed around the damaged section and the annulus between the beam and the jacket was filled with the grout (Fig. 7). The diameter of the FRP jacket was based on the curvature of the available joint.

The test specimens were labelled in the following manner: specimen condition-type of repair system. The first letters U and D stand for undamaged and damaged beam, respectively, while the last letters J and S identify the beams repaired with GFRP jacket and GFRP sleeve (continuous GFRP shell), respectively, while 0 means no repair was used. The letters D and J are followed by a lower-case letter, t or b, which stand for top and bottom, respectively, to signify the damage location, or the joint location of the jacket, if used. Finally, letter E was added at the end of a specimen's label to refer to the epoxy coating applied inside the jacket. The first specimen U-0 (Fig. 5a) served as an undamaged control specimen. The second and third specimens represented by U-Jt (Fig. 5b) and U-JtE (Fig. 5c), respectively, were

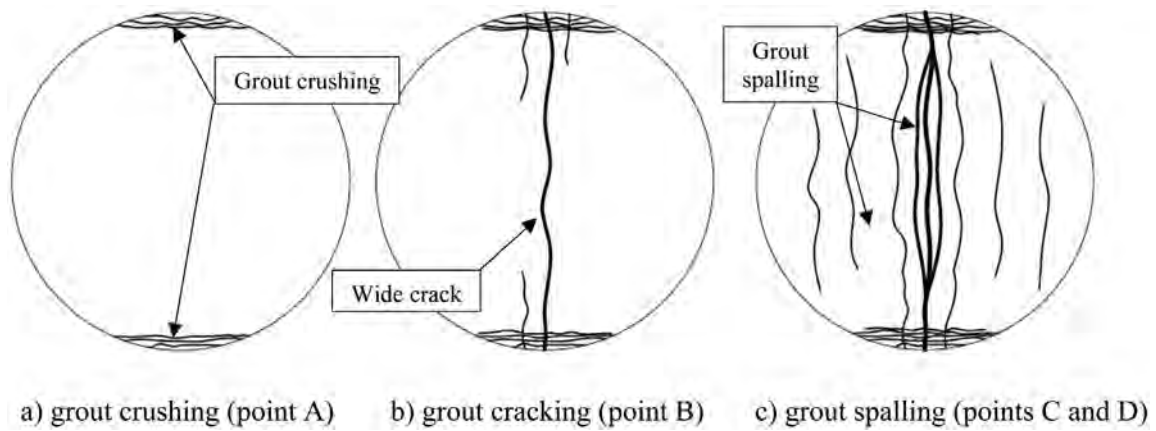


Fig. 4. Schematic diagram of the failure mode of grout-filled FRP tubes.

prepared without any damages and were wrapped with GFRP jacket and GFRP jacket coated with epoxy, respectively, to evaluate the influence of the epoxy coating on the jacket effectiveness. Both of the beams had the FRP joint location at the top of the specimens. The fourth beam U-S (Fig. 5d) was also prepared with no damage but it was wrapped with continuous GFRP shell (no joint) to determine the effectiveness of the joint in the repair system. The fifth beam Db-0 (Fig. 5e) served as the damaged control specimen as it was fabricated with simulated damage and it was not repaired with the FRP jacket. The sixth beam Db-Jt and seventh beam Db-Jb (Fig. 5f and 5g, respectively) were both prepared with simulated corrosion damage at the bottom and repaired with the novel FRP jacket, but in the former specimen, the joint was placed at the top while in the latter, the joint was located at the bottom. The joint location was varied to determine the behaviour of the joint in the compression and tension zones. The current industry

practice is to locate the joint away from the damage as asset owners are concerned that the joint may provide a pathway for moisture to reach the damaged locations in the existing structures. The final specimen Dt-Jb (Fig. 5h) is similar to the Db-Jb, except the damage location being placed at the top of the beam. The behaviour of the last three specimens was evaluated to determine the effectiveness of the repair system as well as the influence of joint and damage locations.

### 2.3. Test program and instrumentation

Fig. 8 shows the test setup and instrumentation employed in this study to investigate the flexural behaviour of the reinforced concrete beams repaired with the novel FRP jacket. The four-point static bending test was employed for this purpose. The specimens were simply supported with a clear span and a shear span of 2700 mm and 900 mm,

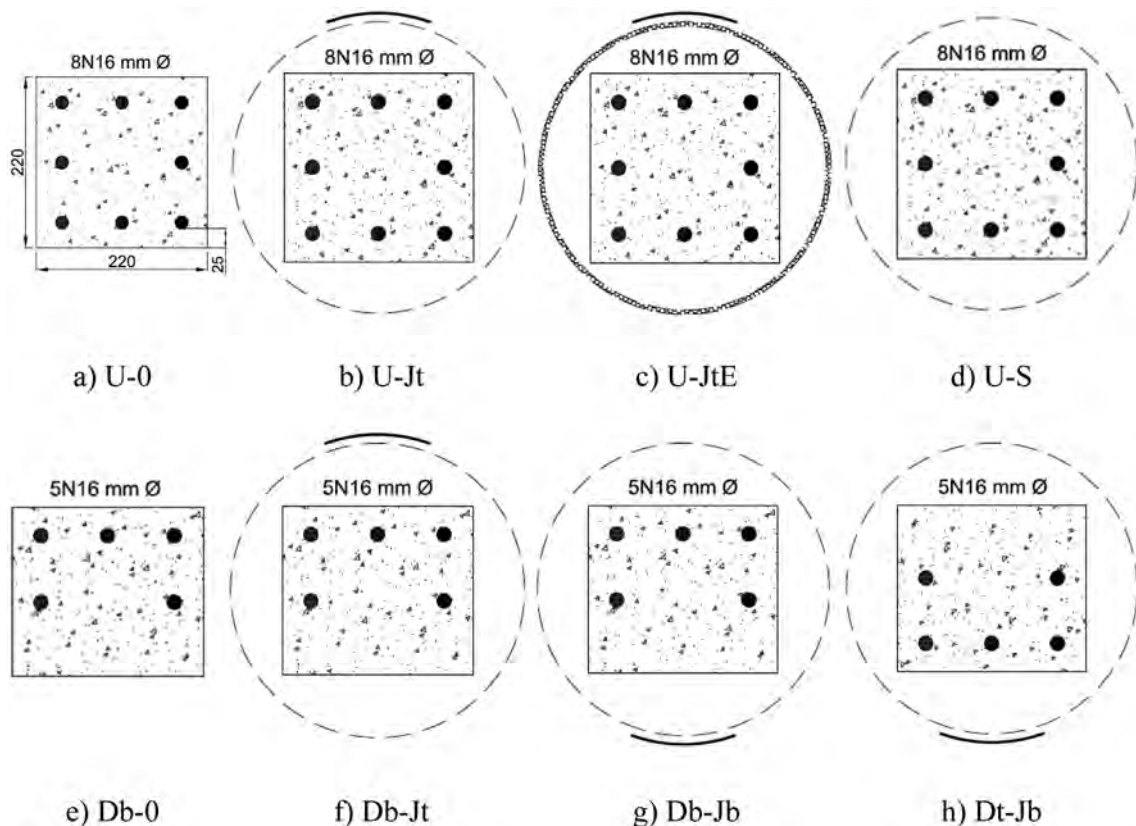


Fig. 5. Details and configuration of test specimens.

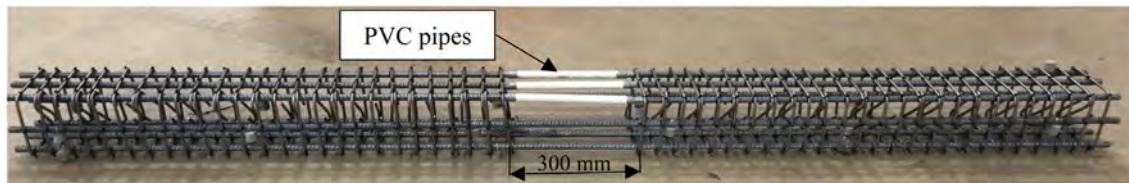


Fig. 6. Fabrication of beams reinforcement cage with simulated damage.



Fig. 7. Installation of GFRP jackets over the beams.

respectively. Bonded resistance strain gauges were mounted longitudinally onto the top concrete (CT), top (ST) and bottom (SB) reinforcement layer, longitudinally (JkC or JkT depending if the gauge is in the compression or tension side) and radially (JkH) onto GFRP jacket, and longitudinally (JnL) and radially onto the key (JnF) and teeth (JnT) of the joint. All the strain gauges were attached at mid-span of the test region.

The beams were subjected to monotonically increasing loads through a spreader I-beam using a 2000 kN electric hydraulic pump and were tested to failure in displacement control while observing the pre- and post-peak behaviour. The magnitude of the applied load was measured with a 500 kN capacity load cell, whereas the corresponding deformations were measured with a string potentiometer and laser displacement sensor. The strain, load and deflection readings were recorded with the help of system 5000 data logger, while the failure propagations were manually observed and video recorded during the entire test.

### 3. Results and observations

This section presents the test results and observations from this experimental work. Table 1 summarises the ultimate load ( $P_u$ ), mid-span deflection at ultimate load ( $\Delta_u$ ) and failure mode of each specimen.

#### 3.1. Cracks propagation and failure mode

Fig. 9 shows the crack propagation on the tested beams. The numbers marked on the beam near the cracks represent the magnitude of the applied load in kN. The experimental cracking moment of the control specimen, U-0, was 8.1 kN.m. For U-0 (Fig. 9a), fine vertical flexural cracks were first developed between the loading point at the bottom of the beam at a load of 16 kN (7.2 kN.m). This is comparable to the theoretical cracking moment of beam U-0 (6.8 kN.m). As the applied load increased, the cracks widened and propagated upward, while new vertical cracks formed along the beam length up to approximately

half of the shear span. Then, the specimen failed due to yielding of the bottom most steel followed by concrete crushing at the top mid-span as shown in Fig. 10a. For beam Db-0, the cracks were initiated at 5 kN and were concentrated near the damaged region as shown in Fig. 9b. While the applied load increased, the crack at the edge of the damaged region became significantly wide, which was followed by concrete crushing at the top (Fig. 11b).

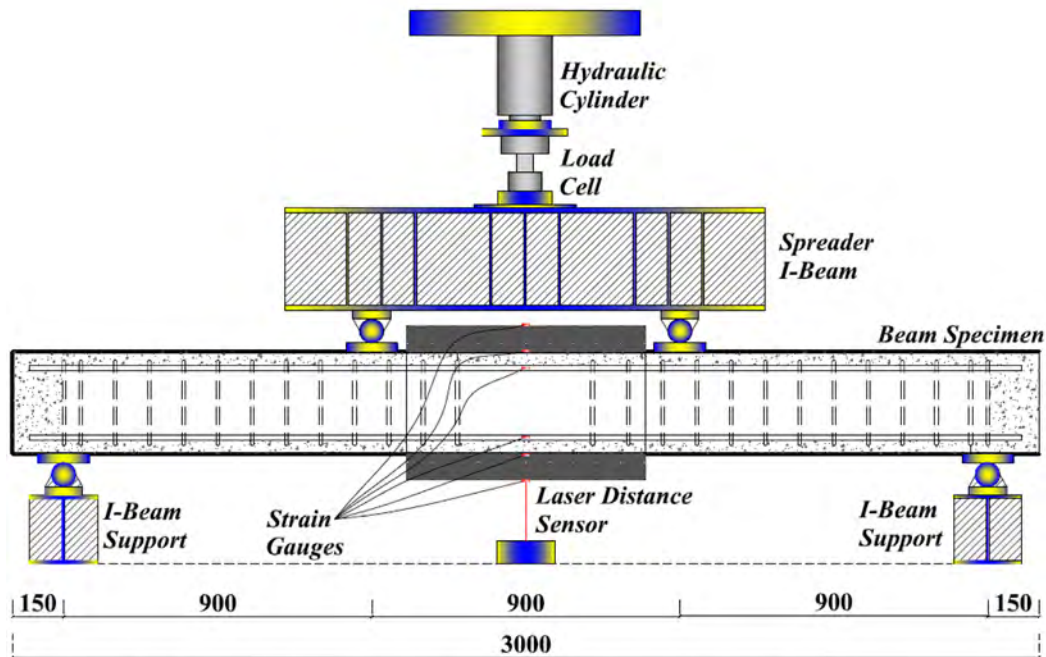
Placing the jacket around the damaged member resulted in shifting of the cracks' concentration to the concrete adjacent to both ends of the jacket. As shown in Fig. 11c-11e, beams U-Jt, U-JtE, and U-S exhibited flexural failure induced by tension steel yielding at mid-span, but the cracks were observed at the bottom concrete at the ends of the jacketed region at an applied load of 20 kN (Fig. 9c). Shear cracks were also observed in the concrete between the jacket and supports for beams U-Jt, U-JtE, and U-S. Interestingly, the post-failure examination of the tested specimens showed that no cracks were generated at the bottom concrete underneath the jacket (Fig. 12c) as the presence of the jacket delayed the steel yielding and protected the concrete underneath from cracking. Relatively wide cracks, however, were observed in the grout underneath the joint, with additional wide cracks at the corners in beams U-Jt and U-JtE (Fig. 10a and 10b), whereas beam U-S exhibited well distributed cracks in the grout with slight concentration of cracks at the corners (Fig. 10c). The failure of the damaged repaired specimens (Db-Jt, Db-Jb and Dt-Jb) was mainly governed by the joint failure as the teeth ripped off from the joint and resulted in opening the jacket (Fig. 12a and 12b). However, the width of crack underneath the joint of beams Db-Jt (Figs. 10d and 11f) and Db-Jb (Fig. 10e and 11g), which have simulated steel corrosion located in the tension area, was substantially large. However, the crack width underneath the joint of beam Dt-Jb (Fig. 10f and 11h) was slightly narrower than that of beams Db-Jt and Db-Jb.

#### 3.2. Load-deformation response

Fig. 13 depicts the relationship between the experimental bending load and the mid-span deflection of the tested beams. For beam U-0, the load-deflection curve started as a linear branch wherein the deflection increased linearly with the applied load which represented the beam's uncracked condition up to an applied load of 16 kN and a deformation of 7 mm. Vertical cracks then appeared at the bottom concrete within the pure moment zone (Fig. 9a), which resulted in a slight reduction in the slope of the curve. This marked the beginning of the cracked condition of the beam, and effective transfer of stresses to the tension steel. Next, it was followed by an almost linear response up to an applied load of 150 kN and a deflection of 33 mm, where the steel started yielding, and then by a nonlinear behaviour until the final failure occurred by concrete crushing (Fig. 11a) in the compression zone at a load of 168 kN and a deflection of 48 mm. For beam Db-0, the load-deformation curve started with short linear behaviour up to an applied load of 10 kN and a deformation of 7 mm where the first concrete crack occurred. Next, the load increased with a reduced stiffness up to 58 kN load and 28 mm deformation accompanied by several minor load-drops, which can be attributed to the severe cracking in the damaged concrete portion (Fig. 9b and 11b). Finally, the post-peak behaviour started with a slight drop and long flat plateau until unloading of the specimen.



a) Actual test setup



b) Schematic diagram of the test (all dimensions in mm)

Fig. 8. Four-point static bending test set-up.

For specimen U-Jt, the load increased linearly up to 150 kN with a deformation of 28 mm and the load-deformation curve provided no indication regarding the initiation of stress-transfer between the concrete and bottom steel. After this point, there was a short transition zone where the steel started yielding and initiated the next stage. This stage is characterised by a slightly ascending segment with few drops

attributed to the widening of cracks at the bottom and concrete crushing at the top on both sides of the jacket, which corresponds to the ultimate failure of this beam (Fig. 11c). Beams Dt-Jb, U-S and U-JtE exhibited similar behaviour to that of U-Jt, but the transition zone was observed at applied loads of 157 kN, 159 kN and 167 kN, respectively, at a deformation of around 27 mm. Beam Db-Jb behaved linearly up to

**Table 1**  
Load, deformation and the failure mode of the tested beams.

Beam	$P_u$ , kN	$\Delta_u$ , mm	Failure Mode
U-0	160	48	Bottom steel layer yielding followed by top concrete crushing and steel buckling
U-Jt	169	48	Bottom steel layer yielding followed by large cracks on the bottom concrete near the jacket ends and no damage in the jacket. Shear concrete cracks and localised grout cracks were observed
U-JtE	189	51	Bottom steel layer yielding followed by well distributed and relatively small cracks on the bottom concrete near the jacket ends and no damage was observed in the jacket. Shear concrete cracks and localised grout cracks were observed
U-S	184	74	Bottom steel layer yielding and followed by flexural concrete cracks near the jacket ends and no damage in the jacket. Shear concrete cracks and well-distributed grout cracks were observed
Db-0	58	37	Middle steel layer yielding followed by top concrete crushing and steel buckling
Db-Jt	60	19	Middle steel layer yielding followed by large cracks on the bottom concrete near the jacket ends. Large grout cracks and significantly wide grout crack underneath the joint were observed, which was followed by rupture of the jacket teeth
Db-Jb	92	32	Middle steel layer yielding followed by large cracks on the bottom concrete near the jacket ends. Large and wide grout cracks were observed underneath the joint, followed by rupture of the jacket teeth
Dt-Jb	183	89	Bottom steel layer yielding followed by large cracks on the bottom concrete near the jacket ends. Large grout cracks were followed by jacket teeth rupture. Shear concrete cracks were observed between the jacket and supports

an applied load of 72 kN and a deformation of 18 mm. Then, the load increase became non-linear due to concrete and grout cracking (Fig. 10c and 11g) up to the ultimate load of 92 kN at a deformation of 32 mm. After that, the load-deformation curve descended until the jacket opening which marked the ultimate failure of the beam as shown in Fig. 11g. Finally, beam Db-Jt behaved linearly up to an applied load of 51 kN and 13 mm deformation. After that, the load dropped down to 43 kN and went up again to a peak value of 60 kN and a deformation of 19 mm. Then the curve moved downwards until the final failure.

**4. Discussion**

*4.1. Effectiveness of the FRP jacket in repairing RC beams with steel corrosion*

The effectiveness of the FRP jacket in repairing concrete beams with steel corrosion was evaluated by studying the behaviour of specimen Db-Jb and comparing it with the behaviour of control specimens (U-0 and Db-0). Simulating 37.5% steel corrosion damage in beam Db-0 resulted in the development of first crack at a lower load magnitude (5 kN) compared to U-0 due to the reduced cross-sectional area. It also reduced its flexural capacity by 64% in comparison with beam U-0. This

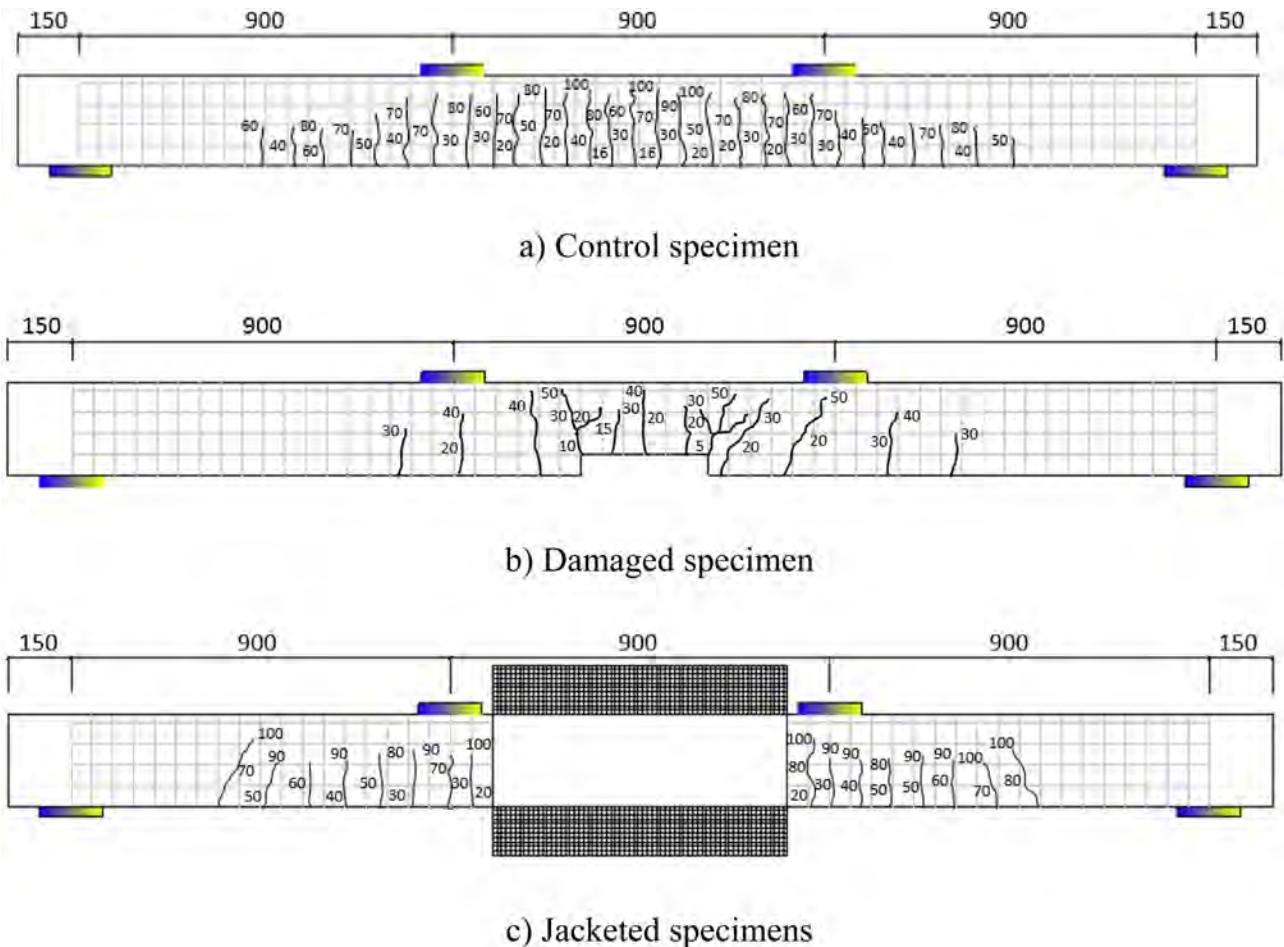


**Fig. 9.** Crack pattern of tested beams.

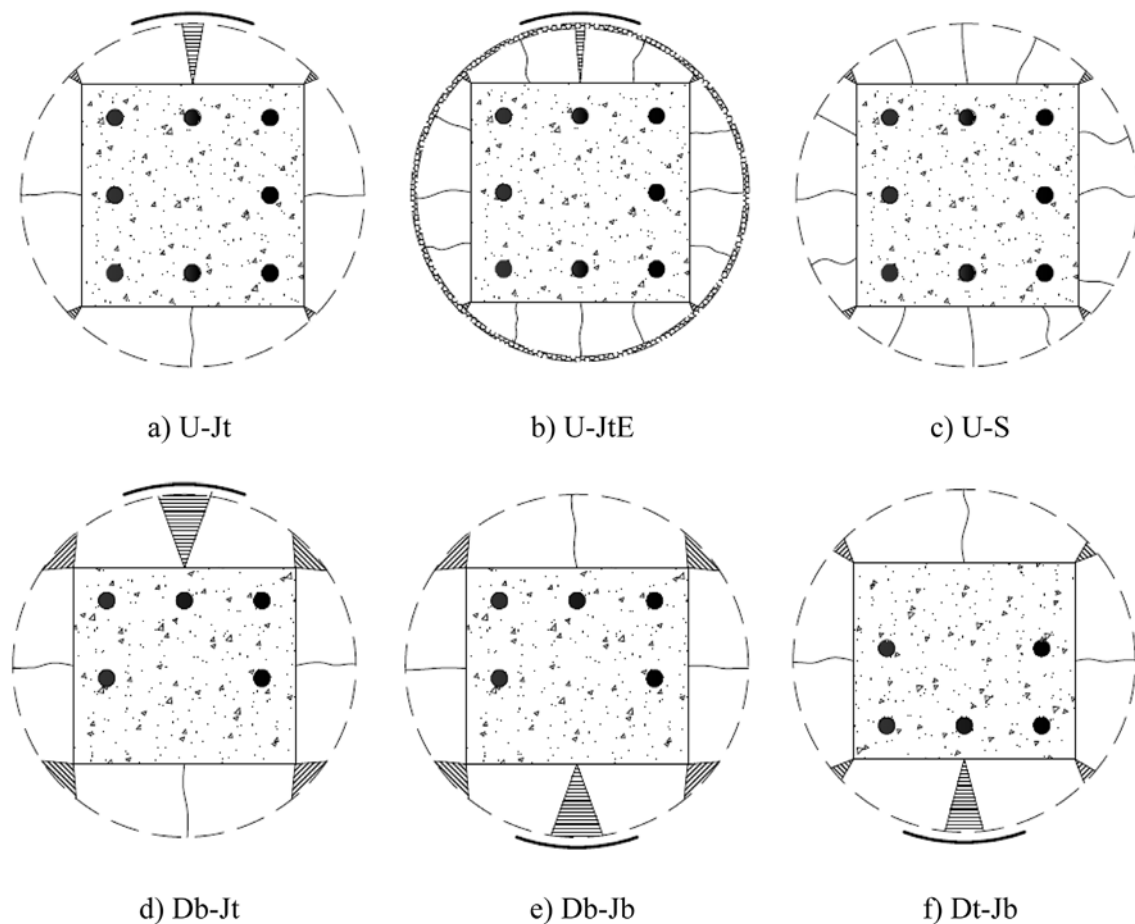


Fig. 10. Propagation of cracks in the grout infill.

reduction is reasonably comparable to that reported by Torres-Acosta et al. [12] where an average of 60% reduction in the flexural load capacity was observed for RC beams with 30% loss of rebar diameter due to simulated corrosion.

Use of FRP jacket in beam Db-Jb protected the concrete from cracking and the top steel from buckling as the jacket resisted the concrete expansion. This can be seen from Fig. 14 wherein the strain in top steel was increasing at a faster rate in beam Db-0 compared to that in beam Db-Jb, which means that, at the same load level, the top steel is more stressed in beam Db-0 than that of Db-Jb. Moreover, beam Db-0 exhibited a sharp drop in the load-strain curve at 20 kN (Fig. 14a) due to the widening of cracks before failing by buckling of the top steel at a strain of  $850 \mu\epsilon$  and a load of 58 kN with concrete crushing. On the other hand, the jacket was activated when cracks began to develop in the grout at a load of 50 kN. As shown in Fig. 14b, the strain at JnL and JnT increased rapidly, and the gauge at JkH was damaged and failed to record the strains. This result suggested that the jacket acted as a tensile reinforcement due to the discontinuity in the bottom steel. Due to the relatively low tensile strength of the grout, a severe large crack was developed beneath the joint as shown in Figs. 10e and 11g. The presence of the jacket however confined the grout and resisted its crack widening until the failure of the jacket. This explains the reason for restoration of 55% original flexural capacity in beam Db-Jb after the repair with FRP. However, it is believed that higher degree of restoration could be achieved by using grouts with higher tensile strength as it will minimise the severity of the localised cracks which opens up the joint of the jacket. Shamsuddoha [70] suggested the use of high tensile strength grouts to maximise the effectiveness of FRP composite repair system for steel pipelines.

#### 4.2. Joint location effect on the FRP jacket effectiveness

Comparative evaluation on the behaviour of beams Db-Jt and Db-Jb was done to investigate the influence of the location of the joint on the effectiveness of the FRP jacket in repairing beams with steel corrosion. The results suggest that placing the joint of the jacket away from the compression zone will result in more effective utilisation of the repair system. As shown in Fig. 14d, JnT strain in beam Db-Jt increased linearly with the applied load at the early stages of loading until an applied load of 24 kN. After which, the strain started to increase rapidly and nonlinearly due to concrete expansion and grout cracking beneath the joint (Fig. 10d). As a result, the joint's teeth were ripped off at a load of 60 kN and a JnT strain of  $480 \mu\epsilon$ , which was followed by the buckling of top steel at  $150 \mu\epsilon$  (Fig. 14d). On the other hand, the presence of the continuous part of the jacket in the compression side of beam Db-Jb confined the top concrete and resisted its expansion which delayed the grout cracking and prevented the top steel buckling. However, once the cracks developed and widened in the grout, especially underneath the joint (Fig. 11d), the specimen failed at the joint by ripping off the teeth. This comparison explains why beam Db-Jb, where the joint was located at the bottom, experienced a 50% higher ultimate flexural strength capacity than that of beam Db-Jt, where the joint was located at the top. In addition, since the FRP joint was manufactured by pultrusion process with relatively high thickness and mostly longitudinal fibres, the beam Db-Jb performed better in tension as it carried direct tensile stresses as shown in Fig. 14b where JnL strain was nearly  $1000 \mu\epsilon$ . Similar observation was reported by Mohamed and Masmoudi [71] as they found that by increasing the thickness of FRP tube in concrete-filled FRP tubes, the flexural strength increased by 20%.

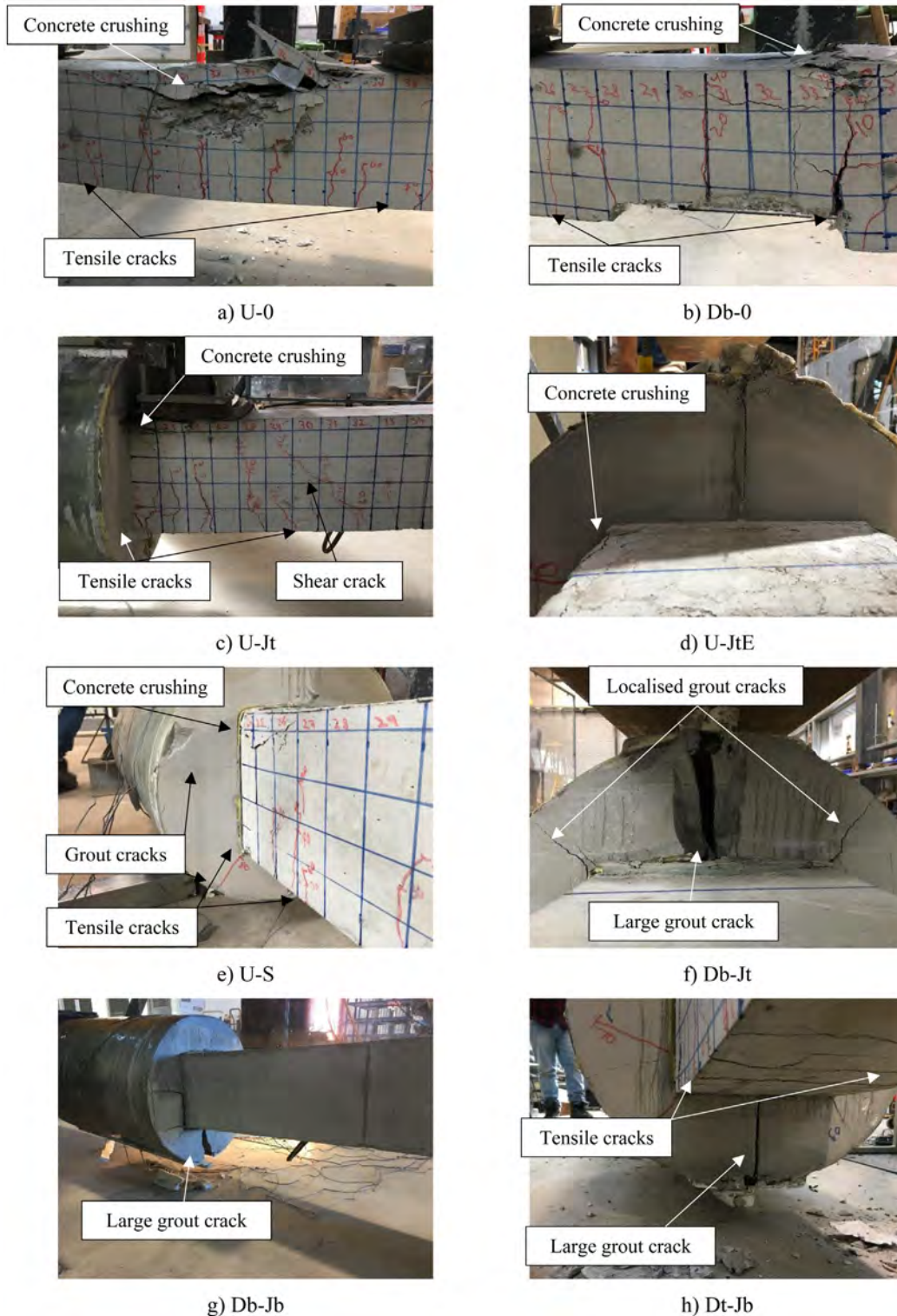


Fig. 11. Failure mode of the tested specimens.

4.3. Damage location effect on the FRP jacket effectiveness

The comparison of the behaviour of beams Db-Jb and Dt-Jb showed that the damage location affects the effectiveness of the FRP jacket. The results suggest that if the damage location is at the bottom, the repair system will be activated earlier to manage the tensile stresses but locating the damage on top will delay the activation of repair system because its contribution will be mainly on the compression side. This

explains why the FRP jacket has restored only 55% of the original flexural strength for beam Db-Jb while 114% strength restoration was achieved in beam Dt-Jb. Despite the difference in the flexural strength capacity, the ultimate failure of beams Db-Jb and Dt-Jb was governed by the joint failure as the teeth ripped off and opened the jacket. Prior to final failure, the grout crack width underneath the joint, however, was narrower in beam Dt-Jb compared to beam Db-Jb. This can be explained by the fact that in beam Dt-Jb where the damage was on top,

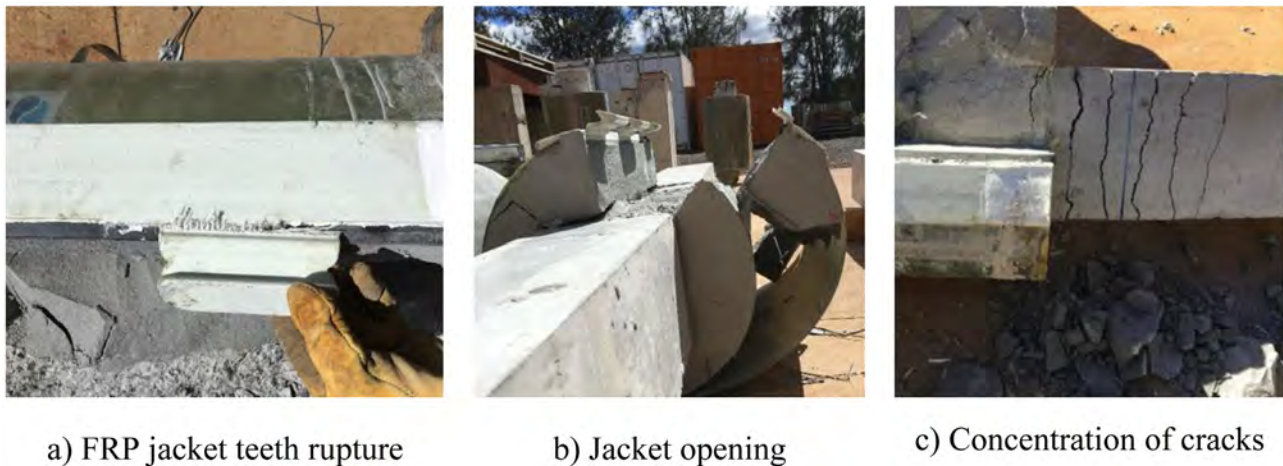


Fig. 12. Failure of the jacket.

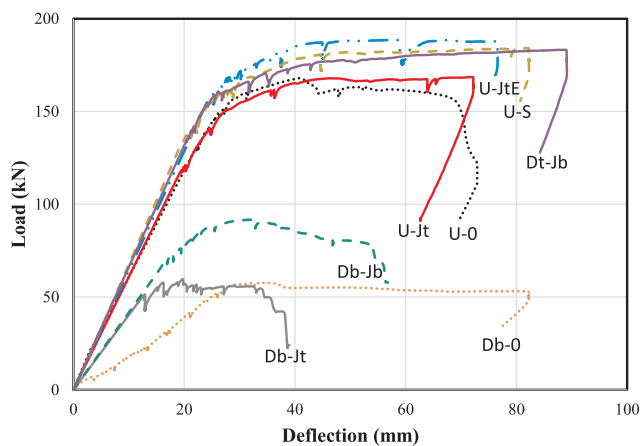


Fig. 13. Load-deflection curves of the tested specimens.

the bottom reinforcement carried most of the tensile stresses up to an applied load of 170 kN as shown in Fig. 14c where SB exhibited strain up to  $1200 \mu\epsilon$ , which was the highest amongst the components of Dt-Jb. After that, the cracks' width significantly increased due to the concrete expansion which resulted in stressing and opening of the joint. The jacket on the compression side, JkC, exhibited almost linearly increasing load-strain curve as it resisted the grout expansion due to cracks that were generated and spread from the top concrete that experienced crushing. However, since the jacket was opened from both ends, the stresses at the middle were shifted to the adjacent parts of the jacket which resulted in yielding of the bottom reinforcement that resulted in large cracking near the bottom concrete as shown in Fig. 11h. In beam Db-Jb, the discontinuity in the bottom reinforcements resulted in higher tensile stresses being carried by the jacket and grout compared to beam Dt-Jb as shown in Fig. 14b where JnT strain started to increase rapidly at an applied load of 50 kN, while it was nearly zero up to an applied load of 160 kN in beam Dt-Jb. As a result, a severe large crack was developed in the grout at a lower load (50 kN) in beam Db-Jb in comparison with beam Dt-Jb.

#### 4.4. Effectiveness of the novel GFRP joint

The efficiency of the novel joint was evaluated by comparing the flexural behaviour of beams U-Jt (jacket with joint) and U-S (sleeve without joint). The behaviour of beam U-Jt indicates that there is a very small gap between the joint edges, and the jacket is activated immediately after the closure of the gap due to concrete/grout expansion. This gap allowed the grout to develop its first crack underneath the

joint, and the crack continued to widen with increased loading which resulted in further stressing of the joint which led to opening and failing of the joint. Thus, the beam U-S showed slightly higher enhancement (by 9%) in the flexural capacity than that of the beam U-Jt as the former specimen carried higher strains due to the joint/gap absence and fibre continuity. This observation is in agreement with that of Mohammed et al. [52], where the same repair system was used for restoring the axial integrity of RC columns.

The activation load of the bottom reinforcement of beam U-S was four times higher than that of U-Jt, and it was the highest amongst all other tested specimens as shown in Fig. 15a and 15b. Moreover, the bottom steel, SB, of beam U-S did not reach strain yield limit as it was below  $2000 \mu\epsilon$ , while in beam U-Jt, it was around  $2250 \mu\epsilon$ . The underlying reason for this response is the effective stress distribution around the sleeve due to the continuity of fibres, which resulted in more even stress distribution and crack propagation in the grout of beam U-S compared to beam U-Jt (Fig. 10). However, despite the difference in the strength enhancement, the ultimate failures of U-Jt and U-S were governed by the bottom steel yielding and concrete cracking outside the jacket, and not within the repair system. Nevertheless, the hoop/transverse joint, JnT, showed strain reading of  $1080 \mu\epsilon$  at failure, which is only about 30% of the joint transverse strain capacity of  $3500 \mu\epsilon$  discussed before. This could be attributed to the multiaxial stresses that were generated at the joint region due to the gap underneath the joint that resulted from the cracking of grout. This decrease resulted in utilisation of the FRP shell capacity by around 10% only. However, the design of the current system effectively restored and enhanced the flexural strength of beams by 114% and 55% for beams with damage on the top compression zone and the bottom tension zone, respectively. Additional modifications can be done to increase the restoration performance, and to extend the application of the system for additional strengthening purposes.

#### 4.5. Epoxy coating effect on the FRP jacket effectiveness

The modification of the internal surface of the FRP jacket in beam U-JtE, by coating the surface with 5 mm coarse aggregates using epoxy grout as an adhesive resulted in enhanced stress transfer between the grout and the jacket, and provided better stress distribution and crack propagation in the grout of beam U-JtE (Fig. 16b) in comparison with beam U-Jt (Fig. 16a). The enhanced composite action between the jacket and grout enabled the repair system to carry additional load and resulted in better confinement of the top concrete and top steel as shown in Fig. 16b where JnL and JkC exhibited higher strains than ST. While in beam U-Jt, the grout exhibited development of wide cracks and activation of ST at a load of around 100 kN (Fig. 16a). As a result,

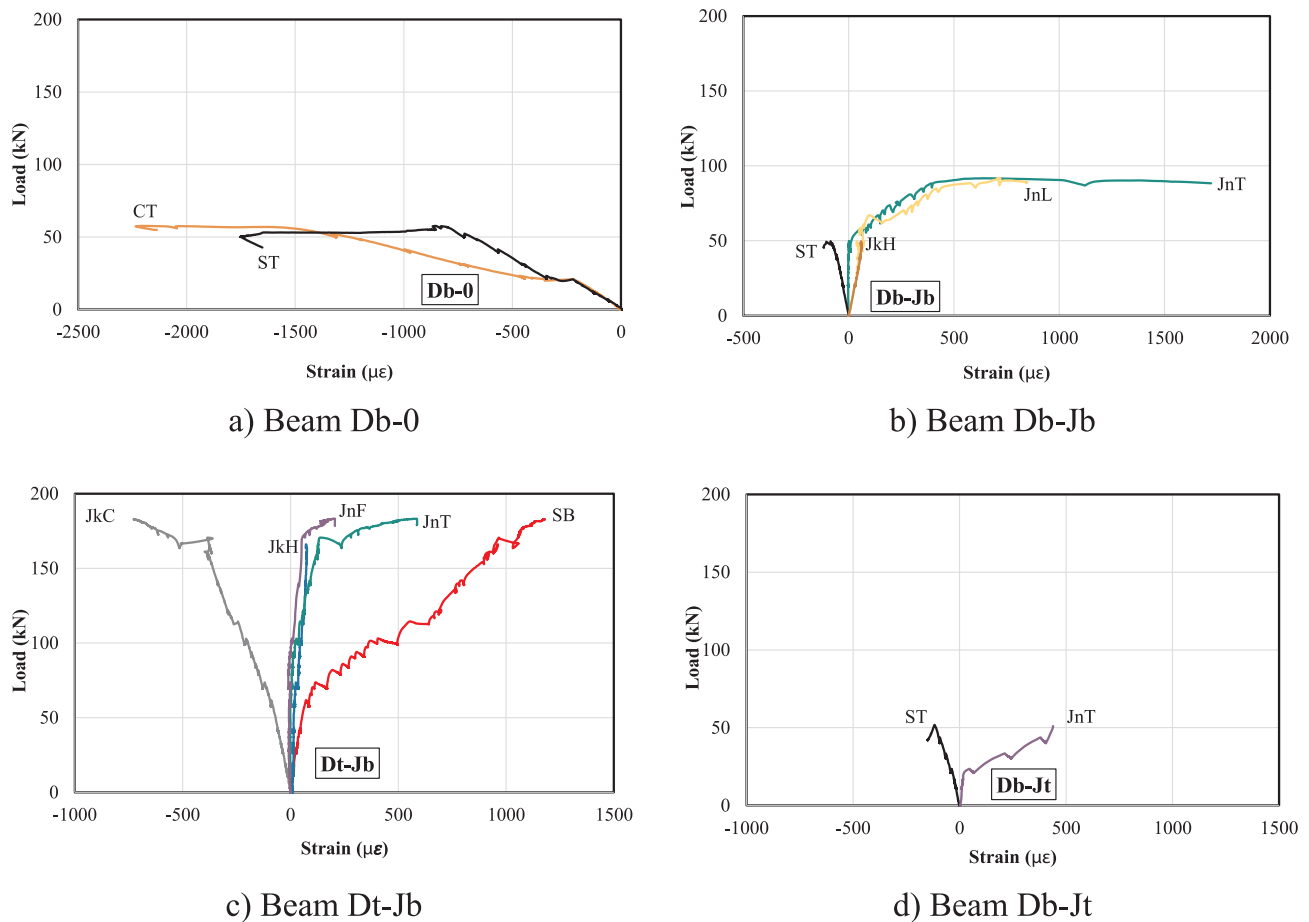


Fig. 14. Load-strain curves of the tested beams.

the flexural load capacity of the jacketed specimen (U-JtE) with internal epoxy coating was higher by 12% when compared to beam U-Jt without epoxy coating as presented in Table 1. This observation corroborates the findings of Aydın and Sarıbiyık [72] where a 10% increase was observed in the flexural strength when the interior surface of square GFRP beam was sand blasted before filling it with concrete. However, both specimens (beams U-Jt and U-JtE) failed outside the jacketed region by bottom steel yielding followed by concrete crushing at the top next to the jacket as shown in Fig. 11c and 11d.

### 5. Fibre model analysis

Theoretical model based on the Fibre Model Analysis (FMA) was implemented to evaluate the maximum flexural load capacity of damaged RC beams repaired with the novel FRP repair system. The developed model is useful to estimate the flexural capacity restoration of the repaired RC beams.

#### 5.1. Fibre model analysis

The behaviour of repaired RC beams in flexure was predicted using a simple FMA. The FMA is a one dimensional, layer-by-layer approach

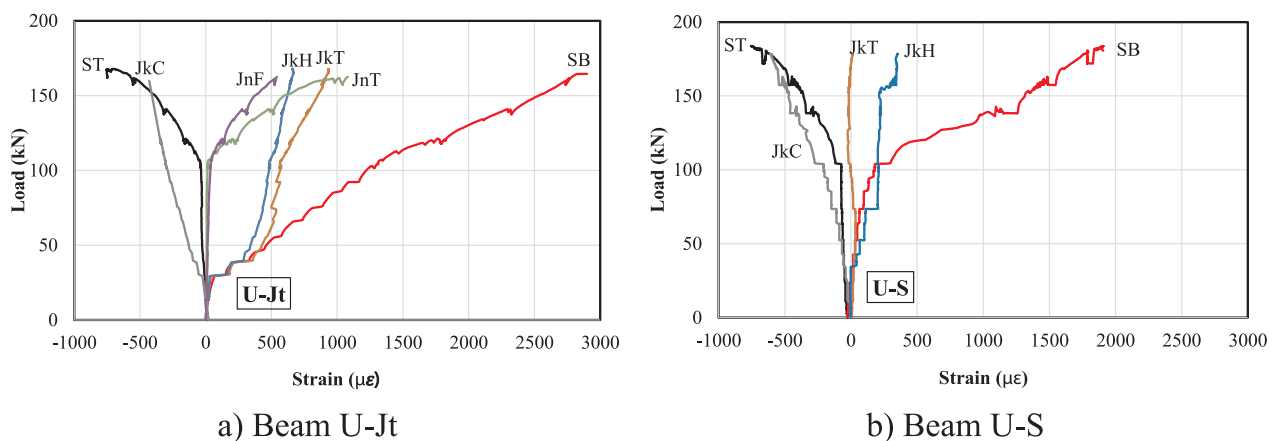


Fig. 15. Load-strain curves of the tested beams.

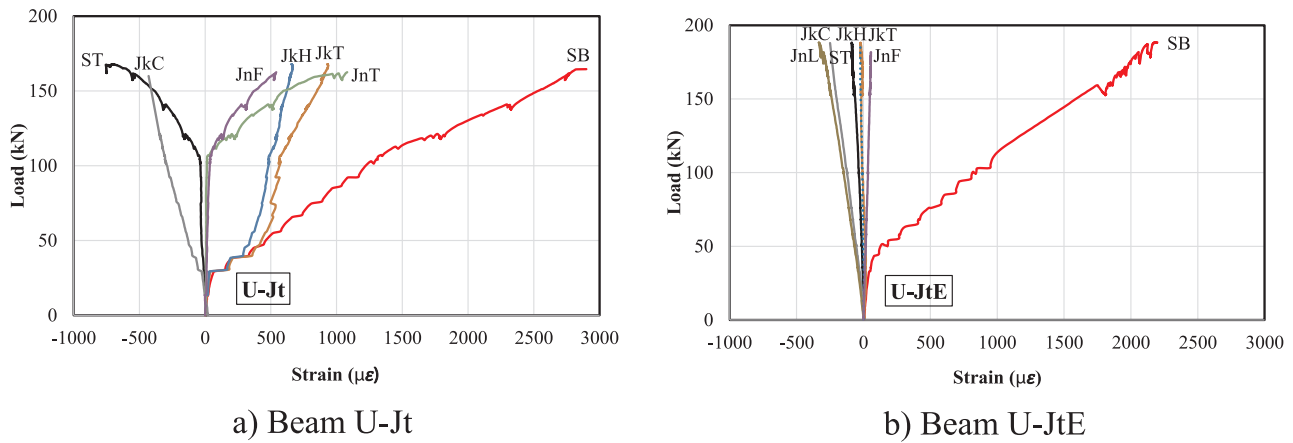


Fig. 16. Load deflection curves of beams repaired with epoxy coated jacket.

to evaluate the sectional forces corresponding to a given strain distribution at a specific section [73–79]. An important advantage of the FMA is that it can account for the different behaviour of constituent materials of composite structures. This method is successfully used by Manalo and Aravinthan [74] in analysing and evaluating the behaviour of glued fibre composite sandwich beams in flexure. It also has been used by other researchers to predict the behaviour of concrete structures reinforced with fibre composite materials. Duthinh and Starnes [80] presented an iterative numerical approach to predict the ductile behaviour and flexural strength enhancement of RC beams bonded with FRP strips. El-Hacha et al. [81] analysed the flexural behaviour of concrete beams strengthened with near-surface mounted FRP reinforcement using simple plane section analysis. This method is adopted in this study to predict the ultimate load of damaged RC beams repaired with the novel FRP jacket. The nominal flexural capacity of RC beams was calculated from the constitutive material behaviours using strain compatibility and internal force equilibrium principles. Since the proposed system is for repair and restoration, only beams U-0, Db-0 and Db-Jb were considered in the FMA. A perfect bonding is assumed between adjacent layers of the jacketed RC beams. It is also assumed that the strains are directly proportional to the distance from neutral axis. The stress at each layer is determined from the constitutive behaviour of the materials. The internal force at each layer was calculated by multiplying the stress with the area of correspondent layer and the cross-sectional force equilibrium was applied. During summation of forces, the net tensile force was equated to the net compressive force. MS Excel spreadsheet program was used to analyse the flexural behaviour of the RC beams using the FMA.

The basic assumptions in FMA on the flexural behaviour of the RC beams are illustrated in Fig. 17. When the concrete and grout are still uncracked, all the layers or element  $i$  (with thickness  $t_i$ ) contribute to the moment capacity of the section. When the concrete and grout crack, their contribution in tension is neglected. The constitutive material behaviour for the concrete, steel and confined grout is shown in Fig. 18. For concrete, Popovics [82] model was adopted for the stress-strain behaviour (Fig. 18a), the steel was simplified with a bilinear behaviour, i.e. linear elastic before yielding and a constant stress after yield (Fig. 18b). The contribution of the FRP jacket was incorporated in the FMA by considering the confined properties of the grout inside the FRP tube in tension (Fig. 3), and in compression (Fig. 18c) as reported by Mohammed et al. [51].

FMA analysis starts by assuming a compressive strain value at the topmost layer of the RC beam. For a given top strain, the bottom strain is solved by an iterative procedure until the summation of forces is equal to zero. The corresponding neutral axis depth,  $d_n$  for these set of top and bottom strains which satisfies the force equilibrium is calculated by using Eq. (1). Moreover, the strain  $\epsilon_i$  at each layer  $i$  is related to the topmost strain through linear strain across the section, which can be determined by using Eq. (2). Then, the stress in the layer is determined from the constitutive stress-strain curve of the materials in Fig. 18.

$$d_n = \frac{d_3 \times \epsilon_c \text{ con}}{(\epsilon_c \text{ con} + \epsilon_t s_3)} \tag{1}$$

$$\epsilon_i = \frac{\epsilon_c \text{ con} \times (d_n - d_i)}{d_n} \tag{2}$$

where  $d_n$  is the neutral axis depth,  $d_3$  is the distance from the topmost

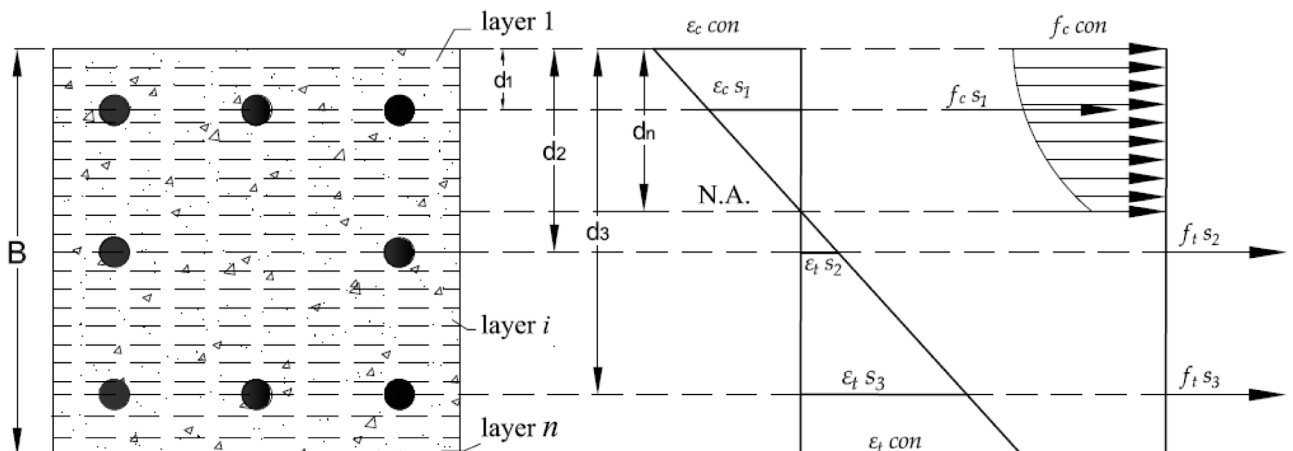


Fig. 17. Basic assumptions in Fibre Model Analysis.

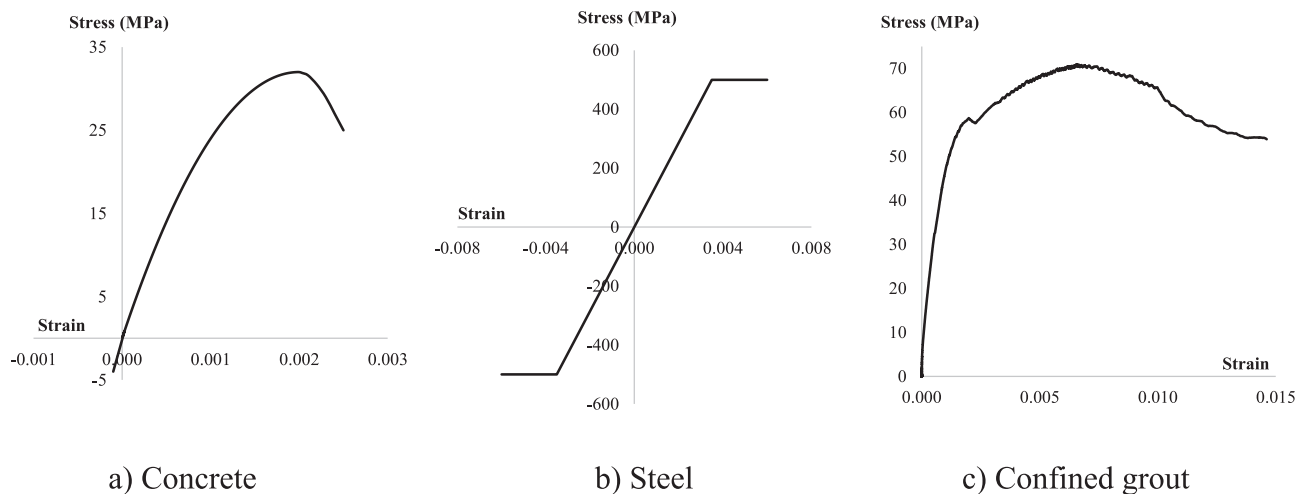


Fig. 18. Constitutive models for basic materials of RC beam.

surface to the bottom steel,  $\epsilon_c$  con is the strain at the top concrete,  $\epsilon_s$  s3 is the strain at the bottom steel,  $\epsilon_i$  is the strain at each element and  $d_i$  is the distance from the top surface to the corresponding element. Finally, the force equilibrium equation is given by Equation (3):

$$\sum P = \sum_{i=1}^n f_{i\ con} A_{i\ con} + \sum_{i=1}^n f_{i\ st} A_{i\ st} + \sum_{i=1}^n f_{i\ in\ fill} A_{i\ in\ fill} \tag{3}$$

where P is the summation of forces,  $f_{i\ con}$  is the concrete strength at layer  $i$ ,  $A_{i\ con}$  is the concrete area at layer  $i$ ,  $f_{i\ st}$  is the steel strength at layer  $i$ ,  $A_{i\ st}$  is the steel area at layer  $i$ ,  $f_{i\ in\ fill}$  is the grout-infill strength at layer  $i$  and  $A_{i\ in\ fill}$  is the grout-infill area at layer  $i$ .

5.2. Predicted results and comparison with the experiment

The ultimate load capacity and strain readings of the beams obtained from the FMA are compared with the experimental values of the tested specimens as shown in Table 2. The comparison shows that there is an excellent agreement between the predicted and experimental values of the beams, where the predicted values are within 97% of the experimental values. This means that the assumption made for the current FMA is validated by the test results and can be used for further applications. However, the strain value at the joint measured by FMA is much higher than the experimental values for beam Db-Jb. This difference is attributed to the wide cracks observed in the grout (Figs. 10e and 11g) where the strain is lost at the interface between the grout and the joint as the crack width of the grout was significantly higher than the joint hoop displacement. This point resembles point B in Fig. 3 where the grout experienced severe and wide cracking in the grout-filled GFRP tubes under splitting tensile load (Fig. 4b). Interestingly, the hoop strain recorded on the GFRP tube at point B was equal to  $5000\ \mu\epsilon$ , which is very close to the value calculated by FMA at bottom most

location of beam Db-Jb ( $4965\ \mu\epsilon$ ). Finally, it is to be noted that the assumptions made may be only applicable to the repair system investigated in this study and may need calibration for other types of prefabricated composite repair systems.

6. Conclusions

The behaviour of reinforced concrete beams with simulated corrosion damage and repaired with a novel FRP jacket system was investigated under 4-point static bending tests. The effects of damage location in the concrete member, joint location and internal surface coating of the jacket were evaluated, and a simplified theoretical analysis was implemented to predict the capacity of the repaired beams. Based on the results, the following conclusions were made:

- The effectiveness of the novel repair system was highly influenced by the tensile strength of the grout infill and the joint capacity as the failure of the jacket is initiated by the grout cracking beneath the joint which resulted in opening and failing of the teeth at the joint.
- Placing the joint away from the compression zone resulted in a more effective utilisation of the composite jacket as a repair system. The crushing and volume expansion of top concrete and grout resulted in opening of the joint and failure at the teeth. The provision of jacket in the compression side however confined the top concrete and resisted its expansion which delayed the buckling of top steel.
- The FRP jacket is more effective in repairing flexural members with the damage located at the top than at the bottom. Only 55% restoration of the original flexural strength of the beam was achieved when the damage was at the bottom whereas 114% strength restoration was achieved when the damage was at the top.
- The provision of epoxy and coarse aggregate coating inside the

Table 2 Actual and predicted load (P, kN) and strain ( $\mu\epsilon$ ) values of RC beams.

Beam	FMA			Experiment			Top strain, FMA/Experiment	P, FMA/Experiment
	Top steel strain	Bottom, middle steel/joint strain	P	Top steel strain	Bottom steel/joint strain	P		
U-0	1300	3540 <sup>1</sup>	158	1700	3630 <sup>1</sup>	160	0.76	0.99
Db-0	560	3520 <sup>2</sup>	56	760	-	58	0.74	0.97
Db-Jb	830	4965 <sup>3</sup>	91	118*	1721 <sup>3</sup>	92	-*	0.99

<sup>1</sup> There were no bottom steel reinforcement nor joint/jacket to attach strain gauges on.  
<sup>\*</sup> The strain gauge stopped recording at an applied load of 50 kN, which is almost half of the failure load.  
<sup>1</sup> Strain at the mid-span of bottom steel reinforcement.  
<sup>2</sup> Strain at the mid-span of middle steel reinforcement.  
<sup>3</sup> Longitudinal strain at the joint of the jacket.

GFRP jacket surface resulted in better stress distribution and cracks propagation in the grout than the one without coating. The enhanced composite action of the repair system components due to coating improved the flexural strength capacity by 12% when compared with the jacketed specimen without coating.

- The simplified FMA can reliably predict the flexural capacity of the damaged beams repaired with FRP jacket by considering confined tensile and compressive properties of the grout. Comparison between the predicted and experimental results show the predictions to be within 97% of the experimental values.

#### Declaration of Competing Interest

The authors declare that they have no known competing financial interests or personal relationships that could have appeared to influence the work reported in this paper.

#### Acknowledgements

The authors gratefully acknowledge Joinlox™ Pty. Ltd., Australia for the financial, materials and technical support in conducting this study. The second author acknowledges the scholarship granted by the Australian Government Endeavour Executive Leadership Award to undertake his professional development at the Centre for Integration of Composites into Infrastructure (CICI), West Virginia University, Morgantown, USA.

#### Appendix A. Supplementary data

Supplementary data to this article can be found online at <https://doi.org/10.1016/j.compstruct.2019.111634>.

#### References

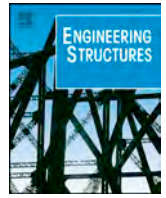
- [1] Shi X, Xie N, Fortune K, Gong J. Durability of steel reinforced concrete in chloride environments: an overview. *Constr Build Mater* 2012;30:125–38.
- [2] Güneşli E, Gesoğlu M, Karaboğa F, Mermerdaş K. Corrosion behavior of reinforcing steel embedded in chloride contaminated concretes with and without metakaolin. *Compos B Eng* 2013;45(1):1288–95.
- [3] Coronelli D, Gambarova P. Structural assessment of corroded reinforced concrete beams: modeling guidelines. *J Struct Eng* 2004;130(8):1214–24.
- [4] Auyeung Y, Balaguru P, Chung L. Bond behavior of corroded reinforcement bars. *Mater J* 2000;97(2):214–20.
- [5] Triantafyllou GG, Rousakis TC, Karabinis AI. Effect of patch repair and strengthening with EBR and NSM CFRP laminates for RC beams with low, medium and heavy corrosion. *Compos B Eng* 2018;133:101–11.
- [6] Page C. Corrosion and its control in reinforced concrete. The Institute of Concrete Technology Yearbook 1999. 1998. p. 37–51.
- [7] Du Y, Clark LA, Chan AH. Impact of reinforcement corrosion on ductile behavior of reinforced concrete beams. *ACI Struct J* 2007;104(3):285.
- [8] Rodriguez J, Ortega L, Casal J. Load carrying capacity of concrete structures with corroded reinforcement. *Constr Build Mater* 1997;11(4):239–48.
- [9] Val DV. Deterioration of strength of RC beams due to corrosion and its influence on beam reliability. *J Struct Eng* 2007;133(9):1297–306.
- [10] Manalo AC, Mohammed AA, Maranan G. Novel Composites Jacket for Repair of Concrete Columns. Special Publication 327 2018;3(1-3):12.
- [11] Manalo AC, Mohammed AA, Maranan GB. Novel Composites Jacket for Repair of Concrete Structures, Proceedings of the 13th Fiber Reinforced Polymer for Reinforced Concrete Structures (FRPRCS13). Anaheim, California: United States of America; 2017.
- [12] Torres-Acosta AA, Navarro-Gutierrez S, Terán-Guillén J. Residual flexure capacity of corroded reinforced concrete beams. *Eng Struct* 2007;29(6):1145–52.
- [13] Azam R, El-Sayed AK, Soudki K. Behaviour of reinforced concrete beams without stirrups subjected to steel reinforcement corrosion. *J Civil Eng Manage* 2016;22(2):146–53.
- [14] Cassidy M, Waldie J, Palanisamy S. A Method to Estimate the Cost of Corrosion for Australian Defence Force Aircraft. (2015).
- [15] Vandoros KG, Dritsos SE. Concrete jacket construction detail effectiveness when strengthening RC columns. *Constr Build Mater* 2008;22(3):264–76.
- [16] Chalioris CE, Thermou GE, Pantazopoulou SJ. Behaviour of rehabilitated RC beams with self-compacting concrete jacketing—analytical model and test results. *Constr Build Mater* 2014;55:257–73.
- [17] Belal MF, Mohamed HM, Morad SA. Behavior of reinforced concrete columns strengthened by steel jacket. *HBRC J* 2015;11(2):201–12.
- [18] Li J, Gong J, Wang L. Seismic behavior of corrosion-damaged reinforced concrete columns strengthened using combined carbon fiber-reinforced polymer and steel jacket. *Constr Build Mater* 2009;23(7):2653–63.
- [19] Delatte N. Failure, distress and repair of concrete structures. Elsevier; 2009.
- [20] Sakr M, El Naggar M, Nehdi M. Interface characteristics and laboratory constructability tests of novel fiber-reinforced polymer/concrete piles. *J Compos Constr* 2005;9(3):274–83.
- [21] Guades E, Aravinthan T, Islam M, Manalo A. A review on the driving performance of FRP composite piles. *Compos Struct* 2012;94(6):1932–42.
- [22] Al-saadi AU, Aravinthan T, Lokuge W. Structural applications of fibre reinforced polymer (FRP) composite tubes: A review of columns members. *Compos Struct* 2018;204:513–24.
- [23] Oller E, Pujol M, Mari A. Contribution of externally bonded FRP shear reinforcement to the shear strength of RC beams. *Compos Part B: Eng* 2018.
- [24] Pessiki S, Harries KA, Kestner JT, Ricles JM. Axial behavior of reinforced concrete columns confined with FRP jackets. *J Compos Constr* 2001;5(4):237–45.
- [25] Teng J, Chen J, Smith ST, Lam L. Behaviour and strength of FRP-strengthened RC structures: a state-of-the-art review. *Proc Inst Civil Eng-Struct Build* 2003;156(1):51–62.
- [26] Ozbakkaloglu T. Compressive behavior of concrete-filled FRP tube columns: assessment of critical column parameters. *Eng Struct* 2013;51:188–99.
- [27] Lau K-T, Zhou L-M. Mechanical performance of composite-strengthened concrete structures. *Compos B Eng* 2001;32(1):21–31.
- [28] Belarbi A, Bae S-W. An experimental study on the effect of environmental exposures and corrosion on RC columns with FRP composite jackets. *Compos B Eng* 2007;38(5):674–84.
- [29] Naughton A, Fan M, Bregulla J. Fire resistance characterisation of hemp fibre reinforced polyester composites for use in the construction industry. *Compos B Eng* 2014;60:546–54.
- [30] Rousakis TC. Reusable and recyclable nonbonded composite tapes and ropes for concrete columns confinement. *Compos B Eng* 2016;103:15–22.
- [31] ACI Committee 440.2R. Guide for the Design and Construction of Externally Bonded FRP Systems for Strengthening Concrete Structures (ACI 440.2R-08). Farmington Hills, MI: American Concrete Institute; 2008.
- [32] Manalo AC, Karunasena W, Sirimanna C, Maranan GB. Investigation into fibre composites jacket with an innovative joining system. *Constr Build Mater* 2014;65:270–81.
- [33] Mohammed AA, Manalo AC, Maranan GB, Zhuge Y, Pettigrew J. FRP jacket assembly for retrofitting concrete structures. Proceedings of the 6th Asia-Pacific Conference on FRP in Structures. 2017.
- [34] Nanni A, Norris MS. FRP jacketed concrete under flexure and combined flexure-compression. *Constr Build Mater* 1995;9(5):273–81.
- [35] Teng J, Lam L. Compressive behavior of carbon fiber reinforced polymer-confined concrete in elliptical columns. *J Struct Eng* 2002;128(12):1535–43.
- [36] Berthet J, Ferrier E, Hamelin P. Compressive behavior of concrete externally confined by composite jackets. Part A: experimental study, *Construction and Building Materials* 2005;19(3):223–32.
- [37] Chen W, Pham TM, Sichebe H, Chen L, Hao H. Experimental study of flexural behaviour of RC beams strengthened by longitudinal and U-shaped basalt FRP sheet. *Compos B Eng* 2018;134:114–26.
- [38] Eslami A, Ronagh HR. Effect of FRP wrapping in seismic performance of RC buildings with and without special detailing – A case study. *Compos B Eng* 2013;45(1):1265–74.
- [39] Vijay P, Soti PR, GangaRao HV, Lampo RG, Clarkson JD. Repair and Strengthening of Submerged Steel Piles Using GFRP Composites. *J Bridge Eng* 2016;04016038.
- [40] Karagah H, Dawood M, Belarbi A. Experimental Study of Full-Scale Corroded Steel Bridge Piles Repaired Underwater with Grout-Filled Fiber-Reinforced Polymer Jackets. *J Compos Constr* 2018;22(3):04018008.
- [41] Beddier A, Zitoun R, Collombet F, Grunevald Y, Abadlia M, Bourahla N. Compressive behaviour of concrete elements confined with GFRP-prefabricated bonded shells. *Eur J Environ Civil Eng* 2015;19(1):65–80.
- [42] Lopez-Anido R, Michael AP, Sandford TC, Goodell B. Repair of wood piles using prefabricated fiber-reinforced polymer composite shells. *J Perform Constr Facil* 2005;19(1):78–87.
- [43] Monti G, Nisticò N, Santini S. Design of FRP jackets for upgrade of circular bridge piers. *J Compos Constr* 2001;5(2):94–101.
- [44] Pantelides CP, Gergely J, Reaveley LD, Volny VA. Retrofit of RC bridge pier with FRP advanced composites. *J Struct Eng* 1999;125(10):1094–9.
- [45] Parks J, Brown D, Ameli M, Pantelides CP, Reaveley L. Repair of damaged precast RC bridge columns with grouted splice sleeve connections using CFRP shells and plastic hinge relocation. *Earthquake Engineering Research Institute* 2014.
- [46] Lopez-Anido R, Michael AP, Sandford TC. Fiber Reinforced Polymer Composite-Wood Pile Interface Characterization by Push-Out Tests. *J Compos Constr* 2004;8(4):360–8.
- [47] Williams J, Pile FRP. Jacket Solution has no 'Pier' in Timber. *Pile Restoration* 2009.
- [48] Choi E, Rhee I, Park J, Cho B-S. Seismic retrofit of plain concrete piers of railroad bridges using composite of FRP-steel plates. *Compos B Eng* 2011;42(5):1097–107.
- [49] Sen R, Mullins G. Application of FRP composites for underwater piles repair. *Compos B Eng* 2007;38(5):751–8.
- [50] Joinlox™, PileJax™ – Pile Repair Jackets, 2014. <http://www.joinlox.com/pilejax/>.
- [51] Mohammed AA, Manalo AC, Maranan GB, Zhuge Y, Vijay PV. Comparative study on the behaviour of different infill materials for pre-fabricated fibre composite repair systems. *Constr Build Mater* 2018;172:770–80.
- [52] Mohammed AA, Manalo AC, Maranan GB, Zhuge Y, Vijay P, Pettigrew J. Behavior of Damaged Concrete Columns Repaired with Novel FRP Jacket. *J Compos Constr* 2019;23(3):04019013.
- [53] AS/NZS4671 Steel Reinforcing Materials, AS/NZS4671-2001 Steel Reinforcing

- Materials, Sydney (Australia) (2001).
- [54] ASTM Standard C143/C143M-05a, C143/C143M-05a. Standard Test Method for Slump of Hydraulic-Cement Concrete. West Conshohocken, PA: ASTM International; 2005.
- [55] ASTM C39/C39M-15a, C39/C39M-15a, Standard Test Method for Compressive Strength of Cylindrical Concrete Specimens (2015).
- [56] ASTM C31/C31M-12, C31/C31M-12. Standard Practice for Making and Curing Concrete Test Specimens in the Field. West Conshohocken, PA: ASTM International; 2012. Doi: 10.1520/C0031\_C0031M-12, 2012.
- [57] ISO 1172. ISO 1172: 1996 Textile glass reinforced plastics, Prepregs, moulding compounds and laminates, Determination of the textile-glass and mineral-filler content. International Organization for Standardization; 1996. p. 1996.
- [58] Parvin A, Jamwal AS. Performance of externally FRP reinforced columns for changes in angle and thickness of the wrap and concrete strength. *Compos Struct* 2006;73(4):451–7.
- [59] Hajsadeghi M, Alaei FJ, Shahmohammadi A. Investigation on behaviour of square/rectangular reinforced concrete columns retrofitted with FRP jacket. *J Civil Eng Manage* 2011;17(3):400–8.
- [60] ISO 527-1. ISO 527-1:1995 Plastics – determination of tensile properties: General principles. International Organization for Standardization; 1995.
- [61] ISO. 14126, ISO 14126: 1999-Fibre-Reinforced Plastic Composites. Determination of Compressive Properties in the In-Plane Direction. International Organization for Standardization; 1999.
- [62] Shamsuddoha M, Islam MM, Aravinthan T, Manalo A, Lau K-T. Effectiveness of using fibre-reinforced polymer composites for underwater steel pipeline repairs. *Compos Struct* 2013;100:40–54.
- [63] Bluey, Technical Data Sheet: BluCem GP60 Construction Grout, 2017.
- [64] ASTM C496/C496M. ASTM C496/C496M-11 Standard Test Method for Splitting Tensile Strength of Cylindrical Concrete Specimens. ASTM International; 2011.
- [65] Abdel-Hay AS, Fawzy YAG. Behavior of partially defected R.C columns strengthened using steel jackets. *HBRC J* 2015;11(2):194–200.
- [66] Maaddawy TE. Behavior of corrosion-damaged RC columns wrapped with FRP under combined flexural and axial loading. *Cem Concr Compos* 2008;30(6):524–34.
- [67] da Fonseca BS, Castela A, Silva MA, Duarte R, Ferreira M, Montemor M. Influence of GFRP Confinement of Reinforced Concrete Columns on the Corrosion of Reinforcing Steel in a Salt Water Environment. *J Mater Civ Eng* 2014;27(1):04014107.
- [68] Manalo A, Sirimanna C, Karunasena W, McGarva L, Falzon P. Pre-impregnated carbon fibre reinforced composite system for patch repair of steel I-beams. *Constr Build Mater* 2016;105:365–76.
- [69] Liu X, Nanni A, Silva PF. Rehabilitation of compression steel members using FRP pipes filled with non-expansive and expansive light-weight concrete. *Adv Struct Eng* 2005;8(2):129–42.
- [70] Shamsuddoha M. Behaviour of Infilled Rehabilitation System with Composites for Steel Pipe. University of Southern Queensland; 2014.
- [71] Mohamed HM, Masmoudi R. Flexural strength and behavior of steel and FRP-reinforced concrete-filled FRP tube beams. *Eng Struct* 2010;32(11):3789–800.
- [72] Aydın F, Sarıbyık M. Investigation of flexural behaviors of hybrid beams formed with GFRP box section and concrete. *Constr Build Mater* 2013;41:563–9.
- [73] Park RL, Park R, Paulay T. Reinforced concrete structures. John Wiley & Sons; 1975.
- [74] Manalo A, Aravinthan T. Behaviour of glued fibre composite sandwich structure in flexure: Experiment and Fibre Model Analysis. *Mater Des* 2012;39:458–68.
- [75] Manalo A, Aravinthan T, Mutsuyoshi H, Matsui T. Composite behaviour of a hybrid FRP bridge girder and concrete deck. *Adv Struct Eng* 2012;15(4):589–600.
- [76] Muttashar M, Manalo A, Karunasena W, Lokuge W. Flexural behaviour of multi-celled GFRP composite beams with concrete infill: Experiment and theoretical analysis. *Compos Struct* 2017;159:21–33.
- [77] Manalo A, Surendar S, van Erp G, Benmokrane B. Flexural behavior of an FRP sandwich system with glass-fiber skins and a phenolic core at elevated in-service temperature. *Compos Struct* 2016;152:96–105.
- [78] Muttashar M, Manalo A, Karunasena W, Lokuge W. Influence of infill concrete strength on the flexural behaviour of pultruded GFRP square beams. *Compos Struct* 2016;145:58–67.
- [79] Manalo A. Behaviour of fibre composite sandwich structures under short and asymmetrical beam shear tests. *Compos Struct* 2013;99:339–49.
- [80] Duthinh D, Starnes M. Strength and ductility of concrete beams reinforced with carbon fiber-reinforced polymer plates and steel. *J Compos Constr* 2004;8(1):59–69.
- [81] El-Hacha R, Rizkalla S, Kotynia R. Modelling of reinforced concrete flexural members strengthened with near-surface mounted FRP reinforcement. 7th Int. Symp. on Fiber Reinforced Polymer (FRP) Reinforcement for Concrete Structures (FRPRCS-7). 2005. p. 1681–700.
- [82] Popovics S. A numerical approach to the complete stress-strain curve of concrete. *Cem Concr Res* 1973;3(5):583–99.

## Chapter 6

### **Experimental and numerical evaluations on the behaviour of structures repaired using prefabricated FRP composites jacket**

The results of the experimental investigations in Chapters 4 and 5 showed that the novel prefabricated FRP jacket can restore the strength and stiffness of deteriorated concrete structures. A more in-depth investigations of the effect of critical design parameters were then implemented through FE analysis. The FE analysis of the damaged structures repaired with the FRP jacket was implemented using ABAQUS/Explicit considering the damaged plasticity model for concrete, bilinear model for steel and linear elastic behaviour of the FRP composites. A perfect bond between the repair system components was assumed where tie constraint was selected as an interaction criterion between the concrete-grout-jacket elements. This assumption is based on the observed behaviour in Chapter 3 wherein the lateral expansion of the grout pushed the jacket outward resulting in full contact and tensioning the jacket circumferentially. The developed FE model accurately simulated the behaviour and failure mechanism of the corroded RC columns repaired with the novel prefabricated FRP repair system. Moreover, the FE analysis provided a better understanding on the behaviour of the repaired system and showed internal stress concentration at the damaged region which suggests that the joint of the jacket should be placed away from the damaged area to effectively utilise the composite jacket. Furthermore, the developed FE model was used to investigate the effect of the hoop tensile strength of the joint on the effectiveness of the repair system and the behaviour of the repaired structures. The FE analyses results showed that a joint with tensile strength of at least 20% of the novel GFRP jacket's hoop strength can significantly improve the axial strength capacity of the repaired column. Beyond this 20% level, the failure of the repaired system changes from failure of the GFRP jacket to the failure of the existing structures. From these results, it was concluded that the jacket can be effectively used to restore the strength capacity of damaged concrete members. Moreover, optimisation of the joint strength will lead to further exploitation of the novel jacket as a strengthening system. The next chapter highlights the significant outcomes of this study and recommend the future research directions where the unexplored benefits of the novel system can be revealed.



## Experimental and numerical evaluations on the behaviour of structures repaired using prefabricated FRP composites jacket



Ali A. Mohammed<sup>a,b,\*</sup>, Allan C. Manalo<sup>a</sup>, Wahid Ferdous<sup>a</sup>, Yan Zhuge<sup>c</sup>, P.V. Vijay<sup>d</sup>, John Pettigrew<sup>e</sup>

<sup>a</sup> Centre for Future Materials (CFM), School of Civil Engineering and Surveying, University of Southern Queensland, Toowoomba 4350, Australia

<sup>b</sup> Environmental Engineering Department, College of Engineering, The University of Mustansiriyah, Baghdad, Iraq

<sup>c</sup> School of Natural & Built Environments, University of South Australia, Adelaide 5001, Australia

<sup>d</sup> Department of Civil and Environmental Engineering, West Virginia University, WV 26506, USA

<sup>e</sup> CEO, Joinlox Pty Ltd., Brisbane, QLD 4105, Australia

### ARTICLE INFO

#### Keywords:

Damage  
Corrosion  
Structural rehabilitation  
Repair  
Jacketing  
FRP  
Composites  
Prefabricated FRP composite jacket  
FRP joint  
Numerical analysis  
Finite element

### ABSTRACT

Fibre reinforced polymer (FRP) composite jackets have become a popular option for repairing deteriorated structures due to the superior characteristics of composite materials in resisting corrosion and in providing a high strength but lightweight repair system. Recently, a novel prefabricated FRP composite jacket with an easy-fit and self-locking mechanical joining system was developed. This paper presents the experimental and numerical studies on the effectiveness of the FRP jacket in repairing reinforced concrete (RC) columns with simulated corrosion damage under uniaxial compressive loading. The experimental results showed that the jacket successfully stabilised and restored the axial strength capacity of the damaged concrete columns. Moreover, the results of the finite element (FE) analysis revealed that the joint of the jacket should be placed away from the damaged zone to minimise stress concentration and to effectively utilise the jacket as a repair system. Finally, a joint strength of at least 20% of the hoop tensile strength of the jacket is effective in repairing damaged structures.

### 1. Introduction

Maintaining the existing structures in a good state of service is a major challenge for many transport authorities around the world due to the constant weathering and environmental distress [1–4]. The weathering affects the load-carrying capacity and durability of reinforced concrete (RC) structures due to the corrosion of steel rebars as chloride and moisture reach the surface of steel rebar through cracks [5]. The cost of repair also causes a huge burden on nations' economies. The United States, Canada, Europe, and Australia spend a staggering combined amount of \$30 billion per year for the repair and maintenance of highway RC bridges affected by steel corrosion [6,7]. In addition, there are many deficient steel infrastructures around the world that require structural retrofit to alleviate the detrimental effects of corrosion leading to restrictions on their intended usage and load carrying capacities [8]. A common technique to retrofit steel structures is welding or bolting of new steel reinforcement onto degraded

structures. In case of a highway or offshore structural system, the facility may have to be partially or fully shut down during welding repair for safety reasons which substantially increases the total cost of the repair [9]. Compounding this problem is the recurring issue of durability in the traditional repair techniques such as concrete and steel jacketing [10–12] as they are made with the same materials used in existing structures, which will be affected again by the same factors that attacked the original structures [13,14]. In addition, concrete and steel jackets are bulky and heavy, which add weight to the repaired structures and may attract more loads in seismic events due to the increased stiffness of the repaired members [15,16]. Implementing these traditional repair systems in the repair of underwater structures is also difficult, labour-intensive and costly. Hence, there is a need for alternative techniques to overcome the drawbacks of using traditional materials in a repair system.

In the last two decades, fibre reinforced polymer (FRP) composites have become popular due to their high strength, lightweight and ability

\* Corresponding author at: Centre for Future Materials (CFM), School of Civil Engineering and Surveying, University of Southern Queensland, Toowoomba 4350, Australia.

E-mail addresses: [ali.mohammed@usq.edu.au](mailto:ali.mohammed@usq.edu.au) (A.A. Mohammed), [allan.manalo@usq.edu.au](mailto:allan.manalo@usq.edu.au) (A.C. Manalo), [wahid.ferdous@usq.edu.au](mailto:wahid.ferdous@usq.edu.au) (W. Ferdous), [yan.zhuge@unisa.edu.au](mailto:yan.zhuge@unisa.edu.au) (Y. Zhuge), [p.vijay@mail.wvu.edu](mailto:p.vijay@mail.wvu.edu) (P.V. Vijay), [johnp@joinlox.com](mailto:johnp@joinlox.com) (J. Pettigrew).

<https://doi.org/10.1016/j.engstruct.2020.110358>

Received 16 August 2019; Received in revised form 4 February 2020; Accepted 7 February 2020

0141-0296/ © 2020 Elsevier Ltd. All rights reserved.

to minimise the durability issues that accompany the use of traditional materials [17–21]. As a repair system, FRP composites have been widely used to rehabilitate damaged infrastructure, maintain their serviceability and prolong their service life-span [22–27]. The prefabricated FRP repair systems have been a preferred solution as they are easy and quick to install, can be manufactured under controlled conditions with high quality and can serve as permanent form work depending upon application. Vijay et al. [28] utilised prefabricated glass fibre reinforced polymer (GFRP) composite jackets to rehabilitate damaged H-shaped steel bridge columns in East Lynn Lake Bridge, West Virginia, USA. This repair system was installed around the damaged columns, then wrapped with prepreg FRP fabrics on the outer perimeter. Prefabricated FRP shells were also used to protect and restore the structural strength of decayed wooden columns in Portland Harbor, Maine, USA [29]. A similar repair technique was also used to restore the waterfront structures in New York City [22]. However, the above mentioned prefabricated jackets lack a simple and reliable joining system that can provide structural continuity along the hoop direction. Therefore, prefabricated FRP jackets with innovative and effective joints should be explored further for developing more effective, simple, and rapid repair system.

Recently a prefabricated GFRP jacket with an innovative joining system has been developed for bridge column repair (Fig. 1). This repair system is quick and easy to install due to its self-locking joining system consisting of two interlocking edges that can easily fit into each other like teeth of a zipper. Due to the innovative self-locking joining system, the proposed system can be installed up to 10 times faster than the other column repair methods [30], thus substantially reducing the installation time and labour/equipment cost. This simple and rapidly installable system works by wrapping the FRP jacket around the damaged column in addition to serving as an environmental-shield and a permanent formwork for the grout-infill that is used to fill the gap between the core column and the outer FRP shell. An appropriate grout is used to fill the gap between the damaged core and the composite jacket. Manalo et al. [10] evaluated the effectiveness of this FRP jacket numerically using Strand7 finite element program and experimentally tested the jacket with the application of internal pressure. The results showed that the FRP jacket can sustain an internal pressure of up to 2 MPa, which considerably exceeds the industry standard for internal bursting pressure required of a concrete column repair system and a permanent concrete formwork jacket. Mohammed et al. [31] evaluated the most suitable grout-infills that would effectively transfer the loads from the damaged structure to the repair system and utilise the inherent

strength and stiffness properties of the fibre composite materials. They concluded that the behaviour of the composite FRP jacket was strongly influenced by the grout's compressive strength and the modulus of elasticity. While the actual behaviour of this prefabricated FRP repair system has been investigated in some detail as reported by Mohammed et al. [11], its structural contribution to the damaged RC members is still not fully understood.

This study experimentally and numerically investigates the behaviour of damaged RC columns repaired with the novel prefabricated FRP composite jacket. The failure mechanism of the different components of the repair system especially the existing damaged structure and the grout which are covered and hidden by the jacket are studied in detail. This study also provides a useful evaluation of the effectiveness of the prefabricated FRP jacket in repairing damaged concrete structures and further optimisation of the joint strength. The results of this study will provide a better understanding on the behaviour of damaged concrete structures repaired with the prefabricated FRP jacket. It will also help to expand the application of this novel repair system for the maintenance and rehabilitation of other types of engineering structures leading to more efficient and economical rehabilitation due to less installation time, lower labour and equipment costs, and minimized delay in transport of goods and traffic.

## 2. Experimental work

This section presents the experimental work conducted to evaluate the effectiveness of the prefabricated FRP jacket in repairing RC columns with simulated steel corrosion damage. It also details the material properties, the preparation of the large-scale specimens, the test setup and instrumentation, and discusses the experimental results.

### 2.1. Materials and specimens

Table 1 details the experimental test specimens and depicts their cross-sections at mid-height. All the columns are 1 m high, 250 mm in diameter, have a 30 mm concrete cover and are reinforced by eight longitudinal steel bars of 16 mm diameter. Steel ligatures were used as transverse reinforcements with a spacing of 50 mm centre-to-centre. The RC columns were fabricated with ordinary Portland cement concrete of 30.5 MPa compressive strength and 26 GPa modulus of elasticity tested as per ASTM C39/C39M-15a [32]. In addition, reinforcing steels of 500 MPa and 250 MPa yield strength were used for the main bars and ligatures, respectively, based on the information provided by

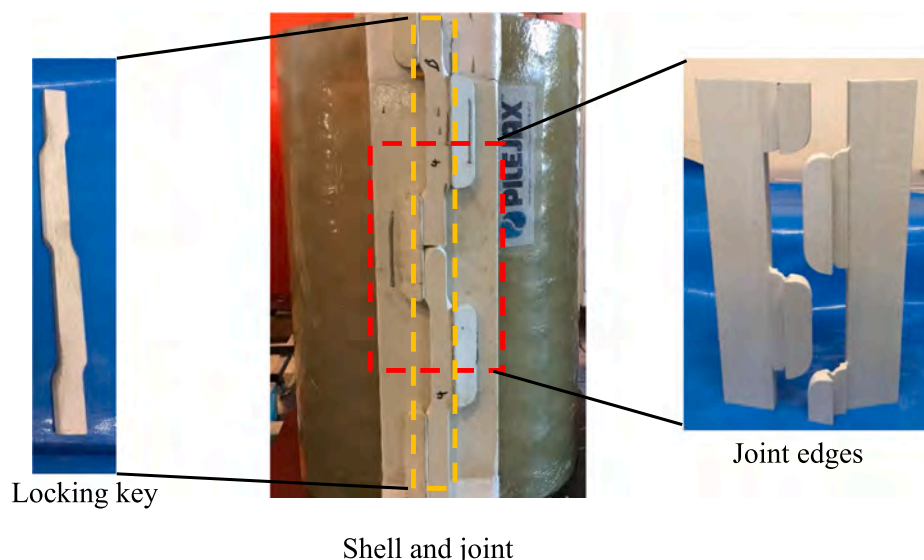
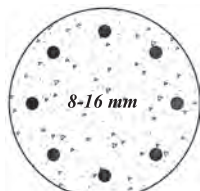
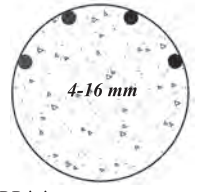
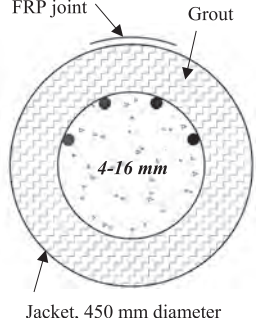


Fig. 1. Novel GFRP Jacket.

**Table 1**  
Experimental test specimens.

Specimen	Description	Cross-section
Column C-1	Undamaged RC column	
Column C-2	RC column with 50% corrosion damage	
Column C-3	RC column with 50% corrosion damage repaired with novel FRP jacket	

the manufacturer and determined according to Steel Reinforcing Material AS/NZS4671-2001 [33]. Except for steel, rest of the materials used in this study were tested and characterized and the detailed behaviour can be found in [11,31]. The first column (C-1) was fabricated with no damage and served as a control specimen. As a second control specimen with damage, column C-2 was made with 50% simulated steel corrosion, and 100% concrete cover damage in the middle region (Fig. 2). It should be noted that the actual by-products of steel corrosion have a higher volume and exert outward pressure on the surrounding concrete which causes cracking and spalling of the concrete cover and

leads to loss of structural integrity. The steel corrosion was simulated by replacing the steel bars with non-structural PVC pipes for a length of 300 mm at mid-height of the column as shown in Fig. 2a. The PVC pipes helped in maintaining the alignment of the damaged longitudinal steel bars at both ends and prevented the concrete from occupying the removed steel volume. This approach was used to simulate the actual condition of reinforcement loss wherein the severity of corrosion may not be constant throughout the surface, thus creating asymmetric behaviour under loading. Moreover, this approach of simulating the corrosion damage was adopted by a few researchers [25,34] showing good correlation with the actual behaviour of corrosion-damaged structures. It was also found that the adopted approach has more detrimental effect on the compressive strength capacity of the reinforced concrete columns [27]. The part damaged by corrosion was wrapped with bubble wrap to eliminate the concrete cover as the corrosion is accompanied with cover damage (Fig. 2b). Columns with other levels of corrosion damage were also investigated and the findings are published in [11].

The technique used in simulating the steel corrosion damage is similar to that of Manalo et al. [25] and Karagah et al. [34] wherein they machined the steel to reduce the cross-sectional area due to corrosion. Ligatures were not provided in the middle region of column C2 where the corrosion was simulated since the lateral reinforcement was not functional and was ignored in the design of actual columns with severe corrosion [11,35]. Finally, the third column (C-3) was cast in a similar manner to that of column C-2 but wrapped with the novel prefabricated FRP jacket made of E-glass fibres impregnated with vinyl ester resin, and having the dimensions of 450 mm diameter and 3 mm thickness. The GFRP shell was fabricated by the filament winding method, while the GFRP joint was manufactured through the pultrusion process. The mechanical properties of the FRP jacket are presented in Table 3 and were used as inputs for the numerical model. The annulus between the core and the outer FRP shell was filled with shrinkage-compensating cementitious grout. The compressive strength and modulus of elasticity of the cementitious grout were 48.2 MPa and 34.3 GPa, respectively, based on the testing as per ASTM C39/C39M-15a [27].

2.2. Test set-up

The fabricated specimens were tested under a concentric axial load, following the test setup shown in Fig. 3. The load was applied using a vertical hydraulic jack of 2500 kN capacity, where the centre of jacket



(a) Corrosion damage (b) Concrete cover damage (c) Damaged column

Fig. 2. Fabrication of column specimens.

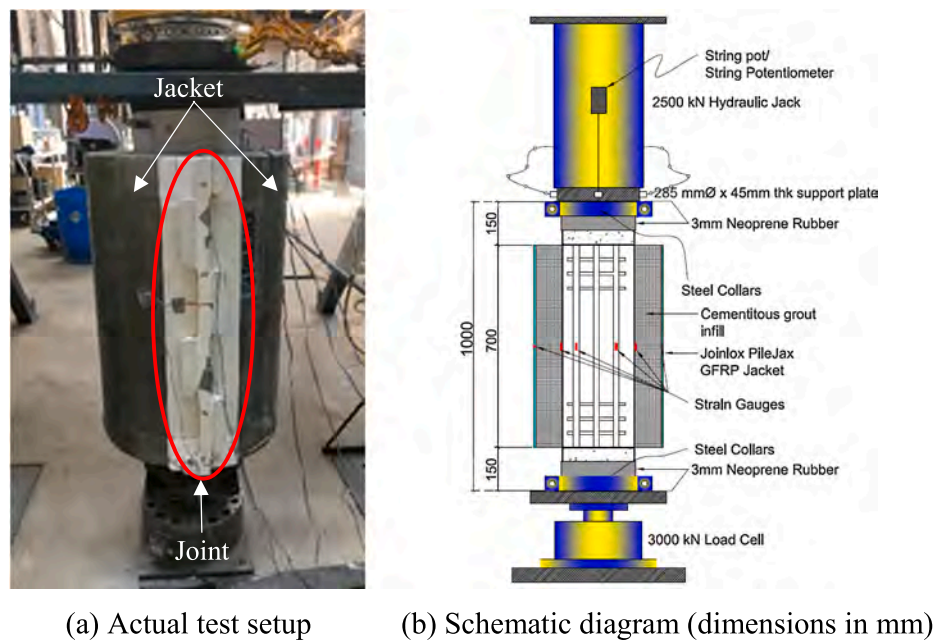


Fig. 3. Test set-up of columns.

coincided with the centre of the tested columns. In addition, the flexible socket apparatus used in conjunction with the load cell during testing is designed to ensure concentric loading throughout the entire stage of loading. Two pairs of steel collars measuring 50 mm wide and 10 mm thick were used to confine the columns at the top and bottom ends to ensure the occurrence of failure within the test region. A neoprene rubber pad with 3 mm thickness was provided at the top and bottom surfaces of the column to provide a uniform load application over the cross section. The strains at the critical regions of concrete, longitudinal reinforcement, and GFRP jacket were measured using strain gauges generally mounted at the mid-height of the columns as shown in Fig. 3b. The columns were subjected to monotonically increasing axial concentric loads until failure using 2500 kN hydraulic actuator, whereas the corresponding deformations were measured with a string pot. The pre- and post-peak behaviour including strain, load, and deflection, were recorded using the System 5000 data logger, whereas the failure modes were manually observed and recorded.

### 2.3. Results and discussion

This section presents the experimental results and observations of the tested columns. The results in terms of maximum axial load capacity, strain, and failure modes of the test specimens are summarised in Table 2.

#### 2.3.1. Failure behaviour

Fig. 4 depicts the failure mode of the tested columns. For column C-1, minor concrete cracking and spalling were observed at both ends of the concrete column prior to the peak load. Once the applied load reached the peak value, column C-1 failed by simultaneous crushing of concrete and buckling of the steel reinforcement at mid-height as

shown in Fig. 4a. Column C-2 failed by global outward buckling of steel reinforcement first, which was followed by less severe concrete core crushing (Fig. 4b), but with a relatively lower magnitude of load given the simulated damages. In column C-3, the failure was initiated by buckling of the longitudinal steel bars which radially pushed and cracked the concrete and the grout towards the outer perimeter resulting in circumferential tensioning of the jacket until the joint teeth were ripped off (Fig. 4c). This resulted in opening and complete detachment of the jacket from the repaired member.

#### 2.3.2. Load-strain behaviour

Fig. 5 depicts the experimental load-strain behaviour of the different material components of the tested columns. For column C-1, the steel and concrete strain increased linearly with the applied load, then it became nonlinear near the 1500 kN load due to cracking and spalling of the concrete cover that led to concrete strain gauge damage. Up to this stage, the strain gauges on two opposite sides of concrete column showed comparable readings (around  $700 \mu\epsilon$  at 1300 kN) which indicates that the loading is applied along the centre of the column. After that, the steel strain kept increasing with the applied load, but at a higher rate, until the steel finally buckled at a load of 2319 kN and a strain of  $-2470 \mu\epsilon$ . Column C-2 experienced linear elastic steel strain behaviour until the concrete crushed and steel buckled at an applied load of 1028 kN and a steel strain of  $-1050 \mu\epsilon$ . Interestingly, it was noted that the failure load of column C-2 is 20% lower than its theoretical capacity (1281 kN). This could be attributed to the eccentricity effect that resulted from asymmetric geometry of the damaged steel (Table 1). Finally, in column C-3, the steel strain increased linearly with the load until 1325 kN followed by a significant drop in the load and a fast increase in the steel strain indicating the buckling of steel and crushing of concrete, wherein the joint exhibited negligible strain

**Table 2**  
Axial load capacity, stiffness and failure mode of the tested columns.

Specimen	Load, kN	Failure strain, $\mu\epsilon$	Location	Failure Mode
C-1	2319	-2470	Steel	Simultaneous steel buckling and concrete crushing
C-2	1028	-1050	Steel	Steel buckling followed by concrete crushing
C-3	2208	226	Joint	Steel buckling followed by radial stressing of concrete and grout along with circumferential tensioning of the jacket and failure of the teeth at the joint

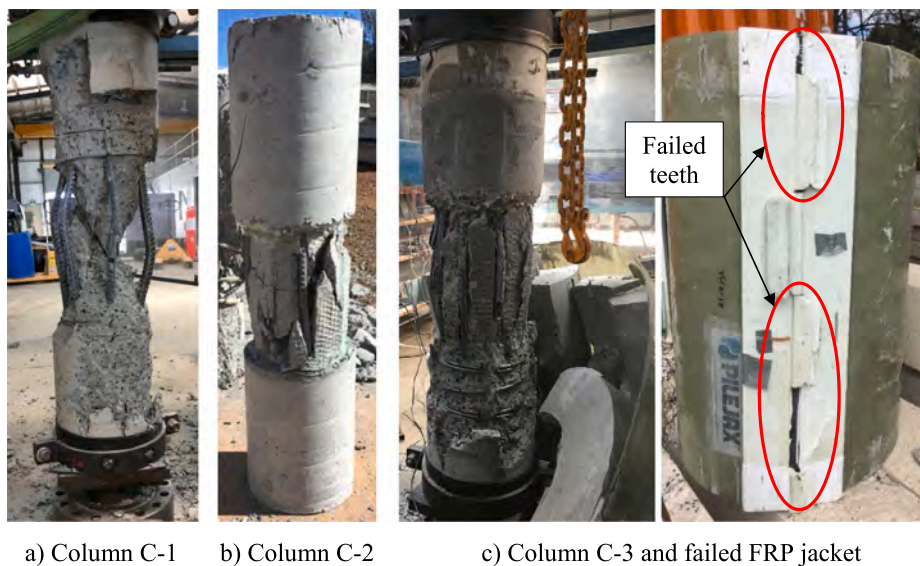


Fig. 4. Failure mode of the tested columns.

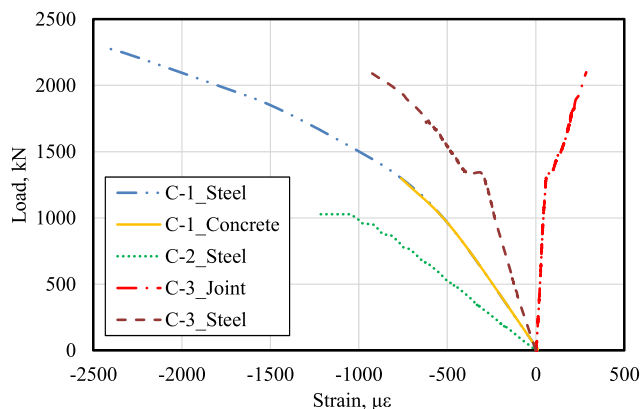


Fig. 5. Experimental load-strain behaviour of the tested columns.

values until it was at the verge of steel buckling. At the point of steel buckling, the grout transferred the radial stresses that were being generated by the column to the jacket as a result of the increased lateral expansion of the core column. The joint strain then started to increase until the teeth of the FRP jacket were ripped off (Fig. 4c) at a circumferential strain of 226  $\mu\epsilon$  at an applied load of 2208 kN (Fig. 5). Interestingly, the eccentric behaviour of the steel bars with simulated corrosion damage was not as obvious in column C-3 as compared to column C-2 due to the presence of the novel FRP jacket which reduced the eccentricity effect and stabilized the damaged column.

#### 2.4. Summary of the experimental work

The novel FRP jacket is experimentally established as an effective repair system for RC columns with corrosion damage. The results showed that simulating 50% corrosion damage resulted in reducing the axial strength capacity by 56% (2319 vs 1028 kN, Table 2) compared to the column with no damage (column C1). Providing the FRP jacket to repair the damaged column stabilized the damaged column by reducing the eccentricity effect of the steel bars with simulated corrosion damage and restored its axial strength capacity by 95% (2319 vs 2208 kN, Table 2). However, the above experimental work involved only one type of columns, i.e. RC columns. Also, the failure of the repair system was governed by the teeth rupture of the FRP joint. Hence, developing and using a numerical model to simulate the behaviour of the tested columns will help to better understand the behaviour of each

component and the effect of increasing the joint strength on the overall axial strength capacity of the repaired member.

### 3. FE simulation of columns repaired with GFRP jacket

Finite element analysis was conducted for a better understanding of the behaviour of the repaired columns with the prefabricated FRP jacket, particularly the behaviour inside the repaired part of the columns which was not visible during loading due to the surrounding repair system. Moreover, the FE analysis provides a better insight into the sequence of failure of the internal parts. The finite element analysis was implemented using Abaqus software analysis package [36].

#### 3.1. Constitutive material behaviour

The constitutive models of the four main materials, i.e. concrete, grout, steel and FRP of the repair system are summarised in Table 3. For concrete and cementitious grout, Concrete Damaged Plasticity Model, which is predefined in Abaqus software and commonly used for modelling of RC structures [36–40], was used to model the nonlinear

Table 3  
Material properties of concrete, grout, steel and GFRP.

Material	Property	Value
Concrete	Compressive strength, $f_{cu}$ (MPa)	30.5
	Tensile strength, $f_t$ (MPa)	2.3
	Modulus, $E_c$ (GPa)	26
	Poisson's ratio	0.2
Grout	Compressive strength, $f_{cug}$ (MPa)	48.2
	Tensile strength, $f_{tg}$ (MPa)	2.52
	Modulus, $E_{cg}$ (GPa)	34
	Poisson's ratio	0.2
Steel	Yield strength of main steel, $f_y$ (MPa)	500
	Yield strength of secondary steel, $f_{ys}$ (MPa)	250
	Yield strain, $\epsilon_y$ ( $\mu\epsilon$ )	2500
	Modulus, $E_s$ (GPa)	200
	Poisson's ratio	0.3
GFRP jacket	Tensile strength, $f_{frp}$ (MPa)	297
	Modulus, $E_{frp}$ (GPa)	24
GFRP joint	Longitudinal tensile strength, $f_{frpl}$ (MPa)	256
	Modulus, $E_{frpl}$ (GPa)	25
	Hoop tensile strength, $f_{frph}$ (MPa)	37
	Modulus, $E_{frph}$ (GPa)	11

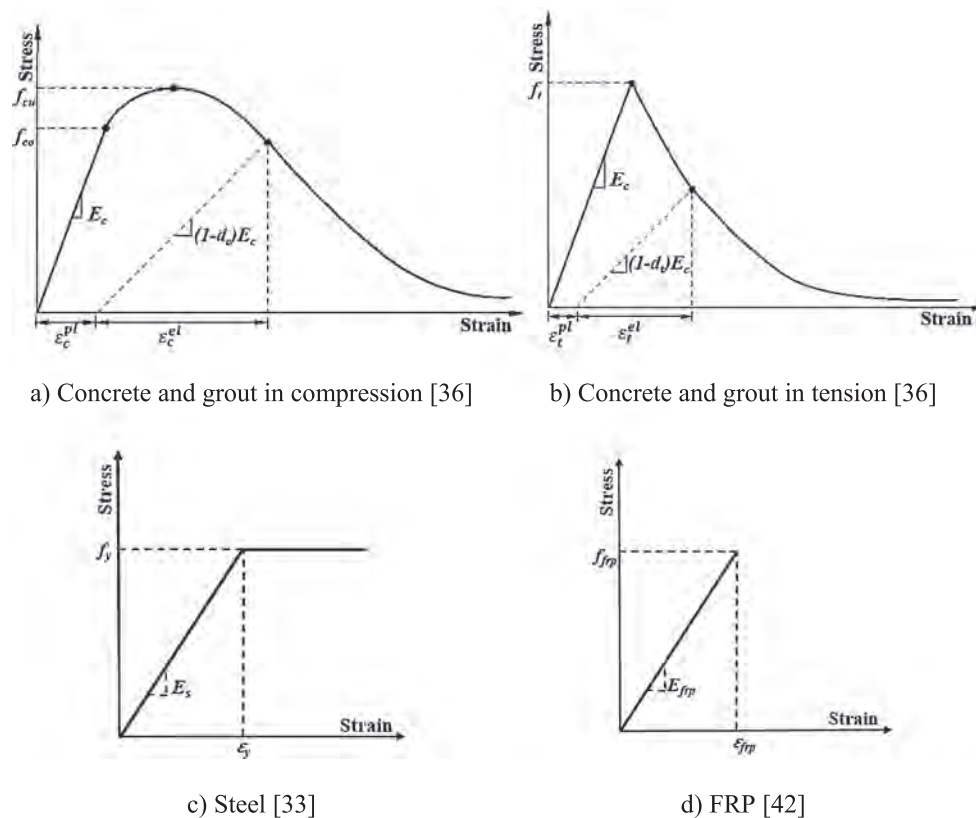


Fig. 6. Constitutive models of components materials [42].

behaviour of concrete and grout in compression and tension (Fig. 6a and b). The Damaged Plasticity Model presumes that the two main failure criteria are compressive crushing and tensile cracking of the concrete material. It requires three parameters in the form of a dilation angle  $\Psi$ , shape factor for yield surface  $K_C$  and a ratio of initial biaxial compressive yield stress to initial uniaxial compressive yield stress. The values corresponding to those three parameters are taken as equal to 31, 1.16 and 0.667, respectively, for both concrete and grout based on the Abaqus recommendations for Concrete Damaged Plasticity Model and previous research findings [33–35]. The compressive strength, tensile strength, modulus of elasticity and Poisson's ratio of concrete and cementitious grout which were measured using cylinder tests are reported in Table 3.

Since steel exhibits the same behaviour in tension and compression despite the time and environmental conditions [41], an elastic and perfectly plastic stress strain curve was assumed for the behaviour of main and secondary reinforcement in tension and compression as shown in Fig. 6c. The properties of the deformed steel bars as provided by the manufacturer are listed in Table 3.

The behaviour of the FRP composite jacket and the joint is assumed to be linearly elastic until failure as depicted in Fig. 6d. Since the FRP shell is made of four layers of fibres with a stacking sequence of  $-45^\circ/+45^\circ/-45^\circ/+45^\circ$  with respect to the hoop direction, it was modelled with a simplified geometry as an isotropic material, instead of four plies of fibre impregnated with epoxy, using the properties that were obtained from the material characterisation tests as listed in Table 3. The joint was modelled as a lamina with different properties in the longitudinal and hoop direction as reported in Table 3.

### 3.2. Development of the FE model

Fig. 7 depicts the modelled RC columns and the novel prefabricated FRP repair system. The concrete columns and steel reinforcement bars were modelled as 3D deformable solid parts and meshed using 8-noded

hexahedral element with reduced integration (C3D8R) on the outer parts and 6-noded wedge element (C3D6) for the core parts to generate a uniform mesh and avoid the distortion and the hour-glassing problem in numerical simulations [40]. The grout was also modelled using a 3D deformable solid but fully meshed using 6-noded wedge element (C3D6) to avoid the shear locking effect [36]. The jacket was modelled as 3D deformable shell and meshed using quadrilateral element S4R. Finally, since the joint geometry is not a main parameter in this analysis and it is already fully investigated by Manalo et al. [10], it was modelled as a shell element with different strength and modulus properties in the longitudinal and hoop direction as listed in Table 3.

The steel cage was modelled as an embedded part within the concrete, and perfect bond was assumed using the tie constraint as an interaction criterion between the concrete-grout-jacket elements. This type of constraint allows the fusion of two different regions together even when the meshes created on the surfaces of the regions are dissimilar. Fixed supports were introduced as a boundary condition at the bottom end of the column. Other constraints applied on the top and bottom ends of the columns as shown in Fig. 7 were the steel collars used in the experimental work. Next, the specimens were loaded by concentric force at the centre point of the top end of the columns and the coupling feature that Abaqus offers was used to distribute the load uniformly onto the top surface of the columns.

### 3.3. FE results and validation with experimental work

This section discusses the numerical behaviour of columns C1 to C3 and compares them with the results obtained from the experimental investigation. As shown in Fig. 8a, there is an excellent agreement between the experimental and numerical behaviour of the failing components, i.e. steel for columns C-1 and C-2, and the joints for C-3. However, a slight difference in the slope of the load-strain behaviour of the longitudinal steel was observed between the experimental and the FE results due to the presence of the steel clamps in the actual RC

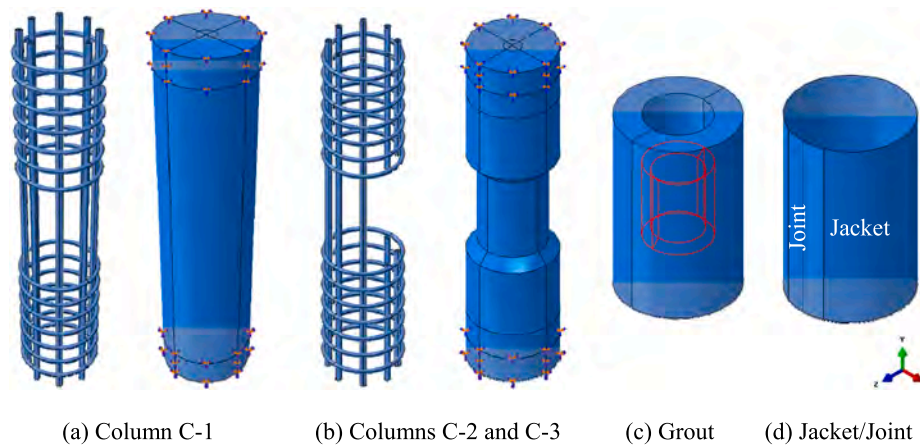


Fig. 7. Modelled columns and repair system.

columns which may have provided additional stiffness and restraint to the steel bars, and confined the concrete at the top and bottom portion of the column. A good correlation was also observed between the experimental and numerical load-strain behaviour of the longitudinal steel in column C-2 and of the joint in column C-3.

With regards to the numerical behaviour of each specimen, the steel and concrete of column C-1 behaved linearly, in nearly perfectly matching curves, up to an applied load of 1700 kN (Fig. 8b). Subsequently, a slight decrease in the slope of the steel and concrete load-strain curve was observed due to concrete cracking at the top end near the loading point as shown in Fig. 9a. This behaviour was also observed in the experimental results at a comparable applied load (1500 kN) as presented earlier under the section of experimental work. However, the strain kept increasing with the applied load until the final failure at mid height where the concrete crushed, and the longitudinal steel buckled at a strain of 2600  $\mu\epsilon$  as shown in Fig. 9b.

For column C-2, the strain in both concrete and steel on the opposite sides of the damaged region increased linearly with the applied load

with matching slopes until the longitudinal steel buckled and the surrounding concrete crushed at an applied load of around 1028 kN and strain values of 1010  $\mu\epsilon$  and 1017  $\mu\epsilon$  for concrete and steel, respectively (Fig. 8b and 9c). However, the load-strain curves of concrete and steel bars near the damaged bars (referred to with a \* in Fig. 8c) showed slightly different behaviour compared to the bars at the undamaged portion of the column. The concrete strain in the damaged region increased at a much lower slope than that in the opposite undamaged side. The strain on the damaged side was 2.9 times higher than the undamaged side as shown in Fig. 8c. Also, the steel bars near the damaged region exhibited higher compressive strains than those located on the opposite side of the damage by 278  $\mu\epsilon$ . The high level of strains in the damaged region clearly indicate the eccentricity effect that was observed in the experimental work. High strains are due to the asymmetric geometry of the simulated corroded bars which caused high bending stresses in the damaged region.

Finally, for column C-3, the axial strains of steel and concrete increased rapidly in a linear manner with the load up to 1500 kN.

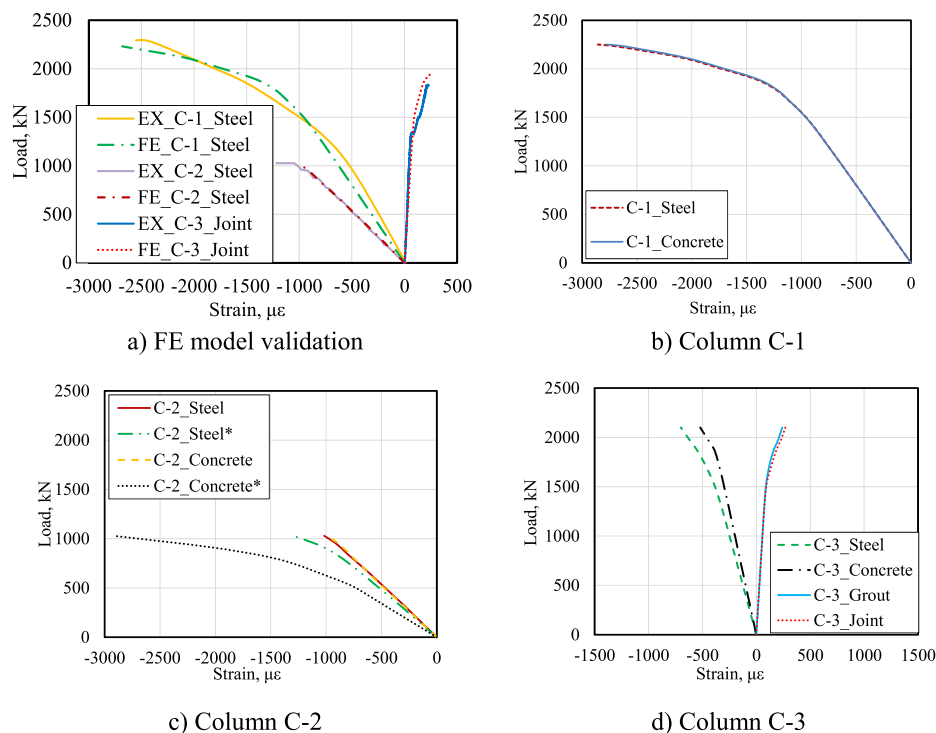


Fig. 8. Validation and numerical load-strain behaviour of the tested columns.

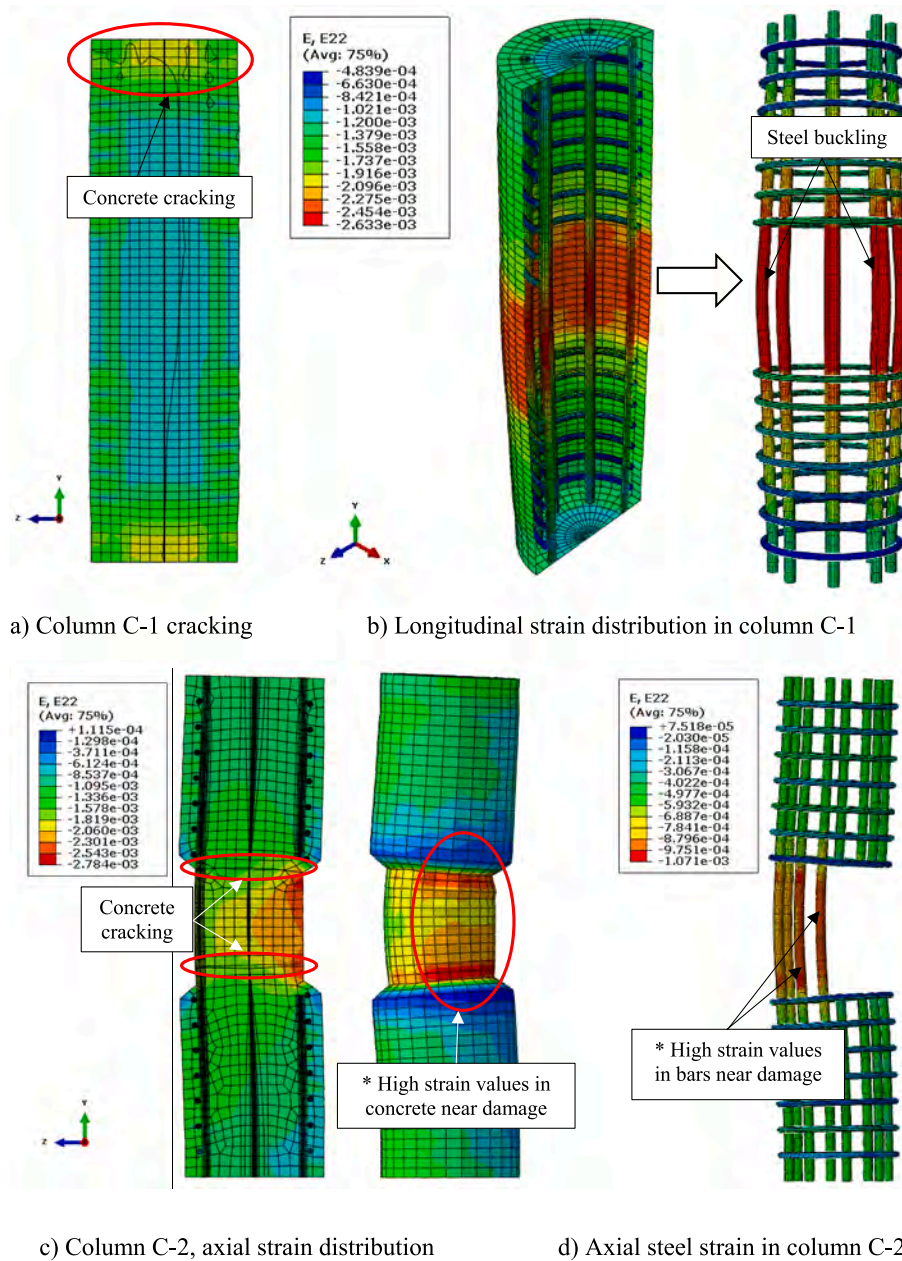


Fig. 9. Failure mode of simulated columns.

Subsequently, the axial strains kept increasing with a reduced slope until an applied load of 1980 kN, whereas the specimen failed at the joint at a strain of  $220 \mu\epsilon$  (Fig. 9e). This behaviour is comparable to the experimental work where the reduction in the slope of the FE analysis (Fig. 8d) represents the drop in the stiffness in the tested column (Fig. 5) due to buckling of the longitudinal steel. The longitudinal steel buckling pushed the grout radially outwards and resulted in higher stresses being carried by the grout and eventually by the jacket/joint. The increased stresses led to the development of cracks in the grout (Fig. 9f) which resulted in minor strain dissipation within the grout. Therefore, higher strain values were measured on the joint than the grout when the applied load exceeded 1500 kN as shown in Fig. 8d. This observation corroborates the findings of Sum and Leong [43] where the authors indicated that the development of cracks in the grout affects its efficiency in transferring the stresses within the components of the FRP repair system. However, slightly higher strain values were observed at the joint in the FE model than the experimental model at the same load level, especially within the linear part of the curve. The

reason behind that could be the presence of gaps at the interface between the grout and the FRP shell/joint which resulted in strain dissipation in that zone. This kind of gaps may also occur in actual applications which can be considered as a limitation of the grout material used because gaps/voids at the surface of the grout might develop during the curing process due to water vaporization.

### 3.4. Effect of joint strength on the behaviour of repaired columns

The experimental results and FE analyses revealed that the failure of the repair system is governed by grout cracking and hoop tensile strength capacity of the joint, which is only 12% of the ultimate hoop strength of the jacket. The limited strength capacity of the current joint design is due to the manufacturing limitations of the pultrusion process where most of the fibres are oriented in the longitudinal direction. The findings from both the experimental and FE simulation highlighted the importance of investigating the effect of the joint strength in improving the overall strength of the repaired system and the restoration capacity

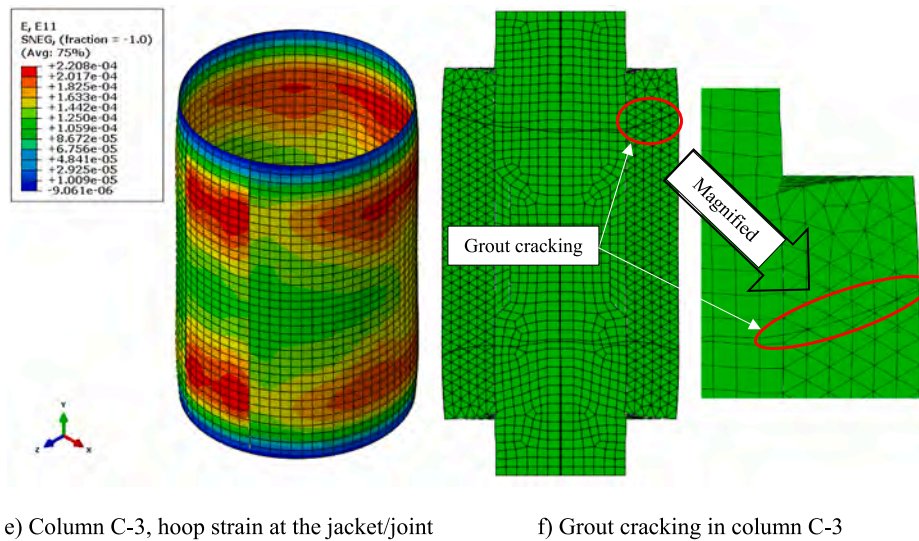


Fig. 9. (continued)

of the novel FRP repair system. This investigation is conducted using the developed FE model by increasing the joint strength as a function of the ultimate hoop tensile strength of the jacket from the current efficiency of 12% to 100% at 10% intervals.

Fig. 10 shows the increase in the axial strength capacity of the repaired column ( $P_c/P$ ) corresponding to the increase in the joint strength/jacket strength ( $f_{frph}/f_{frp}$ ) based on the results of the FE analysis. As shown in the figure, improving the joint strength from its original capacity (12% of the jacket strength) to 20% of the jacket strength resulted in substantial improvement where the axial strength capacity of the repaired column increased by 1.5 times. However, improving the joint strength from 20% up to 100% of the jacket strength at 10% intervals resulted in a marginal strength gain compared to what was achieved in the first increment from 12% to 20% as shown in Fig. 10. This can be attributed to the failure mode of the system changing from rupturing of the joint to compressive failure of the existing structure just outside of the repaired portion. This damage is initiated by crushing of the concrete and buckling of the longitudinal bars with some cracking in the grout inside the jacket.

### 3.5. Summary of the FE simulation

The developed FE model successfully simulated the behaviour of the tested reinforced concrete columns with simulated corrosion damage. The FE analysis results highlighted and confirmed the eccentric effect that resulted from the asymmetric geometry of the corroded bars where stress concentration was observed in concrete and steel locations at the

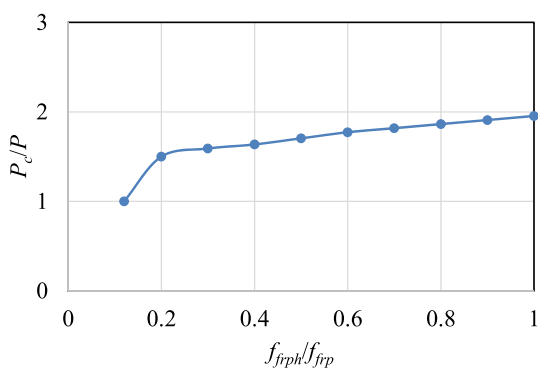


Fig. 10. Level of joint strength improvement ( $f_{frph}/f_{frp}$ ) versus axial strength enhancement of the repaired member ( $P_c/P$ ).

damaged portion. This observation suggests that it would be useful to consider the placement of the joint away from the damage zone of the column being repaired, whenever applicable, so that the high strength properties of the fibre composite jacket can be effectively utilized. Finally, the parametric investigation revealed that the FRP jacket will be effective if the innovative joint strength can be increased to at least 20% of the hoop tensile strength of the novel GFRP jacket. These results will help the engineers in effectively and safely design prefabricated composite jackets in structures repair.

### 4. Conclusions

In this study, the behaviour and failure mechanism of the corroded RC columns repaired using a novel prefabricated FRP repair system was investigated experimentally and numerically. Based on the results of the experimental and numerical analyses, the following conclusions are made:

- The simulated steel corrosion (50%) and concrete cover damage (100%) reduced the axial stiffness and capacity of the column by 40% and 55%, respectively due to compression buckling of the longitudinal bars and concrete crushing at the damaged portion of the column.
- The provision of the novel prefabricated FRP composite jacket stabilised the damaged column by reducing the eccentricity effect of the corroded steel and restored fully the axial stiffness and the strength capacity by 95% compared to the undamaged column. The repaired column failed by steel buckling and concrete crushing at the damaged portion which pushed and cracked the grout radially and ripped off the joint teeth.
- The behaviour of the damaged and repaired columns can be simulated reliably by considering the damaged plasticity model for concrete, bilinear model for steel and linear elastic behaviour of the FRP composites. The FE analysis provided a better understanding on the behaviour of the repaired system and showed internal stress concentration at the damaged region which suggests that the joint of the jacket should be placed away from the damaged area to effectively utilise the composite jacket.
- A joint with tensile strength of at least 20% of the novel GFRP jacket's hoop strength can significantly improve the axial strength capacity of the repaired column. Beyond this 20% level, the failure of the repaired system changes from failure of the GFRP jacket to the failure of the existing structures.

The experimental and numerical works in this study revealed the high potential of the prefabricated FRP composite jacket to provide a safe, quick to install and reliable repair system. However, new research areas can be further explored to better understand the effect of critical design parameter on the behaviour of deteriorated structures repaired with prefabricated composite jackets including the types of grouts, different sizes for the damaged columns and jacket. Moreover, a more detailed cost/benefit analysis is recommended for future study to highlight the cost effectiveness of the novel prefabricated FRP jacket in comparison with other conventional repair systems.

### Declaration of Competing Interest

The authors declare that they have no known competing financial interests or personal relationships that could have appeared to influence the work reported in this paper.

### Acknowledgements

The authors gratefully acknowledge Joinlox Pty Ltd., Australia for the financial, materials, and technical support in conducting this study. The authors are also grateful to the Innovation Connections Fund given by the Australian Government for the successful implementation of this research project. The second author acknowledges the scholarship granted by the Australian Government Endeavour Executive Leadership Award to undertake his professional development at the Centre for Integration of Composites into Infrastructure (CICI), West Virginia University, Morgantown, USA.

### References

- Chellis R. Deterioration and preservation of piles. *Pile Found* 1961;339–72.
- Baileys RT. Timber structures and the marine environment, Ports' 95, ASCE, 1995, p. 703–10.
- Bazinnet S, Cercone L, Worth F. Innovative FRP piling repair without the use of coffer dams. *Int Sampe Sympos Exhibit, Sampe* 1999;1999:2201–6.
- Val DV, Stewart MG, Melchers RE. Effect of reinforcement corrosion on reliability of highway bridges. *Eng Struct* 1998;20(11):1010–9.
- Li X, Wang J, Bao Y, Chen G. Cyclic behavior of damaged reinforced concrete columns repaired with high-performance fiber-reinforced cementitious composite. *Eng Struct* 2017;136:26–35.
- Azam R, El-Sayed AK, Soudki K. Behaviour of reinforced concrete beams without stirrups subjected to steel reinforcement corrosion. *J Civil Eng Manage* 2016;22(2):146–53.
- M. Cassidy, J. Waldie, S. Palanisamy, A Method to Estimate the Cost of Corrosion for Australian Defence Force Aircraft, (2015).
- Holloway L. Advanced fibre polymer composite structural systems used in bridge engineering. *ICE Manual Bridge Eng* 2008;34525.
- Gholami M, Sam ARM, Yatim JM, Tahir MM. A review on steel/CFRP strengthening systems focusing environmental performance. *Constr Build Mater* 2013;47:301–10.
- Manalo AC, Karunasena W, Sirimanna C, Maranan GB. Investigation into fibre composites jacket with an innovative joining system. *Constr Build Mater* 2014;65:270–81.
- Mohammed AA, Manalo AC, Maranan GB, Zhuge Y, Vijay P, Pettigrew J. Behavior of damaged concrete columns repaired with novel FRP jacket. *J Compos Constr* 2019;23(3):04019013.
- Zhao X-L, Zhang L. State-of-the-art review on FRP strengthened steel structures. *Eng Struct* 2007;29(8):1808–23.
- Vandoros KG, Dritsos SE. Concrete jacket construction detail effectiveness when strengthening RC columns. *Constr Build Mater* 2008;22(3):264–76.
- Belal MF, Mohamed HM, Morad SA. Behavior of reinforced concrete columns strengthened by steel jacket. *HBRC J* 2015;11(2):201–12.
- Beddiar A, Zitouni R, Collombet F, Grunevald Y, Abadlia M, Bourahla N. Compressive behaviour of concrete elements confined with GFRP-prefabricated bonded shells. *Eur J Environ Civil Eng* 2015;19(1):65–80.
- Olmos Navarrete BA, Jara Guerrero JM, Gómez Soberón MDLCTJ, Jara Díaz M. Influence of RC jacketing on the seismic vulnerability of RC bridges. *Eng Struct* 2016;123:236–46.
- AlAjarmeh O, Manalo A, Benmokrane B, Karunasena W, Mendis P, Nguyen K. Compressive behavior of axially loaded circular hollow concrete columns reinforced with GFRP bars and spirals. *Constr Build Mater* 2019;194:12–23.
- Mohammed AA, Manalo AC, Maranan GB, Zhuge Y, Pettigrew J. FRP jacket assembly for retrofitting concrete structures. *Proceedings of the 6th Asia-Pacific Conference on FRP in Structures*. 2017.
- Manalo AC, Mohammed AA, Maranan GB. Novel composites jacket for repair of concrete structures. *Proceedings of the 13th Fiber Reinforced Polymer for Reinforced Concrete Structures (FRPRCS13)*, Anaheim, California, United States of America. 2017.
- Bakis C, Bank LC, Brown V, Cosenza E, Davalos J, Lesko J, et al. Fiber-reinforced polymer composites for construction-state-of-the-art review. *J Compos Constr* 2002;6(2):73–87.
- Kim YJ. State of the practice of FRP composites in highway bridges. *Eng Struct* 2019;179:1–8.
- Williams J. FRP Pile Jacket Solution has no 'Pier' in Timber Pile Restoration; 2009.
- Lopez-Anido R, Michael AP, Sandford TC. Fiber reinforced polymer composite-wood pile interface characterization by push-out tests. *J Compos Constr* 2004;8(4):360–8.
- Sen R, Mullins G. Application of FRP composites for underwater piles repair. *Compos B Eng* 2007;38(5):751–8.
- Manalo A, Sirimanna C, Karunasena W, McGarva L, Falzon P. Pre-impregnated carbon fibre reinforced composite system for patch repair of steel I-beams. *Constr Build Mater* 2016;105:365–76.
- Haddad RH, Al-Rousan RZ, Al-Sedyiri BK. Repair of shear-deficient and sulfate-damaged reinforced concrete beams using FRP composites. *Eng Struct* 2013;56:228–38.
- Mohammed AA, Manalo AC, Maranan GB, Muttashar M, Zhuge Y, Vijay P, et al. Effectiveness of a novel composite jacket in repairing damaged reinforced concrete structures subject to flexural loads. *Compos Struct* 2019;111634.
- Vijay P, Soti PR, GangaRao HV, Lampo RG, Clarkson JD. Repair and strengthening of submerged steel piles using GFRP composites. *J Bridge Eng* 2016. 04016038.
- Lopez-Anido R, Michael AP, Sandford TC, Goodell B. Repair of wood piles using prefabricated fiber-reinforced polymer composite shells. *J Perform Constr Facil* 2005;19(1):78–87.
- Joinlox™, PILEJAX™ Fastest Pile Repair Systems, 2019. <http://www.joinlox.com/product/pilejax/>.
- Mohammed AA, Manalo AC, Maranan GB, Zhuge Y, Vijay PV. Comparative study on the behaviour of different infill materials for pre-fabricated fibre composite repair systems. *Constr Build Mater* 2018;172:770–80.
- ASTM C39/C39M, ASTM C39/C39M-15a Standard Test Method for Compressive Strength of Cylindrical Concrete Specimens, ASTM International; 2015.
- AS/NZS4671 Steel Reinforcing Materials, AS/NZS4671-2001 Steel Reinforcing Materials, Sydney (Australia); 2001.
- Karagah H, Dawood M, Belarbi A. Experimental study of full-scale corroded steel bridge piles repaired underwater with grout-filled fiber-reinforced polymer jackets. *J Compos Constr* 2018;22(3):04018008.
- Abdel-Hay AS, Fawzy YAG. Behavior of partially defected R.C columns strengthened using steel jackets. *HBRC J* 2015;11(2):194–200.
- Abaqus, Abaqus 6.13, Dassault Systemes Simulia Corp Providence, RI, USA; 2019.
- Elchalakani M, Karrech A, Dong M, Ali MM, Yang B. Experiments and finite element analysis of GFRP reinforced geopolymer concrete rectangular columns subjected to concentric and eccentric axial loading. *Structures* 2018;273–89.
- Ibrahim AMA, Fahmy MFM, Wu Z. 3D finite element modeling of bond-controlled behavior of steel and basalt FRP-reinforced concrete square bridge columns under lateral loading. *Compos Struct* 2016;143:33–52.
- Alfarah B, López-Almansa F, Oller S. New methodology for calculating damage variables evolution in Plastic Damage Model for RC structures. *Eng Struct* 2017;132:70–86.
- Genikomsou AS, Polak MA. Finite element analysis of punching shear of concrete slabs using damaged plasticity model in ABAQUS. *Eng Struct* 2015;98:38–48.
- Kwak H-G, Filippou FC. Finite element analysis of reinforced concrete structures under monotonic loads, Department of Civil Engineering, University of California Berkeley, CA; 1990.
- ACI-Committee, Guide for the Design and Construction of Externally Bonded FRP Systems for Strengthening Concrete Structures (ACI 440.2R-08), American Concrete Institute, Farmington Hills, MI; 2008.
- Sum W, Leong K. Numerical study of annular flaws/defects affecting the integrity of grouted composite sleeve repairs on pipelines. *J Reinf Plast Compos* 2013. 0731684413503721.

## Chapter 7

### Conclusions

Prefabricated FRP composite jackets have become very attractive repair technique for deteriorating structures, particularly those exposed to the marine environment. A novel FRP jacket with innovative joining system that can easily fit into each other and ensuring uniform stress distribution along the repair system was developed. The initial investigations showed that the novel FRP jacket has the potential to provide structural continuity along the hoop direction. However, the low cost-to-performance benefits of the repair system are not investigated yet and its structural contribution to the repaired structure is still unknown. This study focused on investigating the behaviour of damaged RC structures repaired with the prefabricated FRP jacket to evaluate the effectiveness of the repair system through experimental, theoretical and numerical studies. From this extensive and systematic studies, many new findings were gained and highlighted in the following sections:

#### *Review of the current repair practice*

The state-of-the-art research, development and practice in prefabricated FRP repair systems were critically reviewed to identify the challenges of these repair systems and identify new opportunities for their effective utilisation.

Important factors affecting the design and behaviour of structures repaired with the prefabricated FRP system have been identified and analysed. From the critical review, the following conclusions were drawn:

- Repairing the damaged structures using either concrete or steel jackets or timber splicing is impractical for infrastructure exposed to aggressive environments. These conventional materials will lead to never-ending repair cycles as they are subjected to the same environment which caused damage to the existing structure.
- FRP composite jacketing systems offer superior properties in terms of corrosion resistance, lightweight and durability compared to conventional repair systems and are compatible with steel, concrete and timber structures. Prefabricated FRP composite repair systems are more preferable than the wet lay-up as the former systems are easier, quicker, safer to install, require lesser workers on site, lead

to minimal resource wastage and have higher quality as they are manufactured under well controlled conditions.

- An effective joint is the key to provide structural continuity for prefabricated FRP jackets. The joining schemes should offer a composite repair system that is quick and safe to install, and can be easily implemented for prefabricated FRP repair systems.
- The effectiveness of the prefabricated FRP composite jackets is governed by the thickness and orientation of the fibres within the jacket, the type and properties of infill grout, and the level of damage and shape of the existing structures.

From the above findings, understanding the effects of these design parameters will lead to an optimal and safe design of prefabricated FRP jacket repair systems. Moreover, the contribution of prefabricated FRP jackets to the structural capacity of the repaired structure should be determined to effectively and safely design composite repair systems to extend the service life of structurally deficient structures. It was also identified that the type and properties of the grout infill plays a vital role in transferring the stresses between the damaged structure and the composite repair system.

#### ***Effect of grout properties on the behaviour of prefabricated FRP jacket***

The effect of using concrete, cementitious and epoxy based grout infills on the behaviour of prefabricated composite repair system was investigated by filling GFRP tubes with grouts of compressive strength and modulus of elasticity ranging from 10 MPa to 70 MPa and from 10 GPa to 35 GPa, respectively. All specimens were tested under concentric axial loading until failure. Based on the experimental results, the following conclusions were drawn:

- The type of the grout infill has a major role in the overall behaviour of the composite repair system. The brittle failure behaviour of the cementitious and epoxy grouts led to localised failure in the FRP repair system while the progressive cracking and crushing of the concrete infill resulted in effective utilisation of the high strength properties of the composite materials.
- High compressive strength infill material will limit the capacity to transfer the stresses uniformly around the GFRP tubes due to the increased brittleness. This resulted in the strength and strain enhancement ratios of only 1.3 and 1.0,

respectively for the GFRP repair system filled with epoxy grouts but up to 6.2 and 38 times, respectively for the tubes filled with the lowest strength and modulus concrete.

- The provision of epoxy and coarse aggregates inside the GFRP tube surface enhanced the stress transfer between the tube and infill. This consequently improved the load capacity, ductility and energy absorption by at least 10%. It also prevented the propagation of fibre rupture around the composite repair system leading to a more ductile behaviour than the one without roughened surface.
- Theoretical model which considers the axial and hoop rupture strains of the fibre in the FRP tubes can accurately predict the overall compressive behaviour of GFRP repair system filled with grouts. This model is very useful in determining the appropriate elastic and strength properties of the grout infill for repairing existing structures with prefabricated composite jackets.

The above study demonstrated that the different grout properties significantly affect the behaviour of the prefabricated FRP jacket. The cementitious grout was found effective as an infill between prefabricated FRP jacket and damaged RC structures due to its sufficiently high compressive strength and stiffness which enabled it to yield a strength and strain enhancement equivalent to 1.6 and 5.9, respectively.

#### ***Axial behaviour of damaged RC columns repaired with the novel jacket***

The effectiveness of the novel FRP jacket was evaluated by investigating the axial behaviour of damaged RC columns repaired with the novel jacket. The effect of different parameters i.e. level of steel corrosion, level of concrete cover damage, and the shape effect on the efficiency of the novel FRP jacket were evaluated. The core columns were 1000 mm in height and 250 mm in diameter, all columns were tested until failure under concentric axial load. The main findings of this study are as below:

- The behaviour of the prefabricated FRP repair system in repairing damaged RC columns is governed by the capacity of the grout infill followed by the failure of the teeth at the joint location.

- The GFRP jacket was effective in restoring the axial load capacity of the RC columns with 25% and 50% corrosion damage, by 99% and 95%, respectively, as the repair system stabilized and restored the strength of the damaged columns.
- The GFRP jacket restored the axial load capacity by 95% for the specimen with a 50% spalled concrete cover. However, this percentage decreased by 13% in the specimen with 100% spalled concrete cover due to the change in the interaction/bond between the undamaged steel bars and the grout infill.
- The GFRP jacket was more effective in repairing circular than square columns as the damaged square column exhibited 43% lower axial load capacity than that of the circular section due to the stress concentration at the corners with the joint location.
- A theoretical model that considers the partial confinement effect of the FRP jacket accurately predicted the ultimate axial load capacity of the repaired RC columns. This model is very useful in determining the extent of damage for which the FRP jacket is capable of restoring the structural integrity of a damaged column member.

From this study, it can be concluded that the novel FRP jacket can restore the axial strength and stiffness of damaged RC member. Since the submerged piles are subjected to lateral loads from water, tides and waves which create flexural stresses, the flexural behaviour of the damaged members repaired using the novel repair system was also investigated.

***Flexural behaviour of damaged RC members repaired with the novel jacket.***

The effectiveness of prefabricated FRP composite jacket as a repair system for damaged RC members subjected to flexural loads was investigated. The effect of damage location in the concrete member, joint location and internal surface coating of the jacket on the flexural behaviour of damaged RC members repaired with the FRP jacket were studied. Eight large scale specimens of 3000 mm length and 220 mm by 220 mm cross-section were prepared and tested under four points bending test. Based on the results, the following conclusions were made:

- The behaviour of flexural members repaired with prefabricated jacket was highly influenced by the tensile strength of the grout infill and the joint capacity as the failure of the jacket is initiated by the grout cracking beneath the joint which resulted in opening and failing of the teeth at the joint.
- Placing the joint away from the compression zone resulted in a more effective utilisation of the composite jacket as 53% higher flexural strength capacity was achieved compared to the case when the joint was at the compression zone.
- The FRP jacket is more effective in repairing flexural members with the damage located at the top than at the bottom. Only 55% restoration of the original flexural strength of the beam was achieved when the damage was at the bottom whereas 114% strength restoration was achieved when the damage was at the top.
- The provision of epoxy and coarse aggregate coating inside the GFRP jacket surface resulted in better stress distribution and cracks propagation in the grout than the one without coating. The enhanced composite action of the repair system components due to coating improved the flexural strength capacity by 12% when compared with the jacketed specimen without coating.
- The simplified FMA can reliably predict the flexural capacity of the damaged beams repaired with FRP jacket by considering confined tensile and compressive properties of the grout. Comparison between the predicted and experimental results show the predictions to be within 97% of the experimental values.

The experimental studies clearly demonstrated the effectiveness of the prefabricated FRP composite jacket in repairing RC piles subjected to flexural loads. It also identified the effect of important parameters on the repair system efficiency, such as joint location, damage location and bonding effects. The effect of these important design parameters was investigated in detail using the FE analysis.

### ***Numerical investigation on the behaviour of structures repaired with FRP jacket***

The behaviour of the corroded RC column repaired with prefabricated FRP jacket was investigated numerically using ABAQUS. The developed numerical model was then used to evaluate the effect of the joint hoop tensile strength on the effectiveness of the novel FRP jacket in repairing damaged structures. Based on the results of the numerical analyses, the following conclusions are made:

- The behaviour of the damaged and repaired column can be simulated reliably by considering the damaged plasticity model for concrete, bilinear model for steel and linear elastic behaviour of the FRP composites.
- The FE analysis provided a better understanding on the behaviour of the repaired system and revealed that the joint of the jacket should be placed away from the damaged area to minimise premature failure of the jacket and effectively utilise the composite FRP jacket.
- Improving the joint by at least 20% of the prefabricated composite jacket tensile strength substantially enhanced the axial strength of the repaired members. Beyond this improvement level, the failure mode of the repaired member changed from the FRP joint to the existing structures where the concrete crushed outside the FRP jacket.

### ***Contribution of the study***

This study provided an in-depth understanding of the behaviour of damaged concrete structures repaired with a prefabricated FRP composite jacket with a novel joint. This research also explored the low cost-to-performance benefits of the novel repair system and evaluated its effectiveness in repairing structures with defects. This output resulted in utilising the FRP jacket in many actual repair projects in Australia and overseas as shown in Figure 7.1. Moreover, the results obtained from this study provided a useful design tools for engineers to safely design a highly durable and reliable repair system that can fully restore the strength of the damaged structure. The main contribution of this study can be summarised as follow:

- Understanding the behaviour and determining suitable grout system that can effectively transfer the stress between the repaired structure and prefabricated FRP jacket.

- Effectiveness of prefabricated FRP jacket in repairing damaged RC structures with different level of reinforcement corrosion and concrete cover damage subjected to concentric axial loads.
- Understanding the effects of joint location and damage location on the behaviour of structures repaired with prefabricated FRP jacket subjected to flexural loads.
- Simple theoretical tools to safely design and predict the overall behaviour of grout, damaged RC columns and RC beams repaired with prefabricated FRP jacket.
- Numerical model that can accurately describe the overall behaviour of the damaged RC structures repaired using the prefabricated composite jacket.



Figure 7.1. Novel FRP jacket utilisation in actual repair project

### ***Directions of future research***

This study extensively investigated the effectiveness of the prefabricated FRP system and demonstrated the high potential of this repair system to restore the capacity of damaged structures. Based on the outcome of this study, several opportunities and new research areas can be further explored to better understand the effect of critical design parameters on the behaviour of the repaired structures, which are:

1. Three different types of grouts, i.e. concrete, cementitious and epoxy based grout, with compressive strength and modulus of elasticity ranging from 10 MPa to 70 MPa and from 10 GPa to 35 GPa, respectively, were investigated in this study as infills for the repair system. Further research considering other types of cost-effective grouts with different range of properties should be conducted to optimise the design and utilisation of the repair system.
2. The maximum diameter of the tested RC columns was limited to 250 mm due to the capacity of the testing equipment, while the prefabricated FRP composite jacket could be produced with a minimum diameter of 450 mm due to the curvature of the joint. These two limitations resulted in a grout thickness of 100 mm. Investigations on the behaviour of damaged RC structures repaired with the novel FRP repair system considering different size for the piles and jacket to yield different grout thickness should be explored as this might better simulate the behaviour of actual repaired structures.
3. This study investigated the effectiveness of the novel composite FRP jacket in repairing damaged RC structures with normal concrete compressive strength ( $\approx 30$  MPa) due to the capacity of test equipment. There is an opportunity to conduct research on the effectiveness of the prefabricated FRP jacket in repairing RC structures with high and/or ultra-high compressive strength, which is typical for bridges.
4. The design of the current repair system and the innovative joint is sufficient for structural repair/restoration. Further improvements and investigations are necessary to modify the joint and strengthen it, particularly in the transverse direction to extend the jacket's application to strengthening applications.
5. The developed FMA model accurately predicted the flexural behaviour of the successfully repaired specimen considering the confined tensile and mechanical properties of the grout-infill. However, this developed model is not applicable for repaired structures with premature failure of the joining system as the grout-infill was not confined. Hence, further studies to develop prediction equation that can accurately describe the behaviour of these systems are recommended.
6. Bridge piers used in marine structures have high probability to be hit by boats, thus, investigation on the behaviour of the repair system under impact loads is important for safer design consideration.

## References

- Azam, R., El-Sayed, A. K., and Soudki, K. (2016). "Behaviour of reinforced concrete beams without stirrups subjected to steel reinforcement corrosion." *Journal of Civil Engineering and Management*, 22(2), 146-153.
- Beddiar, A., Zitoune, R., Collombet, F., Grunevald, Y., Abadlia, M., and Bourahla, N. (2015). "Compressive behaviour of concrete elements confined with GFRP-prefabricated bonded shells." *European Journal of Environmental and Civil Engineering*, 19(1), 65-80.
- Berthet, J., Ferrier, E., and Hamelin, P. (2005). "Compressive behavior of concrete externally confined by composite jackets. Part A: experimental study." *Construction and Building Materials*, 19(3), 223-232.
- Cassidy, M., Waldie, J., and Palanisamy, S. (2015). "A Method to Estimate the Cost of Corrosion for Australian Defence Force Aircraft."
- Manalo, A. C., Karunasena, W., Sirimanna, C., and Maranan, G. B. (2014). "Investigation into fibre composites jacket with an innovative joining system." *Construction and Building Materials*, 65, 270-281.
- Sakr, M., El Naggat, M., and Nehdi, M. (2005). "Interface characteristics and laboratory constructability tests of novel fiber-reinforced polymer/concrete piles." *Journal of Composites for Construction*, 9(3), 274-283.
- Vandoros, K. G., and Dritsos, S. E. (2008). "Concrete jacket construction detail effectiveness when strengthening RC columns." *Construction and Building Materials*, 22(3), 264-27

## **Appendix A: Recognitions and Awards**

During my PhD study, my efforts and achievements have been recognized by the University of Southern Queensland and other external organisations/authorities through several awards and recognitions as presented below:

- 2017 Best Poster Award, Centre for Future Material, USQ (Winner)
- 2018 Best Publication Award, Centre for Future Material, USQ (Winner)
- 2018 Wiley Better Future Award, USQ Pitch Club Challenge, (Winner)
- 2018 JEC Asia Innovation Awards, Infrastructure and Civil Engineering Category (Winner).
- 2019 Certificate of Appreciation (Active Postgrads Club\_President), USQ

## Appendix B: Refereed Conference Papers and Project Poster

1. Ali A. Mohammed, Allan C. Manalo, Gingham B Maranan, Yan Zhuge and John Pettigrew (2017). Composite repair systems for damaged concrete columns. *Advanced Composites Innovation Conference*, 28-30 March, Gold Coast, Australia.
2. Ali A. Mohammed, Allan C. Manalo, Gingham B Maranan, Yan Zhuge and John Pettigrew (2017). FRP jacket assembly for retrofitting concrete structures. *Sixth Asia-Pacific Conference on FRP in Structures (APFIS 2017)*, 19-21 July, Singapore.
3. Allan C. Manalo, Ali A. Mohammed, and Gingham B. Maranan (2017). Novel Composites Jacket for Repair of Concrete Columns. *The Thirteenth International Symposium on Fiber-Reinforced Polymer Reinforcement for Concrete Structures (FRPRCS-13)*, 14-15 October, Anaheim, California, USA.
4. Ali A. Mohammed (2018). Effectiveness of a novel FRP jacket in repairing concrete columns with steel corrosion. *The First Inaugural Young Researchers Conference*, 8 December, University of Queensland, Brisbane, Australia.
5. Ali A. Mohammed, Allan C. Manalo, Gingham B. Maranan, Yan Zhuge and John Pettigrew (2018). Effectiveness of a novel FRP jacket in repairing concrete columns with steel corrosion. *Eleventh Asian-Australasian Conference on Composite Materials*, 29 July – 1 August, Cairns, Australia.
6. Ali A. Mohammed, Allan C. Manalo, Gingham B. Maranan and Yan Zhuge (2018). *Ninth International Conference on Fibre-Reinforced Polymer (FRP) Composites in Civil Engineering (CICE 2018)*, 17-19 July, Paris, France.
7. Ali A. Mohammed (2019). Prefabricated composite jacket for repairing of damaged concrete structures. *The Second Inaugural Young Researchers Conference*, 30 November, Queensland University of Technology, Brisbane, Australia.
8. Ali A. Mohammed, Allan C. Manalo, Gingham B Maranan, Yan Zhuge and John Pettigrew (2019). Prefabricated composite jacket for concrete pile repair. *Seventh Asia-Pacific Conference on FRP in Structures (APFIS 2019)*, 10-13 December. Surfers Paradise, Gold Coast, Australia.

# Novel Composite Jacket for Structural Repair

Researcher: Ali A. Mohammed  
Supervisory team: Prof Allan Manalo & Prof Yan Zhuge



## Introduction

- Corrosion damage costs Australia more than \$13 billion per year.
- Deteriorating structures are more economical to rehabilitate than to rebuild.



Deterioration of timber, steel and concrete structures  
Source: <http://www.structuremag.org/article.asp?articleid=141>

## Current repair systems

- Fibre reinforced polymer (FRP) composite jackets are versatile materials for rehabilitating damaged structures due to their high-strength, light-weight and high durability.
- Most available prefabricated FRP composite repair systems lack an effective joint capable of providing structural continuity around the repaired member.



Currently available FRP jacket systems  
Source: <http://www.dorloging.com/forums.php?showthread=1414>

## Proposed solution

- FRP composite jacket with an innovative joining system.
- The FRP jacket works by wrapping the damaged pile and placing a grout in between to fill the gap.
- The performance of this FRP jacket is not yet fully explored and its structural contribution is still unknown.



Jacket and joining system  
Source: <http://www.repair.com/epccom>

## Research Objectives

### Main objective:

- Evaluate the efficiency of a novel FRP jacket as a repair system for structurally deficient structures.

### Specific objectives:

- Determine the most appropriate infill for the FRP jacket.
- Investigate the axial and flexural behaviour of concrete structures repaired with the novel FRP jacket.
- Develop analytical and numerical models to predict the behaviour of structures repaired with the novel FRP jacket.



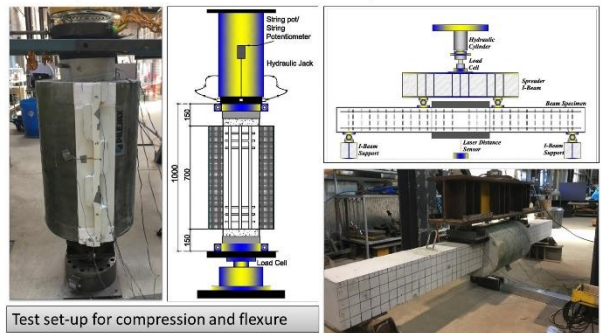
## Research Methodology

### 1. Characterisation of different grout infills



Compression and splitting tensile tests

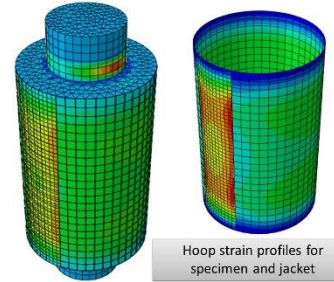
### 2. Compressive and flexural behaviour of repaired structures



Test set-up for compression and flexure

### 3. Theoretical and numerical modelling

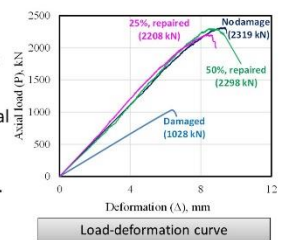
FE analysis is being performed using Abaqus version 6.13, to simulate the overall behaviour and the effect of important parameters such as the type of existing structure, properties of grout and the jacket.



Hoop strain profiles for specimen and jacket

## Research Result

- The provision of the FRP jacket restored the axial capacity of concrete columns with 25% and 50% corrosion damage up to 99% and 95%, respectively.
- The jacket is effective in repairing flexural members when the joint is placed away from the compressive zone to minimise the hoop stress in the interlocking teeth.



## Research Outcome

- The successful completion of this research resulted in utilising the novel jacket in several repair projects in Australia and overseas.



Bridge repair using novel FRP jacket  
Source: <http://www.compositematerials.com/news/usa/golden-collaborate-composites-cable-composite-repair-system>



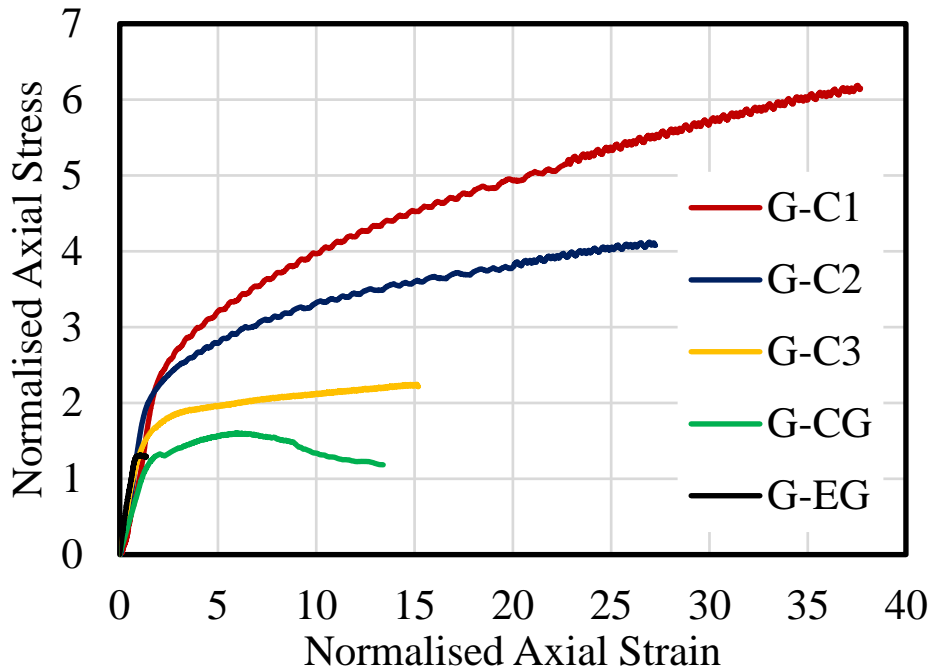
## Appendix C: Full Experimental Results of Chapter 3

### C.1 Test results summary of grout infills and grout filled GFRP tubes

Grout Infills						Grout-filled GFRP Tubes					
Specimen	P <sub>c</sub> kN	P <sub>c-ave</sub> kN	σ <sub>c</sub> MPa	σ <sub>c-ave</sub> MPa	S <sub>c</sub> MPa	Specimen	P <sub>c</sub> kN	P <sub>c-ave</sub> kN	σ <sub>c</sub> , MPa	σ <sub>c-ave</sub> , MPa	S <sub>c</sub> , MPa
C1-1	92		11.7			C-C1-1	656		74.3		
C1-2	94	99	12.0	12.6	1.4	C-C1-2	806	693	91.4	78.5	11.3
C1-3	112		14.3			C-C1-3	616		69.8		
C2-1	113	137	14.4			C-C2-1	562		63.7		
C2-2	121		15.4	17.4	4.4	C-C2-2	649	600	73.5	67.9	5.0
C2-3	176		22.4			C-C2-3	588		66.6		
		-				C-C2-1*	631		71.5		
						C-C2-2*	664	639	75.3	72.4	2.5
						C-C2-3*	622		70.5		
C3-1	199		25.3			C-C3-1	518		58.8		
C3-2	244	216	31.1	27.5	3.1	C-C3-2	462	498	52.4	56.5	3.6
C3-3	206		26.2			C-C3-3	514		58.3		
CG-1	374		47.6			C-CG-1	643		72.8		
CG-2	388	378	49.4	48.2	1.1	C-CG-2	648	645	73.4	73.1	0.3
CG-3	373		47.5			C-CG-3	645		73.1		
EG-1	661		84.2			C-EG-1	737		83.6		
EG-2	604	620	76.9	78.9	4.6	C-EG-2	795	798	90.1	90.5	7.2
EG-3	594		75.6			C-EG-3	863		97.9		

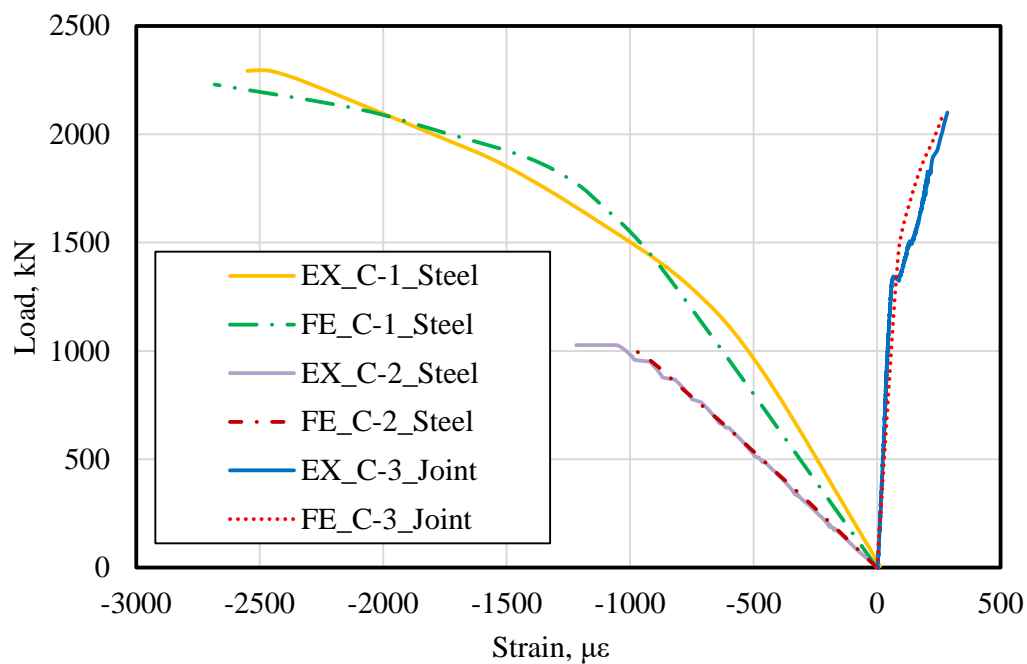
## Appendix D: Revised Published Figures

### D.1 Chapter 3, Figure 12 (Page 33)



Chapter 3, Figure 12. Relation between the normalised axial stress and the normalised axial strain of grout-filled GFRP tubes.

### D.2 Chapter 6, Figure 8a (Page 75)



Chapter 6, Figure 8a. Validation and numerical load-strain behaviour of the tested columns.